Urban Wind Turbines: A Feasibility Study

by

Ben R. Dymock

2719351

dymockb@lsbu.ac.uk

Abstract

There is an existing body of research into noise, vibration and wind regime concerns associated with urban wind turbines demonstrating the detrimental effects of these topics on the energy yield potential and therefore financial worth of an installation. Much of the research has focused on wind regime assessment and optimum roof top placement via CFD modeling offering generalised guidelines showing a potential for wind power to contribute towards lowering London's CO_2 emissions. Unfortunately, without benefiting from appropriate planning assessment, a number of early urban turbines failed and have risked irreversibly tarnishing the concept.

Hitherto no studies have been specifically conducted on the urban potential of building integrated wind turbines. As integration is bespoke, typically determined by the architecture, it is unknown whether existing guidelines for roof mounted wind turbines could be directly applied. It is probable that each installation would merit its own assessment and analysis procedure.

This study aims to investigate the differences between roof mounted and building integrated turbines in terms of assessment, operation and urban potential. In response to these differences it is intended to demonstrate how a successful installation can be achieved.

Comparisons between two urban sites, one smaller, roof mounted HAWT and one larger, building integrated HAWT have been made via noise, vibration, CFD and atmospheric data recorded and analysed over two years to build a comprehensive understanding of the inherent urban issues.

The prospect of successfully situating an urban turbine is complex in nature and considering the high installation costs and high level of design and engineering required to do so it is imperative that their energy yield provide a satisfactory return on investment and efficient supply of power without adversely impacting upon the surrounding environment or themselves.

This study concludes that a multifaceted approach is necessary to achieve an efficient building integrated turbine, comprised of: (i) accurate local noise surveys to establish the local acoustic environment to inform acceptable turbine operating ranges, (ii) specific noise modeling of manufacturer provided data or, where none is available, acoustic testing of the proposed turbine across all applicable wind speed ranges, (iii) comprehensive vibration assessment, not only of the turbine tower/system but also of the turbine housing and any lower residential floors to ensure no natural frequencies will be excited and to prevent any vibration transmission via appropriate mounting, isolation or damping where necessary, (iv) the acquirement of site specific wind data to inform architectural design, turbine selection and placement. If monitoring at hub height is not possible it has been found that it may be acceptable to monitor in close proximity and then extrapolate the results using CFD analysis and wind profile methods, (v) CFD modeling of the surrounding topography, the turbine mount and/or enclosure. These areas are discussed with potential areas of noise and vibration control and turbine optimisation, specific to the case studies, investigated.

Further to the aforementioned study an investigation into a new method of assessing noise and vibration levels associated with average anemometry recorded wind speeds has been presented so as to attain average levels per wind speed bin without being skewed by impulsive gusts.

Acknowledgments

I would like to express my appreciation to the backers of my research: Brookfield Multiplex and the EPSRC. I would like to thank my lead supervisor Dr Stephen Dance for the direction, support and coffee that helped me through countless hours of data collation. I would also like to thank my two external supervisors: Professor Bridget Shield and Dr Tony Day for your advice and input. I would like to thank Dr. Magliano and her team at the Stoke Mandeville Rheumatology department.

A special thanks to my mum, dad and family for supporting and encouraging me always, to NMC and close friends for much needed distractions and a huge thank you to my wife, Nicola, and son, Joe for your support.

Declaration

This thesis is submitted to London South Bank University in support of my application for the degree of Doctor of Philosophy.

I, Ben Dymock, declare that the work, research and results presented within this thesis are my own having been generated by myself as a result of my own original investigation and research and has not been submitted in any previous application for any degree at any institution.

Ben Dymock

Resources Nomenclature

Technologies, software and prediction models were utilised within this study as described below.

Software

Meteodyne Urbawind is a computational fluid dynamics (CFD) prediction software to simulate and predict wind flow within a user defined environment. 3D representations of turbulence, wind direction and mean wind speeds can be simulated and graphically visualised around urban topography.

Datakustik CadnaA (Computer aided noise abatement Acoustics) is an environmental noise prediction software used to simulate and calculate sound propagation within a user defined environment. 3D representations of cities can be modelled and evaluated in accordance with national standards and regulations. A particularly useful calculation feature of CadnaA is a building evaluation technique whereby instead of evaluating noise levels at single receiver positions an entire structure can be evaluated displaying noise levels at interval points around the external facades of the structure. This structure can then be assigned a specific land use property, residential or industrial etc. CadnaA will then display summed noise levels at these points and informs the user of which levels within the structure infringe upon the relevant standards for the specified area of use.

Trimble SketchUp is a 3D modelling software package, similar to AutoCAD in ability to produce architectural, engineering or environmental models, which can be exported into CadnaA and Urbawind to model the surrounding turbine areas in the Southwark and Elephant and Castle area.

Probability distribution models

Probability distribution models are utilised to predict wind speed frequencies over an observed wind speed range using recorded average wind speed data. This is then used to determine the theoretical power available in the predicted wind regime. Two distribution models (Weibull and Rayleigh) are used in weather forecasting due to their shapes most naturally matching natural trends.

The **Weibull** distribution has two, shape (k) and scale (c), parameters. The **Rayleigh** distribution has a shape parameter of $k = 2$.

The **Modified Maximum Likelihood Method** estimates the two Weibull parameters and is proven, via experimentation, by Seguro and Lambert (2000) and Parcell (2007) as a better fit when applied to wind speed distribution data.

Hardware

The following sound and vibration level meters are utilised throughout the monitoring conducted within this thesis

Svantek SV958: Is a class 1, 4 channel sound and vibration level meter allowing for 3-axis (X, Y & Z) vibration and 1/3rd octave noise data to be recorded simultaneously.

Svantek SV106: A 6 channel human vibration meter allowing for 2 sets of 1/3rd octave X,Y & Z axis vibration data to be recorded simultaneously.

Norsonic 140: A class 1 sound level meter to record 1/3rd octave environmental noise levels.

Contents

Chapter 1 Introductory Overview

Urban wind turbines (UWT) are becoming more common place in response to European legislation to reduce CO_2 emissions. This presents known challenges in relation to noise, vibration and energy production, the last of which is dependent on location, orientation and the wind regime available due to urban topography. There are existing tools and methods available to ensure these concerns are appropriately addressed, but currently there is no specific standard or 'check-list' guidance that combines these intrinsic disciplines to effectively ensure a successful urban installation without giving rise to adverse impact. Therefore several urban installations have overlooked vital issues causing the installation to under-achieve, break or be decommissioned due to local complaint thus tarnishing the public view of wind energy.

Through research, active monitoring of urban sites and peer review this thesis intends to compile a complete set of guidance to ensure successful wind energy installations can be achieved in the urban environment.

Current planning guidance in London requires that all new or refurnished large buildings should produce 20 % of their electrical needs via renewable means (GLA, 2004). The first building in adherence to this policy was the Strata building in Elephant and Castle, also the first building in the world to integrate wind turbine technology into the fabric of its architecture atop of the 140 m structure.

This unique example of urban engineering raises some important questions. What effect will urban architecture and topography have on wind flow and therefore energy production? What effect will such an installation have on the surrounding community? What tools and methods are available to predict, optimise and safeguard such a venture?

Turbine placement and design is typically optimized towards rural areas with higher wind speeds and low turbulent flow away from residential populations. This is starkly different to densely populated, built up environments, which presents some barriers to precisely estimating an installation's potential energy production.

There will be uncertainty over the wind estimate as there is no available recorded wind data for central London. The nearest available data is recorded near Heathrow airport at a 10 m height approximately 20 miles west of central London. The urban topography surrounding the Strata Tower as well as the shape of the structure itself would greatly influence the wind regime. Wind shear over urban areas at the Strata's height are not well known or documented, which would have to be overcome for any existing wind data to be extrapolated and applied.

Due to Health & Safety stipulations the bespoke Strata design has eliminated any yaw system to furl the turbines into the prevailing wind resulting in a permanently fixed position. The architects also faced the Strata tower directly north, towards St Paul's cathedral, resulting in the turbines focused to the south. This is not ideal for London's south-westerly prevailing wind.

Noise and vibration issues need to be considered as the Strata tower is, primarily, a residential building[1], with penthouse apartments directly below the turbine plant level, and located in a heavily populated area surrounded by residential areas.

There are existing methods to evaluate and assess a turbines effect on noise and energy production within a community, albeit a rural one. But does this new and unique installation require an equally unique set of assessment criteria and methodology in order to ensure there will be no negative effect on the surrounding community while simultaneously realising its energy production capabilities? Therefore, the following points are investigated to compile a set of criteria and methodology applicable for UWTs:

- How the urban environment impacts upon potential energy generation capabilities of a turbine site by real-time, in situ, monitoring of energy production;
- To observe and assess the influence of urban topography over atmospheric conditions via real time monitoring, which is compared to CFD results to better understand the effect urban architecture has upon the local wind regime. This will contribute towards assessing the appropriateness of CFD application for wind flow predictions in the urban environment;
- Monitor and log the noise at rooftop, representative apartments and local residential areas to investigate the suitability of common environmental noise practice and any associated impacts upon a densely populated urban area;
- Noise map prediction for community noise annoyance in order to quantify turbine related noise in the context of the complex aural environment of the urban area; and
- To assess any turbine induced vibration upon the structure and residential apartments in order to quantify if any constraints are required for turbines and residential developments to coexist. Common vibration monitoring techniques are assessed and a new, high resolution technique is proposed as a more insightful and appropriate method.

In order to gain insight into whether the aforementioned criteria and methodology could be applicable to other urban installations a smaller, more traditional wind turbine was placed at a 40 m height upon the London South Bank University (LSBU) Tower Block roof. There are distinct differences between the installations as highlighted in Table 1 and Figure 1 and 2.

The Strata's three, 9 m diameter, 18 kW rated wind turbines were designed to meet the Mayor's initial London targets of generating 8 % of the energy needs of the building, see Figure 3. The buildings overall carbon emissions were expected to be 15 % lower than the Mayor of London's good practice benchmark, which was set to achieve the 2050 target of a 60 % CO_2 reduction. The LSBU Proven 6 kW turbine is a traditional horizontal axis wind turbine (HAWT), installed in 2013 for research purposes with hope it would contribute to the Tower Block's electricity requirements. It is located 600 m north-west of the Strata tower. These differences provide a prime opportunity in evaluating different turbine design and technology within the same urban environment, but both sites raise certain concerns.

[1] The floor below the turbine level contains penthouse apartments, the last of which sold for £2 million, an investment that would not be made in a noisy, vibrating environment.

	Norwin 18 kW (STRATA)	Proven 6 kW (LSBU)
HUB HEIGHT	135 m	49 m
BLADES	5	3
ROTOR DIAMETER	8.5 m	5.6 m
RATED RPM	1000	200
POWER REGULATION	Air brakes / pitch-able blades	Mechanical Braking
RATED POWER	18 kW	6 kW
PREDICTED ANNUAL POWER	45-100 MWh/annum	6 - 12 MWh/annum
YAW MECHANISM	None/fixed	YES
TOWER TYPE	12.5 DEG tilted custom mast	9 m tapered monopole
DESIGN	Norwin, custom design	Proven, standard design

Table 1: Displays the specifications of the Strata and LSBU turbine sites.

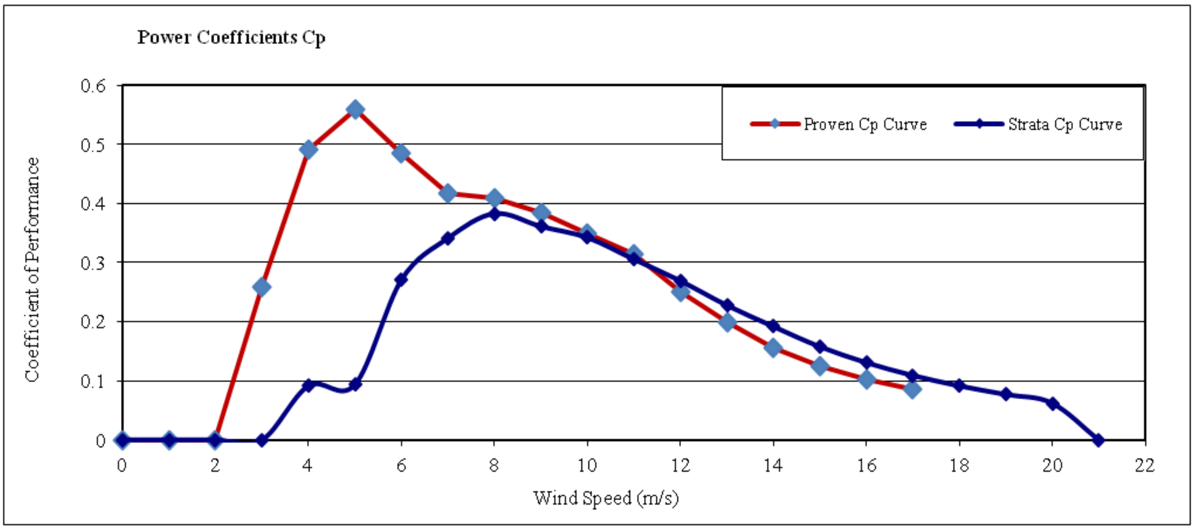

Figure 1: Displays the Power Coefficients (C_p) curve for the Strata and LSBU turbines.

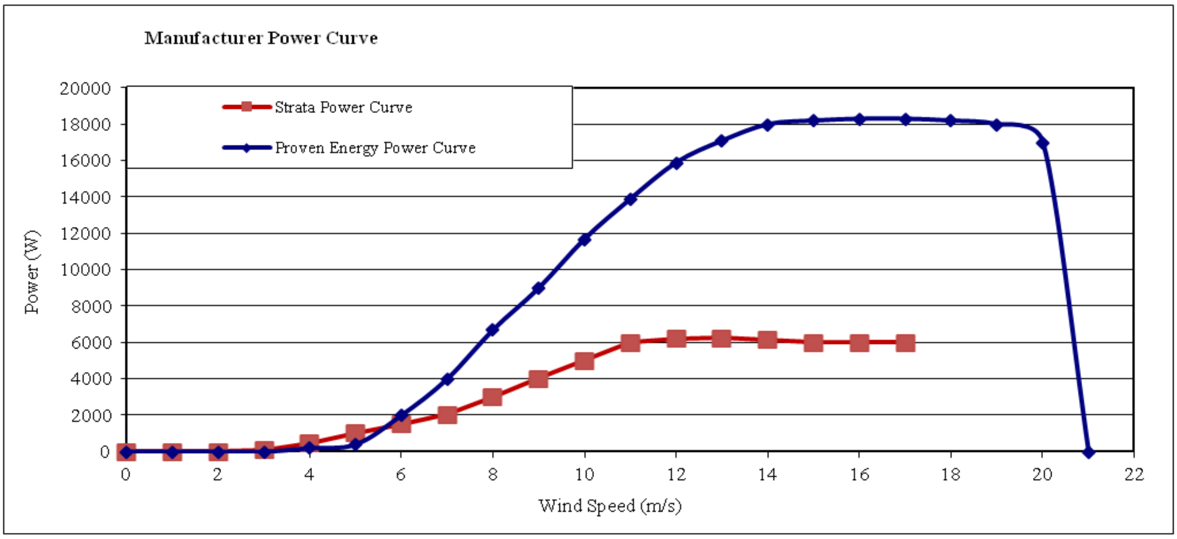

Figure 2: Displays the Energy Power Curve for the Strata and LSBU turbines.

Figure 3: Displays the Strata tower's three Norwin 18 kW and the LSBU Proven 6kW turbines.

The Strata site is an innovative application of an existing technology, the output of the turbines was predicted to be between 45-100 MWh per annum. Similarly, the LSBU turbine, see Figure 3, although a more traditional HAWT system, is being placed into an urban environment, which also presents new, un-anticipated variables in its energy production capabilities. These stark differences will allow for a valuable comparison of existing and bespoke turbine technology within the same urban area.

In order to investigate these topics a literature review is given in Chapter 2 to achieve an effective insight into existing and new turbine technology, to understand the appropriateness of the inclusion of turbines into the urban environment along with any challenges that may arise. This investigation gave the author an understanding of relevant noise and vibration issues applicable to wind turbines along with appropriate monitoring techniques to investigate both sites. An insight into wind resources, topographical effects on wind shear and direction through applying computational fluid dynamic (CFD) techniques is also given in Chapter 2 to gauge the effect of urban configurations on wind flow. This understanding provided a greater appreciation for the energy production capabilities and potential of urban sites.

Methodology for monitoring and recording noise, vibration, atmospheric and energy production data for both the Strata and LSBU sites is presented in Chapter 3. The inherent problems and methods to overcome such challenges are highlighted and discussed. In addition Chapter 3 contents information on data collection periods, parameters and instrumentation.

A case study of results are laid out in Chapter 4 and 5 where all gathered results are presented and compared to relevant guidelines and standards; all infringements of which are highlighted and discussed.

Recorded discrepancies and anomalies are presented in Chapter 6, along with an economic overview of both sites and the authors suggestions for future work in Chapter 7.

The investigation's conclusions and closing remarks are then summarised in Chapter 8.

This investigation hopes to effectively assess an UWT’s appropriateness in the urban environment so it may harmoniously integrate into the community without disruption and annoyance to local residents while contributing to lowering London's CO_2 emissions.

Chapter 2 Literature Review

Current literature on the topics outlined in Chapter 1 are reviewed and summarized in this chapter.

2.1 Historical design, testing & implementation of wind turbines

Commercial development of wind turbines began following the development of the lead-acid battery by Camille Alphonse Faure in 1880 and Sir William Thomson suggesting utilizing wind power to charge such batteries in 1881.

By 1895 the first wind tunnel was developed (by Danish professor Poul LaCour) and throughout the 20th century wind turbine design and implementation was developed and fine tuned from the modest 2.5 kW, 32 V DC Marcellus – Jacobs turbine of the 1930s to the mammoth NASA/DOE/Boeing 98 m diameter, 3.2 MW MOD 5B turbine of the 1990s. This developmental period has seen extensive research and improvement in rotor design, variable speed controls, power trains, generators, gearboxes and towers, culminating in the published IEC 61400 standards, to help set a uniform basis for turbine design.

By February 2015 the world's total installed wind power capacity was 370 GW (WWEA, 2015), driven by very well documented and understood technology.

These vast, technological developments are still mainly focused on wind farm installations in rural areas away from the built environment using typical monopole, three bladed designs. This configuration ensures optimized turbine placement in relation to maximum wind power and uninterrupted flow with minimal turbulence due to local geographical topography.

In 2006 the Department for Business, Enterprise and Regulatory Reform (BERR) introduced the Low Carbon Building Programme (LCBP), which offered set-up grants for up to 50 % of the installation costs, for renewable energy technologies installed into public buildings and businesses. This was later replaced by the Renewable Heat Incentive (RHI) in 2011, which along with Feed in tariffs (FIT) was introduced via the Energy Act (2008) to encourage renewable energy production by paying the suppliers on a £ per kWh basis for electricity produced. Since their introduction these incentives have paid approximately £500,000 every year to owners of small scale renewable energy systems (Grover, 2013). By 2014 approximately 5000 wind turbines had been registered.

These installations were, for the most part, set in rural areas but in line with the London Plan a small percentage of small wind turbines (SWT) were installed in urban areas. A strong interest was initially shown by local authorities across the UK and Ireland with urban turbine installations being introduced very quickly in Huddersfield, Sheffield, Harrogate, Basingstoke, Wandsworth (Case, 2007).

Unfortunately, these installations did not benefit from appropriate forethought and resulted in complaints of excessive noise, vibration and structural damage to support structures and the turbines blades. The installations were, therefore, determined to be uneconomical and were replaced by photo-voltaic (PV) systems or decommissioned receiving some negative press along the way, tarnishing the notion of wind turbines being an effective contributor towards urban renewable energy (Anderson, 2008).

As the urban wind regime inherently offers lower annual wind speeds, more turbulent flow, rough uneven ground urban topography it is important to find the least turbulent areas of cities, which may

be on the roof tops of high rise buildings. Not only is appropriate placement imperative but appropriate technology suited to the environment is key. Urban turbines would need to provide a lower rated wind speeds and lower cut out speeds to withstand the urban wind regime (Sarl, 2012).
In 2006, following a spate of similarly unsuccessful installations the Energy, Environment and Technology Research Centre found that although there is a viable market for UWTs many turbine manufacturers were using inferior quality materials and craftsmanship, there being no standards or regulation in place to assess their technical quality. It also found that a majority of product performance information was not verified (Abohela, 2011).
Years after the first introduction of government incentives in 2006 it was found that the SWT industry could still not establish a dominant technological design for turbines in urban areas. Large-scale wind farm technology has become understood, regulated and successfully deployed within rural areas, but due to SWT technology rapidly penetrating the market while still being in early development stages significant discrepancies between commercially available turbines, manufacturers and installation methods were still apparent (Simic et al. 2013). Supplied data (if any at all) was mostly based on computer simulations alone (Grieser, 2013).
In 2008, however, the world saw an interesting development where, for the first time, larger scale UWT were incorporated into a developments design rather than retrofitted onto an existing structure. The Bahrain World Trade Centre, see Figure 4 (a 240 m high, 50 floor complex) formed from two towers linked by three sky bridges, each holding a 225 kW, 29 m diameter wind turbine predicted to produce up to 13 % (1.3 GWh p.a.) of the buildings electrical needs (BBC, 2008). This was the world's first Building Augmented Wind Turbine (BAWT) where architecture of the building was a determining factor in the turbine installation, augmented to concentrate and accelerate wind flow towards the turbines (Hasse, 2015). BAWTs give architects the opportunity to respond to their concerns about climate change via environmentally friendly, iconic designs where the form of the building plays a significant role in harnessing wind power (Cristia, 2010).
But still, many people find the design of a conventional wind turbine unattractive and where aesthetic and safety measures (of wildlife and surrounding residents) are still a concern these urban energy systems could be further integrated within the architecture of urban environments.

Figure 4: Depicts the world's first building augmented and integrated turbines. The Bahrain world trade centre on the left (BAWT) and London's Strata tower on the right (BIWT).

In 2010, in South London's Elephant and Castle, the Strata Tower became the world's first Building Integrated Wind Turbine (BIWT). This building architecturally encapsulates wind turbines into a specially designed rooftop. The Strata tower is a 140 m height, 43 storey residential tower block with a specially designed venturi enclosure designed into the building's architecture to hold three 19 kW rated, 9 m diameter turbines. These turbines are expected to provide 50 MWh of energy per annum equating to 8-12 % of the building electrical needs (Norwin, 2010). In 2015 the Eiffel tower in Paris had two BIWTs (vertical axis) installed upon its 122 m height second level, see Figure 5. They are expected to generate approximately 10 MWhs of electricity per year. This is enough electricity to power the Eiffel towers first floor restaurants, shops, exhibitions and other such tourist facilities (BBC, 2015).

As the world becomes more aware for the need to combat climate change, this new breed of urban turbine installation may present one solution to increasing renewable energy within the built environment, or alternatively, spaces where open land is sparse. However, it has often been considered that conventional horizontal axis wind turbines would not integrate easily or effectively with architectural designs (Miles, 2006). This, along with the fact that bespoke designs are not verified and tested, or are supplied with computer generated simulated data means that BIWTs and HAWTs require physical monitoring and assessment within the urban environment.

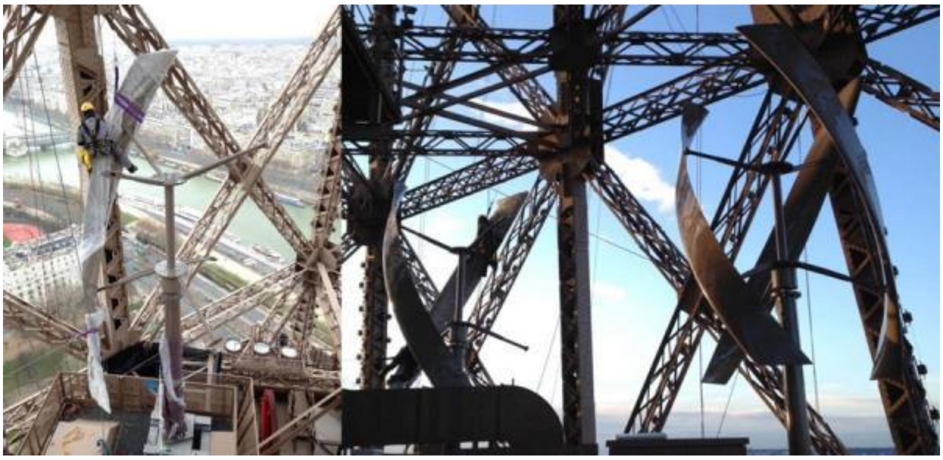

Figure 5: Depicts the Eiffel tower installed VAWTs, expected to generate 10 MWh p.a.

2.1 London Guidance Policy

In 2002 a Mayoral report entitled 'London's Warning' (GLA, 2002) was published outlining the changes in weather patterns and knock-on serious financial implications that climate change would bring to London.

In 2004 the Energy white paper (GLA, 2004) was published setting UK targets of producing 10 % of our electricity from renewable sources by 2010, further extended to 20 % by 2020. This was to show the first steps on putting the UK on a path to reduce carbon dioxide (CO_2) emissions by 80 % in 2050 (Booker, 2010).

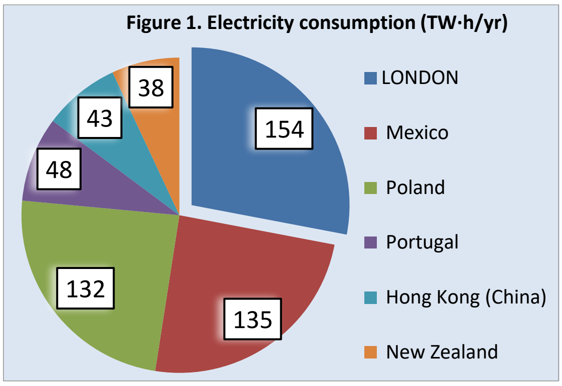

Figure 6: Displays London's electricity consumption at the time the GLA Energy white paper was published. Figure demonstrates that London itself consumes more energy than entire nations.

London's individual electrical consumption at the time of writing the energy white paper was 154 TWhs a year, see Figure 6, incidentally more than Portugal or Ireland. Clearly London's contribution to climate change is highly significant and therefore the Mayor deemed it suitable for London to set its own target of reducing CO_2 emissions by 23 % by 2016. He released 'the London Plan', which put forth the following new policies and strategies relating to renewable energy use in London:

• **London Plan policy 4A.9**

"The Mayor will and boroughs should require major developments to show how the development would generate a proportion of the site's electricity or heat needs from renewables, wherever feasible" (GLA, 2004, p13)

• **The Mayor's Energy Strategy proposal 13**

"To contribute to meeting London's targets for the generation of renewable energy, the Mayor will expect applications referable to him to generate at least ten per cent of the site's energy needs (power and heat) from renewable energy on the site where feasible. Boroughs should develop appropriate planning policies to reflect this strategic policy" (GLA, 2004, p13).

Major developments are defined to include 500 dwellings, 30,000 m^2 commercial space in the city, 20,000 m^2 and 15,000 m^2 of commercial space in and outside Central London respectively.

The mayor also encourages that renewable energy sources be integrated into existing roof spaces, where practicable and that provision be made at the design stage for all new developments to integrate renewable energy sources into new buildings.

There has been a growing interest in wind turbines being located in urban areas, previously considered unsuitable, in order to supplement the large demands of office, residential and business premises.

Research has found that per kWh of electricity generated, the majority of environmental impacts from the wind turbine are lower than from grid electricity (e.g. 26% lower terrestrial toxicity, 92% lower global warming). However, due to the steel production, processing required to manufacture wind turbines depletion of abiotic elements, fresh-water and human toxicity rates are 82%, 74% and 53% lower for grid electricity, respectively.

The research also suggests that wind turbines are more environmentally sustainable than solar PV for 7 out of 11 environmental categories apart from the cases of fossil resource depletion, fresh-water, human and terrestrial toxicities, which are higher, again due to the use of steel (Greening, 2013). It can therefore be seen that urban turbines may offer a viable solution to meeting the criteria for new builds mandated in the London Plan policy 4A.9 and The Mayor's Energy Strategy proposal[2] making the development of these technologies important if targets are to be realised. London's energy strategy also includes local and micro-generation renewable energy schemes (Booker, 2010).

The first major development to propose such a plan was the Strata Tower in south London. In 2005 plans were put forward by Brookfield Multiplex (BFMP) to build the tower in Elephant and Castle, a unique building to be the first to adhere to the Energy Strategy Proposal as well as the first to implement such renewable technology into the residential-led design.

The content of aims and objectives of the London Plan have not changed dramatically to this day, aiming to combat climate change while providing sustainable development in line with the National Planning Policy Framework (NPPF).

The building sector currently accounts for 40% of energy consumption within European Union (Francisco, 2015), which led to Directive 2010/31/EU on the energy performance of buildings being drafted, which provides guiding principles for Member States regarding the energy performance of buildings. One of these guidelines concerns the minimum requirements for energy efficiency during the design of new buildings.

While encouraging renewable integration into the urban environment the EU directive, London Plan and NPPF all strive to simultaneously minimise noise pollution. They act to conserve the natural environment by preventing new and existing developments from contributing to noise pollution to avoid significant adverse effects on health and quality of life. However, they do not address the issue of noise and vibration specifically related to renewable energy sources.

For wind turbines to be a viable option in the urban environment while adhering to the London Plan and NPPF's policies the likely challenges that may occur must be understood.

2.2 Noise

The implications of urban wind turbine noise will now be discussed.

2.2.1 Noise Sources

The four main, distinctive types of sound that active wind turbines may produce are listed below:

- Tonal: Defined as a sound containing a prominent frequency, characterised by a definite pitch.
- Broadband: A noise where sound pressure is equally distributed over a broad frequency range, typically 20 - 4000 Hz.
- Low Frequency: Noise of predominantly low frequency content, 20 - 100 Hz.

[2] A comparison of other urban turbine sites are listed in APPENDIX A.

- Impulsive: Short, sharp transients, impulses or thumping sounds varying with amplitude and time.

These distinctive sounds can be further categorised as either mechanical or aerodynamic noise. Mechanical noise is generated by any structural mechanisms of the turbine (i.e. the gearbox, yaw system, bearings) and would most commonly present itself as low frequency noise. Mechanical faults or defects could generate discrete tones, which may be more perceivable and therefore increase likelihood of noise annoyance than broadband noise at the same level (Moorhouse, 2007). Mechanical sound may be amplified and transmitted further through the turbine hub, nacelle or tower (RERL, 2002). Tonal noise can also be attributed to imperfections or dents on the turbine blades.

Aerodynamic noise is more usually associated with broadband noise generated by the flow of air around the blades and turbine tower. These noises are often subjectively described onomatopoeically as 'whooshing, 'thumping' or 'swishing' noises. The frequency content of such sounds is related to the wind and blade's rotational speed. At higher wind speeds it is predominantly caused by a turbulent air field flowing around the blade's tips and at lower wind speeds the trailing edge of the blades, known as boundary layer turbulence (ETSU-R-97).

The blade pass frequency (BPF) should also be considered, which is related to the rotation speed of the turbine blades. The Strata and LSBU turbines would exhibit the characteristics listed in Table 2 derived from Equation 1.

	RATED RPM	**BLADES**	**BPF (rpm/60 * blades)**
STRATA	200	5	16.6 Hz
LSBU	200	3	10 Hz

Table 2: Compares the BPF of the LSBU and Strata turbines.

$$BPF = \frac{RPM}{60}.n$$

Equation 1: To calculate BPF where n = number of blades.

Technological advancements have contributed to reducing aerodynamic and mechanical noise although they can still occur through damage. Other sources of turbine noise can include the following, see Figures 7 -11:

- A coupling between the blades movement and the wake from the truss tower causing a low frequency impulsive noise (often associated with down-wind rotors). This would usually cause infrasonic noise, which could be focused and amplified in urban areas due to building reflections.
- Higher blade-tip speeds as well as the turbulent boundary layer interacting with the trailing edge can cause high frequency noise (whistling or swishing sound). This ‘swishing’ sound is the most common description in noise annoyance surveys (M.V. Lowson, 1993).
- Rotational harmonies can be observed due to constant fluctuation of aerodynamic loads acting upon a constantly moving rotor blade through localized turbulent flows.

- Separated boundary layer turbulence noise can be generated by convection of the turbulent boundary layer into the wake of the airfoil.
- Noise from in-flow turbulence generally creates low-mid frequency noise and can occur from high wind shears.
- Yaw error noise occurs when there is misalignment of the rotor hub in relation to the wind direction. When yaw error is high a reduction in low frequency noise can be seen due to reduced aerodynamic loading. In contrast, high frequency noise can be increased due to yaw error. This could be overcome through utilisation of a wind directing venturi.

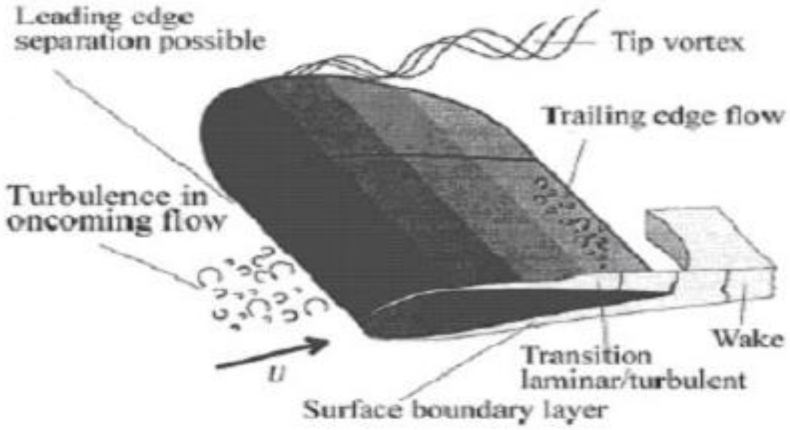

Figure 7:Aerodynamic Noise Sources of Wind Turbines (Wind Turbine Noise, Wagner et al 1996)

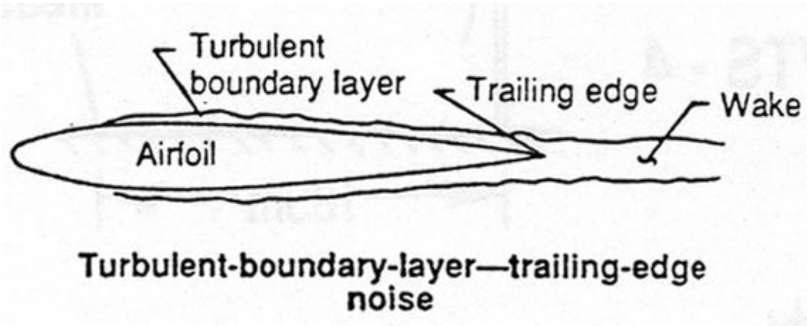

Figure 8:Trailing Edge Noise (Assessment & Prediction of Wind Turbine Noise, M.V. Lowson 1993)

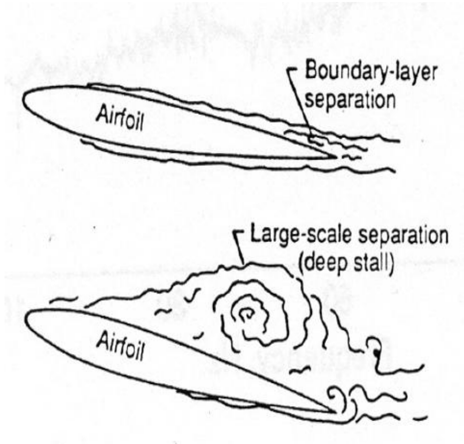

Figure 9:Separated Boundary Layer Noise (M.V. Lowson 1993)

Figure 10: Blade Swish (Courtesy of Oerlemans, Sijtsma and Mendez, 2007)

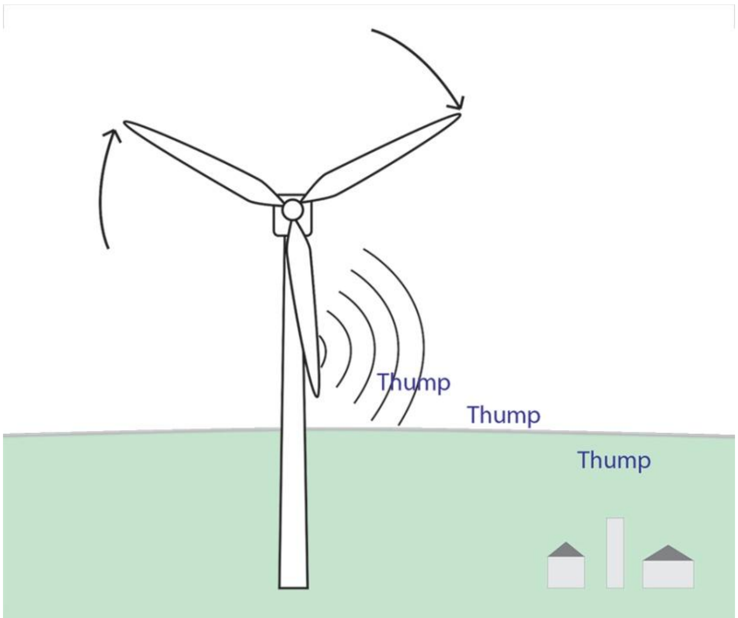

Figure 11: Blade Passing Thump

Any noise created within the built up, urban environment has the potential to be exacerbated by interactions of sound with the abundant reflective facades and surfaces within the urban environment. Turbine noise could be reduced using a better blade shapes design (using pitch control in large scale) and with a good gearbox acoustic isolation. The employment of SWTs in urban areas would help combat noise issues related to larger scale turbines as small wind turbines do not have gearboxes or other noisy mechanical systems, and manufacturers therefore have more room within the nacelle to make them quieter through better sound insulation, lower rotor speeds and adjustments to blade geometry (Lack, 2010).

Other specific noise issues relating to urban turbines atop of high rise building could include:

- Air temperature differs at altitude causing sound to bend towards the denser, cooler air; therefore, although not typical, if the ground is cooler than the air above sound can bend down towards the ground, thus extending its typical propagation distance (Moorhouse et al, 2007).
- Noise emanating from wind turbines as well as background, ambient noise levels will rise as a function of wind speed and therefore vary with altitude due to wind shear, which is heightened over rough, urban topography. This could lead to high wind speeds at altitude diminishing towards the ground, making turbine noise more apparent at street level.
- The wind itself could also mask any turbine noise.
- Wind direction is also a strong factor to consider in wind noise as any residential areas downwind of the turbine will experience greater noise levels than those upwind.

When assessing the impacts associated with any noise source it is useful to know its noise characteristics because different models of wind turbine may exhibit different noise mechanisms, E.g. tonal or impulsive noise, which may be considered more intrusive than continuous or broadband noise (Waye and Ohrstrom, 2002). Ideally this data would be provided by the manufacturer. This can then be assessed and quantified in terms of the relevant criteria applicable at the time. However, recent research conducted by the University of Nottingham has found that there is a gap in the research of noise from smaller UWT and therefore noise continues to frequently pose a barrier to their widespread implementation (Taylor, 2013).

Previous research investigating possible links between wind turbine noise and human health, covering both peer-reviewed articles and popular literature concluded that turbines can be a source of annoyance to some people and that reported health effects could be statistically associated with wind turbine noise sound pressure levels over 40dBA (Knopper and Ollson, 2011). However, it was concluded that much of the existing research examining wind turbine noise focused on rural locations and that there is a gap in research for smaller-scale urban BIWTs (Devine-Wright, 2005). Rural areas are typically quiet with background noise levels below 40 dBA not being uncommon. In contrast, background noise levels can frequently reach levels 65-75 dBA in urban areas.

It has also been found that previous research into the perception of, and annoyance due to, wind turbine noise was limited yet a weak relationship between noise levels and annoyance was presented, varying considerably depending on the turbine type (Waye and Ohrstrom, 2002). Wind turbine noise characteristics could vary wildly due to lack of existing regulations, data and manufacturing standards as sound power levels are not typically published for smaller turbines (Gipe, 2009). It has been found that many manufacturers fail to carry out acoustic testing on their products at all (Sarl, 2012).

Research has also shown that people are more likely to report higher levels of noise, more frequently, due to wind turbines if they can actually see the wind turbine from their property. This could be because those who can see a turbine are living closest to the turbine and therefore more likely to perceive the noise as there are less physical barriers separating them. However, it has also been suggested that the visibility of a noise source increases the likelihood of annoyance and complaint when compared to not being able to see the noise source at the same noise levels (Devine-Wright, 2005).

This could be particularly damning for the BAWTs as they are ideally placed upon high-rise roof tops, away from surrounding obstacles therefore inherently being highly visible from all directions, above potential noise barriers. Therefore, research into more architecturally intertwined BIWTs could be valuable research as it may disguise the installations true visual character, avoiding complaint and annoyance, while also providing natural barrier attenuation/screening of noise into the surrounding areas.

The lack of urban wind turbine precedence and manufacturer provided data means that future planning conditions should be set on a case-by-case basis based on the existing noise regulations, conditions and intended turbine technology relative to the specific urban environment it is to be placed within (Lack, 2010).

This raises an important consideration for any planned urban turbine evaluation; to what should the turbine noise levels be assessed? This will be evaluated in the following section.

2.2.2 UK Noise Policy for Wind Turbine Noise Assessment

A study into how methodology and national standards for wind turbine noise assessment has developed in UK is now undertaken. Reviewing how monitoring procedures and criteria have developed over time to protect residential amenity will highlight any issues in applying these principles within the urban environment.

The first policy to specifically highlight wind turbine noise as a factor to be considered was Planning Policy Guidance Note on Renewable Energy (PPG22) released in 1993. PPG22 was published by the Department of the Environment and the Welsh Office to explain renewable technologies role in reducing greenhouse gas emissions, outline relevant legislation and highlight environmental considerations for installation. PPG22 states that wind turbine sites should be located so that ambient noise levels around noise sensitive developments (such as residential areas) should be kept to acceptable limits. These levels are to help determine the wind turbines distance from occupied buildings and wind farm levels at 350 m are suggested to be 35 - 45 dBA.

PPG22 refers to the already existing British standard BS4142:19903 - ' Method for rating industrial noise affecting mixed residential and industrial areas' as a suitable set of guidelines to adhere to when assessing turbine noise due to low level background noise assessment.

BS4142 demonstrates that complaints may occur when noise levels rise over background noise levels by certain given amounts and is proposed to rate noise at a given receiver position but not quantitatively assess community annoyance or nuisance. BS4142 states that L_{Aeq} measurements are taken but not when the wind speed exceed 5 m/s. This speed limit is imposed to reduce the effects and influence of microphone generated wakes (turbulence) and therefore self-generated noise[4]. This

[3] BS4142 was revised in 2014. However, the 1990 is first considered in order to provide a chronological overview of wind noise policy development.

[4] The use of wind shields is discussed later in this chapter Wind Shields2.2.3.

is not entirely suitable for wind farms as turbines would ideally be located in strong wind resource areas demonstrating higher wind speeds. The L_{Aeq} parameter may also not be entirely suitable as wind turbine noise is, mostly, a steady source that could be masked by any short-term transient noise from passing aircraft, trains or other such environmental and industrial noise that contributes to an L_{Aeq} measurement. PPG22 was later superseded by PPS22 (Planning Policy Statement 22), published by the Office of the Deputy Prime Minister in 2004. Due to the limitations in BS4142 applicability to wind turbine noise PPS22 suggests that the ETSU-R-97 report be employed to assess and rate wind turbine noise.

ETSU-R-97, published in 1996, was written by a 'Working Group' on wind turbine noise in an attempt to advise developers on appropriate and effective procedure of environmental noise assessment of wind farms. Although the Department of Trade and Industry set up the 'Working Group' ETSU-R-97 is not a government report and does not replace any government guidance. ETSU-R-97 also draws inspiration from international guidance and legislation found in the USA, Denmark, Netherlands and Germany. It provides a framework for measurements and noise level limits to avoid community annoyance in neighbourhoods surrounding turbine sites while being mindful not to overly stifle renewable energy production and development and burden local authorities.

One of the main aims of this report is to ensure that an urban turbine installation is configured, installed and operates in a manor so as to avoid complaint of noise nuisance, annoyance or sleep disturbance, topics which are reviewed in detail in PPG24 and by the WHO (Environmental Health Criteria 12 – Noise).

It is made clear in ETSU-R-97 that guidance is not intended to adversely hinder or restrict renewable technology development or installation. In unison with PPG24 the 'Working Group' intend to offer '... advice on how the planning system can be used to minimise the adverse impact of noise without placing unreasonable restrictions on development or adding unduly to the costs and administrative burdens of business.' ETSU-R-97 further quotes PPG24 by stating that '...much of the development which is necessary for the creation of jobs and the construction and improvement of essential infrastructure will generate noise. The planning system should not place unjustifiable obstacles in the way of such development. Nevertheless, local planning authorities must ensure that development does not cause an unacceptable degree of disturbance'. It is clear that ETSU-R-97 strives to be fair in the balance of peace and tranquillity with progress and development.

ETSU-R-97 states that noise limits are to be set relative to existing local background noise levels at the nearest noise sensitive properties and that as background and turbine noise levels increase as a function of wind speed, measurements should be taken over the full spectrum of locally measured wind speeds. $L_{90\ 10min}$, A-weighted measurements are made to capture the background noise level, thus avoiding the measurement of other transient sounds in the environment such as automobiles, trains, planes etc. Noise should be limited to levels 5 dBA above background noise levels per wind speed bin for both day and night except in low level noise environments where the $L_{A90\ 10\ min}$ measurements should be contained within 35 - 40 dBA.

A fixed night time limit is also suggested to 43 dBA, which is based on PPG24 35 dBA sleep disturbance criteria. The level difference derives from the PPG24 criteria being based on internal levels measured with L_{Aeq} and therefore a 10 dB open-window attenuation allowance is made with a -2 dB allowance due to L_{A90} parameter rather than L_{Aeq}.

Wind speed measurements are to be taken up to 12 m/s at a 10 m height, or if recorded at a differing height, should be adjusted to a 10 m measurement. The 12 m/s cap is due to the rarity of such measured speeds, the difficulty in reliable measurement capture due to high wind effects on the microphone. If noise limits are satisfied below this speed then likelihood of complaint is minimal above due the elevated background noise levels caused by the force of the wind.

The $L_{Aeq\ 10min}$ measurement period is different from BS4142 suggested 5 min interval so that measurements would coincide with traditional 10 min wind speed measurements and help ensure an alignment of results.

A microphone height of 1.2 - 1.5 m above ground is suggested in accordance with BS4142 in a position to minimise reflections from buildings at least 10 m from building facade. It is recommended that at least 1 weeks' worth of data is recorded, which should ideally include 20 - 30 night time L_{A90} measurements within +- 2 m/s of the sites critical wind speed. The noise limit evaluations are to be applied to broadband noise from the wind and turbine but further advice is given to any tonal noise, predominantly described onomatopoeically as blade 'swish', which is caused by the amplitude modulation of the noise created as the turbine blades pass through the air. This sound is rhythmic and tonal in nature and dependent on tip speed and the blade profile. A 3 dB variation in level (or more via narrow-band analysis) may result in close proximity to the turbine at distances less than 50 m from the turbine tower, which would lessen with greater distance due to atmospheric absorption.

When ETSU-R-97 was drafted it offered a penalty scale for tonal noise based on existing standards as well as personal/ professional experience as there was no official standard method available within the UK. However, with the advent of the updated BS4142-2014 which now include objective tonal assessment methods and defined penalties the guidance now considers the Joint Nordic Method, which is also highlighted in ETSU-R-97.

ETSU-R-97 came under some scrutiny from external peers over interpretation of methodology, apparent inconsistencies in noise limits and it's omission of consideration of wind shear and it's appropriateness came under question. In 2012 acting for the Department of Energy and Climate Change (DECC) the Institute of Acoustics (IOA) set up a noise working group (NWG) to publish the 'Good Practice Guidance on Noise Assessments of Wind Farms', which was published in 2013 with additional guidance notes published in 2014.

In 2014 the Department for Communities and Local Government published the Planning Practice Guidance for Renewable and Low Carbon Energy guide to supersede the 2013 'Planning for Renewable Energy: A Companion Guide to PPS22' report. Within this updated report ETSU-R-97 is still endorsed for wind turbine noise assessment but this time along with the IOA prepared 'A Good Practice Guidance on Noise Assessments of Wind Farms'.

Other specific acoustic measurement methods are outlined in EN61400-11:2003 'Wind Turbine Generator Systems - Acoustic Noise Measurement Techniques'. This includes the recommendation that measurements be taken level to the nacelle or rotor hub, within a ±15 degree angle of wind direction at time of measurement and at least a distance of R defined in Equation 2. Equation 2 assumes the wind turbine acts a point source in the free field.

$$R = H + \frac{D}{2}$$

Equation 2: To calculate the required measurement distance *R* from a turbine where: *H* = vertical distance from the base of the tower to the rotor hub centre. *D* = rotor blade diameter, as recommended in EN61400.

Clear guidance is given for the assessment of wind turbine noise but the advice given is with wind farm sites in mind, a rural environment with great distances between large turbines (possibly multiple) and quiet residential areas. The Strata and LSBU turbines are located within a busy, heavily populated area of south London so not only is the environment dissimilar but so are the technologies, installations and wind resources. Although one should strive to adhere to guidelines and standards it is equally important to assess their suitability to the individual site in question. It is therefore important, in this instance, to assess more appropriate guidance and standards applicable to built up environment. The guidance presented next provides a greater context for turbine assessment in an urban environment.

National Planning Policy Framework, 2012

The National Planning Policy Framework (NPPF) seeks to conserve and enhance the local environment by preventing developments from contributing to, and / or, being put at an unacceptable risk from, noise pollution. The NPPF stipulates that planning decisions should seek to:

- avoid noise from giving rise to significant adverse impacts on health and quality of life as a result of new development;
- mitigate and minimise adverse impacts on health and quality of life arising from noise from new development, including through the use of conditions;
- recognise that the development will often create some noise and existing businesses wanting to develop in continuance of their business should not have unreasonable restrictions put on them because of changes in nearby land uses since they were established; and
- identify and protect areas of tranquillity which have remained relatively undisturbed by noise and are prized for their recreational and amenity value for this reason.

Noise Policy Statement for England, 2010

The Noise Policy Statement for England (NPSE) was published in March 2010 by the Department for Environment Food and Rural Affairs (DEFRA) and is the overarching statement of noise policy for England. It applies to all forms of noise other than occupational noise, setting out the long term vision of Government noise policy to:

- "*Promote good health and a good quality of life through the effective management of noise within the context of Government policy on sustainable development*."

That vision aims, through effective management and control of environmental noise within the context of Government policy to:

- avoid significant adverse effects on health and quality of life;
- mitigate and minimise adverse effects on health and quality of life; and
- where possible, contribute to the improvement of health and quality of life.

The Explanatory Note to the NPSE introduces three concepts to the assessment of noise in this country:

- No Observed Effect Level (NOEL) – this is the level below which no effect can be detected and below which there is no detectable effect on health and quality of life due to noise;
- Lowest Observable Adverse Effect Level (LOAEL) – this is the level above which adverse effects on health and quality of life can be detected; and
- Significant Observed Adverse Effect Level (SOAEL) – this is the level above which significant adverse effects on health and quality of life occur.

None of these three levels are defined numerically in the NPSE and for the SOAEL the NPSE makes it clear that the noise level is likely to vary depending upon the noise source, the receptor and the time of day/day of the week. The need for more research to investigate what may represent a SOAEL for noise is acknowledged and the NPSE asserts that not stating specific SOAEL levels provides policy flexibility in the period until there is further evidence and guidance.

The London Plan

Specific to London, The Spatial Development Strategy for London was updated with alterations in 2011 and 2015.

Policy 5.3 of The London Plan states that major development proposals should include measures to achieve sustainable design principles through minimising noise pollution.

Policy 7.15 states that development proposals should seek to manage noise by:

- avoiding significant adverse noise effects on health and quality of life as a result of new development;
- mitigating and minimising the existing and potential adverse effects of noise on, from, within, as a result of, or in the vicinity of, new development without placing unreasonable restrictions on development or adding unduly to the costs and administrative burdens of business;
- separating new noise sensitive development from major industrial noise sources through the use of distance, screening or internal layout; and

- promoting new technologies and improved practices to reduce noise at source, and on the transmission path from source to receiver.

The Mayor's Ambient Noise Strategy, 2004

The Strategy sets out policies to protect and improve noise environments within London while seeking to build a more sustainable City.

Planning Practice Guidance, 2014

In March 2014, the Department for Communities and Local Government (DCLG) released updated Planning Practice Guidance (PPG) which included reference to Noise.

The PPG provides advice concerning noise exposure, and its effects, and puts the NPSE guidelines into context. The PPG states that local authorities should take account of the acoustic environment and considerr whether or not:

- a significant adverse effect is occurring or likely to occur;
- an adverse effect is occurring or likely to occur; and
- a good standard of amenity can be achieved.

The PPG introduced the concepts of the No Observed Adverse Effect Level (NOAEL) and Unacceptable Adverse Effect Level (UAEL). NOAEL differs from NOEL in that it represents a situation where the acoustic character of an area can be slightly affected as long as there is no perceived change in the quality of life. SOAEL represents a situation where noise is 'noticeable' and 'disruptive', and should be 'avoided'. UAEL represents a situation where noise is noticeable, very disruptive and should be prevented. Thus, the national policy approach is to avoid noise above the SOAEL.

The PPG explains the appropriate response for each noise exposure category:

- No Observed Effect: There is no effect and the noise is not perceived.
- No Observed Adverse Effect (NOAEL): Noise can be heard, perceived as noticeable but not intrusive. Noise may also slightly affect the acoustic character of the area. It must not, however, cause any change in behaviour or attitude or cause a perceived change in the quality of life,.
- Observed Adverse Effect: Noise can be heard and perceived as noticeable and intrusive. It may cause small changes in behaviour and/or attitude, e.g. turning up volume of television; speaking more loudly; where there is no alternative ventilation, having to close windows for some of the time because of the noise. Potential for some sleep disturbance. It could affect the acoustic character of the area such that there is a perceived change in the quality of life.
- Significant Observed Adverse Effect (SOAEL): Noise is perceived as noticeable and disruptive causing a material change in behaviour and/or attitude, e.g. avoiding certain activities during periods of intrusion; where there is no alternative ventilation, having to keep windows closed most of the time because of the noise. Potential for sleep disturbance

resulting in difficulty in getting to sleep, premature awakening and difficulty in getting back to sleep. Quality of life diminished due to change in acoustic character of the area. This should be avoided.

- Unacceptable Adverse Effect: Noise is perceived as noticeable and very disruptive. Extensive and regular changes in behaviour and/or an inability to mitigate effect of noise leading to psychological stress or physiological effects, e.g. regular sleep deprivation/awakening; loss of appetite, significant, medically definable harm, e.g. auditory and non-auditory. This should be prevented against.

The subjective nature of noise means there is not a simple relationship between noise levels and its effect. This would depend on how various factors combine in any particular situation, including:

- the level of the noise together with the time of day it occurs;
- for non-continuous sources of noise, the number of noise events, and the frequency and pattern of occurrence of the noise;
- spectral content of the noise and the tonal or impulsive character of the noise; and
- the acoustic character of the local area.

British Standard 4142: 2014 Methods for Rating and Assessing Industrial and Commercial Sound

BS 4142:2014 has already been highlighted as influencing ETSU-R-97's guidance but is now overviewed in the context of the urban environment. It describes methods for rating and assessing sound of an industrial and/or commercial nature to investigatee complaints and assess sound from proposed, new, modified or additional sources of sound of an industrial/commercial nature.

The procedure compares the measured (or predicted) sound level from the source (specific sound level - $L_{Aeq,T}$) immediately outside of the dwellings with the background sound level ($L_{A90,T}$) that exists in the absence of the source in question. If the sound is tonal, impulsive, intermittent or otherwise distinctive in character at the assessment location then a character correction of between 0 dB and +9 dB is added to the specific sound level to obtain the rating level ($L_{Ar,Tr}$).

After making any relevant corrections the background sound level is subtracted from the rating level and an initial estimate of the potential impact of the sound source is made where typically, the greater this difference, the greater the magnitude of the impact.

- a difference of around +10 dB or more is likely to be an indication of a significant adverse impact, depending on the context;
- a difference of around +5 dB or more is likely to be an indication of an adverse impact, depending on the context; and

- the lower the rating level is relative to the measured background sound level, the less likely it is that the specific sound source will have an adverse impact or a significant adverse impact. Where the rating level does not exceed the background sound level, this is an indication of the specific sound source having a low impact, depending on the context.

The standard places emphasis upon the context in which the sound occurs in arriving at any decision. This may include the nature of the local environment, the level and character of the background noise climate, the sensitivity of the receptor and whether the residential premises incorporate design measures that ensure good internal acoustic conditions such as façade treatment, ventilation and acoustic screening.

World Health Organisation Guidelines for Community Noise, 1999

The World Health Organisation (WHO) document '*Guidelines for Community Noise*' provides a range of aspirational noise targets aimed at protecting the health and well-being of the community. It sets out noise goals to minimise the adverse effects of noise on health whilst recognising that the recommended guidelines are already exceeded in many urban areas and alongside many roads.

The guideline strives to ensure the critical effects of noise on sleep, annoyance and speech interference are avoided. The WHO guidelines strive to protect the most vulnerable and sensitive of the population by setting values at the level of the lowest adverse health effect below which the occurrence rates of particular effects can be assumed to be negligible.

Noise limits aim to prevent the majority of the population being moderately or seriously annoyed by noise and ensure a good night's sleep. A summary of the recommended WHO guideline values is presented in Table 3.

Specific Environment	Critical Health Effect(s)	$L_{Aeq,T}$ (dB)	Time Period	$L_{Amax,fast}$ (dB)
Outdoor Living Areas	Serious annoyance, daytime and evening	55	Day	n/a
	Moderate annoyance, daytime and evening	50	Day	n/a
Indoor Living Areas	Speech intelligibility and moderate annoyance, daytime and evening	35	Day	n/a
Inside Bedrooms	Sleep disturbance, night-time	30	Night	45
Outside Bedrooms	Sleep disturbance, window open (outdoor values)	45	Night	60

Table 3: WHO Guidelines Noise Levels to Protect the Health and Wellbeing of the Community

British Standard 8233: 2014 Guidance on Sound Insulation and Noise Reduction for Buildings

BS 8233 builds on the WHO guidelines, providing guidance for the control of noise in and around buildings. It recommends internal ambient noise criteria for a range of indoor spaces including residential land uses to prevent the local residents being impacted upon by noise. The indoor ambient noise levels for habitable room spaces relevant to this assessment are presented in Table **4**.

Activity	Location	Daytime L_{Aeq},16hr (07:00 to 23:00)	Night-Time L_{Aeq},8hr (23:00 to 07:00)
Resting	Living room	35 dB	n/a
Dining	Dining room / area	40 dB	n/a
Sleeping	Bedroom	35 dB	30 dB

Table 4: BS 8233 Guideline Noise Levels for Residential Spaces

While internal levels set by BS8233 and WHO guidelines protect residential health and sleep patterns, external levels may be unrealistic depending on the area and pre-existing conditions.

Considering we are focused on the urban environment ETSU-R-97 does not seem wholly appropriate or capable to assess the potential significance or scale of impact a turbine may have. In spite of ETSU-R-97s guidelines to measure against existing conditions it does not offer the same scope that NPPF, NPSE and DCLGs PPG do to give wider context to the existing noise climate and predict the likelihood of an adverse effect occurrence on local residents in order to achieve a good standard of amenity.

It is therefore deemed more appropriate to consider the guidance set out in NPPF, NPSE, DCLGs PPG and BS4142 along with ETSU-R-97 for wind turbine noise assessment in an urban environment. This would ensure that noise sources (and their associated character) introduced into an area will be evaluated in terms of its contribution to the local environments existing noise climate.

Therefore noise impact assessments from urban turbines would consider the following criteria, see Table 5:

<table>
<tr><th>Standard / Policy</th><th colspan="3">Criteria</th></tr>
<tr><td>BS 4142:2014</td><td colspan="3">Existing L_{Aeq} - 10 dB</td></tr>
<tr><td>ETSU-R 97</td><td colspan="3">Existing L_{Aeq} + 5 dB</td></tr>
<tr><td rowspan="3">BS 8233:2014 / WHO 1999</td><td></td><td>Day</td><td>Night</td></tr>
<tr><td>Living spaces</td><td>35 dB</td><td>n/a</td></tr>
<tr><td>Bedroom spaces</td><td>35 dB</td><td>30 dB</td></tr>
</table>

Table 5: Review of Relevant Noise Criteria for Urban Turbines.

2.2.3 Wind Shields

Wind shields are an important necessity in any environmental noise arsenal as they reduce the effects of microphone self-noise in high winds, protect the microphone and keep it clean. For noise surveys taken in high wind speeds on a turbine site or at altitude wind induced self-noise may present a problem.

Wind induced microphone self-noise is generated by pressure fluctuations within the turbulent flow caused by the microphone capsule itself. The air flow is disrupted by its interaction with the microphones geometry, size and shape and causes unwanted pressure fluctuations picked up by the microphones diaphragm. A wind shield will reduce this effect while allowing un-attenuated noise to be picked up by the microphone. the larger surface area of the shield averages out local pressure fluctuations. Strasberg's research in 1987 showed that wind shield noise was approximately inversely proportional to its diameter.

In light of this a 100 mm diameter dual layer windshield will be used for turbine noise measurements in high wind speeds in accordance with the IOA Good Practice Guide to application of ETSU-R-97 (pg 8, IOA, 2013).

2.3 Vibration

Key points for consideration regarding wind turbine vibration within the urban environment are now discussed. Turbines induced vibrations could be dangerous for constructions and therefore for any rooftop wind turbines, BAWT or BIWT, this factor should be considered before installation (Lack, 2010).

Key issues to analyse are discomfort, structural/mechanical damage and re-radiated, structural borne noise. Any airborne noise heard simultaneously to structural borne vibration may enhance a person's perception of vibration, which is also true of vibrational knock-on effects, such as rattling of windows. High speed winds, especially impulsive gusts can cause building vibration for turbine sites, the root causes of which are the rotating blades and dynamics of wind power on the tower and the gearbox, which may be radiated through any connecting mechanical components of the installation. Turbine blades are not completely rigid and therefore random wind loads may excite natural modes of the blades. To understand this effect the energy content of the wind must be known and examined at each point along the blades at its natural frequencies. These effects can be amplified when individual or parts of, blades pass through gusts of wind.

Any torsional vibrations experienced by the blades can usually be disregarded as they will typical be above the exciting frequencies due to the blade stiffness. It is, however, essential to avoid resonant oscillations when designing a turbine blade as this could cause fatigue and failure. Appropriate damping can distance blades natural frequencies from their rotational frequency.

Due to constantly fluctuating wind speeds, and therefore fluctuating rotational speed, variable speed turbines will have a varying load over time. This mixed with a complex drive chain, which will also be rotating at variable speeds over time, can present complicated vibration analysis issues. A variable speed and load system will present differing peaks in amplitude and frequency spectrum throughout its lifecycle, which can make it hard to isolate exact locations of structural fatigue. Therefore to effectively treat vibration at a turbine site it is imperative to assess the sites most common mode of operation and take measures against potential dominant noise and vibration generation frequencies (Case, 2007). This can be done through adequate wind speed or energy production measurements and is essential to avoid inappropriate isolation.

As there are residential apartments and employee offices on the floors below the turbines at both sites it is important to establish that any vibration transmitted throughout the structure of building is of low enough amplitude so as to not generate adverse comments from the residents. Reinforced concrete roofs may be able to absorb vibrations from the turbine or heavy, inertia bases could be implemented as support structures (Ragheb, 2014) but care should be taken to ensure that problem frequencies are effectively negated through such a design. Failure to do so could see an installation fail or be prematurely decommissioned due to structural stress and damage to the roof top, turbine mounting or the turbine itself. This has been mentioned in Huddersfield and Dublin (Abohela, 2011).

BS5228:2009 part 2 'Code of practice for noise and vibration control on construction and open sites - Part 2: Vibration' expresses human response and thresholds to vibration levels in peak particle velocity (mm/s). It suggests that vibrations above a perception threshold of 0.14 - 0.3 mm/s can disturb. startle, cause annoyance or interfere with work activities. Within a residential setting vibrations of such magnitude could cause sleep disturbance or anxiety as is discussed along with vibrations effects on physical health in BS6841:1987 'Measurement and evaluation of human exposure to whole-body mechanical vibration and repeated shock'. BS6841 recommends the use of RMS acceleration (m/s^2) to express vibration magnitude quoting the average perception threshold of humans to be 0.015 m/s^2. BS6841 also outlines human comfort levels per vibration level as presented in Table 6.

R.M.S Acceleration [m/s^2]	**Level of Comfort**
< 0.315	Not uncomfortable
0.315 - 0.63	Little uncomfortable
0.5 - 1	Fairly uncomfortable
0.8 - 1.6	Uncomfortable
1.25 - 2.5	Very uncomfortable
> 2	Extremely uncomfortable

Table 6: Human comfort levels of RMS acceleration vibration as described in BS6841:1987.

RMS acceleration is obtained by taking the square root of the sum of squared vibration amplitudes measured over a chosen time period. BS6841 does stress that occasional or intermittent peak sources (such as gusts of wind) may be underestimated using this method, in which case an assessment in terms of vibration dose values (VDV) is recommended, the advised method for evaluating vibration effects on health as defined in Equation **3**.

$$VDV = \left(\int_0^T a^4(t)dt \right)^{0.25}$$

Equation 3: Displays the defining equation of VDV Where VDV = vibration dose value ($m/s^{1.75}$).

VDV assesses continuous, intermittent and impulsive vibration over time. *a(t)* is the frequency weighted acceleration (m/s^2) using W_b or W_d filters as appropriate (z and x-y directions) and T equals the total time period of the measurement, in seconds. It is clear that this measurement differs from RMS acceleration by averaging the quad-root rather than the square-root and is often denoted as RMQ. RMS and RMQ results would differ depending on the number of events and amplitude over a given time period. An RMS results would be more influenced by the number of recorded events over a given time period whereas RMQ would be more influenced by the peak value recorded over the same period.

VDV is to be measured over a day period and the overall exposure level evaluated or if the source of vibration is known to be steady and continuous then one representative measurement may be extrapolated into a full day exposure value. There is also guidance on how to evaluate an overall estimated VDV (eVDV) from RMS acceleration measurements with a low crest factor where the vibration source is constant.

Likelihood of complaint due to building vibrations will differ in differing environments.

BS 6472-1:2008 gives examples of human response to vibration exposure in buildings in the 1-80 Hz frequency range and offers acceptable vibration magnitude limits in varying environments along with multiplying factors to be used in accordance with type of building, vibration and time in order to avoid complaints, presented in Table 7. This is based on likelihood of complaint rather than hazard to health in BS6841 using VDV levels.

Measurements taken on X, Y and Z axes in RMS and VDV are compared to axes specific weighting curves to determine if the measured vibration levels are within acceptable regulation human exposure limits, which differ with frequency and direction as demonstrated in Figure 12. Appropriate frequency weightings are presented to in the graph to reflect the exposure. Typically a weighted peak acceleration of 0.015 m/s^2 will be perceivable to most people but for periods of vibration under one second perception thresholds can be higher.

Place and time	**Low probability of adverse comment** $m \cdot s^{1.75}$	**Adverse Comment Possible** $m \cdot s^{1.75}$	**Adverse comment probable** $m \cdot s^{1.75}$
Residential buildings - 16 h day	0.2 to 0.4	0.4 to 0.8	0.8 to 1.6
Residential buildings - 8 h night	0.1 to 0.2	0.2 to 0.4	0.4 to 0.8

Table 7 - Vibration dose value ranges which might result in various probabilities of adverse comment within residential buildings. **NOTE** For offices and workshops, multiplying factors of 2 and 4 respectively should be applied to the above vibration dose value ranges for a 16 hr day.

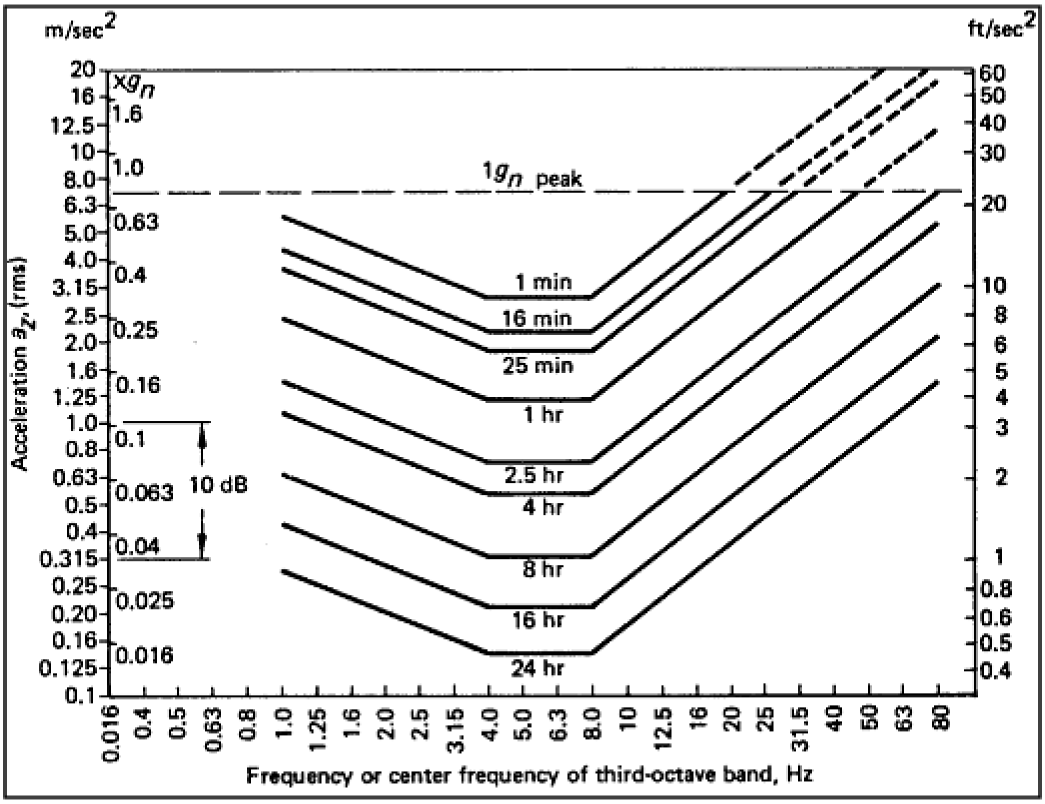

Figure 12: Human exposure to vibration values as described in BS6472-1:2008.

Deisadze, L, proposed in his work at the Worcester Polytechnic Institute that scale model testing of vibration could be conducted to evaluate potential structural transmission paths and determine the effectiveness of isolator mounts (Deisadze, 2013). Deisadze's work focused on amplitude and resonances in the time domain only and did not undertake any natural frequency analysis for tested structures. Due to complex transfer functions and natural frequencies of building elements this kind of behaviour is incredibly difficult to predict and the results gained from any scale modelling may only be uniquely beneficial to that specific model. If vibration transmission throughout a structure is anticipated or suspected to be a problem specific testing and monitoring should be conducted on the structure in question. This way natural frequencies of structural elements can be determined, pre-empted and treated before an installation is commissioned.

When assessing a potential wind turbine site in an urban setting certain limits or conditions may be required in order for activities within the building to not be hindered. It may then be beneficial to evaluate vibration levels over a series of wind speeds in order to assess an acceptable wind speed range of operation for the wind turbine.

BS ISO 5348:1998 (Mechanical vibration and shock. Mechanical mounting of accelerometers) suggests appropriate mounts for transducers[5], which should allow complete sympathetic motion of the transducer relative to the vibrating surface, without change or distortion. The natural frequency of the mounting should not be close to the measured vibration frequency, therefore a simple, rigid mounting of relatively small mass relative to the surface being measured should be chosen. Transducers must

[5] Suggested mounting types and the benefits thereof are displayed in 0.

not negate the structural contact or resonance to negatively affect the results. Measurements should, if possible, be taken on the floor of the room as this would typically be the main entry point into the body. If this is not possible allowances must be made and reported for the transfer function between these two surfaces.

Wind speed measurements are typically averaged over a given time period. These time periods may include periods of wind gusts, which become diluted into a lower, average speed. If a VDV measurement were to be taken over the same time period in an attempt to correlate the two any peak vibration associated with the gust will skew the result not giving an accurate representation of the vibration levels associated with that average wind speed. This would not accurately allow for acceptable working ranges of wind speeds to be determined and other methods would be required for this level of analysis to take place.

2.4 Topography

The installation of small and medium-size wind turbines on the rooftops of high buildings has been often suggested by architects and project developers as a potential solution for achieving sustainable energy in building design. In such locations, however, because of the presence of buildings and other adjacent obstructions, wind is normally turbulent, unstable and weak, in terms of direction and speed. (Tabrizi, 2014).

Securing an optimum position for urban wind turbine placement is crucial to extract maximum amount of energy from the available wind. Wind flow within an urban area can be an extremely complex interaction of wind shears and vortices interacting with buildings of varying size, shape and orientation; a far cry from more orthodox, rural turbine sites. Not only can wind flow be slowed and redirected, but wind speed can increase due to tunnelling effects and be accelerated across rooftops. Surface roughness and its effect on wind shear becomes a major issue due to buildings and obstacles causing a lower average wind speed and a significant increase in complex turbulent flow, which can make wind speed and direction hard to estimate. This is particularly hard to estimate or extrapolate to the heights of high-rise rooftops as there are currently few observations of the urban wind field at heights over rooftop level. Remote sensing instruments such as Doppler lidars could prove a useful tool in these scenarios as they are capable of providing wind speed data at many heights (Lane, 2013). However, this technology is still being tested and not readily available limiting any potential installation to site specific monitoring or extrapolation from wind speeds recorded at lower heights.

Various surface roughness coefficients for different locales, as taken from CIBSE (CIBSE, 2006) are presented in Table 8. These coefficients can be utilised in Equation 4 to extrapolate wind speeds at height above various surfaces and their use in the power law equation (Day 2007):

$$V = V_0 \left(\frac{H}{H_0}\right)^a$$

Equation 4: Displays the wind power law where: V = wind velocity (m/s^2), V_0 is the wind velocity as measured at a reference height (usually 10 m), H is the height (m), H_0 is the reference height (m), $\propto$ is the power factor (or Hellman exponent)for roughness.

It can be observed that a higher surface roughness suggests a lower wind speed at ground level and greater wind shear. This implies that to gain a greater energy yield in urban (rough) areas the higher up and further from obstacles the turbine can be located, the better.
The wind profile power law, stated in Equation 4, gives a good approximation of wind shear up to approximately 50 m in height and is frequently and reliably used in wind farm shear analysis where heights of 50 m are not usually exceeded. However, it may not be entirely appropriate in the urban environment, such as the Strata tower.

Roughness Class	**Roughness Length m**	**Landscape Type**
0	0.0002	Water Surface
0.5	0.0024	Completely open terrain with a smooth surface, e.g. concrete runways in airports, mowed grass, etc.
1	0.03	Open agricultural area without fences and hedgerows and very scattered buildings. Only softly rounded hills.
1.5	0.055	Agricultural land with some houses and 8 metre tall sheltering hedgerows with a distance of approx 1250 metres.
2	0.1	Agricultural land with some houses and 8 metre tall sheltering hedgerows with a distance of approx 500 metres.
2.5	0.2	Agricultural land with some houses and 8 metre tall sheltering hedgerows with a distance of approx 250 metres.
3	0.4	Villages, small towns, agricultural land with many or tall sheltering hedgerows, forests and very rough and uneven terrain.
3.5	0.8	Larger cities with tall buildings.
4	1.6	Very large cities with tall buildings and skyscrapers

Table 8: Surface roughness coefficients, as described in CIBSE 2006, to utilised as part of the wind power law (Equation 4) as the value of: $\propto$, the power factor (or Hellman exponent)for roughness.

Employing a constant Hellman exponent of approximately 0.143 is common in rural environments, such as agricultural land, but will under-estimate surface roughness due to obstacles on the ground displacing wind flow in more built up environments. In any environment with trees, buildings or any other obstructing structure that could impede wind flow a log wind profile law is better utilised with a higher roughness class. The boundary layer wind profile in nature generally appears to be logarithmic (D. Bruce Turner, 1994), therefore Equation 5 better describes the wind profile within the lower portions of the planetary boundary layer (up to approximately 100 m) (Sunderland, 2013). The LSBU tower would fall within the 50 m limit of Equation 4, at a 49 m height, but as the Strata tower turbines are at 135 m and both sites are within a heavily built up area, the log wind profile law may be more applicable. A comparison of results derived from both equations is shown in Table 9.

$$V = V_{ref} \cdot \left(\frac{ln\left(\frac{z}{z_0}\right)}{ln\left(\frac{z_{ref}}{z_0}\right)} \right)$$

Equation 5: Displays the log wind profile law where: V = wind speed at height Z, Z =height above ground level for wind speed V, V_{ref} = known wind speed at height Z_{ref}, Z_{ref} = reference height of known V_{ref}, Z_0 = roughness length (refer to Table 8).

Height [m]	**Wind Speed [m/s]**	
	Log profile law	**Wind power law**
200	13.2	7.7
190	13.0	7.6
180	12.9	7.6
170	12.7	7.5
160	12.6	7.4
150	12.4	7.4
140	12.2	7.3
130	12.0	7.2
120	11.8	7.1
110	11.5	7.0
100	11.3	6.9
90	11.0	6.8
80	10.7	6.7
70	10.3	6.6
60	9.9	6.5
50	9.4	6.3
40	8.8	6.1
30	8.0	5.9
20	6.9	5.5
10	5.0	5.0

Table 9: Displays a comparison of results obtained from the wind power and log profile law equations.

Being able to pre-empt the urban topographies effect on wind flow would be an invaluable tool into assessing UWT placement and potential.

CFD modelling could provide a valuable tool to wind flow assessment. CFD being more flexible than wind tunnels models, particularly in evaluation of the effect of multiple objects and buildings within the urban environment.

A number of institutions have researched UWT placement in Europe, USA and Asia, notably Eindhoven, Loughborough, Reading, Nottingham, Durham, Bath, Illinois and Malaya universities testing SWT placement and the effect of buildings on wind flow. Research has also been conducted to validate the CFD methodology and output by running simulations of wind tunnel experiments conducted by Brown *et al* who measured flow and turbulence around a 2-D array of buildings in a wind tunnel in California, 2000 . Despite some modest over predictions in the region close to the roof, the general trends of CFD results match those of the experiments (Ledo, 2011).

Significant research was based on CFD modelling of wind flow around a single building or simple grid systems, due to processing limitations. This research was successful in understanding wind flow around roof-tops and assessing various roof top configurations to catalogue general 'rules of thumb' to be applied to UWTs. It was found that a wind stream would pass across a roof top at un upward angle of 30-40 degrees from the leading edge over the building leaving a turbulent flow beneath. Therefore, any UWT mast must be above this height where wind speeds could be accelerated to 20-40% higher speeds than those leading up to the building. (Lack, 2010, Lassig, 2016). This height approximates half the roof top width (Ragheb, 2014).

The annual mean wind speed at this location should be at least 5.5 m/s, the mast or rooftop should be approximately 50% taller than other local obstacles/buildings, the turbine should be positioned on the side of the most prevalent wind direction, the lowest position of the rotor has to be above the roof by at least 30% of the building height (Case, 2007 and Müller, 2009).

Due to the required, ideal, height above other local obstacles, it is clear that high-rise buildings have the largest potential for sitting a successful UWT when compared to low-rise buildings (Bahaj, 2007).

These 'rules of thumb' give a useful insight to potential developers considering a UWT installation but these studies were based on single building in isolation. In order to more effectively be able to calculate the energy yield of a UWT it is necessary to know the acceleration of the free stream wind leading up to the building. Mertens acknowledges that it would be laborious to generate such information but nevertheless, important for accurate predictions of the energy yields of BAWT's (Mertens, 2006). CFD modelling has been utilised to assess how building shape influences wind flow towards a UWT.

Different, typical, roof profiles i.e. pitched, pyramidal and flat roofs were simulated in a university of Hong Kong where it was found that turbines mounted on flat roofs are likely to yield higher and more consistent power for the same turbine hub elevation than the other roof profiles (Ledo, 2011).

Further research conducted by the Centre for Energy, Environment and Technology found that curved shapes offer the most potential when it comes to wind energy exploitation. It was shown, via CFD modelling that spherical roof shapes reduce turbulence intensity in all cases while curved edges between wall and roof types increased acceleration. Curved shapes, specifically vaulted and spherical shapes were found to offer the best performance all round in lead-up wind speed, accelerating wind across turbine blades and reducing turbulent flow Francisco, T (2015).

It is also noted that CFD modelling is often utilised post-structural completion in order to verify any installation errors (Ciang, 2008). This would be a far more useful tool if employed pre-build to inform the structural design for optimum energy yield.

A BAWT experiences the acceleration of the free stream wind speed by the building and is therefore aerodynamically integrated with the building. The area around a building with an appreciable acceleration of the free stream wind speed is a fraction of the building area that causes the acceleration. Hence, the rotor area of the BAWT should be small compared to that area in order to profit from the acceleration. Wind turbines with a large rotor compared to the characteristic building size do not solely perform in the accelerated wind close to the building. The power augmentation for those wind turbines can therefore not be found with the cube of the acceleration (Mertens, 2006).

This information could contribute towards orientating a BAWT but it would be more useful to design a structure capable of focusing the wind flow towards a turbine and that the use of a turbine shroud or venturi could accelerate wind speeds across turbine blades, guiding it at an optimum flow angle(Chong, 2012).

It is clear that CFD modelling has become accurate, reliable and a useful tool in assessing the urban topography but due to computational limitations its employment has been limited to general rules of thumb for locating UW and BAWTs (Denoon et al, 2008). For BIWTs like the Strata tower it is important to model the surrounding area and architecture of the turbine housing to fully assess the unique effects of the local topography on the leading free wind stream and wind flow across the turbine blades. It is also important to be able to uniquely model bespoke installations as UWTs may not always be visually appropriate and even contested by local residents therefore requiring architects and designers into integrating wind turbine technology into the architecture like the Strata tower.

BIWTs not only give architects the opportunity to express their concerns about climate change via environmentally friendly designs but also give scope to design a building envelope capable of accelerating and focusing the available wind resource. However, in order to ensure the success and feasibility of such designs, a complete assessment of wind flow characteristics on the proposed site should be undertaken. CFD simulation has the potential to compare designs accurately and effectively as long as the computational power is available.

2.5 Energy Yield

In assessing the economics of wind power it is crucial to monitor a turbine's energy production. Once the local wind resource has been determined the available power in the wind can be calculated using Equation 6.

$$P_0 = \frac{1}{2}\rho A V^3$$

Equation 6: An equation to calculate power in the wind where: P_0 = available power in the wind (*W*), ρ = Air density (kg/m^3), *A* = Swept area of turbine blades (m^2), V^3 = Wind speed cubed (m/s).

A turbines ability to convert this available power to electrical power is capped by what is known as the 'Betz limit'. In 1926 Albert Betz proved mathematically that a wind turbine could not extract more than 16/27 of the available wind energy from the air due to wind speed reduction at the rotor hub. Assuming the average wind speed (V_{Av}) through the rotor is the average of the undisturbed wind speed before the turbine (V_1) and the wind speed after the turbine (V_2) we find that:

$$V_{Av} = \frac{V_1 + V_2}{2}$$

Equation 7: To calculate average wind speed (V_{Av})

And mass (*m*) of the air passing through the rotor during 1 second is:

$$m = \rho A V_{Av}$$

Equation 8: A mass flow rate fluids flow equation where ρ = air density, A = swept area.

Power extracted from the wind by the rotor equals mass times drop in wind speed squared.

$$P = \frac{1}{2}\, m\, ({V_1}^2 - {V_2}^2)$$

Equation 9: Kinetic energy equation

Combining Equation 8 and Equation 9 we get Equation 10:

$$P = \left(\frac{\rho}{4}\right)({V_1}^2 - {V_2}^2)({V_1}^2 + {V_2}^2)\, A$$

Equation 10: Combining Equation 8 and Equation 9.

When compared to the undisturbed potential power available in the air, calculated using Equation 6, we find the ratio between the power extracted and power available in Equation 11.

$$\frac{P}{P_0} = \frac{1}{2}\left(1 - \left(\frac{V_2}{V_1}\right)^2\right)\left(1 + \left(\frac{V_2}{V_1}\right)^2\right)$$

Equation 11: To calculate the ratio of power extracted to power available in the wind.

When P/P_0 is plotted as a function of V_2/V_1 we see that it reaches its maximum at V_2/V_1 = 1/3 with a value of 0.59 (16/27), see Figure 13.

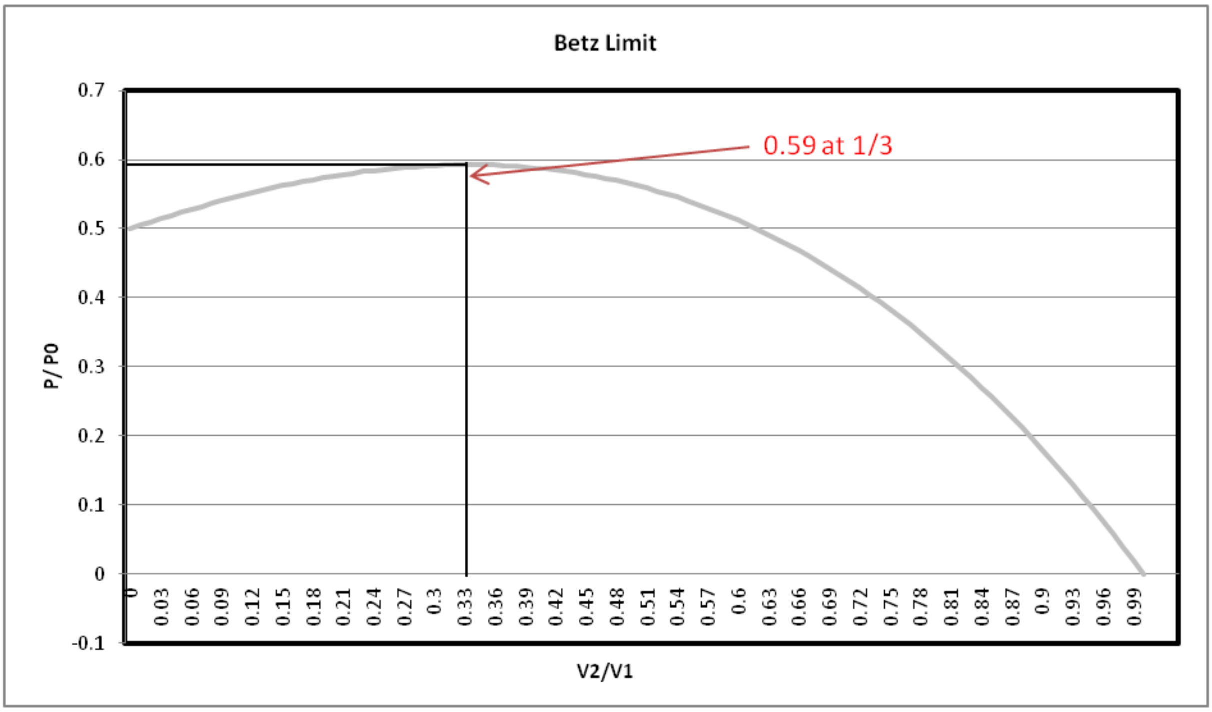

Figure 13: Displays the Betz limit graph demonstrating that a theoretical maximum of 59 % potential energy can be captured from the wind.

Therefore it would be expected that a maximum of 59% of the available energy in the wind could be extracted.

Various performance parameters can help toward assessing turbine efficiency in relation to its location as listed below:

- Coefficient of Power: Ratio of power extracted from the wind by a turbine (59% limit as discussed above).
- Capacity factor: Ratio of net energy production to turbines power rating times the monitored time interval.
- Plant availability factor: Ratio of time the turbines are producing energy during the monitored time span.
- Specific energy output: Turbines energy production output per unit of rotor swept area, given in kilowatt-hours over the monitored time span.

Alongside quantifying the possible physical power extraction from the wind via a turbine it is useful to be able to predict the wind power generating potential of a proposed turbine site in relation to measured wind speeds. An insight into the specific wind regime applicable to the proposed UWT site is crucial as wind speed in the built environment is only a fraction of the wind speed in rural areas. This would necessitate turbines being installed in higher locations to reach the higher, uninterrupted wind speeds. Placing wind turbines on roofs of high rise buildings would increase the wind energy potential yield by 20 - 40%.

Ideally monitoring of this wind regime would require a full year's worth of local anemometry data collected at the proposed hub height. However caution should be had over wind speed measurement devices as research conducted by the University of Natural Resources and Life Sciences in Vienna concluded that differences in measurement results from commercially available anemometry products can vary by up to 60 % (Kirchweger, 2009). Where on site measurements are not possible or data is not available estimations can be made via computational models or statistical models utilising known averaged wind speeds.

Average known wind speeds can be extrapolated within the urban area via computer software like WASP. WASP is a program designed to calculate vertical and horizontal wind climate statistics. It contains different models to describe the wind flow over different areas and terrains. Observed Wind Climate (OWC) Wizard and the WAsP Climate Analyst software can then be employed to analyse time-series wind measurements to provide a statistical summary of the observed, site-specific wind climate (Ciang, 2008).. The software is developed and distributed by the Department of Wind Energy at the Technical University of Denmark.

Statistical prediction models could also be employed. Weibull and Rayleigh probability density functions have been proven suitable in estimating wind speed distribution curves and can be used to estimate the likely wind speed frequency distribution from these averaged results (Carta et al, 2008).

The Weibull method is calculated using two parameters, *k* (shape) and *c* (scale). The shape parameter is equal to the slope of the line in a probability plot and can affect the behaviour of the distribution. The scale parameter determines the width of the distribution curve, if the scale parameter is increased the curve will widen over a greater range of values lowering the peak and vice versa. These parameters can be calculated using the modified maximum likelihood method (MMLM), which has been proven most suitable to physical wind speed measurements (Parcel, 2007).

$$f(v) = \frac{k}{c}\left(\frac{v}{c}\right)^{k-1} exp\left[-\left(\frac{v}{c}\right)^{k}\right]$$

Equation 12: Weibull probability density function where f(v) = the probability of observing wind speed, v = wind speed, k = shape parameter, c = scale parameter

$$k = \left(\frac{\sum_{i=1}^{n} {v_i}^k ln(v_i)P(v_i)}{\sum_{i=1}^{n} {v_i}^k P(v_i)} - \frac{\sum_{i=1}^{n} ln(v_i)P(v_i)}{P(V \geq 0)}\right)^{-1}$$

Equation 13: Modified maximum likelihood method equation used to calculate Weibulls Shape parameter, K.

$$c = \left(\frac{1}{P(V \geq 0)} \sum_{i=1}^{n} {v_i}^k P(v_i)\right)^{1/k}$$

Equation 14: Modified maximum likelihood method equation used to calculate Weibulls scale parameter, C.

The Rayleigh distribution is a specific form of the Weibull method where *k* = 2. The Rayleigh method can be utilised with only mean wind speeds where as more detailed information such as wind speed frequency is required to calculate the *k* and *c* parameters for the Weibull method.

$$f(v) = \frac{\pi V}{2{V_m}^2}\, exp\left[-\frac{\pi}{2}\left(\frac{V}{V_m}\right)^2\right]$$

Equation 15: Rayleigh probability density function where f(v) = probability of observing wind speed, v = wind speed k = 2.

The Weibull method more accurately allows predictions based on varying standard deviation of wind speed frequency per wind speed bin. A Rayleigh shape factor of k = 2 assumes a consistent standard deviation of 52 %. This may be applicable in a more rural, uninterrupted wind flow environment where wind speed fluctuations are likely to more consistent. However, the Rayleigh method does not allow for a more turbulent, fluctuating wind regime that is likely to be found in the urban environment.

A literary search has been conducted on applicable research areas, topics and guidelines. It is time to forge an action plan of data collection and site monitoring method, which is presented in Chapter 3.

Chapter 3 Setup & Methodology

This chapter details the tools, methodology and chosen procedure used throughout the project to capture the required data in order to investigate the established project aims and objectives. Before we can continue, however, some project setbacks must first be addressed.

In August 2012 the Strata Tower turbines ceased turning due to a mechanical fault and have been stationary ever since[6], which has hindered operational noise and vibration data collection. There were also to be atmospheric sensors installed on the Strata rooftop but unfortunately no data logging hardware was ever installed. It has therefore not been possible to collect any site specific wind speed, direction, density or temperature figures.

Fortunately some background noise and vibration data was collected at the Strata turbines along with operational levels before they ceased to turn, so basic site analysis can be conducted with aim to assess the likelihood of residential disturbance from turbine generated noise as well as any negative impact on the surrounding area.

Site specific atmospheric data could have lent itself to a theoretical study using manufacturer power curves, but alas this is not possible either due to a lack of logging sensors. However, planning permission was granted for the author to install a hub-height anemometer and wind vane to log atmospheric data at the LSBU turbine site. This, with the aid of wind power profiles discussed in the previous chapter, can be extrapolated and employed to build a theoretical case study of the Strata's potential energy output along with potential noise and vibration levels based on measurements procured.

A full risk assessment including health and safety dossiers submitted to the LSBU management company are included as part of APPENDIX B and APPENDIX C.

With these technical setbacks in mind the following chapter will outline an action plan to complete the following project objectives for the Strata and LSBU turbine installations:

- Monitor and log local atmospheric data at LSBU.
- Monitor and log real-time energy generation at LSBU.
- Monitor and log background and operation turbine noise at both the Strata and LSBU rooftop, representative apartments, offices and other locations, as appropriate.
- Generate a noise map in both Strata and LSBU surrounding areas for community noise annoyance.
- Monitor vibration at both site's rooftop, representative apartments and other locations, as appropriate.
- Appropriate aerodynamic modelling of wind flow to analyse energy performance for validation purposes of both sites.
- Suggest any design and installation optimisation tips, if appropriate for both sites.

[6] At the time of writing (March 2015) the Strata turbines are still non-operational.

3.1 Wind resource modelling

It is essential to have site specific wind data before a wind turbine site can be appropriately chosen. Without physically measuring site specific data there are extensive wind mapping databases available for public use via the Department of Business, Enterprise and Regulatory Reform, European Wind Atlas and the CIBSE TRY data. This data can be used to estimate available power in the wind and therefore potential energy yield of a proposed site. However, these sources usually only list annual average wind speeds. This necessitates the employment of probability distribution techniques such as the Weibull or Rayleigh distribution methods[7] to gain an estimate of annual wind speed distribution. Another problem is that recorded data is often measured in rural areas or near airports, which although useful for rural wind farm assessment may not be reliable or appropriate for urban areas. The dense and complex urban topography leads to lower annual mean wind speeds and increased turbulent flow causing rapid changes in wind direction, which produces extra stresses on mechanisms and components lowering the life expectancy of a system. It is, therefore more desirable and accurate to accumulate site specific atmospheric data to fully understand the sites wind resource. Once an accurate wind resource is known a good estimate of energy yield can be produced to establish the effectiveness of each site, which will contribute towards determining the feasibility of urban turbines.

Fluid flow is a complex discipline and fully understanding the complex interaction of air particles within an urban environment would be beyond the scope of this investigation, but by utilising CFD tools and running computational simulations of the topography surrounding each site we can assess, with sufficient detail, air flow across urban topography. This simulation using atmospheric data collected from LSBU installed anemometry is used to study the urban topographies effect on the energy generation potential of each site. CFD simulations will also be utilised to investigate 'what if' scenarios to installation optimisation suggestions, if appropriate.

A 1 mile radius 3D model of the area surrounding LSBU and the Strata was built within Trimble SketchUp as displayed in Figure 14.

In an ideal world not bound by computational processing limits a CFD model would have been run on the full 1 mile radius model to give a clear bird's eye view of how wind sweeps across the south of London. Unfortunately, due to the computational power available the models had to be scaled down. Urbawind CFD software was chosen as is it regarded as a robust and fast urban environment modelling tool. As part of the redevelopment of Niigata in Japan The Architectural Institute of Japan (Tomiyanga, Y. 2008) ran varying case studies to compare Urbawind's results with measurements taken before, during and after development had been completed. These case studies varied from a baseline map and simple block construction all the way to the completed construction of a district within Niigata. The results demonstrated the typical error of computations to be at most between 5 - 8.5 %. It was therefore deemed suitable to conduct the wind flow requirements of this project.

---

[7] Discussed in chapter 2.5.

Figure 14: Displays a 1 mile radius of London topography centred on the Strata tower. This model was used in conjunction with Urbawind and CadnaA to assess wind flow and environmental noise propagation.

Due to the complexity and scale of calculations required to run a wind flow simulation Urbawind requires the following, minimum, computer specifications to compute a 300 m x 300 m area in under 2 hours: 2.4 Hz, Quad core, 8 GB RAM computer. A computer of similar spec was available but limited the range of simulations to discrete areas. Figure 15 and Figure 16 represent the 300 m^2 area used for both the Strata tower and the LSBU campus. The prevailing wind for London is from the south west so to evaluate the south westerly winds effect on the turbine sites both installations were placed in the north eastern quadrant to allow maximum flow up to the turbines in order to assess the existing topographies effect on wind flow.

Work conducted by Mick Sagrillo (American Wind Energy Association Newsletter, 2006) demonstrates that to sufficiently overcome ground drag and subsequent turbulence a turbines entire rotor should be mounted at least 30 feet (9.14 m) above anything within a 500 ft (152.4 m) radius. This criteria is sufficiently met as the tallest obstacle within a kilometre of the Strata stands at 85 m, 55 m lower than the Strata turbines hub height.

The 300 m^2 area restriction due to computational power available for Urbawind is therefore not likely to negatively affect modelling results due to the Strata's height, surrounding topographical heights and in line with work presented by the Wind Energy Association. Of course, future construction could invalidate the results.

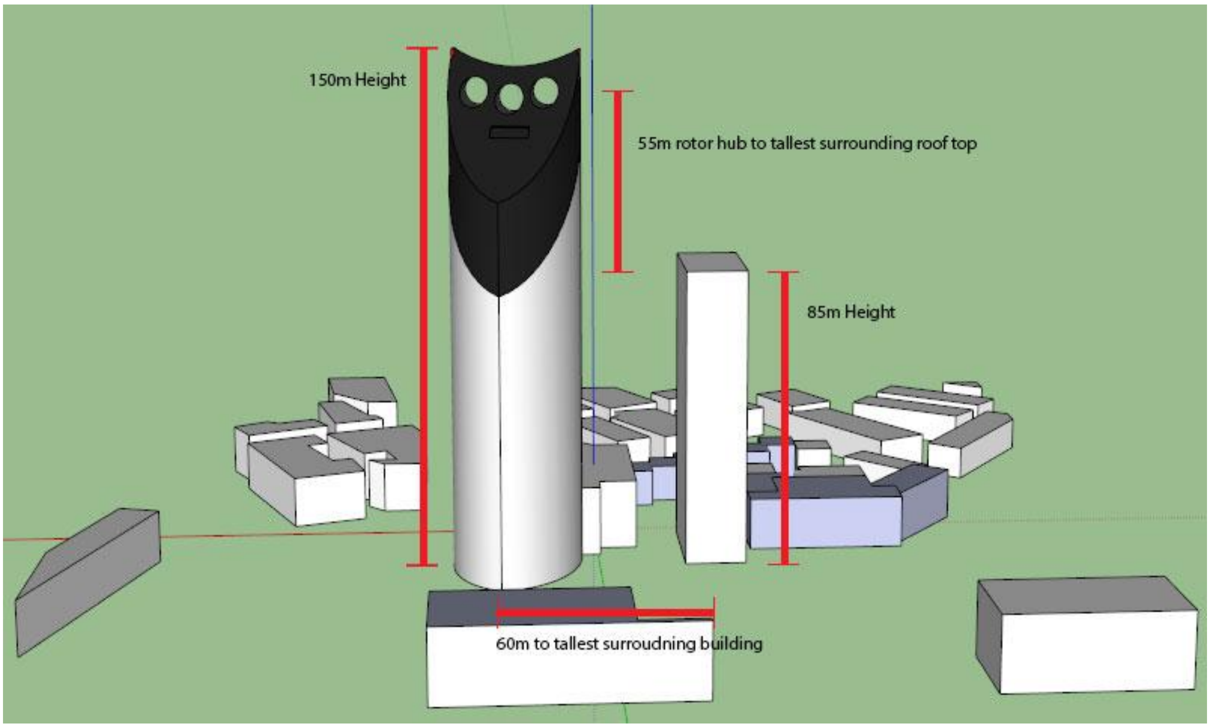

Figure 15: Displays a 300 m^2 model of the Strata tower area

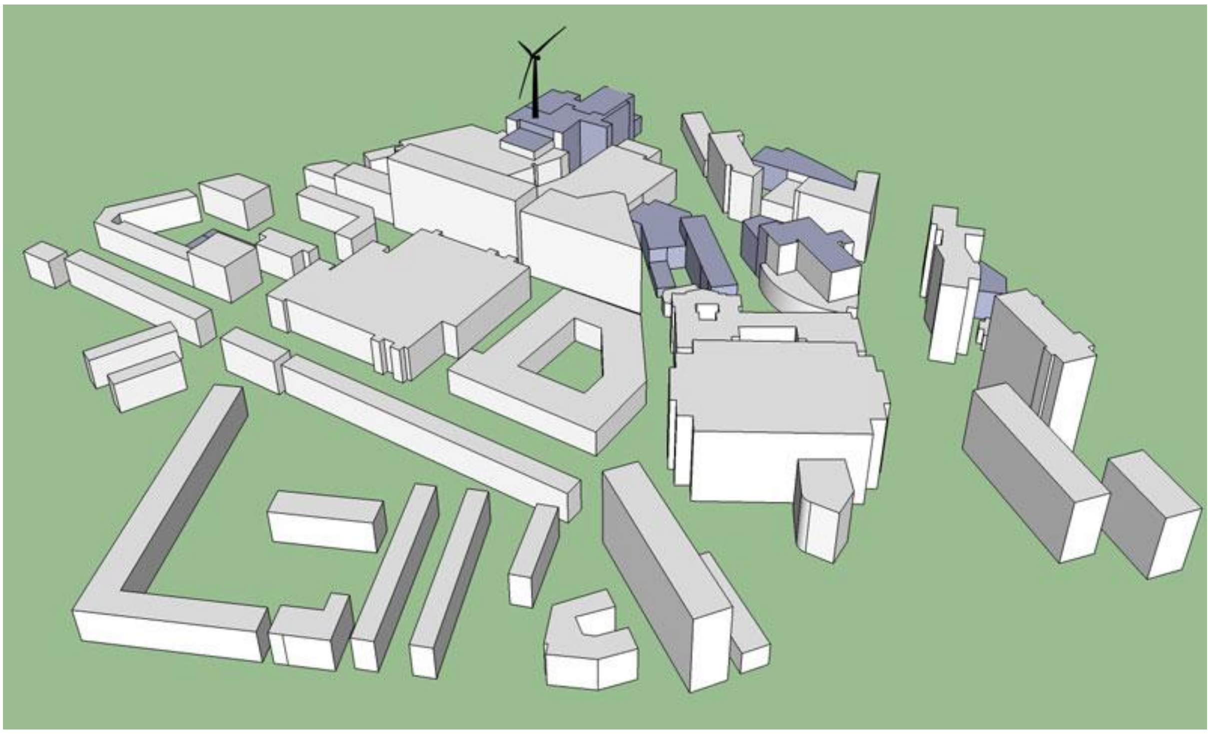

Figure 16: Displays a 300 m^2 model of the LSBU campus including the tower block turbine site

The maximum building height within the LSBU calculation area is 35 m. When compared to the building heights depicted in Figure 14, 97 % of building heights in the area are at or below this height. Showing LSBU's surrounding topography to be typical of the area further demonstrates that the smaller 300 m^2 calculation area centred on the LSBU turbine would be adequate.

Simulations run with Urbawind CFD software will be discussed in chapters 4.4 and 5.4 and used alongside atmospheric data to study the energy yield potential of both sites.

Figure 17: LSBU anemometer mounted on the CEREB rooftop.

As well as the previously mentioned defunct anemometry at the Strata site there are sensors installed at two locations within the LSBU campus. One ultrasonic anemometer and wind vane on the Centre for Efficient and Renewable Energy in Buildings (CEREB) building rooftop and one installed by the author next to the turbine at hub height on the LSBU tower block, Figure 18 shows the anemometers to be 100 m apart. The CEREB anemometer is installed upwind of the tower block anemometer in reference to a prevailing south westerly wind and mounted at 1.5 m on the rooftop next to a 1 m solid safety rail. CFD analysis shows the LSBU anemometer to be in a far clearer, less turbulent, strong wind resource from the south west.

Figure 19 and Figure 24 show the mean wind speed coefficients for the CEREB and LSBU anemometer location, respectively. They show an approximate 50 - 60 % increase in expected wind flow from the south west at the LSBU location. LSBU anemometry readings will more accurately reflect the local wind resource, as it is installed at hub-height to give a reliable insight into LSBU turbine's wind resource. This will aid energy production estimations, the juxtaposition of which against actual energy yield will highlight the manufacturer power curves applicability (or lack of) in the urban environment.

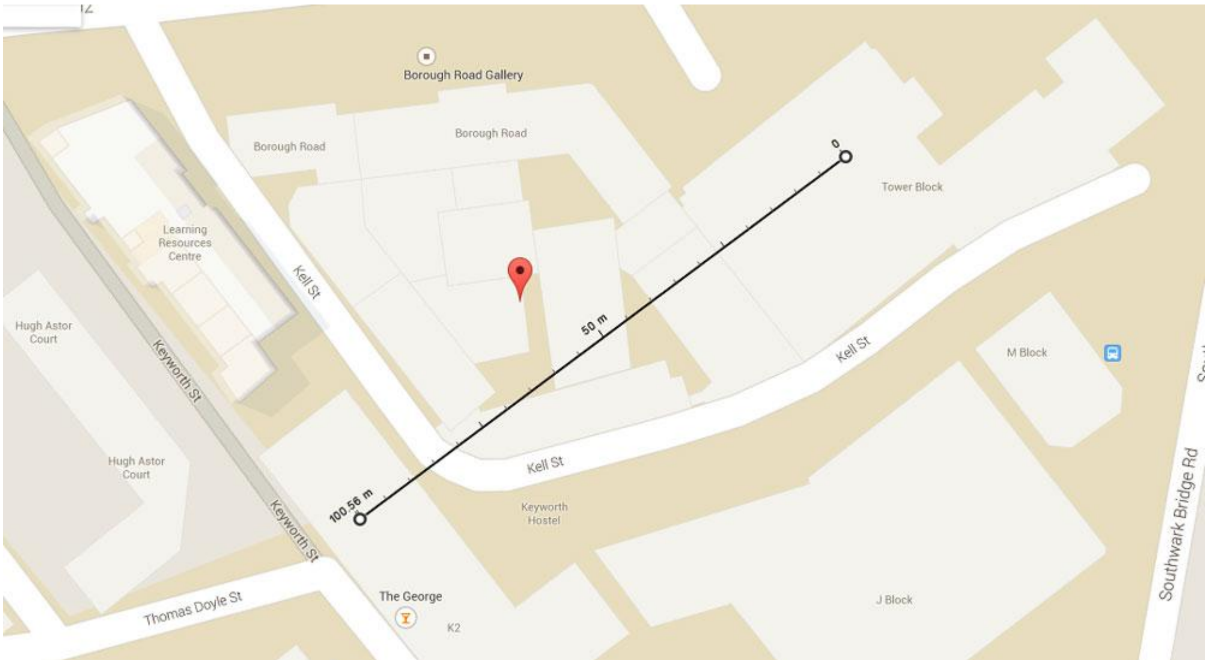

Figure 18: Displays the distance between the CEREB and tower block anemometers

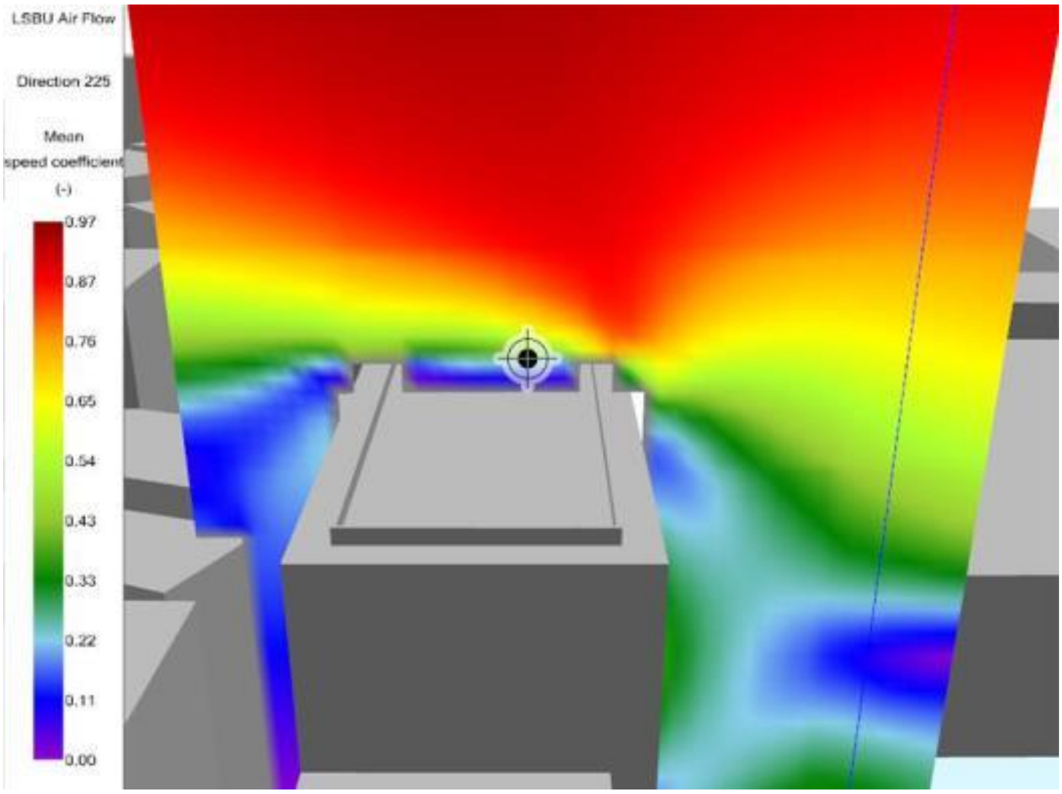

Figure 19: Displays the Urbawind simulated wind flow across the CEREB anemometer

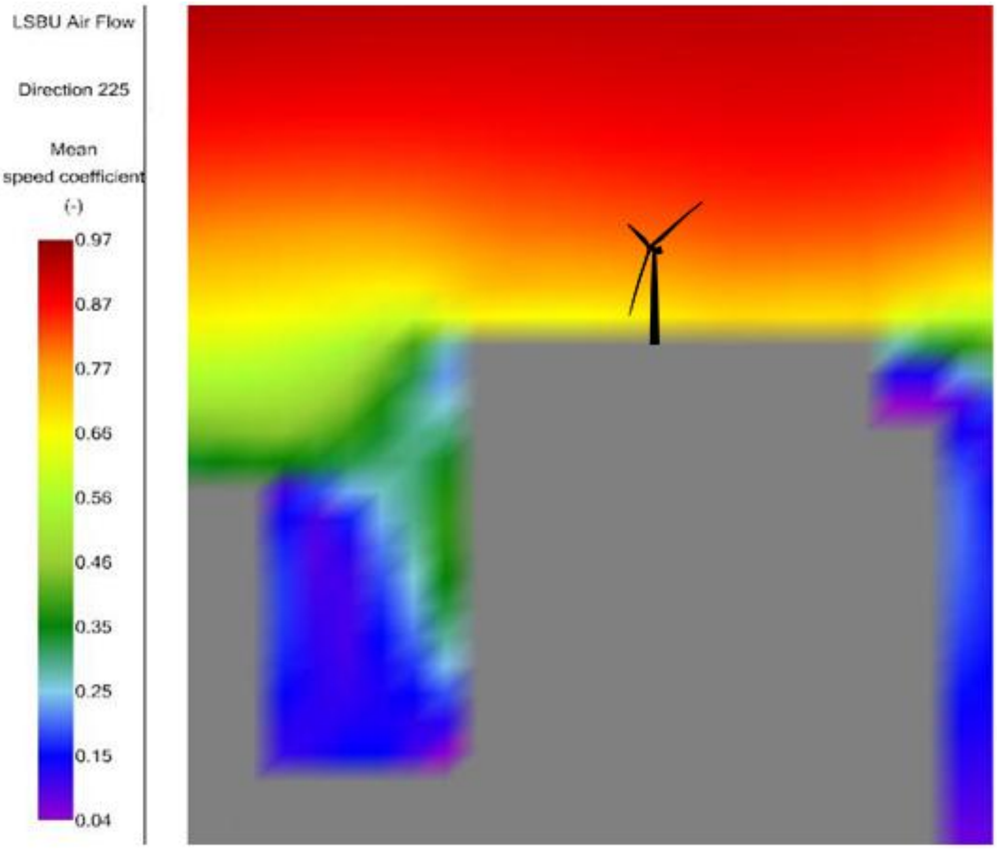

Figure 20: Displays the Urbawind simulated wind flow across the tower block anemometer at hub height

The following atmospheric data will be collected at both CEREB and Tower Block sites:

- Wind speed
- Wind direction
- Temperature
- Atmospheric pressure
- Humidity

Logging and analysing of this data will allow predictions of site potential energy yield and will be compared with theoretical predictions in an effort to further understand the intricacies of urban wind turbine installation and their dos and don'ts. The comparison will also contribute to verifying the chosen CFD analysis model.

Clearer, stronger wind resources can be obtained with increasing height above obstacles, therefore further CFD simulations at greater heights above the Tower Block will be investigated in later sections to demonstrate possible rewards and returns for alternative installations.

3.2 Energy performance of UWT

The previously discussed technological differences between the Strata and LSBU turbine installations shall be further analysed in the following section.

Manufacturer produced power curve and power coefficient data is shown in APPENDIX H & I for the Strata and LSBU installations, respectfully. This data is based on theoretical power available in the wind at constant wind speeds in idealised environments, but due to the complex urban topography it is likely that wind flow will not be as reliable, constant or strong as in a wind tunnel or more rural, open areas. With knowledge of the local wind resource more accurate estimate of potential wind energy production can be calculated.

10 minute interval atmospheric data from the CEREB and Tower Block anemometers was collected and analysed. Data in time series format will include the following:

- Date
- Time
- Measured averaged wind speed (m/s)
- Wind direction
- Humidity
- Barometric Pressure
- Temperature

This data was synchronised with data logged at the LSBU turbine's Windy boy inverter.

When high resolution atmospheric data is not known for energy predictions, Weibull and Rayleigh probability density functions are employed to predict wind speed distribution curves using known average monthly wind speeds. These functions along with the relevant modified maximum likelihood method (MMLM) to calculate the Weibull shape and scale parameters have historically been documented to best represent wind flow characteristics. Previous research and validation work includes research conducted at the University of Bristol's Department of Aerospace (Seguro, Lambert, 2000) and case study analysis conducted in the Canary Islands by the University of Las Palmas's Department of Mechanical Engineering (Carta, Ramiez, Velazquez, 2008).

To test the validity of such methods within the urban environment, LSBU site logged data is formatted into a monthly frequency distribution table and compared with Weibull and Rayleigh probability predicted distribution curves. The power output time series data is then arranged into wind speed bins to calculate the average power per wind speed bin (P_t). The turbine coefficient (C_p) at each wind seed bin is then calculated as a ratio of average power (P_t) to available power (P_0) as shown in Equation 16:

$$C_P = \frac{P_T}{P_0}$$

Equation 16: To calculate the turbines coefficient (C_p), the ratio of P_t to $P_{o.}$

APPENDIX K displays the manufacturer power curve rating and coefficients for both sites. The results are compared with manufacturer predicted data and LSBU site recorded anemometry data. A total of two years worth of data will be assessed thus enabling a site specific power curve and *Cp* data for the installation to be generated. This shall aid the prediction of effectiveness of future turbine designs in similar, urban environments.

Carbon dioxide emission reductions are evaluated assuming a CO_2 factor of 0.568 $kgCO_2/kWh$ as stated in the Building Regulations Approved Document L2A (2006). Insights gained from this portion of study will be the effectiveness of an urban turbine site alongside the applicability of orthodoxy rurally applied prediction models to the urban environment.

3.3 Urban turbine noise

Specific wind noise measurement guidelines discussed in chapter 2.2 will be adhered to as much as possible but due to the unique characteristics of each site certain allowances must be made. The Strata turbines are within a 140 m building in London and it's situ raises some queries. Are we to use this height as the approximate hub height of the turbine or are we to assume the turbine mounting as a base line and take the distance from this to the nacelle as hub height? If Equation 2 is employed in accordance with EN 61400 – 11:2003 and ETSU-R-97 then measurements could either be taken at a 145 m distance from the turbines at ground level or at a 11.25 m distance from the turbines, 140 m above the city. The former is possible, but puts us directly into a heavily built up environment, far from the turbines. Background noise surveys were therefore conducted at the 145 m distance at ground level to obtain a background noise baseline within the area and assess the likelihood for complaint from local residents. These results are compared to measurements taken directly within the turbine venturi to determine if any turbine induced noise would propagate into the surrounding area with enough intensity to cause disturbance.

Due to project circumstance this means that these venturi measurements will (technically) have to be taken within the turbines near-field, where sound pressure and particle velocity are not in phase and within close proximity to the reflecting surfaces of the venturi.

The LSBU site at 49 m above the city on a university rooftop is a more feasible environment as there is a flat surface surrounding the turbine to place measurement apparatus.

How the investigation was conducted for the Strata and LSBU sites is now discussed. Noise monitoring for both sites is divided into noise propagating into the local area and noise propagating into the building. Environmental noise mapping software will be used to determine any anticipated level of annoyance within the local area, in particular at night and the predicted levels will be compared to those measured. Noise levels in the most susceptible positions within the areas to be measured will include the worst case conditions to determine the turbines affect upon any occupants or residential neighbours.

3.3.1 Strata noise measurement setup

To establish a background base line night time measurements have been taken in the surrounding area of the Strata tower. Figure 22 shows the measurement positions taken around a 145 m radius of the Strata building.

The purpose of this monitoring is to establish night time background noise levels in the area at the quietest times of day to determine any threat of disturbance, in particular of sleep. A week long background noise survey was taken around the Strata tower to determine the quietest times of the week and from this survey it was concluded that between 3:30 am - 4:30 am was the ideal time to take measurements as can be seen in Figure 23.

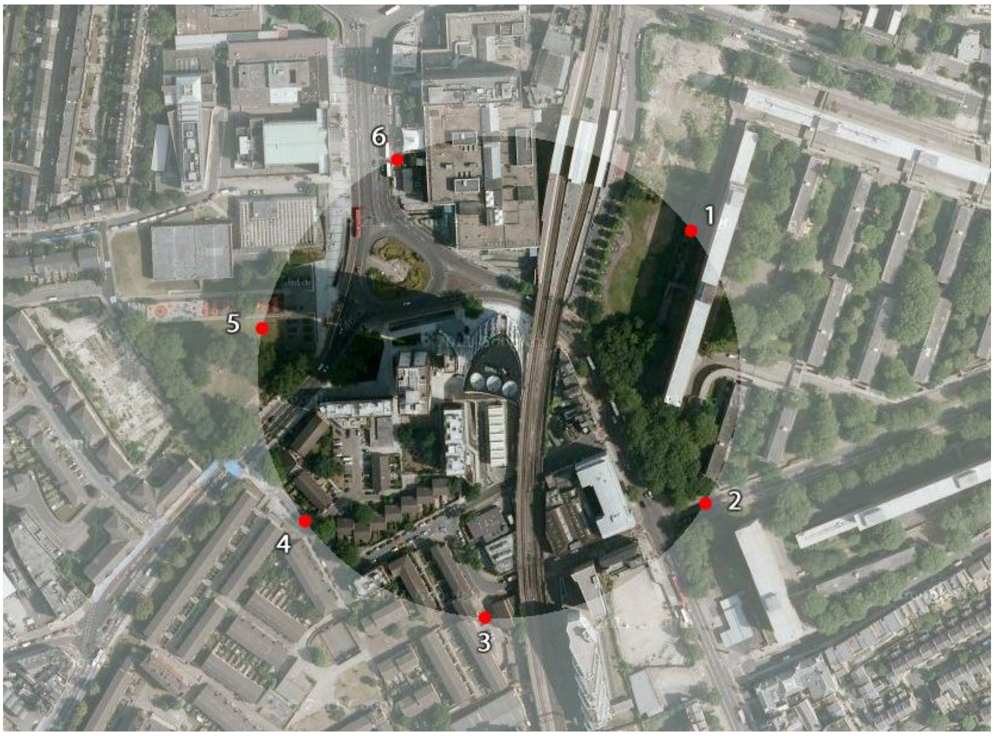

Figure 21: Presents the 145 m radius environmental noise measurement positions around the Strata tower.

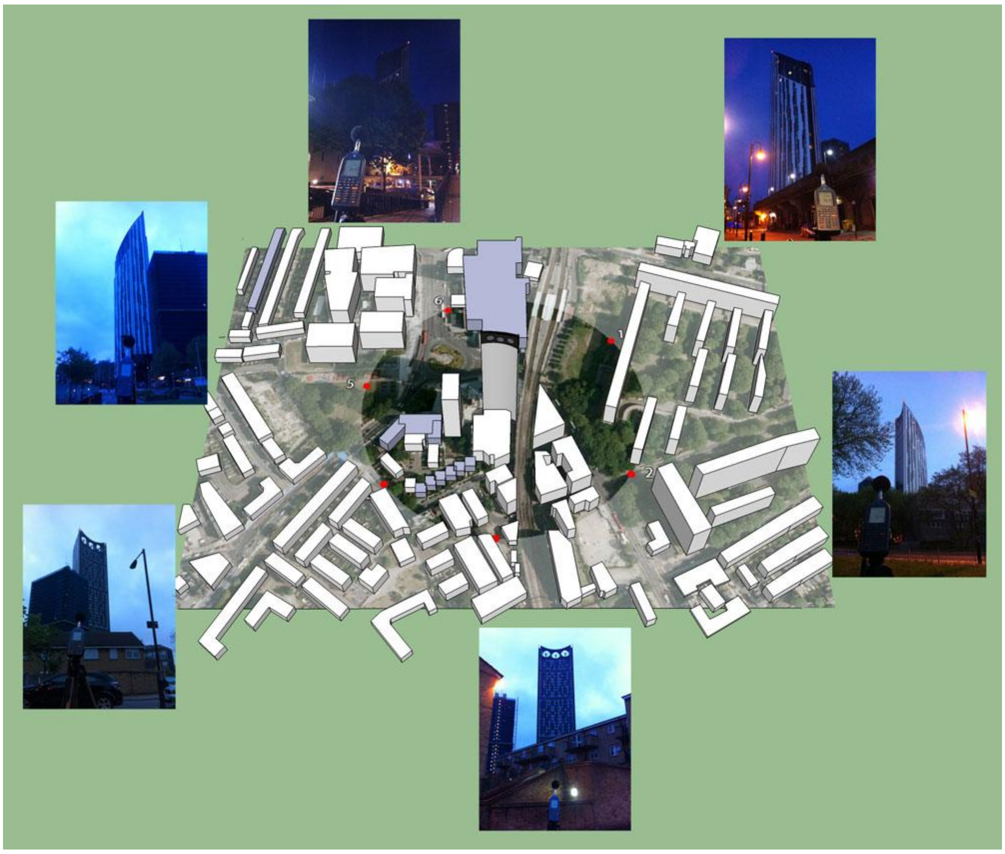

Figure 22: Presents the 145 m radius environmental noise measurement positions around the Strata tower.

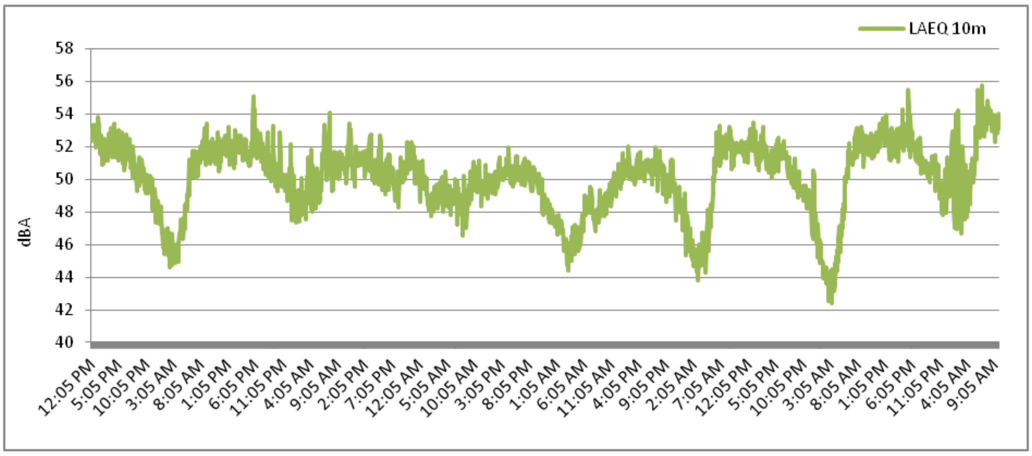

Figure 23: Depicts the background noise levels recorded at the Strata tower turbine positions. These week long, 10 min L_{Aeq} measurements were used to determine the quietest times of day in the local area to conduct an environmental survey in order to assess potential residential sleep disturbance due to turbine noise.

The survey was conducted between 03/05/13 - 30/05/ 2013. Measurements were taken at 6 positions around the Strata 145 m radius, derived from Equation 2 to coincide with standard directives in: EN 61400:2003 and ETSU-R-97. $L_{Aeq,\ 10min}$ measurements were taken with a Norsonic140 and Svantek SV958 class 1 sound level meter under the guidelines set out in BS 7445-1:2003 i.e.

- At least 3.5 m from reflecting surfaces (walls, buildings, structures etc)
- At least 1.2 - 1.5 m from the ground.

The Norsonic 140 was calibrated to 114 dB at 1 kHz and the Svantek to 94 dB at 1 kHz prior to measurements being taken. A colleague was employed to operate a fixed, control sound level meter (SV958) at position 5 marked on Figure 22. This was used to monitor and control any strong deviations from measurements and ensure continuity. The plan was for the Norsonic 140 to act as a floating meter between the other five positions marked on Figure 22 and to take 10 minute L_{Aeq} readings from each. The results are discussed in chapter 4.2.1.

Background noise levels were also taken within the turbine venturi. The aim was to establish the background noise levels at the turbine against wind speed and direction. These results are then compared to measurements taken whilst the turbine is operational to establish the likelihood of complaint for the building residents. Using the Svantek SV958 in this case allowed for 3 channel (X, Y and Z) vibration measurements to be taken simultaneously, see Figure 24. Vibration procedure and data will be discussed in chapter 3.4.1.

Figure 24: Svantek SV 958 at Strata turbine mount to record simultaneous noise and vibration levels.

The turbine venturi is located directly above a maintenance level with access via three hatches leading into each turbine enclosure as shown in Figure 25.

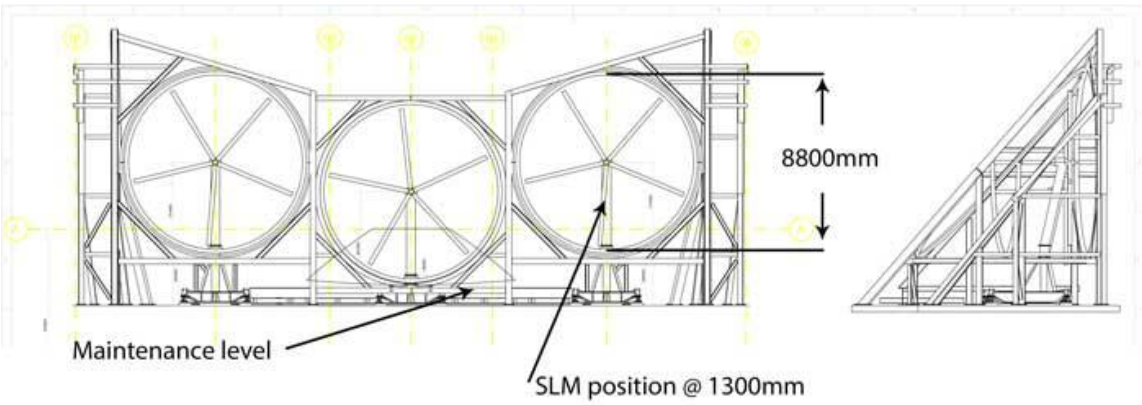

Figure 25: Depicts microphone placement in the Strata turbine venturi.

After calibration the SV958 was installed at the turbine base with its environmental extension kit and wind shield trailed out of the turbine access hatch and securely cable tied to the access ladder to the nacelle. This placement is not ideal, it is close to the tower, which could shadow turbine and wind induced noise, but this is the only place the microphone could be safely secured, see Figures 26 and 27.

Figure 26: Depicts the SV958 environmental microphone placement at the West Strata tower turbine

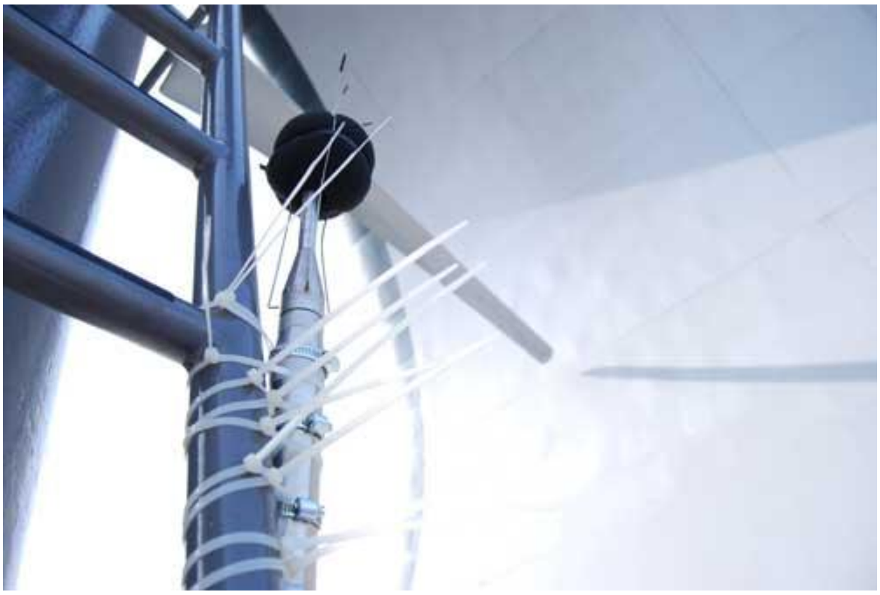

Figure 27: Depicts the SV958 environmental microphone placement at the West Strata tower turbine

Effort was made to secure the microphone close to centre of the venturi and therefore furthest from the surrounding reflective surfaces without being completely shadowed by the tower at a 1.2 m height. The microphone placement from reflected surfaces within the circular enclosure is listed in Figure 28.

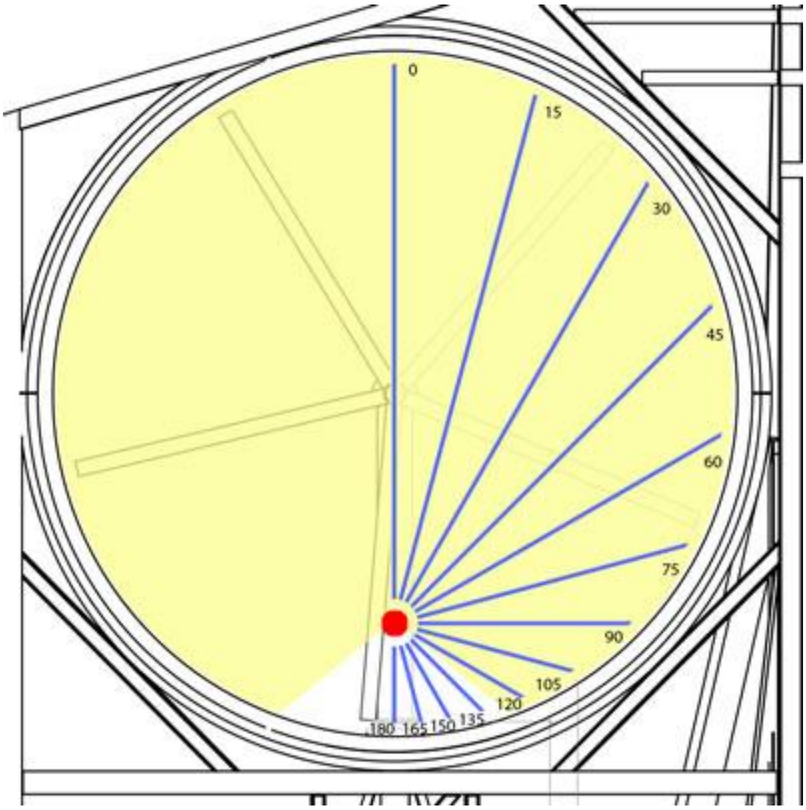

Figure 28: Depicts the Strata tower microphone placement within the west turbine venturi with distances from the nearest reflective facades labelled.

Angle (DEG)	**Distance** (M)
0	7.60
15	7.54
30	7.35
45	7.04
60	6.61
75	6.07
90	5.44
105	4.72
120	3.94
135	3.11
150	2.28
165	1.55
180	1.20

Areas marked in yellow in Figure 28 meet the BS7445: 2003 stipulated 3.5 m distance and at no point does it infringe upon the 1.2 m minimum distance from the ground. The floor of the venturi is shown in Figure 29.

Figure 29: Depicts the Strata's west turbine venturi floor. Two things are apparent: 1) The view is spectacular! 2) There are neither safety rails nor potential anchor points for a more appropriate microphone placement.

Figure 29 not only presents an impressive view but highlights the issue of microphone placement and safety. Located 140 m above built up Elephant and Castle means that strict health and safety considerations must be considered and implemented and it is essential that no parts can fall from the venturi thus eliminating the possibility of a freestanding tripod. The only feasible solution was to secure the microphone in its environmental, weatherproof case to the access ladder behind the turbine mast as shown in Figure 27, however this does present a few points for consideration as the microphone is:

- Placed upwind.
- In a shadow zone of the tower from the blades and any northerly winds.
- Blades passing by the tower could produce a low freq thumping sound with every passing.
- Sound measurements may be taken within the near field of the turbine.
- Only one SLM location available.

The fourth point will now be briefly discussed: a sound field is a region or area in which sound waves are propagating and is made up of two acoustic properties: sound pressure (scalar) and particle velocity (vector). Sound pressure is in phase with particle velocity and propagates following the inverse square law only within the free field, an area of at least 2 wavelengths or at least twice the greatest dimension from the sound source (whichever is greater). The near field is the area before the free field where there is no basic relationship between distance and sound pressure, where sound pressure levels may vary in a non linear fashion as particle velocity and sound pressure are not in phase. In the extreme near field, air next to a sound (or vibrating) source will be incompressible and move in sympathy with the moving surface resulting in a dramatic reduction in sound pressure level.

Traditional sound pressure measurements are usually avoided within the near field for these reasons. In the strictest sense of the terminology the author's microphone is, unfortunately, placed within the near field of the Strata tower as it is 1 m away from the 8.5 m diameter rotating blades. However, as previously discussed in Section 2.3.1, the dominant noise source from turbines and the most common cause of complaint in noise annoyance surveys is the 'swishing' or 'whooshing', which is caused from trailing edge boundary layer turbulence emanating from the blade tips. At distance, the turbine as a whole would be viewed and evaluated as a point source but at this close proximity the blade tips are be viewed as independent, moving noise sources emitting higher, broadband noise. In this case the individual, small sources would always be at the distances discussed in Figure 28.

In order to validate this approach an experiment was conducted. Firstly, a powered fan was set up in an anechoic chamber and while rotating the sound pressure level was measured at various distances. The sound power was then derived from these measurements and compared to see if there were any variance in results due to the microphone position. The results are presented in Figure 30 and Table 10. The results presented in Figure 30 and Table 10 demonstrate that measurements taken directly in front of the powered fan (0.01 m distance) are generally in agreement with measurements taken at a 1 m distance although a variance of 6 - 10 dB is observed at lower (below 125 Hz) and higher (above 1.6 kHz) frequencies. These differences are likely due to noise emanating from the fan's motor, which unlike the blade tips would be in close proximity to the 0.01 m position microphone. In spite of this motor noise there is still generally an agreement within the more dominant frequencies.

As a wind turbine is a passive device, turning in sympathy with the wind it would not produce motor noise. Therefore a second experiment was conducted this time using a 1 m length of wire with a weight at one end. The wire was hand spun to emulate the trailing edge boundary layer turbulence that emanates from turbine blade tips and once again, measurements were taken at varying distances, this time without any interfering motor noise. The results are presented in Figure 31 and Table 10. This time the results are far more in agreement with a maximum difference of 4 dB measured at 200 Hz.

If the powered fan or spun wire systems are to be viewed as one whole noise source then measurements at the 0.01 m position were technically taken within their near field. Nevertheless, measurements taken at distance were in agreement with the derived sound power levels, suggesting that such a method would be acceptable to capture the dominant from trailing edge boundary layer turbulence noise source from turbines.

It is worth noting that finite element analysis of a moving turbine could be an appropriate method for assessing this near field problem. Unfortunately this is outside of the scope of this thesis.

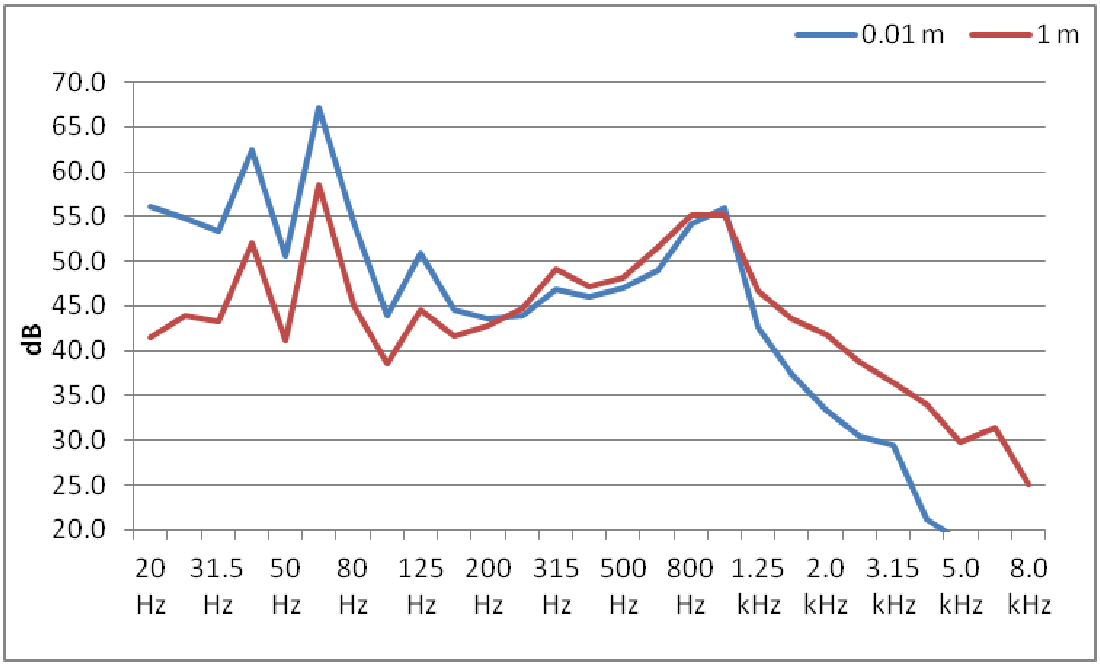

Figure 30:Third Octave Noise Measurements Taken From a Powered Fan in the Near and Far Fields

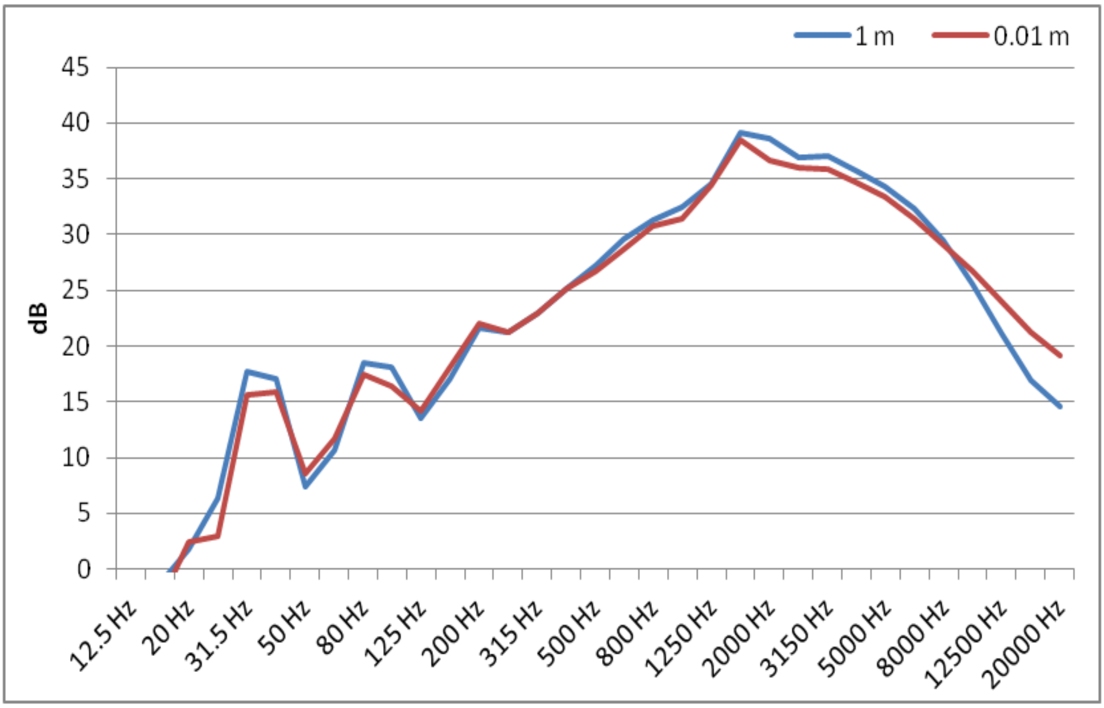

Figure 31: Third Octave Noise Measurements Taken From a Hand Spun Fan in the Near and Far Fields

	Lw dB			
	Powered Fan		Spun Fan	
	0.01 m	1 m	0.01 m	1 m
20 Hz	56	41	2	3
25 Hz	55	44	3	6
31.5 Hz	53	43	16	18
40 Hz	62	52	16	18
50 Hz	51	41	9	11
63 Hz	67	59	12	11
80 Hz	54	45	17	20
100 Hz	44	39	16	19
125 Hz	51	45	14	11
160 Hz	45	42	18	16
200 Hz	44	43	22	18
250 Hz	44	45	21	20
315 Hz	47	49	23	23
400 Hz	46	47	25	26
500 Hz	47	48	27	27
630 Hz	49	52	29	30
800 Hz	54	55	31	31
1.0 kHz	56	55	31	33
1.25 kHz	43	47	34	35
1.6 kHz	37	44	38	40
2.0 kHz	33	42	37	40
2.5 kHz	30	39	36	38
3.15 kHz	29	36	36	38
4.0 kHz	21	34	35	36
5.0 kHz	19	30	33	35
6.3 kHz	16	31	31	33
8.0 kHz	11	25	29	30

Table 10: Sound Power Levels (Lw) Derived From Near and Far Field Measurements

The possible shadow zone created by the tower is also disregarded as a major concern as this would only be an issue with northerly wind and the prevailing wind in London is from the south west.

Faced with no other measurement position options, measurements proceeded with the discussed configuration with special note to be made of any repetitive low frequency peaks in amplitude caused by blade-tower 'thumping'.

The Strata tower's turbines have a rated RPM of 100, this aligned with wind speed and noise data will help isolate any rhythmic amplitude peaks from the produced time domain signal using the Hz - RPM relationship shown in Equation 1.

3.3.2 LSBU noise measurement setup

Noise measurements were also conducted for the LSBU site, which, compared to the Strata site, was a fairly straight forward procedure. The same instrumentation for the Strata was used and background measurements were taken in the position displayed in Figure 32. The SV958 was placed on the turbine roof top at a 12.5 m distance in accordance with the minimum distance described in EN 61400 – 11:2003 and ETSU-R-97 using Equation 2.

Figure 32: Depicts the SV958 placement at the LSBU noise monitoring position, 12.5 m from the turbine tower.

A total of 1200 $L_{Aeq,\ 10\ min}$ measurements were taken between:

- 23/09/13 - 03/10/13 and
- 09/12/13 - 19/12/13

Operational turbine measurements were recorded at the same position in the same manner, procedure and parameters already discussed. Operational turbine measurements were conducted during the following periods:

- 30/09/2013 - 05/10/2013
- 22/10/2013 - 03/11/2013
- 20/12/2013 - 28/02/2014
- 03/03/2014 - 05/02/2015

Measurements are analysed both as a function of time and atmospheric conditions. Background and operational measurements have been assessed in relation to wind speed and direction to ascertain if any discernible difference in levels or frequency content can be noted and therefore the likely threat of annoyance, if any.

An environmental noise survey was conducted within the surrounding areas of the LSBU Tower Block. The intent is to establish a base line background noise level in the area and whether or not it correlates to atmospheric or turbine noise as a function of wind speed. In correlation to ETSU-R-97 this will also allow for an assessment of likelihood of noise from local residents. The LSBU Tower Block is located within a densely built up, urban area so it is possible that other urban factors such as road traffic, bars and social clubs may play a significant part in the local noise profile, see Figure 33. Within the immediate 1 km vicinity there are:

- 7 underground train stations
- 2 over-ground train stations
- Southwark fire station
- 2 hospitals, both with A&E departments
- Ministry of Sound nightclub

As well as numerous bars, cafes and restaurants, along with pedestrian and road traffic, these will all contribute to the typical background noise environment, which must be taken into consideration.

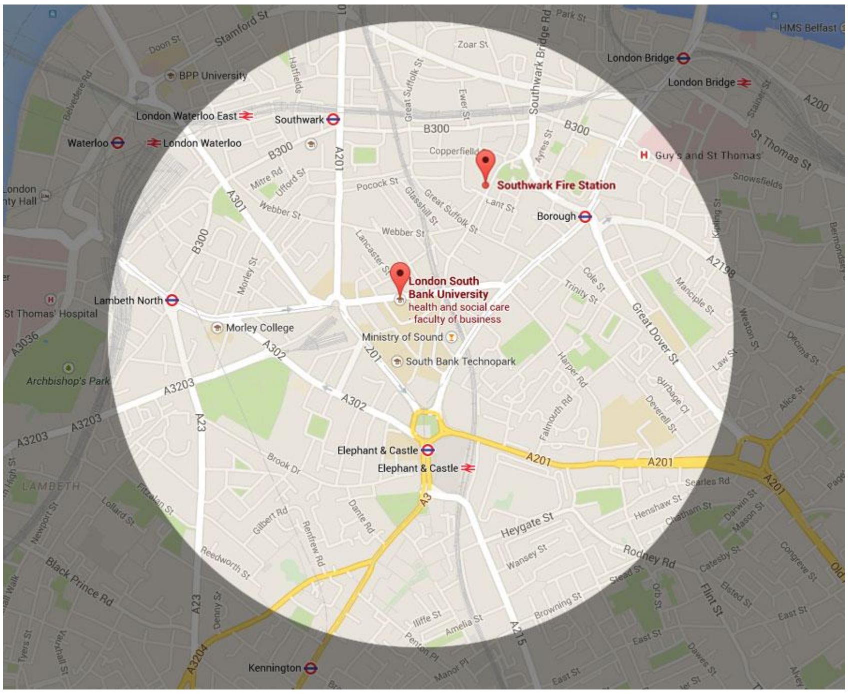

Figure 33: Highlights a 1 km radius of the LSBU Tower Block turbine, emphasising the built up and busy area surrounding it.

Measurement positions are depicted in Figure 34. They were chosen as they represent the closest residential buildings in proximity to the turbine. Position 'T' marks the turbine location and 'C' the control sound level meter. Positions 2 and C are at 42.5 m distances from the turbine hub to adhere to the directives laid out in EN 61400-11:2003 and ETSU-R-97. Positions 1 and 2 are next to the closest residential buildings to assess local likelihood of annoyance. With a local predominant wind from the south west and south east positions 1 and 2 are located downwind of the turbine representing higher risk locations for wind assisted noise propagation.

The survey was conducted over 10 nights between 15/12/14 and 4/1/15 between the hours of 2:00 AM and 5:30 AM. These dates were chosen to collect a 'worst case scenario' data set from the quietest time of day at the quietest time of year. A total of 231 qualifying[8] measurements at comparative positions were taken, New Year's Eve was excluded. Ten minute measurements were taken using two Norsonic 140 and one Svantek SV958 class 1 sound level meters adhering to guidelines set out in BS 7445-1:2003 and ETSU-R-97 i.e.

- At least 3.5 m from reflecting surfaces (walls, buildings, structures etc)
- At least 1.2 - 1.5 m from the ground.

The Norsonic 140s were calibrated to 114 dB and Svantek SV958 to 94 dB @ 1 kHz before measurements were taken.

Measurement parameters captured are:

- L_{Aeq} - to assess time averaged sound level profile.
- $^{1}/_{3}{}^{rd}$ Octave L_{Zeq} - to investigate any tonal or frequency dependent elements.
- L_{A10} - to assess the highest noise levels experienced within the time interval.
- L_{A90} - to assess the background noise level of each interval.

As A-weighting is tailored to the human ear's frequency response it is the appropriate weighting to use to investigating the likelihood of residential complaint. The appropriateness of A-weighting being a true representation human response to sound is in debate in some circles, however it is the accepted and enforced method used in national and international standards for noise annoyance, human comfort and health. Therefore in this assessment for urban turbines and their application in the built environment national criteria and guidance must be followed.

The Svantek SV958 was set up in the turbine location and triggered to record the 10 minute measurements in sync with the power predictor MKII anemometer, which was also set up to record in 10 minute interval readings.

The control Norsonic 140 was then setup at position C to record 10 minute measurements in sync with the SV958 while the remaining Norsonic 140 was used as a roaming sound level meter between positions one, two and three. 10 min measurements were taken in sync with the other instruments.

The three sound level meters were synchronised to ensure measurements were triggered to coincide with each other. The results will be discussed in Chapter 4.2.3.

[8] Qualifying measurements are defined by the author as complete 10 minute interval measurements not being interrupted by extraneous noise sources such as barking dogs, parked sirens, human interference etc.

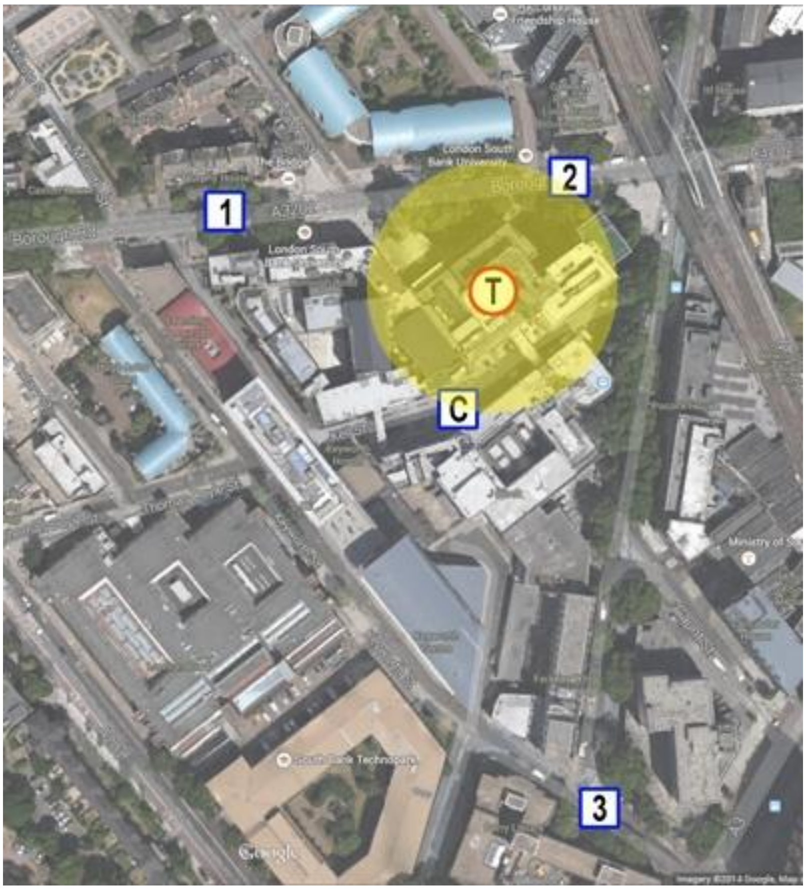

Figure 34: Displays the LSBU environmental noise measurements positions. C = Control position, T = turbine position. Readings were taken between 15/12/14 and 4/1/15.

3.4 Urban turbine vibration

The aim is to monitor vibration from the Strata and LSBU turbines both at the turbine mounting and occupied areas to establish the expected level of annoyance. A Svantek SV958 3 channel vibration meter and SV106 6 channel vibration meter were used to conduct all 5 minute, 1/3 octave band (1 – 20k Hz) X, Y & Z axis RMS acceleration, vibration dosage value (VDV) and PEAK measurements, see Figure 35. All instrumentation was calibrated at 80 Hz for a 30 g accelerometer using a B&K shaker table.

3.4.1 Strata vibration measurement setup

Vibration measurements were recorded simultaneously to noise measurements discussed in the previous section with an accelerometer mounted on the west turbine inertia base. Measurements were also taken on residential levels to assess any structurally transmitted vibration. The background and operational measurement periods are displayed in Table 11, results from which are synchronised with atmospheric data to assess any correlation.

Figure 35: Displays the SV958 vibration meter placement at the Strata's west turbine base.

DATE	LOCATION	STATUS
21.03.2012 - 26.03.2012	TURBINE BASE	BACKGROUND
16.04.2012 - 21.04.2012	RESIDENTIAL LEVEL	BACKGROUND
03.05.2012 - 09.05.2012	TURBINE BASE	BACKGROUND
11.05.2012 - 17.05.2012	TURBINE BASE	OPERATIONAL
18.05.2012 - 24.05.2012	TURBINE BASE	OPERATIONAL
25.05.2012 - 31.05.2012	RESIDENTIAL LEVEL	OPERATIONAL

Table 11: Presents the vibration measurement positions, times and turbine operational or non-operational (background) status taken at the Strata towers west turbine.

All measurements, equipment and technique met the following standards:

- BS 6472-1:2008 - Evaluation of human exposure to vibration in buildings (1 - 80 Hz).
- BS 6841:1987 - Measurement and evaluation of human exposure to whole-body mechanical vibration and repeated shock.
- BS ISO 5348:1998 - Mechanical vibration and shock. Mechanical mounting of accelerometers.
- BS EN ISO 8041:2005 - Human Response to vibration. Measuring instrumentation.

3.4.2 LSBU vibration measurement setup

The LSBU turbine tower is mounted directly on to the frame depicted in Figure 36, which in turn is fixed to the LSBU roof via four steel poles secured through the rooftop and mounted onto the lower level vertical concrete beams as shown in Figure 37 and 38.

Simultaneous vibration measurements will be recorded at the structure base and at the concrete beam the turbine base is mounted upon. These values will be used to determine the structures response to the vibration using the Svantek SV106. These measurements will be synchronised and compared to wind speed in order to assess any correlation. The results obtained from the methodology discussed will be presented in Chapter 4 as part of the LSBU and Strata case studies.

Figure 36: Displays the LSBU turbine's mount.

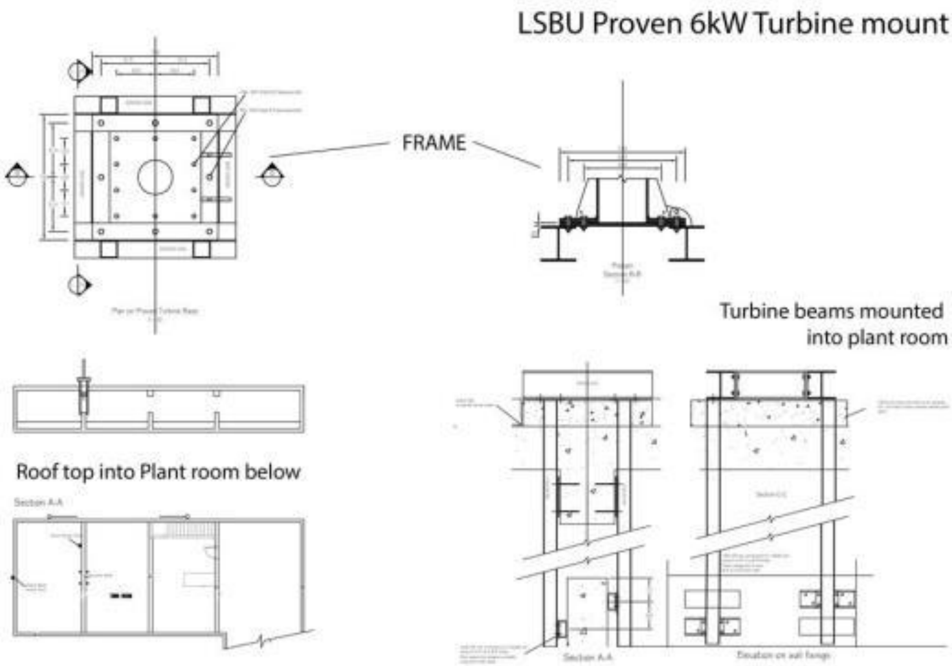

Figure 37: Displays the LSBU turbine mounting plans, showing how it was installed via four steel poles to the concrete beams within the LSBU plant room roof.

Figure 38: Depicts the SV106 vibration meter placement with labelled axis at the LSBU turbine.

Chapter 4 LSBU Case Study

This chapter reports the collated atmospheric, energy performance, noise and vibration data measured at the LSBU turbine site.

4.1 Atmospheric

Atmospheric data was logged between 01/01/13 and 02/02/15 at the CEREB ultrasonic anemometry. A total of 71863 out of a possible 73056, 10 minute interval, data points were collected within this period with a 1.9% of data missing due to logging errors within the server, this information is displayed in Table 12 and Figure 39 - Figure 41.

Year	TOTAL POSSIBLE	TOTAL	MISSING	% MISSING	AVERAGE Wind V [m/s]
2013	35040	34280	760	2.22	0.9
2014	35040	34497	543	1.57	0.8
2015	3168	3082	86	2.79	0.9
TOTAL	**73248**	**71859**	**1389**	**1.93**	**0.8**

Table 12: Displays the total number of wind data collected at the CEREB anemometer including average recorded wind speed (m/s).

Atmospheric data was also collected at the LSBU Tower Block. Due to planning permission restrictions the Tower Block mast could not be erected until 20/08/14 but since then 10 minute interval data has been collected and analysed. A total 18971 out of a possible 23904 data points were collected between 20/08/2014 and 02/02/2015. Unfortunately 17 % of the possible data was missed due to anemometry malfunctions and waiting for replacement parts to be delivered. The captured data is displayed in Table 13 and Figure 42.

TOTAL POSSIBLE	TOTAL	MISSING	MISSING %	AVERAGE Wind V [m/s]
23904	18971	4069	17.02	3.47

Table 13: Displays the wind data figures collected at the LSBU Tower Block including average recorded wind speed (m/s)

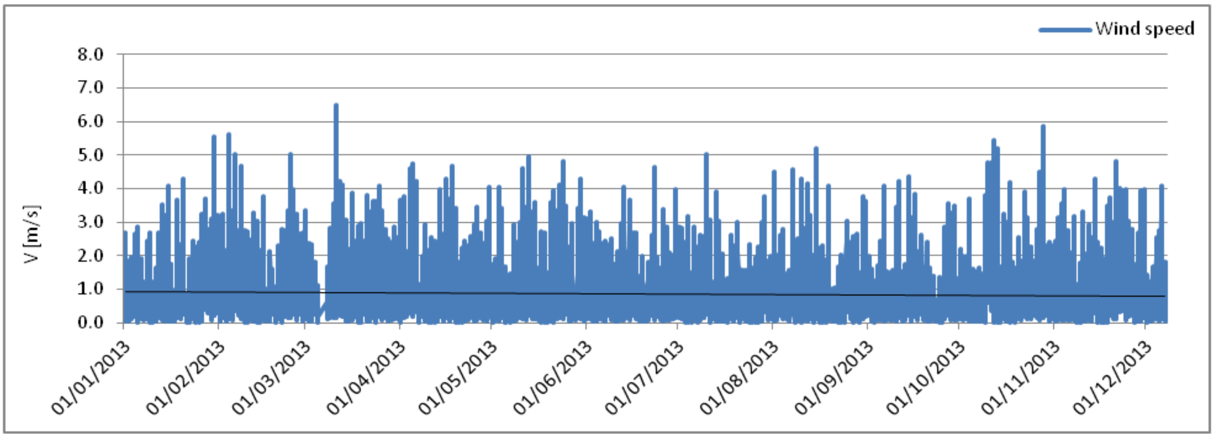

Figure 39: Displays wind speed data collected from the LSBU CEREB anemometer for 2013.

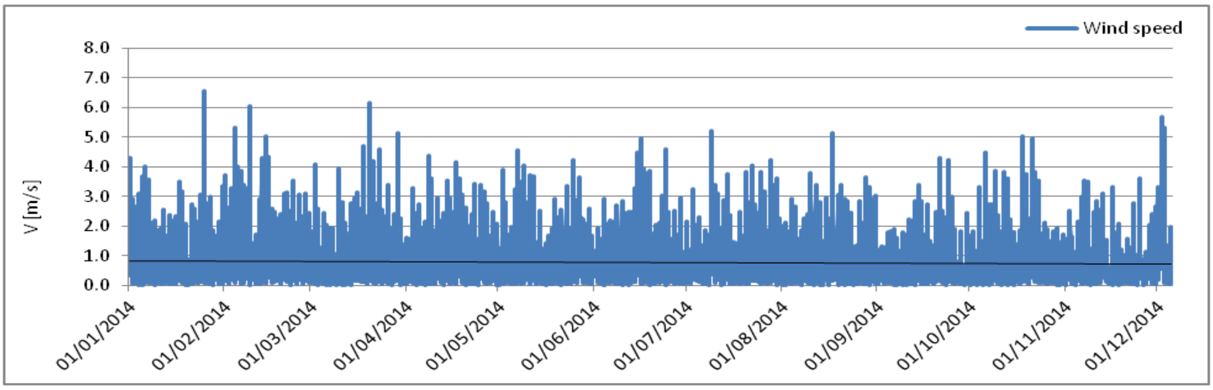

Figure 40: Displays wind speed data collected from the LSBU CEREB anemometer for 2014.

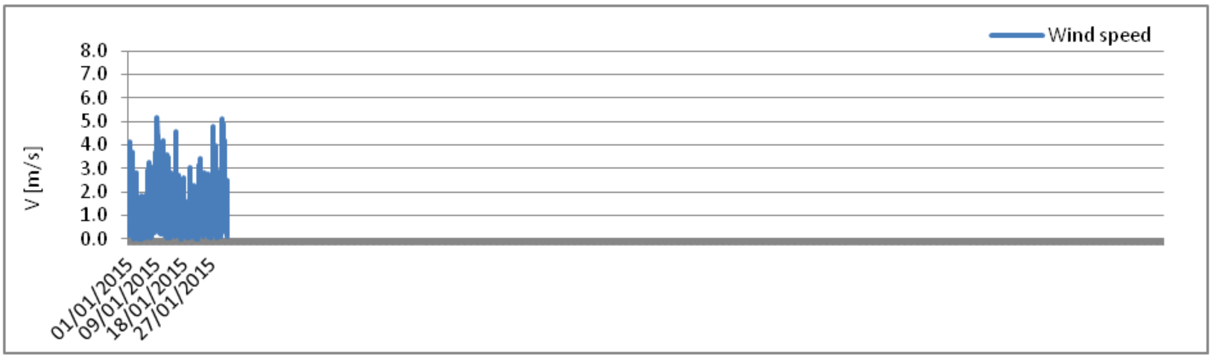

Figure 41: Displays wind speed data collected from the LSBU CEREB anemometer for the 2015 period available. The graph appears empty as monitoring ceased on 02/02/15.

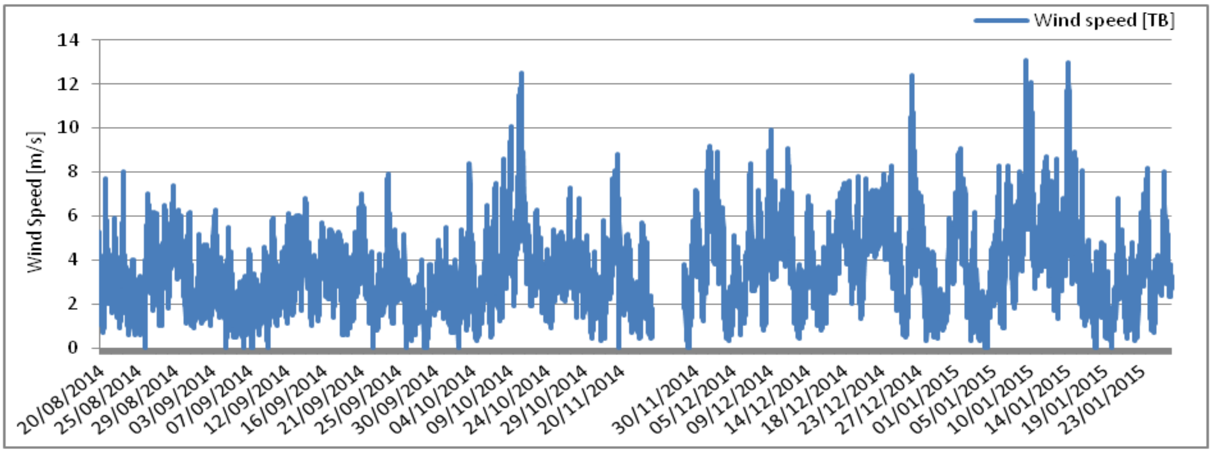

Figure 42: Displays wind speed data collected from the LSBU turbine hub height anemometer from its install date on the 20/08/2014 to the end of monitoring on 02/02/15. The gap appearing after 22/11/2014 is due to the anemometer being offline while waiting for replacement parts.

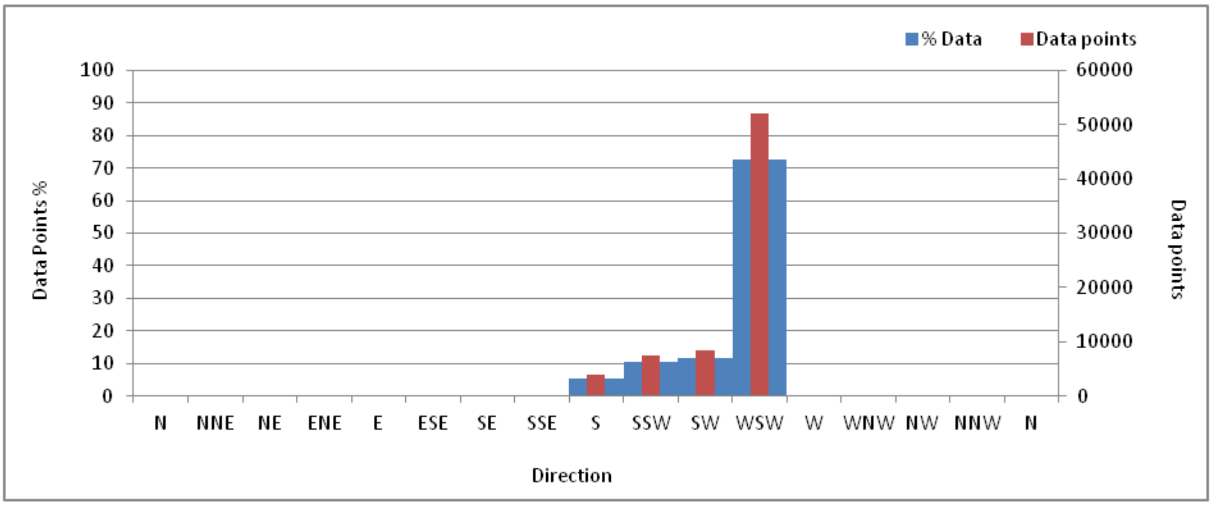

Figure 43: Displays wind direction distribution from data collected at the LSBU CEREB site.

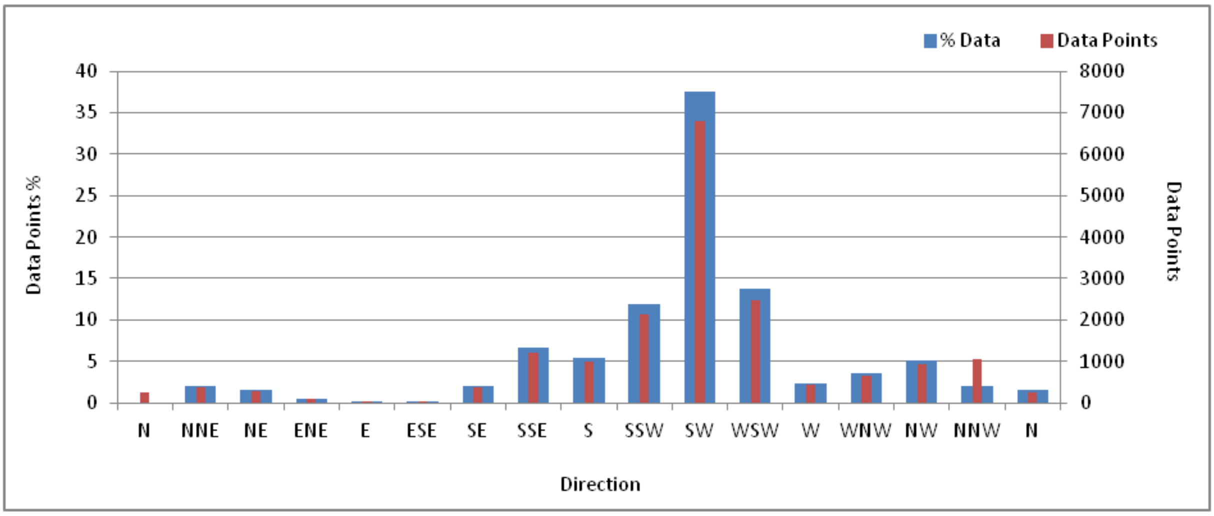

Figure 44: Displays wind direction distribution data collected at the LSBU tower block turbine site.

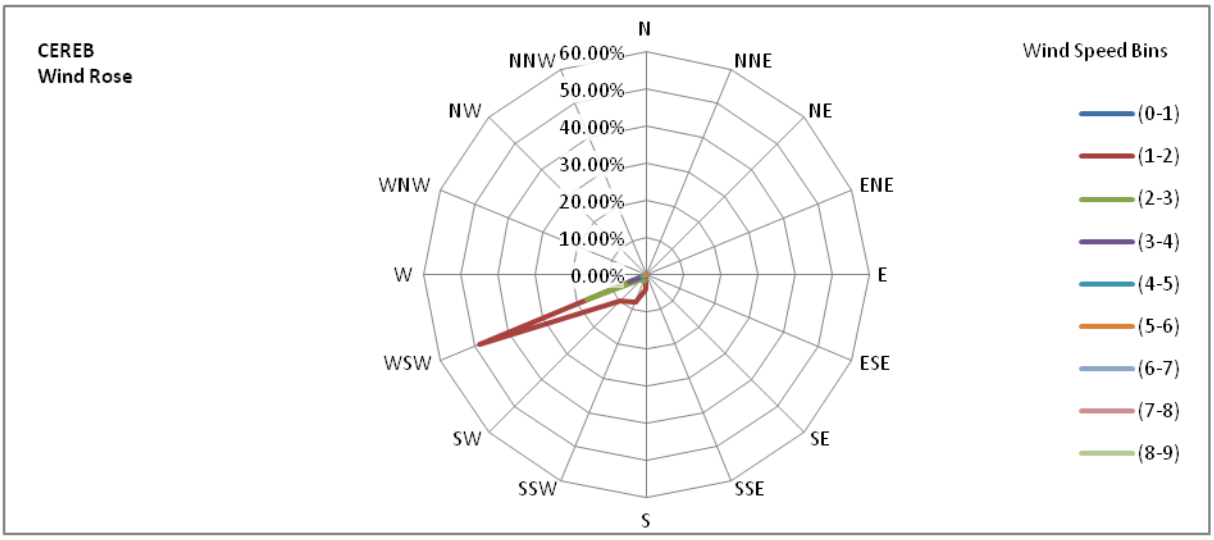

Figure 45: Displays CEREB wind rose.

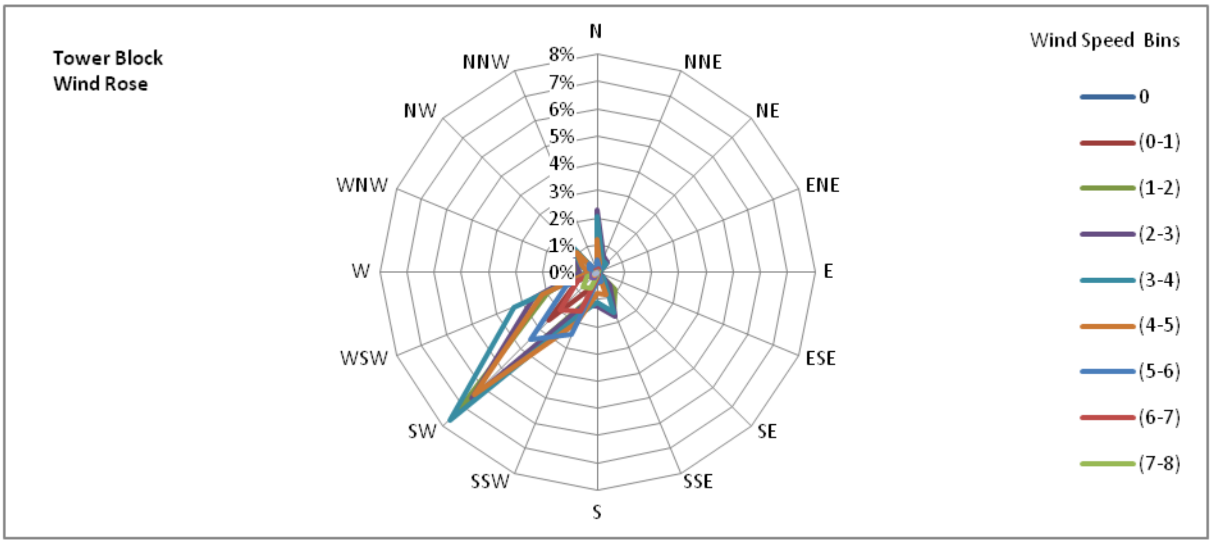

Figure 46: Displays LSBU Tower Block Wind Rose

And in-depth discussion of collected results for this site will now be discussed and extrapolated to theorise the atmospheric conditions at the Strata site.

At first glance there seems to be some discrepancy between the results. The prevailing wind in London is from the south west, which measurements taken at the LSBU position are in harmony with but the anemometry at the CEREB position varies slightly showing a prevailing wind from west-south-west as evident from Figure 43 and Figure 44. This could be attributed to a few factors: the SW - WSW bands represent a 22.5 degree maximum region. Therefore a slight misalignment of either or both of the sensors could contribute to this seeming discordance.

There is also the matter of differing wind speeds to be investigated. The CEREB and Tower Block sites are 100 m apart and approximately at the same height yet consistently lower wind speeds are recorded at the CEREB site. Could one set of data be corrupt? Does this mean that all data from the CEREB anemometry is null and void for our assessment? Lower wind speeds were recorded but were they consistently different? When aligning the recorded data at both positions, displayed in

Figure 47, a moderate correlation of r = 0.5 from the results is observed. This moderate correlation suggests that in spite of the diminished wind speeds demonstrated at CEREB a similar trend in wind speed fluctuations is present. Therefore if a coefficient of mean wind speed can be determined we may be able to quantify how much the wind speed has been reduced by.

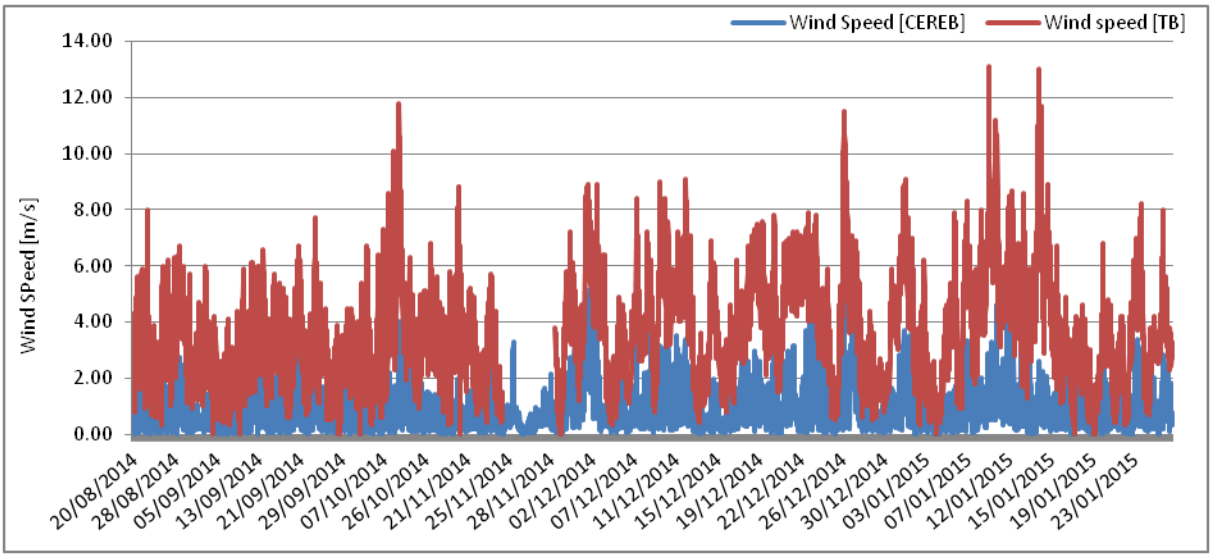

Figure 47: Demonstrates the correlation of wind speed data recorded at tower block and CEREB positions, albeit to a reduced degree.

CFD analysis of the sites was conducted to assess if the local topography could have any direct effect on the recorded wind speeds. A south westerly wind was programmed into the Urbawind simulations across a 1 x 1 m mesh grid area, defined as a plane of interest. The displayed mean wind speed coefficients were produced and displayed in Figure 48, Figure 49 and Figure 50.

Figure 48 and Figure 49 graphically depict a disrupted wind flow with the CEREB building itself acting as an obstacle to wind flow reaching the Tower Block turbine position. The turbine site in Figure 49 is just beyond the turbulent wake (blue area) of the CEREB building and therefore is subjected to greatly reduced mean wind speeds. Urbawind calculates this area to have an average mean wind speed coefficient of approximately 0.87.

Figure 50 depicts high resolution results taken around the CEREB and Tower Block anemometry positions. The CEREB anemometer is at a 1.5 m height above the roof top. However, the roof top is open to public access so has a 1 m solid safety barrier around its perimeter.

Figure 50 shows the interaction of a south westerly wind and the CEREB safety barrier and how this slows and refracts the wind flow around the anemometer position. An Urbawind generated mean speed coefficient of between approximately 0.22-0.43 was calculated at the CEREB anemometer. This is in stark contrast to the higher Urbawind generated coefficient of approximately 0.85-0.90 demonstrated at the Tower Block anemometer. This 50-75 % reduction in wind speeds at the CEREB position satisfactorily explains the diminished speeds recorded at the CEREB site.

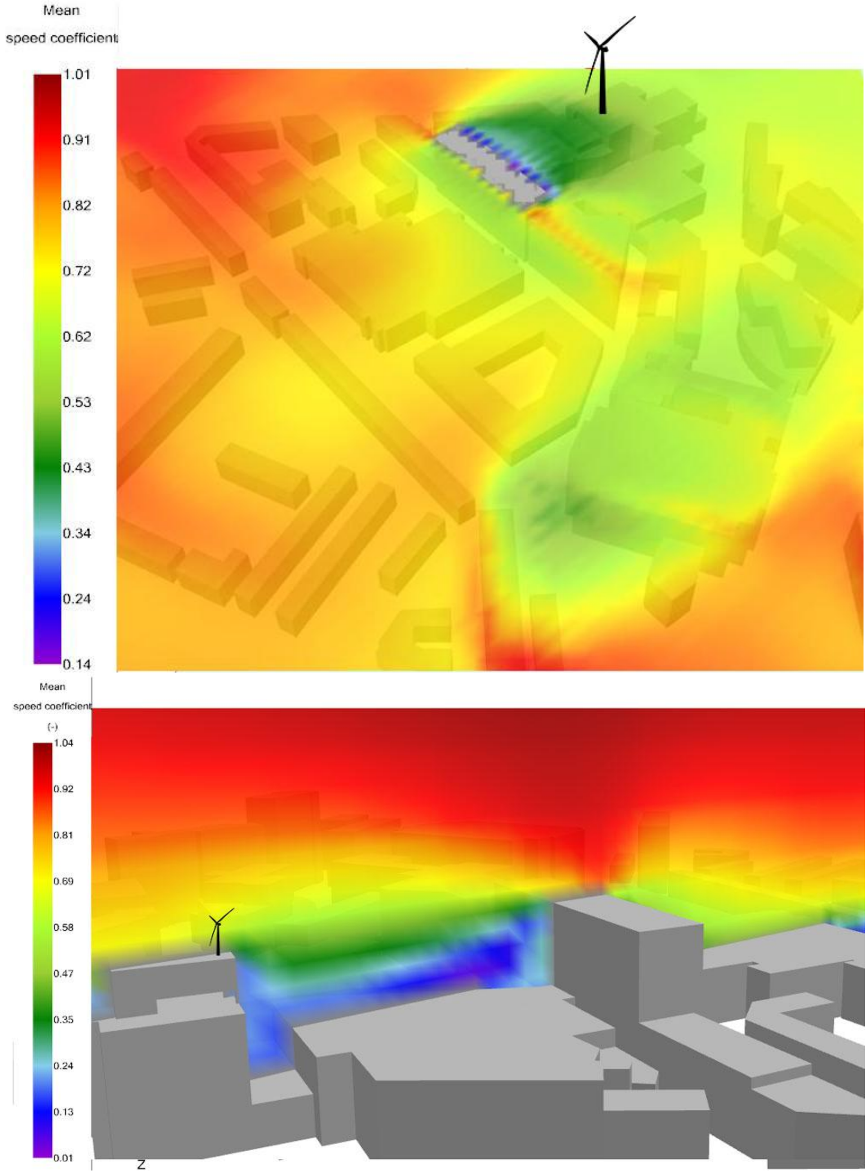

Figure 48: Displays an Urbawind run CFD simulation of a south westerly wind flowing across the LSBU campus from above and the side. It can be seen that a reduced mean wind speed is expected around the CEREB building casting a shadow upon the turbine site marked with a T.

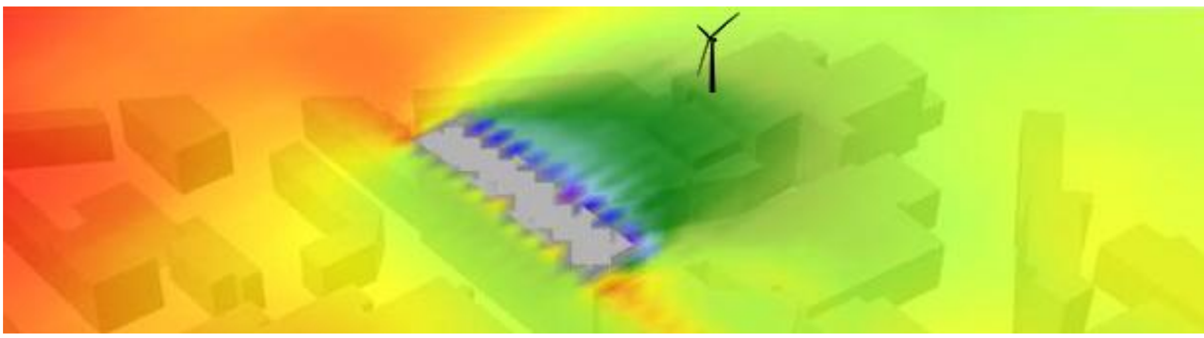

Figure 49: Depicts the LSBU turbine location downwind of diminished wind speeds and turbulent flow caused by the upwind CEREB building.

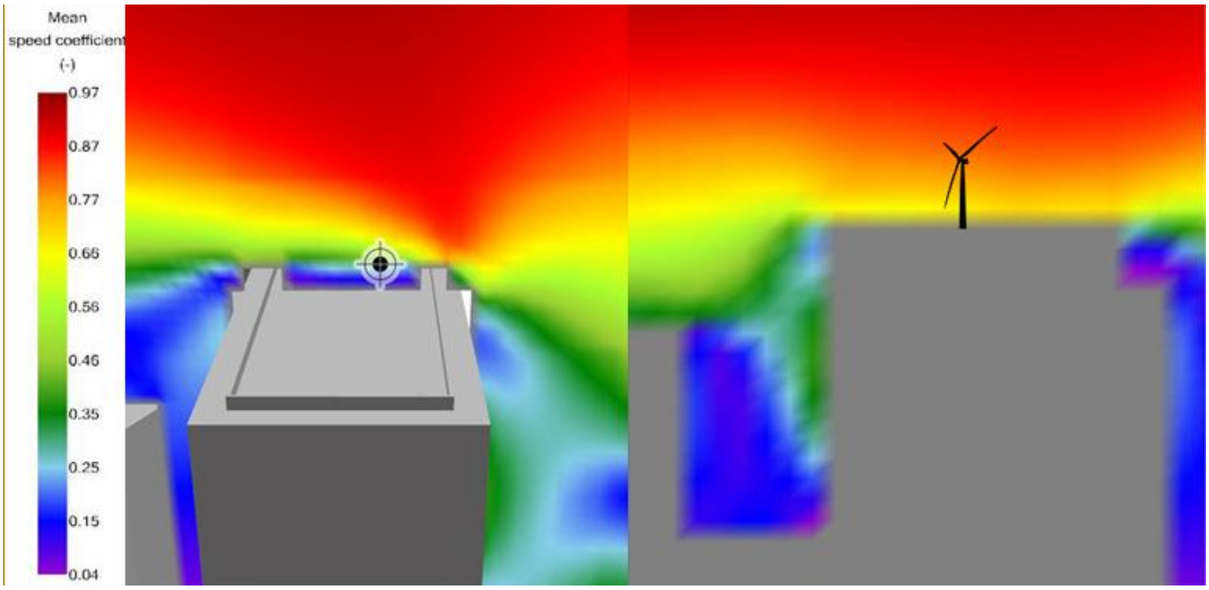

Figure 50: Displays the CEREB and Tower Block anemometry positions and the expected mean wind speed coefficients at both sites. It is clear that the barrier surrounding the CEREB rooftop in the left hand image is drastically reducing wind flow compared to the right hand image of the LSBU site.

Under closer inspection of the synchronised CEREB and Tower Block data we see the CFD prediction somewhat verified as 68 % of the comparative data fell between the Urbawind predicted 25 - 50 % reduction as depicted in Table 14. Table 14 also shows the CFD predicted average wind speed to be 3.7 m/s compared to the measured 3.6 m/s. This part of the investigation, although conducted over a six month period, could be enhanced by a longer trial period of data considering the already outlined losses of data due to technological failure. Further work could contribute towards further certifying CFD predictions.

Total Possible Measurements	23040
Total Recorded Measurements	9787
Missing %	42
Total within CFD Prediction	6638
Total within CFD Prediction %	68
CEREB Average V [m/s]	0.8
Tower Block Average V [m/s]	3.6
CFD Predicted Average V [m/s]	3.7

Table 14: Depicts the comparative data between CEREB and LSBU Tower Block anemometry, which falls between CFD predictions for 49 % of the time.

This exercise also provides a prime example of why prior, site-specific, knowledge and assessment is essential in planning a successful wind turbine installation. At first glance it may seem practical and appropriate to solely use CEREB collected data to assess the wind regime (and therefore wind energy potential) of the Tower Block site as there was already existing anemometry in place. However, in spite of being at the same height and within the same area the CEREB anemometry was experiencing a different wind regime due to its structural orientation.

This dramatic effect topography can have on recorded wind speeds will be summarised in Chapter 6 where LSBU 'what-if' scenarios will be discussed with a view to optimising the site. The knock-on effects to energy generation potential will also be highlighted.

One of the main factors hindering an accurate prediction of energy yield from an urban wind turbine installation is the uncertainty of the local wind regime and a lack of archived averaged wind speed reference data. Incorrectly estimating the available wind resource can be detrimental and negate any planning, technological or financial investment. Current available wind datasets for London have been shown to not be entirely applicable to the urban environment e.g. wind speeds from the NOABL database are recorded at Heathrow with a very different topography to London as shown in chapter 2.4. This can lead to an over estimation of wind speed distribution and energy yield, which can be detrimental, especially when results hover around the cut in speed of the system. Therefore, site specific wind data or an accurate simulation using CFD analysis within the urban environment is intrinsically necessary for an accurate estimate.

LSBU measured data between 2013 - 2015 shows a significant difference in wind speeds when compared to the NOABL data base. NOABL would predict 6 m/s at hub height as opposed to the measured average of 3.5 m/s on the LSBU Tower Block, which in turn is higher than the CEREB measured 1 m/s average.

Weibull and Rayleigh probability density functions were used as auxiliary prediction tools to assess their applicability in the urban environment. The Weibull with MMLM was shown to correlate most closely with measured data, but still over estimated energy production by 30 % compared to Rayleigh's over-estimation of 37 % and power curve method by 56 %[9]. This differs slightly for 2014 where the Weibull method underestimated energy yield by only 8%, Rayleigh over-estimated by 24 % and power curve method by 43%. The difference is attributed to the shift in wind speed bin predictions around the cut in speed of 3-4 m/s for the turbine.

CFD analysis has shown the stark differences in CEREB and Tower Block speed and direction measurements to consistently and predictably be related to the surrounding topography and anemometry placement. CEREB collected speeds were compared to simultaneously measured hub height speeds, the difference of which was shown to be in harmony with CFD predictions for 55 % of the time, with an accurate average wind speed estimation for the site This showed that reliable predictions can be made for hub height wind speeds extrapolated from CEREB wind speed data and demonstrates the practicality and effectiveness of CFD simulations as a wind regime estimation tool.

[9] It should be reiterated at this point that the LSBU turbine output was slightly diminished due to a temporary shut down for maintenance over a 3 week period in August and September 2013.

Variations in recorded directional data were also shown to be in harmony with CFD analysis, showing wind directional results collected at the CEREB site would be skewed further west due to the local topography. From such analysis, optimum placement and configuration can be assessed. For example consider Figure 51; the left hand image shows simulated wind flow from the south west with a coefficient of 0.53 - 0.63 at the current turbine position. The same scenario was run, but with an elevated hub height of +10 m, at which a coefficient of between 0.88 - 0.98 is estimated.

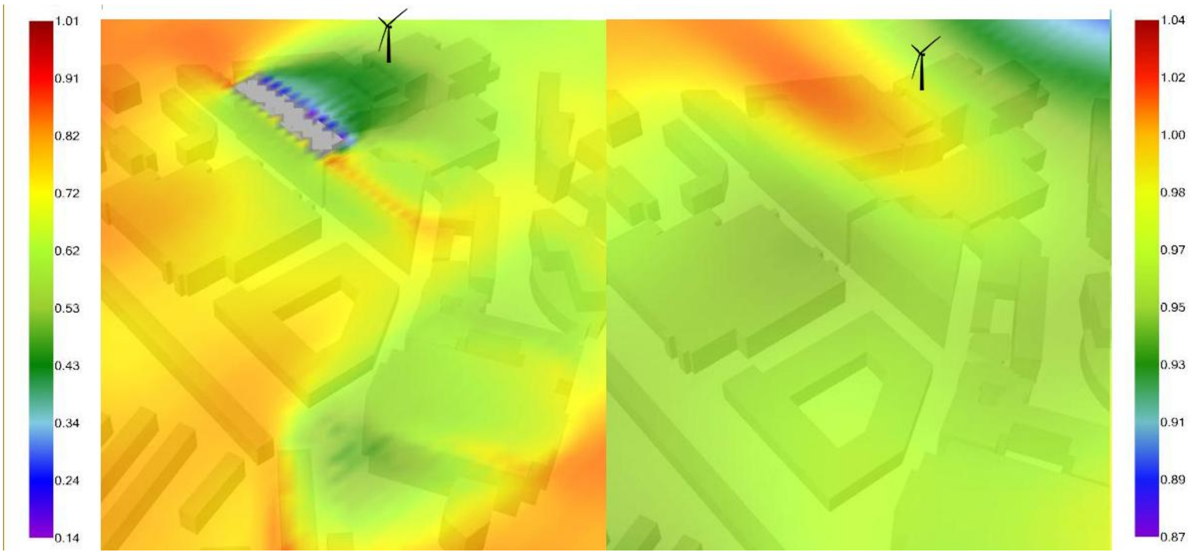

Figure 51: Displays the LSBU Tower Block turbine site. The left hand image depicts CDF mean speed analysis at current hub height and the right shows the same mean speed predictions with an increased 10 m elevation.

Keeping in mind that power in the wind is proportional to velocity cubed (V^3) we can see that a 40 % increase in wind speeds is possible at this new height, an increase that would yield a 2.75 multiple increase in power. Within this section CFD analysis had proven itself to be an invaluable tool in helping to verify results, topographical effects and shows potential as a placement-optimisation tool within the urban environment.

4.2 Noise

The following section will review collected noise measurements captured in the procedures laid out in Chapter 3. Background, operational and environmental noise mapping results was collected for the LSBU site, as far as possible.

4.2.1 Background Measurements

Measurements carried out between 23/09/2013 to 28/09/2013 and 23/12/2013 to 09/01/2013, while the turbine was non-operational, are now to be considered. The data is plotted in Figure 52 and Figure 53.

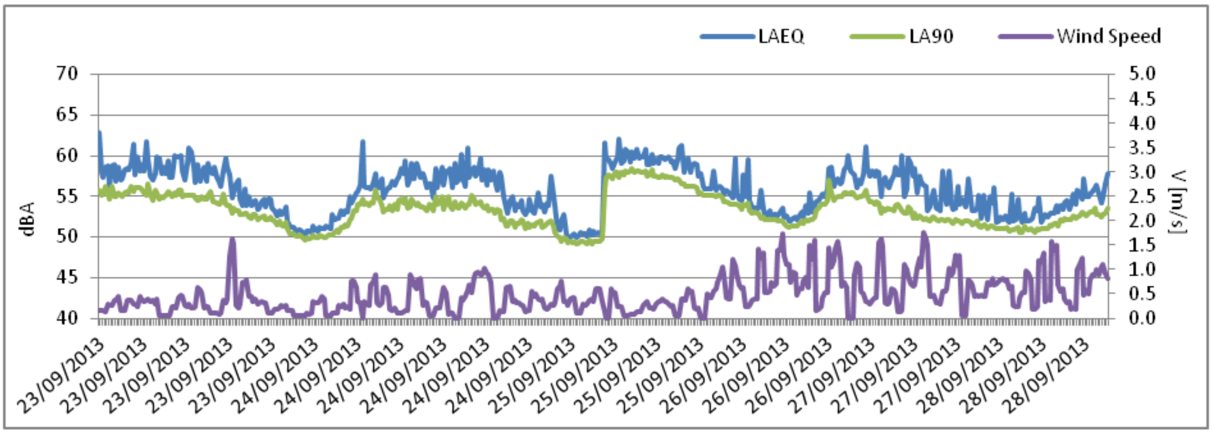

Figure 52: Displays background noise and wind speed levels at the LSBU turbine position in September 2013.

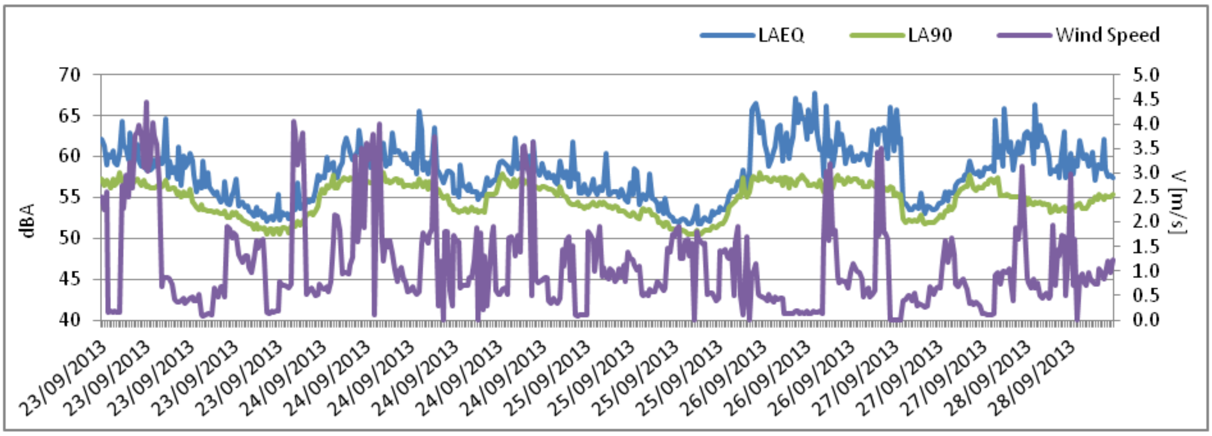

Figure 53: Displays background noise and wind speed levels at the LSBU turbine position in December 2013.

The date plotted in Figure 53 demonstrates no strong correlation between L_{Aeq} and wind speed as shown in Table 15 in spite of a 0.5 dB per wind speed bin being observed in Figure 54. This, along with the consistent, repetitive fluctuation of noise levels recorded suggests the background noise levels within the area are predominantly dictated by other environmental factors such as traffic, HVAC and social sources.

	L_{Aeq}	L_{A10}	L_{A90}	**Wind Speed**
L_{Aeq}	1			
L_{A10}	0.97	1		
L_{A90}	0.89	0.87	1	
Wind Speed	-0.13	-0.15	-0.15	1

Table 15: Displays correlation (r) data for the measured wind speed, L_{Aeq}, L_{A10} and L_{A90} recorded over the September and December background measurement periods at the LSBU turbine position.

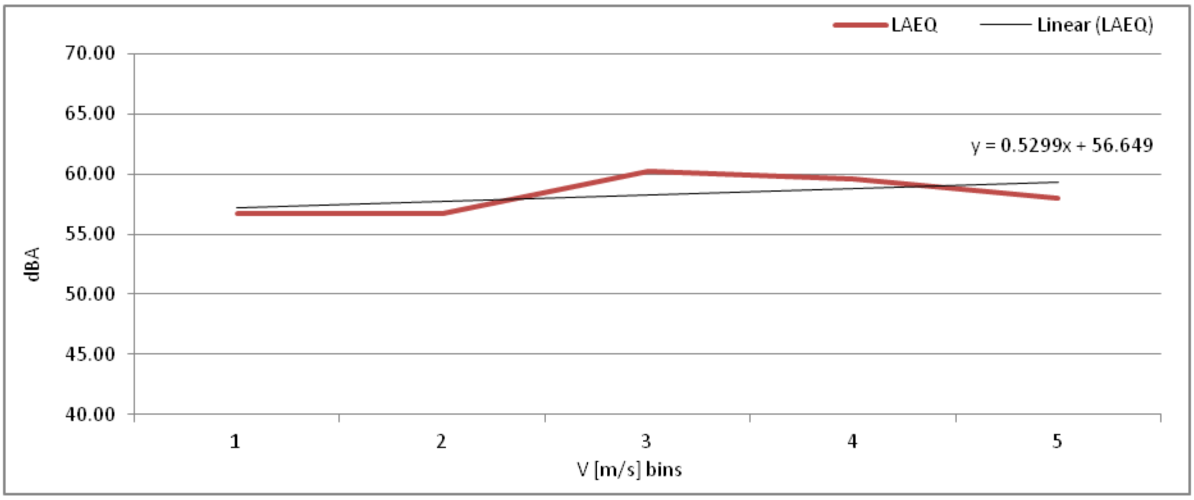

Figure 54: Displays average L_{Aeq} levels as a function of wind speed at the LSBU turbine position. An average 0.5 dB increase per 1 m/s wind speed bin is observed.

4.2.2 Operational

Measurements were then recorded while the LSBU turbine was operational. These measurements were conducted between September 2013 and February 2015 and plotted in Figure 55. Unfortunately full, 24/7, measurements within this period were not possible due to technical and access restrictions.

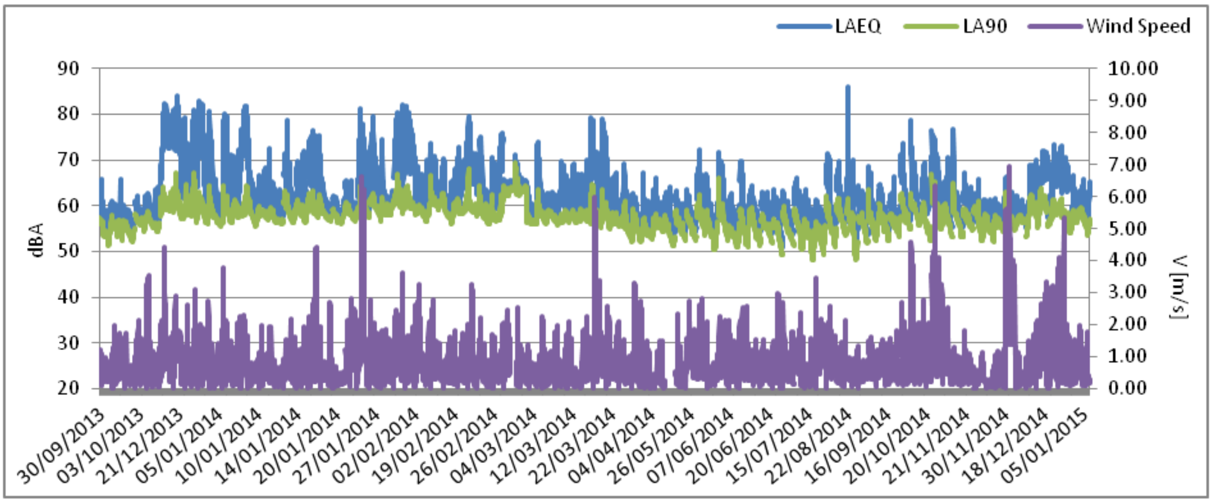

Figure 55: Displays operational noise levels at the LSBU turbine position with wind speed plotted over time.

	L_{Aeq}	L_{A10}	L_{A90}	Wind Speed
L_{Aeq}	1.00			
LA_{10}	0.99	1.00		
L_{A90}	0.80	0.77	1.00	
Wind Speed	0.25	0.25	0.21	1.00

Table 16: Displays correlation (r) values between L_{Aeq}, L_{A10}, L_{A90} and wind speed.

Table 16 displays a slight correlation between noise levels and wind speed and Figure 56 demonstrates a 1 dB increase in noise per wind speed bin. When comparing Figure 54 and Figure 56 a +5 dB shift is observed in the operational results at 1 m/s continuing with a 1 dB increase per wind speed bin. This may, at first, seem to suggest the turbine definitely introduces a high level of noise into the environment but the +5 dB shift occurs below the cut-in speed, where the turbine was not spinning and the 1 dB increase per wind speed bin stays linear through the cut in speed of 3-4 m/s and above where a stepped increase would be expected as the blades begin to turn. This suggests the shift to be environmental in nature and not entirely due to the operational turbine. A more in-depth environmental investigation is therefore conducted to compare simultaneous control, turbine level and street level measurements to get a clearer insight into the turbines relationship with local noise environment.

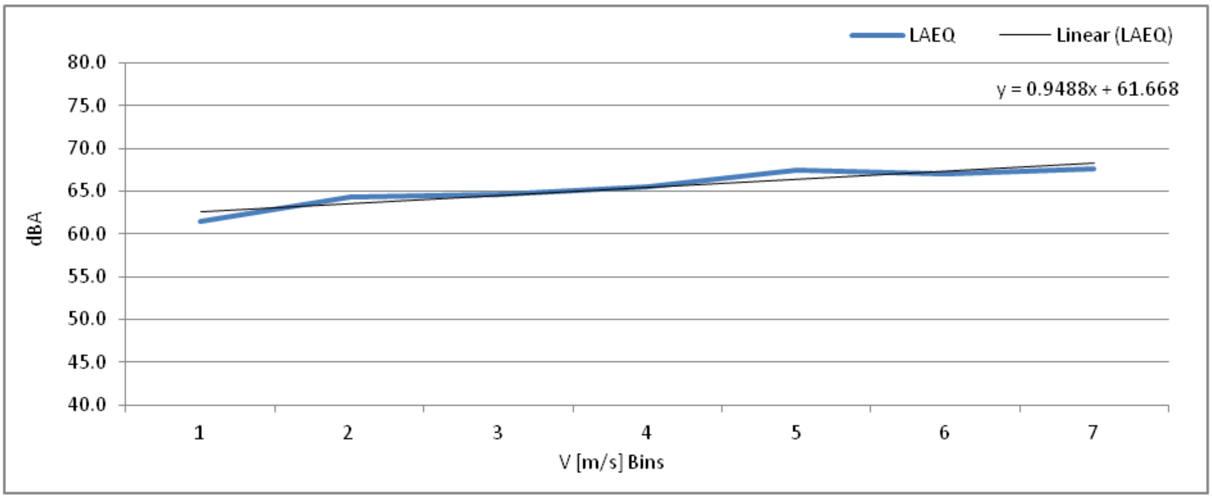

Figure 56: Displays averaged noise level data per wind speed bin. An average increase of 1 dB per 1m/s increase is observed.

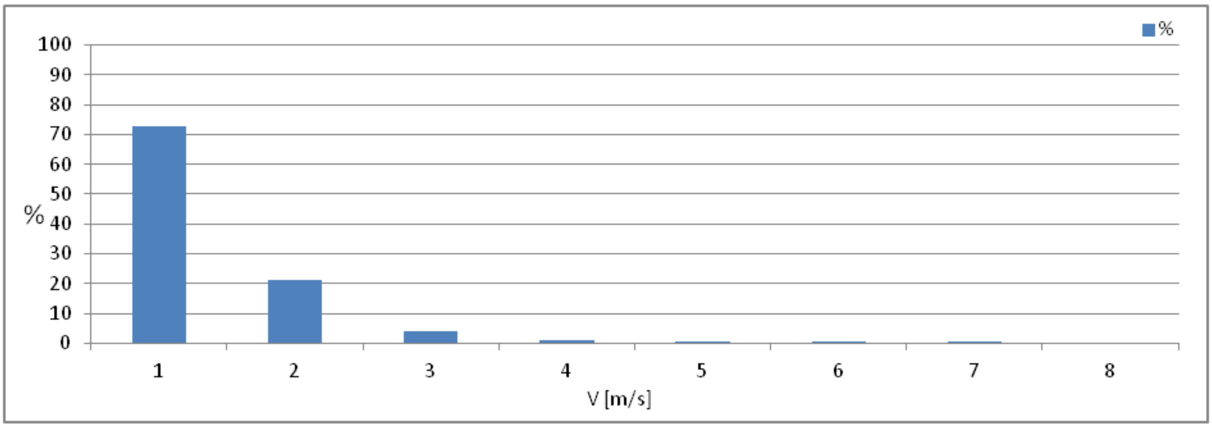

Figure 57: Displays wind speed distribution in wind speed bins as a percentage at the LSBU turbine site.

4.2.3 Environmental mapping

The results listed below were taken between 15/12/14 and 4/01/15 as part of a LSBU environmental noise survey, conducted to establish the background noise environment the LSBU turbine would be placed into and the turbines effect upon this environment. This will be useful in determining the turbine noise emissions contribution towards local, residential annoyance. Noise and wind speed measurements are compared at the turbine position in Figure 58, the control position in Figure 59, the roaming, street level position in Figure 60 and all three sets of results are evaluated against each other in Figure 61.

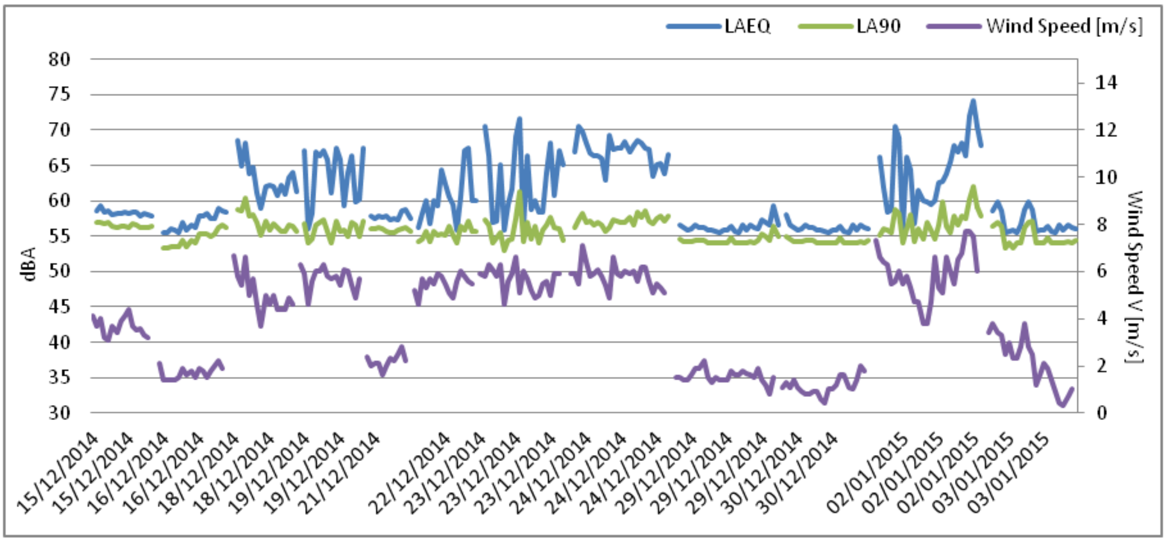

Figure 58: Displays environmental noise measurement results plotted against wind speed; recorded at the LSBU turbine monitoring position.

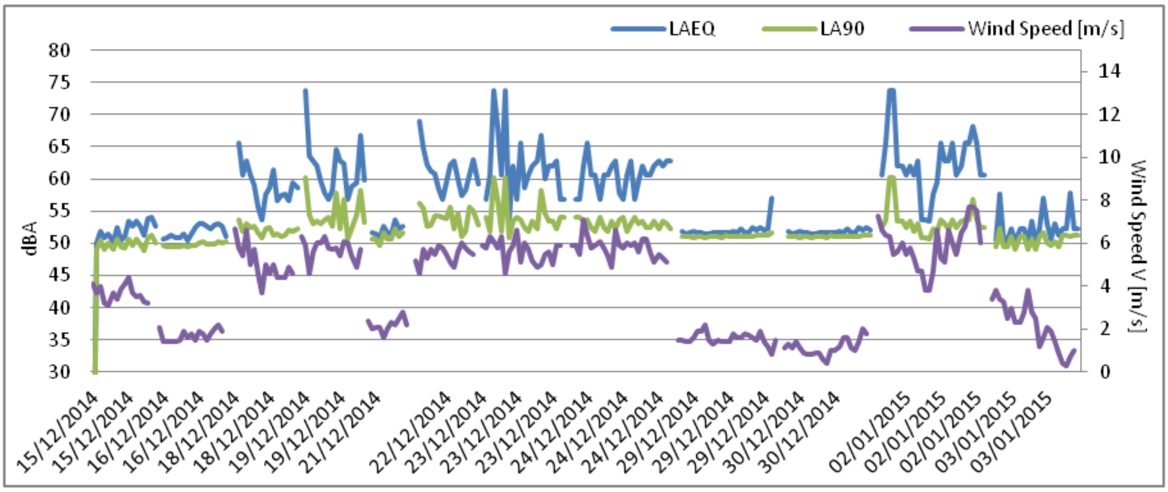

Figure 59: Displays environmental noise measurement results plotted against wind speed; recorded at the LSBU control monitoring position.

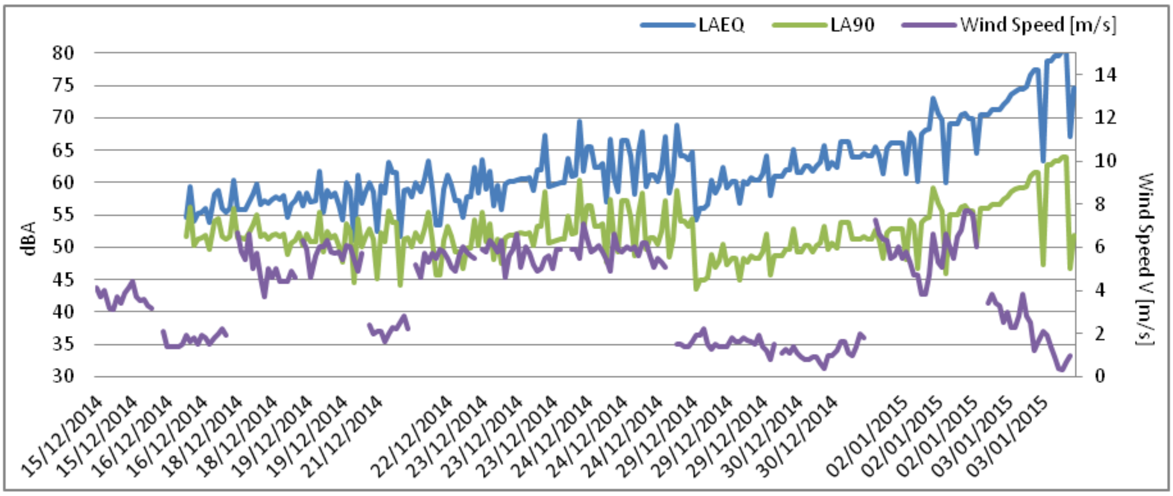

Figure 60: Displays environmental noise measurement results plotted against wind speed; recorded at the LSBU roaming street level monitoring position.

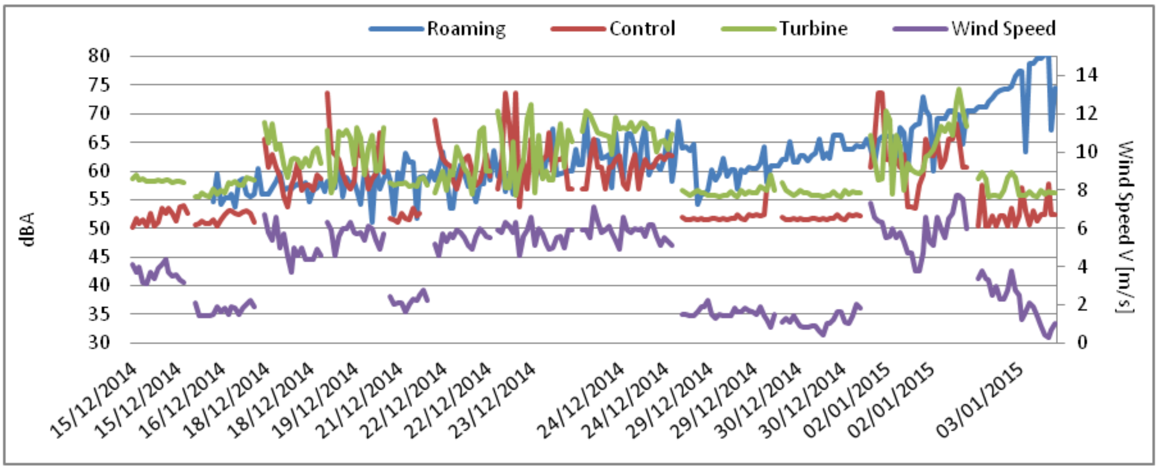

Figure 61: Displays a comparison of measured LAeq results from all (turbine, control and roaming) monitoring positions.

The figures above along with noise levels per wind speed bin displayed in Table 22 suggest other environmental factors outweigh turbine induced noise at wind speeds below 4 m/s for the turbine position and 5-6 m/s for the roaming positions as baseline noise levels stay steady in spite of fluctuating wind speeds. A high average background noise level is demonstrated at the street level roaming positions. Results suggest that above these speeds noise levels increase with wind speed by approximately 1.5-2 dB per wind speed bin. Noise levels measured at positions 1, 2 and 3 did not vary significantly with wind speed and time demonstrating similar noise environments and as positions 1 and 2 are downwind from the local wind resource and are closest to residential areas analysis will focus upon these.

Figure 59 and Table 16 show a direct correlation between wind speed and L_{Aeq} noise level When compared to the measurements taken in the equivalent position on the CEREB building we can see a similar trend in noise as a function of wind speed but at a slightly diminished level. This also shows that though noise levels are increasing with wind speed that direct turbine noise is also a contributor at this level and proximity.

TURBINE	L_{Aeq}	Speed	Direction
L_{Aeq}	1.00		
Speed	0.79	1.00	
Direction	-0.72	-0.88	1.00

Table 17: Displays the correlation (r) between LAeq, wind speed and direction results measured at the LSBU turbine monitoring positions.

Bins	Range V	Freq	Av L_{AEQ}
1	0 <= V < 1	15	56.4
2	1<= V < 2	58	56.4
3	2<= V < 3	19	57.1
4	3<= V < 4	20	58.5
5	4<= V < 5	25	59.8
6	5<= V < 6	70	63.9
7	6<= V < 7	21	65.2
8	7<= V < 8	5	65.0
9	8<= V < 9	0	0.00
	V > 10	0	0
TOTAL		**233**	
AVERAGE SPEED (M/S)		**3.9**	

Table 18: Displays averaged LAeq results per wind speed bin at the LSBU turbine position.

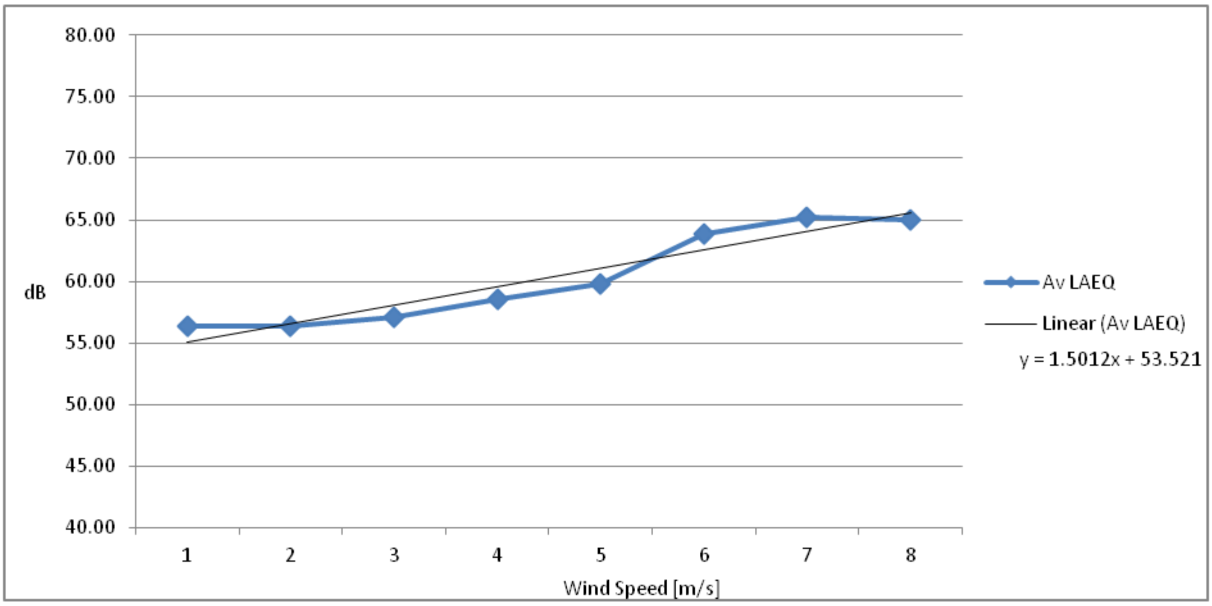

Figure 62: Graphs the averaged L_{Aeq} results per wind speed bin at the LSBU turbine position.

When analysing data for the control position in Table 22 and Figure 63 a high correlation between wind speed and noise is demonstrated, but at much lower noise level than at the turbine monitoring position. At wind speeds below ~3.5 m/s a base line level of 50 - 55 dBA was found, in spite of fluctuating wind speeds, which suggests the local environment factors to be the main contributor of noise at these speeds. A great variance in recorded noise levels can be seen and in a few cases these fluctuations in noise level exceed fluctuations seen in wind speed and at the same time do not always coincide with noise level increases at the turbine level. This may suggest that, in spite of a general agreement in trend between noise and wind speed, other environmental factors are contributing toward the readings, over and above turbine noise.

CONTROL	L_{Aeq}	Speed	Direction
L_{Aeq}	1.00		
Speed	0.81	1.00	
Direction	-0.75	-0.88	1.00

Table 19: Displays correlation (r) between L_{Aeq}, wind speed and direction results measured at the control position.

Bins	**Range V**	**Freq**	**Av L_{AEQ}**
1	0 <= V < 1	14	52.30
2	1 <= V < 2	57	52.08
3	2 <= V < 3	17	51.60
4	3 <= V < 4	21	52.85
5	4 <= V < 5	25	55.92
6	5 <= V < 6	70	60.75
7	6 <= V < 7	21	63.01
8	7 <= V < 8	5	63.64
9	8 <= V < 9	0	0.00
	V > 10	0	0
TOTAL		**230**	
AVERAGE SPEED (M/S)		**3.9**	

Table 20: Displays averaged L_{Aeq} results per wind speed bin at the LSBU control position.

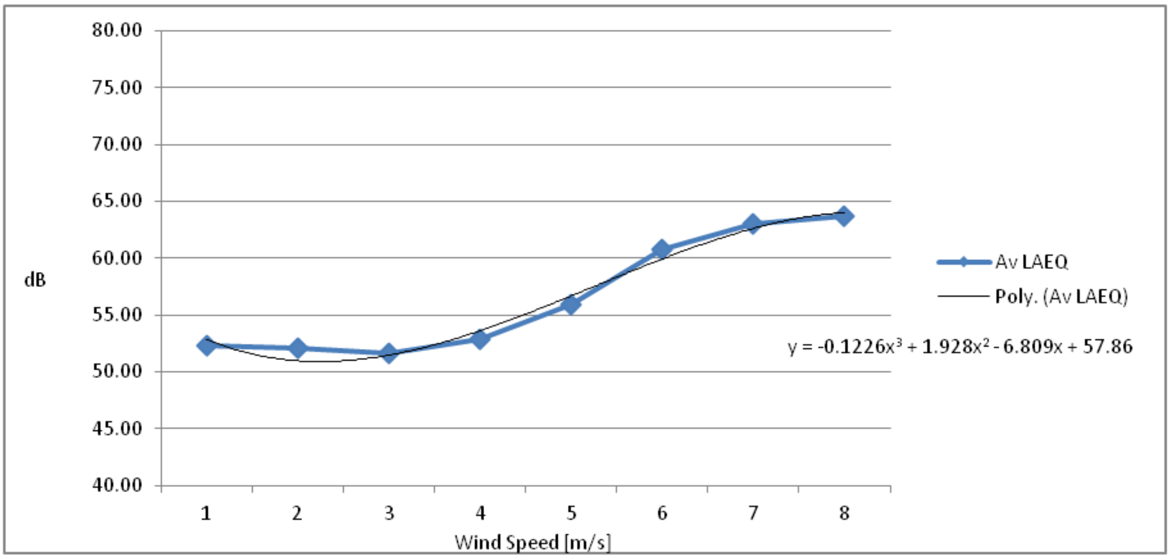

Figure 63: Graphs the averaged L_{Aeq} results per wind speed bin at the LSBU control position.

When looking back to noise measurements taken at the residential area roaming positions around the tower block turbine, Figure 61 displays that noise levels vary significantly at all recorded wind speeds. At wind speeds above the turbine's cut in speed (~3.5 - 4 m/s) there does appear to be a general trend with noise fluctuations shifting in level to match wind speed. However, noise readings at road level do not always shift to coincide with fluctuations in level recorded at the turbine. Quite often noise levels are equal to and greater than the levels recorded at the turbine level, 40 metres above the area, which fit the fluctuating patterns of noise level recorded at the control position. A weaker correlation (r) between wind speed and L_{Aeq} of 0.6 is also apparent from collected results, as shown in Table 21. These factors suggest once again that even though wind speed is influencing noise levels in the area other environmental factors are acting as a strong contributor to the local noise environment. These points may suggest that any turbine induced noise levels perceivable at the turbine level may be masked by the urban environment along with wind induced noise at the road level.

ROAMING	L_{Aeq}	Speed	Direction
L_{Aeq}	1.00		
Speed	0.60	1.00	
Direction	0.50	-0.88	1.00

Table 21: Displays the correlation (r) between L_{Aeq}, wind speed and direction results measured at the LSBU roaming positions.

Bins	Range V	Freq	Av L_{AEQ}
1	0 <= V < 1	15	59.00
2	1<= V < 2	57	58.74
3	2<= V < 3	18	60.08
4	3<= V < 4	20	60.53
5	4<= V < 5	24	59.97
6	5<= V < 6	68	62.41
7	6<= V < 7	21	71.27
8	7<= V < 8	5	75.25
9	8<= V < 9	0	0.00
	V > 10	0	0
TOTAL		**228**	
AVERAGE SPEED (M/S)		**3.9**	

Table 22: Displays the averaged L_{Aeq} results per wind speed bin at the LSBU roaming positions.

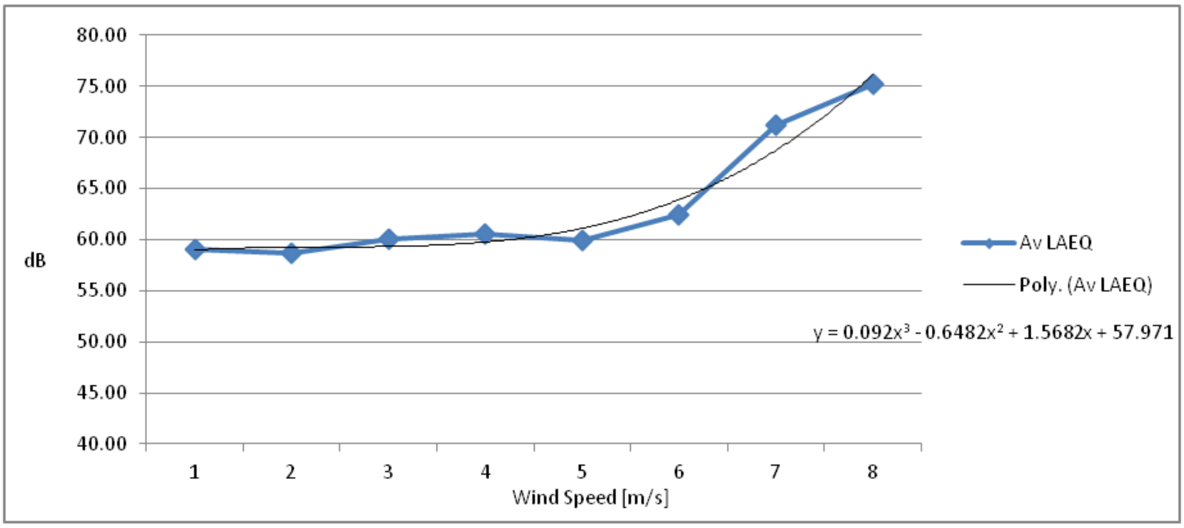

Figure 64: Graphs the averaged L_{Aeq} results per wind speed bin at the LSBU roaming positions.

When comparing L_{A90} and L_{Aeq} results in low wind speeds under 3-4 m/s we see, from Figure 58 - Figure 60, that L_{Aeq} levels remain approximately 1.5 - 2 dB higher than L_{A90} background results as would be expected due to the turbines cut in speed of 3 m/s. However at higher wind speeds, above 4 m/s, a difference of up to 13 dB has been measured at wind speeds measured between 5.5 - 7 m/s at all positions. This suggests that the local wind regime is not constant but a complex mix of high and low speed gusts of wind.

Measurements as a function of wind direction were then plotted and clear relationship of higher wind speeds and noise levels coming directly from the south-south-west is observed and depicted in Figure 66.

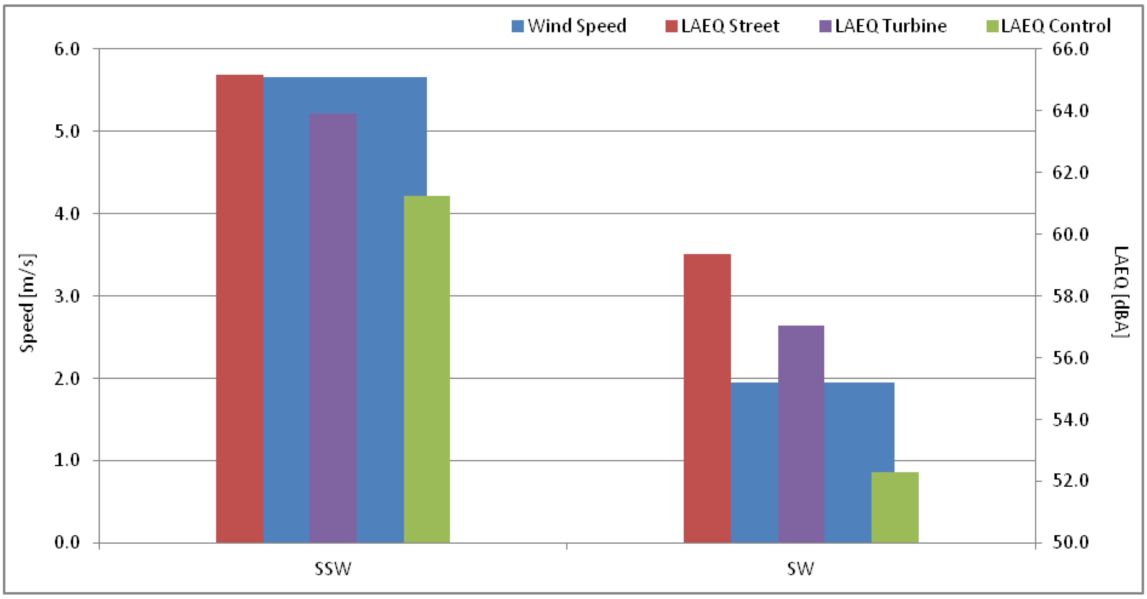

Figure 65: Displays the relationship between the SSW wind direction and recorded higher noise levels at the turbine, control and street measurement positions.

	Wind Speed		Turbine		Street		Control	
	Av. V	Std Dev	Av. L_{AEQ}	Std Dev	Av. L_{AEQ}	Std Dev	Av. L_{AEQ}	Std Dev
SSW	5.7	0.7	63.9	4.2	65.2	6.3	61.3	4.1
SW	2.1	1.1	57.0	1.6	59.3	3.5	52.3	2.0

Table 23**:** Demonstrates a strong relationship between direction and noise measurements recorded at the LSBU turbine, control and roaming street level measurement positions.

A two-sample, two-tailed t-test was performed, not assuming equal variances, to better quantify the variance of results at the turbine measurement position. Firstly for L_{Aeq}: As shown in Table 25 the mean score for the SSW (m=63.8, SD=4.2, N=121) was higher than for the SW (m=57, SD=1.6, N=113) and t stat = 17.35, p <= $1.04^{-36.}$ therefore demonstrating that both sets of data do differ significantly. For wind speed: As shown in

Wind Speed	SSW	SW
Mean	5.7	2.1
Variance	0.5	0.9
Observations	121	113
Hypothesized Mean Difference	0	
t Stat	33.34115	
P(T<=t) two-tail	4.75E-86	
t Critical two-tail	1.971271	

Table 24: the mean score for the SSW (m=5.6, SD=0.7, N=121) was higher than for the SW (M=2, SD=1.1, N=113) and t stat = 33.34, p <= 4.75-86 further demonstrating the stark differences between both sets of data. Complete t-Test data for the street and control measurement positions are included in APPENDIX P.

L_{AEQ}	*SSW*	*SW*
Mean	63.9	57.0
Variance	17.9	1.4
Observations	121	113
Hypothesized Mean Difference	0	
t Stat	17.35419069	
P(T<=t) two-tail	1.03818E-36	
t Critical two-tail	1.977053689	

Table 25: Displays t-Test results for SSW - SW L_{Aeq} comparison data for the turbine position. p<= 1.04^{-36}.

Wind Speed	SSW	SW
Mean	5.7	2.1
Variance	0.5	0.9
Observations	121	113
Hypothesized Mean Difference	0	
t Stat	33.34115	
P(T<=t) two-tail	4.75E-86	
t Critical two-tail	1.971271	

Table 26: Displays t-Test results for SSW - SW wind speed comparison data for the turbine position. p<= 4.78^{-86}

CFD simulations were run to assess the local topographies effect on turbulent flow and mean wind speed from these directions. Figure 66 and Figure 67 display the results and show that although the change in direction does not change the mean wind speed coefficient it does significantly increase turbulent flow at the Tower Block measurement position. The local topography consists of tall buildings lining long roads, creating open, clear pathways for the wind to traverse from a more westerly direction. These CFD simulations show that the more southerly the wind, the more interrupted and turbulent the flow becomes. This increased turbulent flow could contribute towards the higher wind speeds and noise levels captured from the south-south-west.

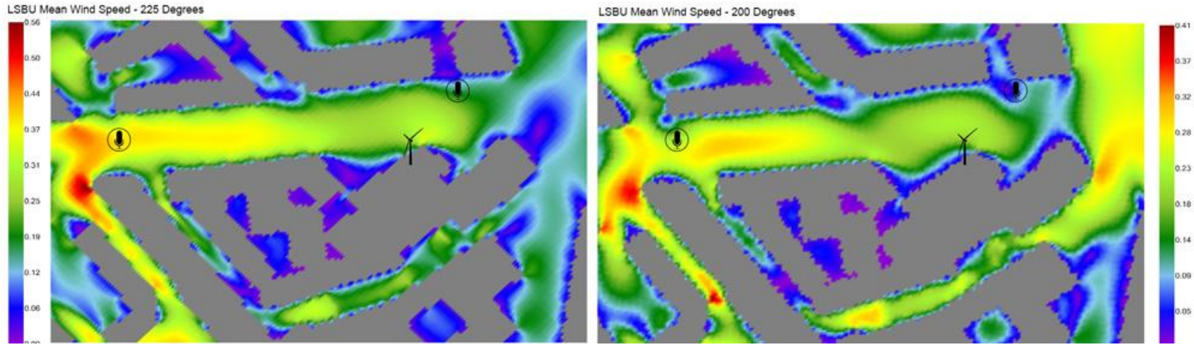

Figure 66: Displays a comparison of mean wind speed coefficients simulated using the dominantly observed south westerly (225 deg) and south-south-westerly (200 deg) winds at the LSBU turbine position. SLM and turbine positions are marked.

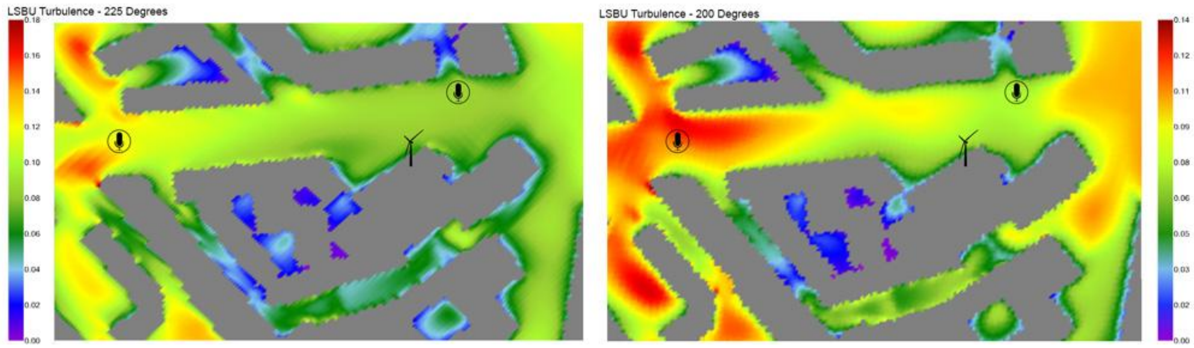

Figure 67: Displays a comparison of turbulent flow coefficients simulated using the dominantly observed south westerly (225 deg) and south-south-westerly (200 deg) winds at the LSBU turbine position. SLM and turbine positions are marked

To further investigate any tonal elements, third octave band analysis is conducted. Figure 68 displays typical 1/3 octave noise levels resulting from select wind speed bins. Please refer to APPENDIX O for full wind speed bin results.

Noise levels remain constant and unvarying in spectral content up to 2-3 m/s wind speeds. The Proven 6 kW LSBU turbine has a cut in speed of approximately 2.5 m/s, suggesting that noise levels recorded at these speeds are when the turbine is non operational and therefore not a contributor. As negligible level increase is seen in Figure 62 - Figure 64 as a function of wind speed, wind noise is not deemed a contributing factor towards these levels and the background environment is outweighing any atmospheric noise at these speeds, as previously discussed. At wind speed bin 3-4 m/s we start to see a slight increase in overall level as well as boost in low frequency content. At wind speed bins above 4 m/s a significant boost in low frequency content is shown at 40 Hz, 80 Hz and 125 Hz bands. A rise in high frequency noise centred around 8-10 kHz bands is also observed.

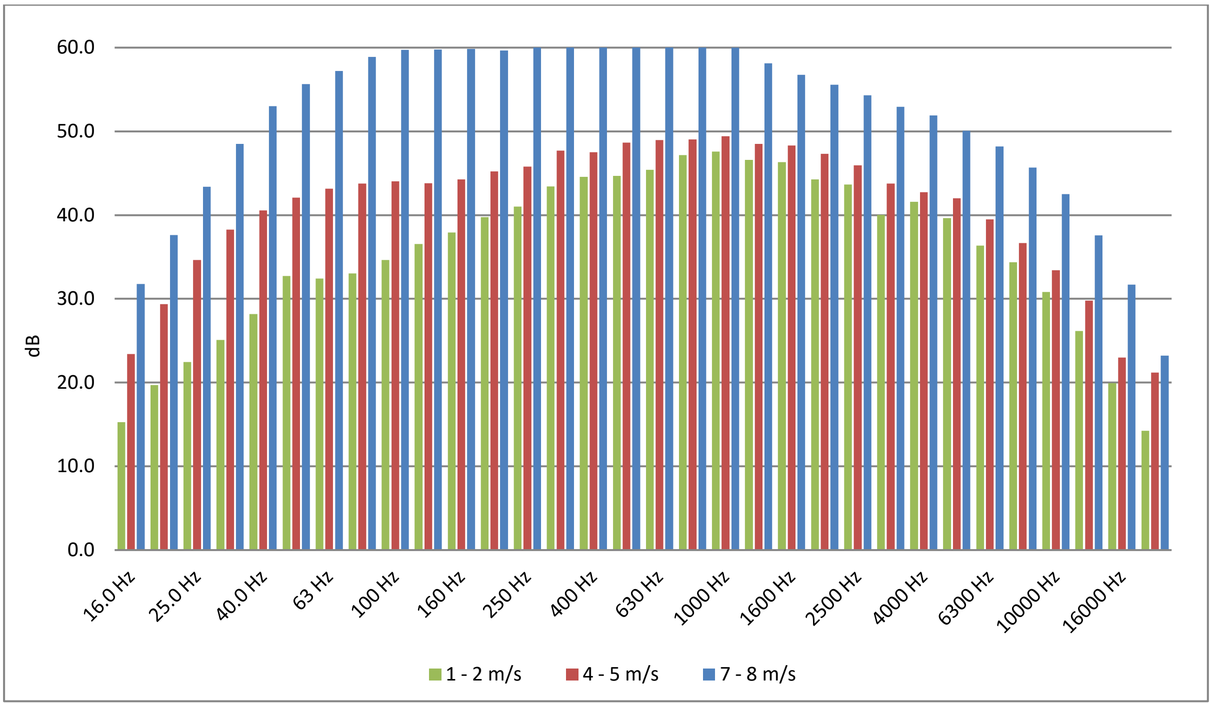

Figure 68 shows a comparison of operational $^{1}/_{3}$ octave noise level results recorded at low, average and high wind speeds at the LSBU turbine monitoring position. An increase in low frequency content is observed with increasing wind speed.

Low frequency noise from turbines can typically be attributed to changes in wind speed experienced by the blades due to the mast and wind shear, although wind shear may not be hugely applicable in such a relatively small scale blade diameter. The spectral content of this noise is dominated by the blade passing frequency and the harmonics there of.

Looking at 4 m/s wind speed with a rotor diameter of 5.5 m and manufacturer rated RPM of 100 the turbines BPF would be 10 Hz as calculated using Equation 1. Observed low frequency noise at the turbine position demonstrates harmonics of this fundamental BPF. Trailing edge noise due to the interaction of the turbulent boundary layer and turbine blades trailing edge is a major source of higher frequency noise from turbines, harmonics of which may be the contributing factor to the increase in high frequency content at higher wind speeds.

Propagation of induced turbine noise into this area will be discussed through the application of computational simulation in the following paragraphs to investigate the expected noise levels in the local area using the recorded levels at the turbine monitoring position. Worst case and average level scenario sound power levels at the turbine position will be investigated using CadnaA by Datakustik noise mapping software to produce a visual noise map at residential areas.

CadnaA software was chosen as is it regarded as a robustly accurate environmental noise propagation modelling tool. As part of a road traffic noise assessment Renzo Tonin & Associates released a paper at the 2008 Australian Acoustical Society conference presenting agreement in results between CadnaA, empirical measurements and other established software packages. Case studies of varying complexity were run to compare CadnaA's results and compared to measured results. The results accuracy was shown to be within ± 2.7 dB and ± 5 dB with an 85 % and 95 %

confidence interval, respectively. It was therefore deemed suitably accurate to conduct the noise propagation requirements of this project.

CadnaA calculates noise propagation in line with the procedures and calculations outlined in ISO 9613 'Attenuation of sound during propagation outdoors' with the accuracies presented in Table 27.

Height (h)	Distance (d)	
	0 < d< 100 m	100 m < d < 1000
0 < h < 5 m	± 3 dB	± 3 dB
5 m < h < 30 m	± 1 dB	± 3 dB

Table 27: Estimated Accuracy of Calculation Results Achieved in line with ISO 9613

A 3D model generated to simulate wind flow around the campus was imported from SketchUp into CadnaA where a 1 x 1 m grid calculation area at a 1.5 m microphone height was set up to reflect physical monitoring positions. Further receiver points and building evaluation[10] points were assigned to monitoring positions and nearest residential buildings.

The turbine was modelled as a point source above a hard plane.

Firstly, a worst case scenario will be investigated. The highest SPL recorded at the turbine monitoring position was 74 dB at a distance of 12.5 m. As a worst case scenario is being investigated a directivity factor of 1 will be used, however it is more likely to be close to 2 as the turbine is situated above a large, hard, reflective surface. The directivity factor (Q) allows for consideration of a sound sources directivity and therefore variations in sound pressure level propagation at varying angles surrounding the source. When the source, or receiver, is in close proximity to a reflecting surface the surface will alter the apparent directional properties and power radiated from the source (Bies and Hansen, 1996). In reference to previous investigations in Section 3.3.1 where the blade tips are viewed as independent, moving point sources then the intensity is independent of the angle around the source and the directivity factor becomes used to assess the level increase due to the sources location in respect to reflecting surfaces. Therefore directivity factor values from (Bies and Hansen, 1996) can be used to best suit the turbines location.

Using these parameters a worst case *Lw* of 106.9 dB is used and the resulting noise map is presented in Figure 69, which shows lower noise levels than recorded in the same positions. This suggests that background environmental noise other than the turbine to be the main contributing factor at these levels.

Predicted levels at the nearest residential properties were in the region of 50-59 dBA, above background noise levels, measured in the area of 50-55 dBA.

Table 28 presents an evaluation of these results compared to relevant criteria outlined in Chapter 2.

[10] Please refer to the Resources Nomenclature for a definition of CadnaA's 'building evaluation' parameter.

Assessment	Criteria	Compliance
ETSU-R-97	5 dB above background levels	No
BS4142	10 dB below background levels	No
WHO	55 dB	Yes
PPG24	NEC B	n/a - Conditions should be imposed
NPPF / LA	10 dB below background levels	No

Table 28: Overview of Highest Turbine Noise Levels Compared to Relevant Criteria.

Table 28 demonstrates that if only turbine noise were to be considered levels would not qualify for the majority of assessments, likely to be viewed as having an impact upon local residents and appropriate action or conditions would be advised. This suggests a likelihood of annoyance, especially when factoring in the new introduction of low frequency blade pass frequency noise[11]. However, noise levels were simultaneously recorded at street level to be higher than those at the turbine level. This along with the turbine noise not being audible at street level for the majority of attended monitoring suggests other environmental factors to be the main contributor of noise including turbulent wind flow due to local topography. A more typical scenario is now assessed using an average SPL of 60.5 dBA. This gives an extrapolated Lw of 90.4 dB with a directivity of 2. Simulating these values produced Figure 70. This time, predicted noise levels are significantly lower than measured, as are the predicted building evaluation levels at the nearest residences. The results compared to relevent standards are presented in Table 29.

Assessment	Criteria	Compliance
ETSU-R-97	5 dB above background levels	Yes
BS4142	10 dB below background levels	Yes
WHO	55 dB	Yes
PPG24	NEC A	Not considered a determining factor
NPPF / LA	10 dB below background levels	Yes

Table 29: Overview of Average Turbine Noise Levels Compared to Relevant Criteria.

This suggests other environmental factors to be the main contributors to the noise levels recorded in the area. The results presented in Table 29 demonstrate the likelihood of annoyance from turbine induced noise is low. Further simulations revealed that at SPLs below 66 dBA not only will levels at the nearest residential buildings be within acceptable noise exposure category limits, but will also fall well below background noise measurements taken at street level and therefore not pose a risk of annoyance. Levels above 66 dBA were only recorded at wind speeds above 6 m/s, were only recorded for 13 % of the time[12].

[11] Please refer to Section4.2.3
[12] Taken from a data set of 103141 results.

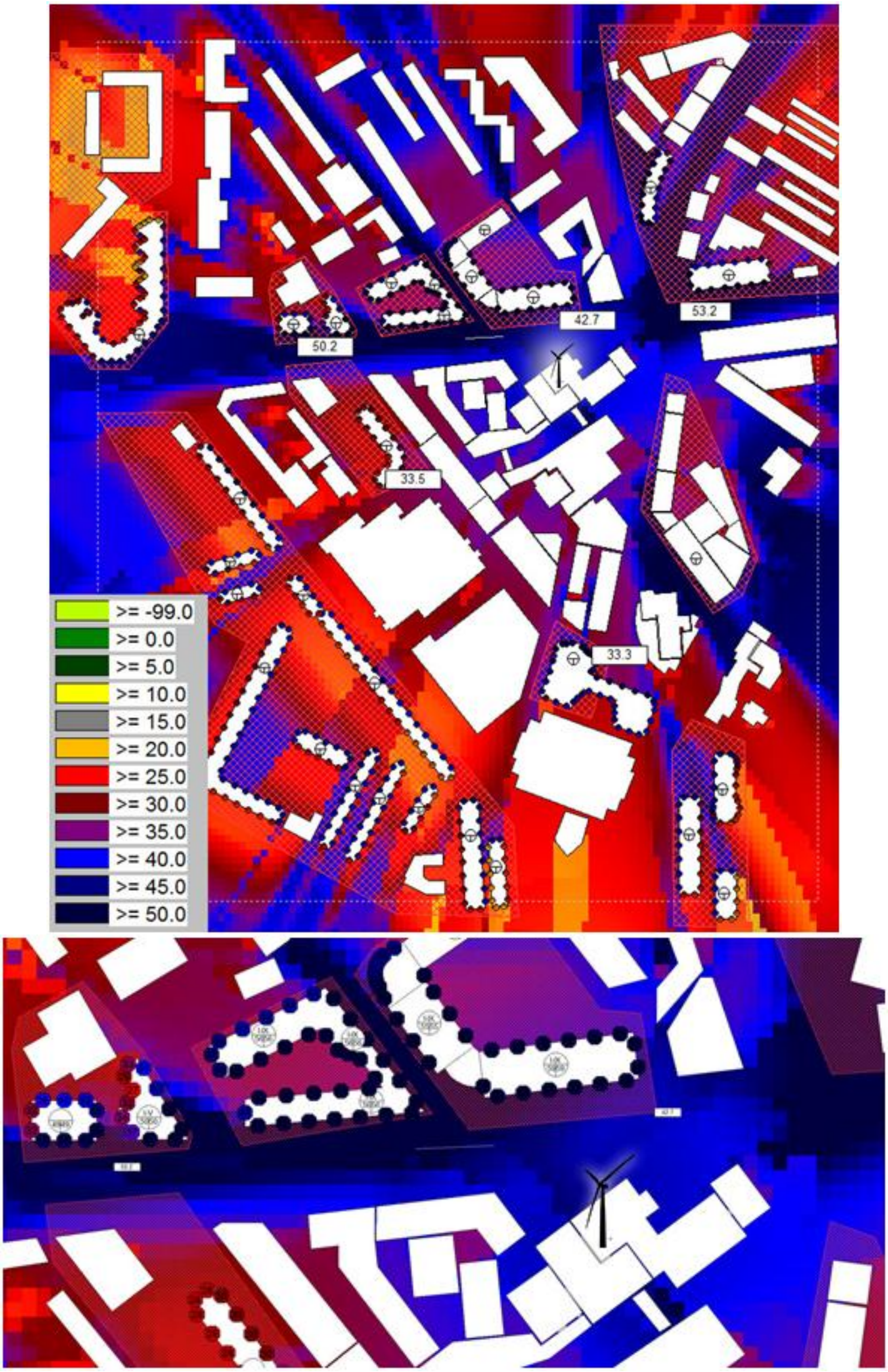

Figure 69: Worst case, operational turbine, scenario L_{Aeq} grid calculations of propagated sound into LSBU residential areas.

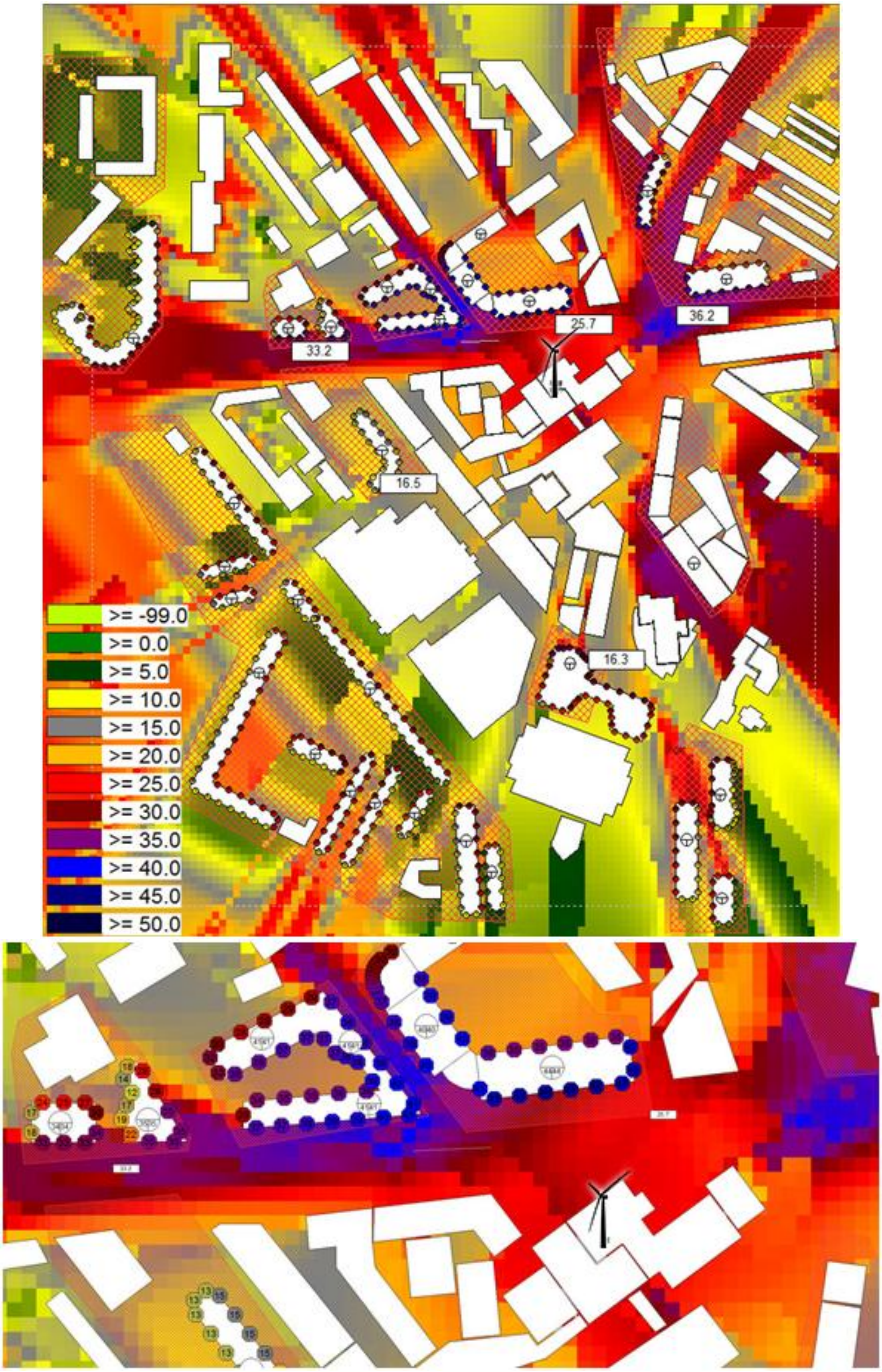

Figure 70 - Displays averaged L_{Aeq} grid calculations of propagated sound into LSBU residential areas.

Environmental measurements and simulations have shown that noise levels from the LSBU turbine will only likely disturb the immediate residents for the higher range of local wind speeds over 6 m/s, experienced approximately for 13 % of the time, and that local environmental noise sources will be the main contributing factors in the local aural environment. LSBU is a university so the working comfort of its employees needs to be assessed. Two main pathways of noise propagation into the top floor of the building will be investigated:

- Directly through the structure of the building. i.e. through the roof level into the offices below.
- From the rooftop around the building and into the offices via the windows.

The LSBU turbine rests upon a concrete plant room resting atop of a concrete roof with direct transmission paths into the main building. Knowing the rooftop to be made of 300 mm concrete slabs with a known density of ~2600 kg/m^3 a superficial mass (surface density) value of 780 kg/m^2 can be calculated. This can be used to calculate a sound reduction per frequency band. The results displayed in Table 30 demonstrate that a significant reduction in sound levels can be expected due to the extensive concrete mass between the turbines and lower maintenance level.

Freq Hz	**$L_{w,K}$ Octave Average**	**$L_{w,K}$ Octave Worst**	**R**
31.5	63.7	75.4	39.8
63	63.7	75.4	45.8
125	64.1	73.6	51.8
250	63.5	66.2	57.8
500	69.3	69.3	63.8
1000	78.8	78.8	69.8
2000	77.9	77.9	75.9
4000	55.5	64.7	81.9
8000	46.9	61.8	87.9
m	780	**kg/m^2**	
ρ	2600	**kg/m^3**	
t	0.3	**(m)**	

Table 30: Displays R values for the LSBU concrete rooftop along with average wind speed noise levels and worst case scenario noise levels.

As well as direct transmission paths from the turbine through the roof into the lower levels noise levels can be estimated entering the buildings areas via diffraction around the outside of the building and in through the glazed office windows, using Equation 17 and Equation 20. A +3 dB penalty is added to Equation 20 for external to internal noise values as the turbine is located upon a hard reflective surface.

$$SPL = L_{w,k} - 20Log(r) + 10Log(Q) - 11 - D_{Atten} + F_{cor}$$

Equation 17: Used to calculate sound pressure levels at distance from a known sound power level where: $L_{w,k}$ = sound power, r = distance, Q = directivity factor, D_{Atten} = Diffraction Attenuation, F_{cor} = Facade Correction = 3 dB.

$$D_{Atten} = 10Log(3 + 20N)$$

Equation 18: Used to calculate Diffraction Attenuation where N = Fresnel Number.

$$N = \frac{2\delta}{\lambda}$$

Equation 19: Used to calculate Fresnel Number (N) where **δ** = path difference, **λ** = wavelength.

$$L_2 = L_1 - R + 10Log(S) - 10Log(A)$$

Equation 20: Used to calculate internal noise levels due to transmission loss via a partition. Where L2 = Internal noise level (dB), L1 = sound level at the turbine. In relation to R = sound reduction of the partition (dB), S = surface area of partition (m2), A = absorption in the receiving room.

Internal (Lin)and external (Lout) results calculated at the Tower Block turbine are shown in

	Hz	**63**	**125**	**250**	**500**	**1000**	**2000**	**4000**	**8000**
Office External	**Lturbine**	63.7	64.1	63.5	69.3	78.8	77.9	55.5	46.9
	Lout	20.4	18.1	14.5	17.4	23.8	20.0	-5.5	-17.1
	Lin	14.3	6.8	0.7	-0.7	-1.4	-12.6	-45.9	-59.3
Office Direct	**Lturbine**	63.7	64.1	63.5	69.3	78.8	77.9	55.5	46.9
	Lin	20.5	15.7	12.6	14.2	16.4	8.2	-22.1	-32.4
Office External	**Lturbine**	75.4	73.6	66.2	69.3	78.8	77.9	64.7	61.8
Worst Case	**Lout**	32.1	27.6	17.3	17.4	23.8	20.0	3.8	-2.2
	Lin	26.0	16.3	3.5	-0.7	-1.4	-12.6	-36.6	-44.4
Office Direct	**Lturbine**	75.4	73.6	66.2	69.3	78.8	77.9	64.7	61.8
Worst Case	**Lin**	32.2	25.2	15.3	14.2	16.4	8.2	-12.8	-17.6

Table 31. All relevant surface area, material make up and absorptive values for internal surfaces, needed to utilise Equation 20 along with theoretical results for direct sound transmission and flanking external levels transmitted through the lower office windows are displayed in APPENDIX G.

	Hz	63	125	250	500	1000	2000	4000	8000
Office External	$L_{turbine}$	63.7	64.1	63.5	69.3	78.8	77.9	55.5	46.9
	L_{out}	20.4	18.1	14.5	17.4	23.8	20.0	-5.5	-17.1
	L_{in}	14.3	6.8	0.7	-0.7	-1.4	-12.6	-45.9	-59.3
Office Direct	$L_{turbine}$	63.7	64.1	63.5	69.3	78.8	77.9	55.5	46.9
	L_{in}	20.5	15.7	12.6	14.2	16.4	8.2	-22.1	-32.4
Office External Worst Case	$L_{turbine}$	75.4	73.6	66.2	69.3	78.8	77.9	64.7	61.8
	L_{out}	32.1	27.6	17.3	17.4	23.8	20.0	3.8	-2.2
	L_{in}	26.0	16.3	3.5	-0.7	-1.4	-12.6	-36.6	-44.4
Office Direct Worst Case	$L_{turbine}$	75.4	73.6	66.2	69.3	78.8	77.9	64.7	61.8
	L_{in}	32.2	25.2	15.3	14.2	16.4	8.2	-12.8	-17.6

Table 31: Displays calculated internal noise levels due to direct transmission and external, propagated noise levels at the LSBU office in closest proximity to the operating Tower Block turbine.

The worst case scenario in Table 81 and Table 82 represents levels measured at wind speeds over 6 m/s, which only happened for 13 % of the measurement period. Averaged and worst case scenario levels for both externally and directly transmitted pathways are calculated to adhere to National Planning policy Framework, WHO environmental health criteria and ETSU-R-97 daytime guidelines. It is noted that externally transmitted sound in the worst case scenario would infringe upon these guidelines if the building were occupied for sleep during the night, which it is not and therefore such enforcements are not applicable.

It should also be noted that both average and worst case scenario externally transmitted pathways are calculated to fall into Noise Exposure Category B if the windows are open, which is not likely due to the higher wind speeds (and therefore higher noise levels) are to be expected in the winter months when warmth is craved over a cooling breeze. But due to the low level of noise predicted no discomfort, distraction, or annoyance is expected.

At wind speeds up to 4 m/s background noise levels from other sources are shown to dominate the local noise environment. At speeds above 4 m/s a significant increase in low frequency noise was demonstrated, likely from in-flow turbulence and blade passing frequency broadband noise due to speed fluctuations and turbulent flow from the tower and passing blades. A slight increase in high frequency content was also demonstrated due to harmonics of tip vortex formation and trailing edge noise. Worst case scenario simulations were investigated using the highest recorded turbine monitoring position noise levels. This produced noise levels at the nearest offices in excess of background noise measurements by up to 5 dB, therefore demonstrating a likelihood of annoyance.

The same simulations run with average noise levels show that turbine noise was predicted far below the thresholds and criteria outlined in relevant criteria when compared to the measured background noise levels in the area (~20 -30 dB below) demonstrating that no likelihood of annoyance would be expected. As worst case conditions were only measured for 26 % of the time at the windiest and therefore noisiest time of year the author feels the likelihood of annoyance from turbine induced noise is low.

4.3 Vibration

4.3.1 LSBU rooftop vibration

Vibration measurements were taken simultaneously on the LSBU turbine mount and the concrete mass beneath the mast. A total of 30,071 data points were recorded between 13/05/13 and 28/11/13 and 17,280 data points recorded between 1/10/14 and 5/1/15.

The measurements consisted of 5 minute averaged RMS accelerations in X,Y,Z directions whereby X is perpendicular, Y parallel and Z vertical to the source. VDV, as well as peak acceleration data was captured and synchronised to the on-site collected atmospheric data, which is displayed in Figure 71. X and Y RMS acceleration results have been omitted as no correlation between them and wind speed was observed (as seen in Table 32), and recorded levels were extremely minimal. It should be noted that results could not be recorded continuously between the periods mentioned as the equipment was moved between sites of interest to capture further vibration data as discussed in chapter 4.3.2. Methodology and meter position is discussed in chapter 3.4.2.

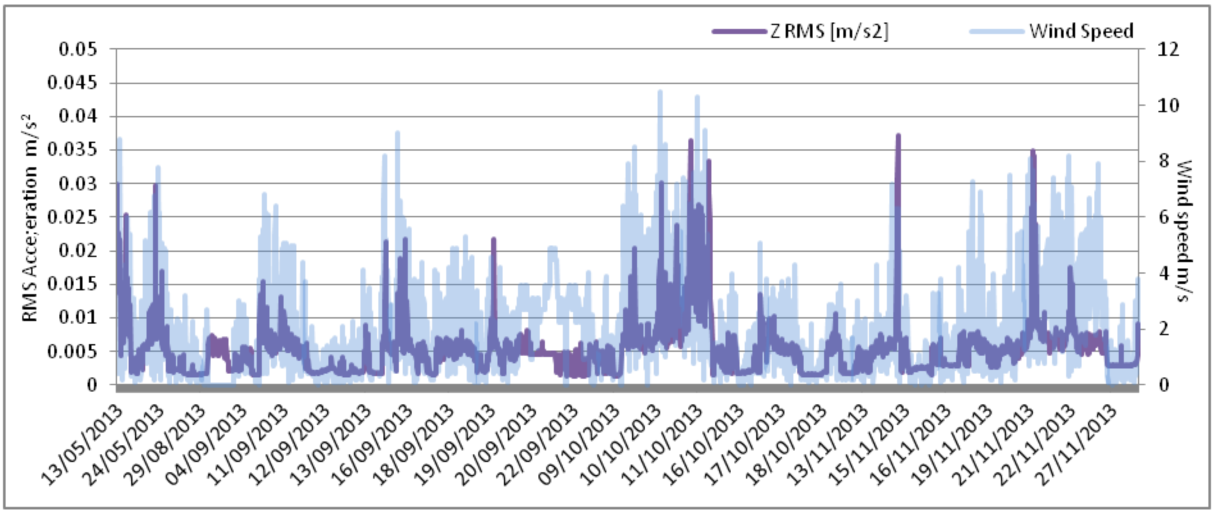

Figure 71: Displays Z-axis RMS acceleration measurements taken at the LSBU turbine mount compared to measured wind speeds. Measurements were taken between 13/05/13 - 28/11/13.

	X RMS [m/s^2]	Z RMS [m/s^2]	Y RMS [m/s^2]	Wind V [m/s]
X RMS [m/s^2]	1.0			
Z RMS [m/s^2]	0.0	1.0		
Y RMS [m/s^2]	0.6	0.0	1.0	
Wind V [m/s]	0.1	**0.4**	0.1	1.0

Table 32: Displays a correlation between wind speed and RMS acceleration on the Z axis of the turbine mount.

Wind can be a source of vibration on tall buildings through gusts induced turbulence on the facades and buffeting and vortex shedding due to air separation around the structure. To investigate any sign of this happening any correlation between wind speed, direction and vibration was investigated.

Although not considered particularly strong (> 0.5) some correlation was observed between Z axis RMS acceleration vibration levels and wind speed is found at the turbine mount and the concrete roof top, as shown in Table 32 and Figure 73. When comparing these simultaneous measurement positions, see Figure 72, a general damping is observed as all levels on the roof top are lower in comparison to those directly monitored at the turbine mount. There is no installed damping or isolation beneath the turbine, although it was requested, therefore this is most likely due to the mass of the concrete structure the turbine is mounted on, see Figures 74 and 75. Appropriate isolation design is offered in chapter 7.1. These results will be further discussed in chapter 4.3.2.

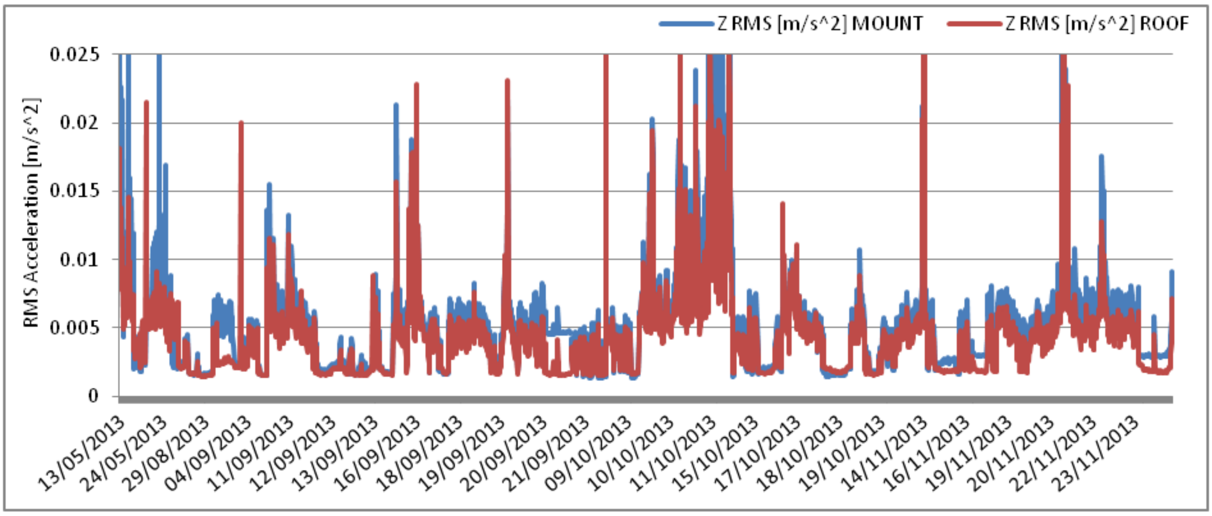

Figure 72: Compares simultaneous Z axis RMS acceleration levels recorded at the LSBU turbine mount and rooftop.

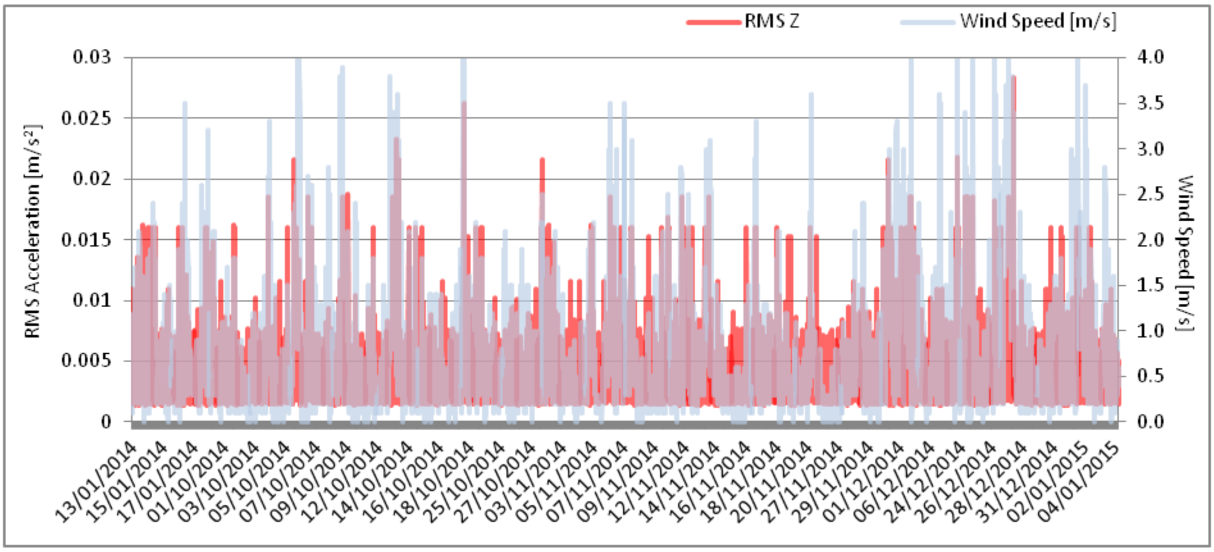

Figure 73: Turbine mount vibration measurements at LSBU, taken between 1/10/14 - 5/1/15.

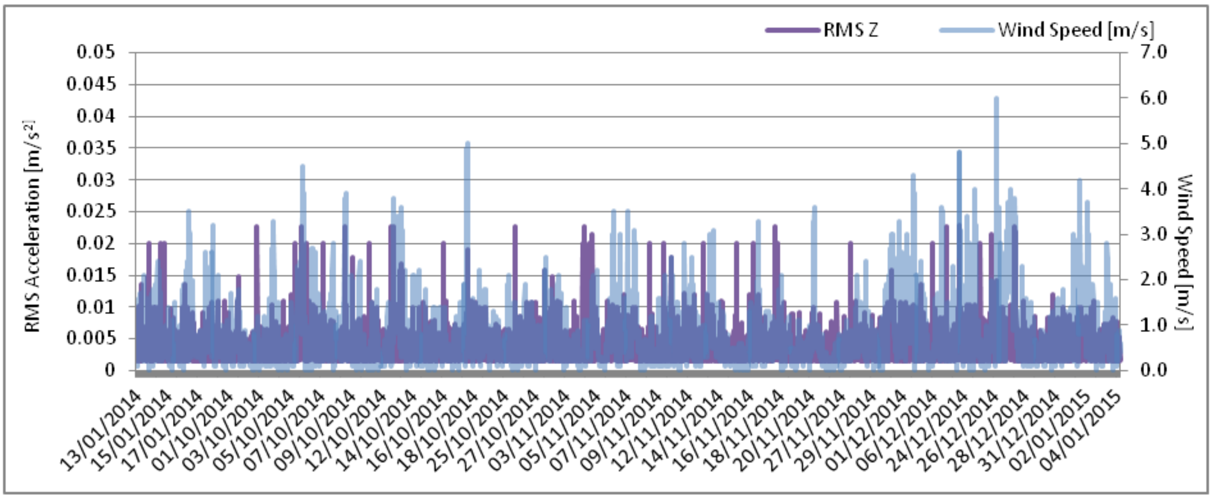

Figure 74: Displays RMS acceleration recorded at the LSBU turbine roof top between 1/10/14 - 5/1/15.

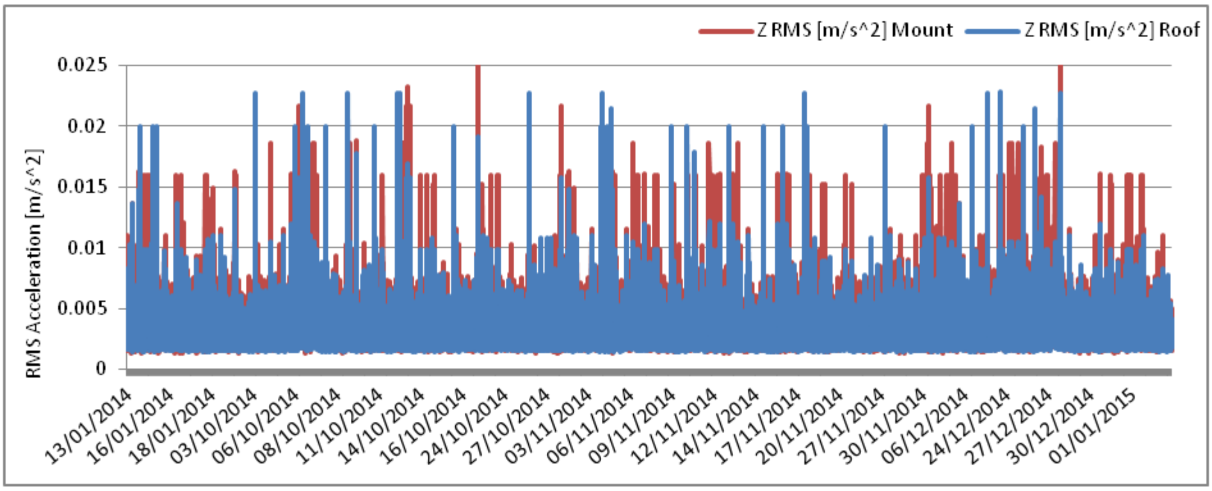

Figure 75: Compares Z axis RMS acceleration recorded at the turbine mount and rooftop positions.

4.3.2 LSBU site & LSBU annoyance case study (T610)

A correlation between wind speed and acceleration was observed in the previous section 4.3.1. The lack of appropriate isolation at the turbine mount allows for observed structural transmission to the roof top, albeit at diminished levels. This attenuation is attributed to the mass of the concrete roof top upon which the turbine is installed. The levels recorded at the rooftop are far below standard guidelines listed in BS6841 and ISO2631, where levels below 0.35 m/s^2 RMS acceleration are not considered to be a threat to comfort. As the turbine is installed on the LSBU Tower Block roof top, two levels (approximately 6 m) above any occupied office space and hence the possibility of annoyance is insignificant, however during periods of high wind speeds, vibrations were reported within the Tower Block that were not seemingly present prior to the turbine installation. These vibrations presented as computer monitors, windows and table-top rattling. These visual effects had a negative effect on the working environment and were a cause for concern.

The LSBU Tower Block, including the roof top plant room, stands 40 m tall and is made up of a ground floor student centre, second level cafeteria and then a following eight office levels before reaching the ninth floor maintenance level/roof top which gives access to an extra tenth level plant room, upon which the turbine is installed. An interesting quirk of the observations was that they were only reported from the fifth and sixth floors of the Tower Block, with no reported vibrations observed or felt in the floors directly under the turbine or the first few floors of the building, the eight floor is full of academics from the School of Engineering. The reports indicated the vibration was intermittent and seemingly coincided with periods of strong winds. It was not reported as continual or to coincide with any other, known, external or internal factors. Access was granted to monitor within one of the offices (T610) where vibration had been observed on the sixth floor of the Tower Block and vibration meter was set up in periods of anticipated high winds over the winter months of 2013 and 2014.

As human response to vibration is more sensitive in the Z axis accelerometers would ideally be mounted on the floor. However, it was not possible to do so in an occupied office space due to measurements being skewed or interrupted by walking, chair scraping or the risk of equipment being a trip hazard. Therefore an accelerometer was mounted to the inner side of an external wall of the office, which leads directly up to the turbine level. This was deemed adequate as any structurally transmitted vibration would most likely be through this direct path. Other than this, methodology, equipment set up and mounting procedure are as outlined in Chapter 3. The results are presented in Figure 76 to Figure 79 and Table 33 - 36.

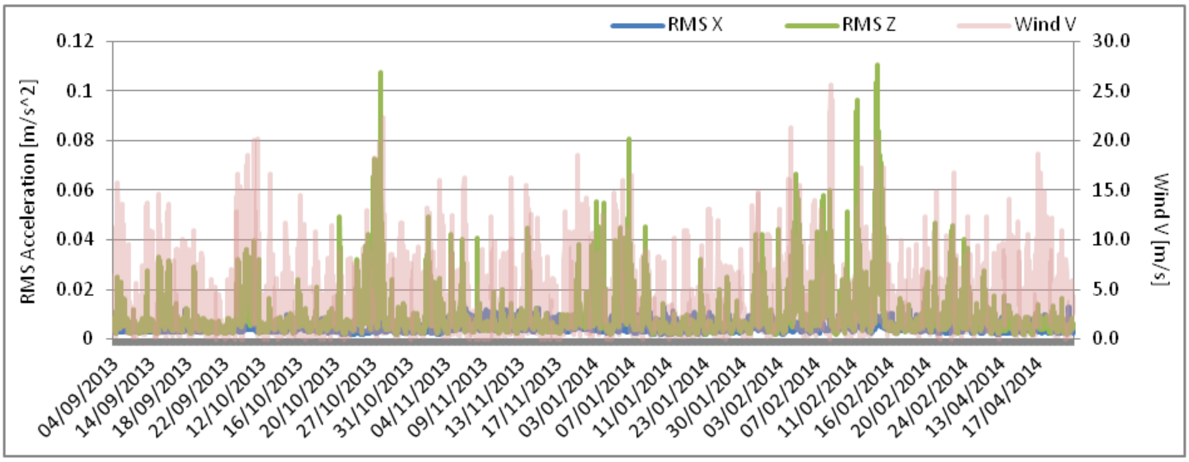

Figure 76: Displays RMS acceleration recorded at the LSBU T610 office external wall and compared to recorded LSBU wind speeds for the 2013 - 2014 winter period.

RMS	X	Z	Y	Wind Speed
X	1.0			
Z	0.0	1.0		
Y	0.3	0.2	1.0	
Wind Speed	0.0	0.8	0.1	1.0

Table 33: Displays a correlation (r) between Z axis RMS acceleration and wind speed for winter 2013- 2014.

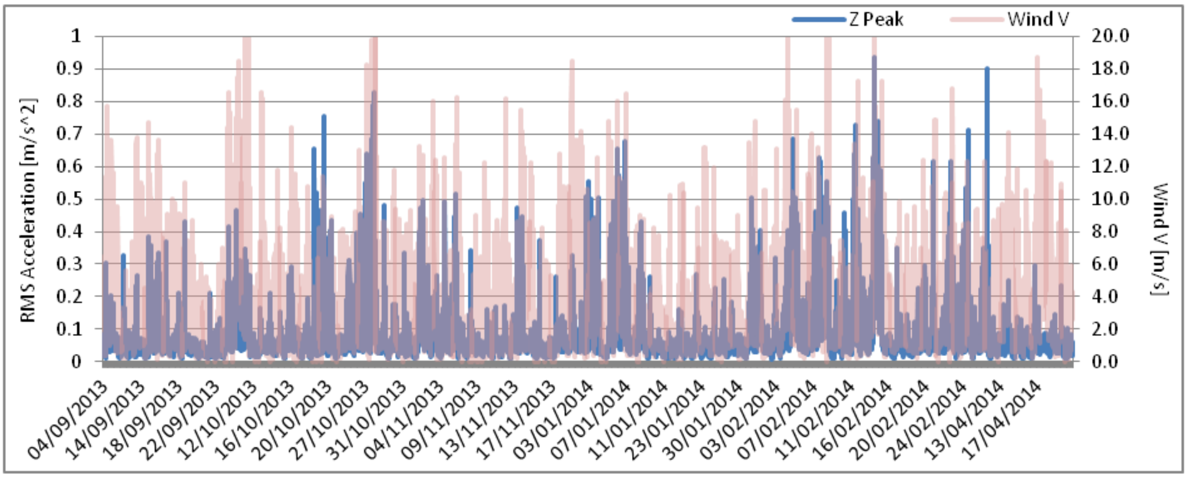

Figure 77: Displays peak RMS acceleration levels recorded at the LSBU T610 office external wall and compared to recorded LSBU wind speeds for the 2013 - 2014 winter period.

Peak	X	Z	Y	Wind Speed
X	1.0			
Z	0.0	1.0		
Y	0.3	0.3	1.0	
Wind Speed	0.0	0.7	0.1	1.0

Table 34: Displays a correlation (r) between Z axis peak RMS acceleration and wind speed for winter 2013-2014.

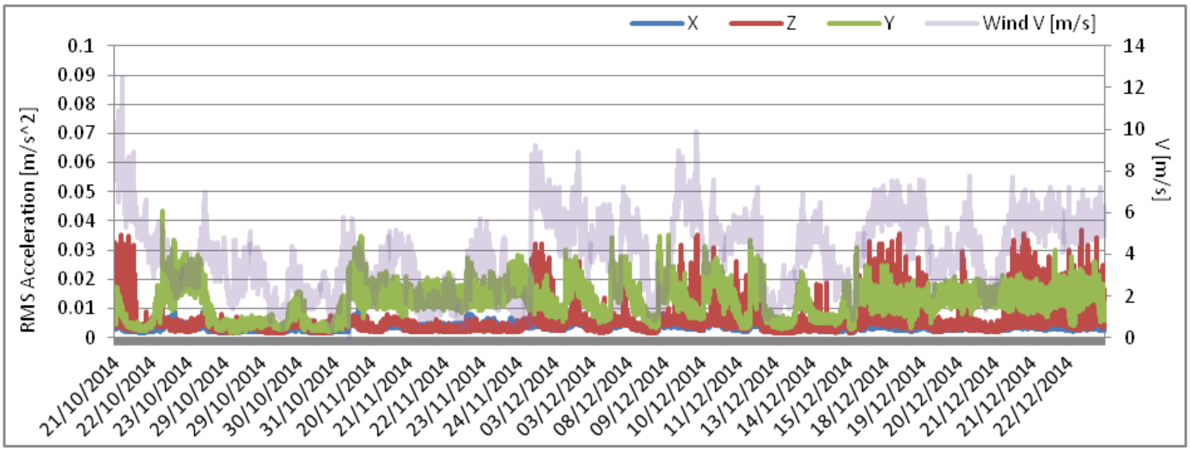

Figure 78: Displays RMS acceleration recorded at the LSBU T610 office external wall compared to recorded LSBU wind speeds for winter 2014 - 2015 period.

RMS	X	Z	Y	Wind Speed
X	1.0			
Z	0.3	1.0		
Y	0.5	0.6	1.0	
Wind Speed	0.0	0.7	0.1	1.0

Table 35: Displays correlation (r) between Z axis RMS acceleration and wind speed for winter 2014- 2015.

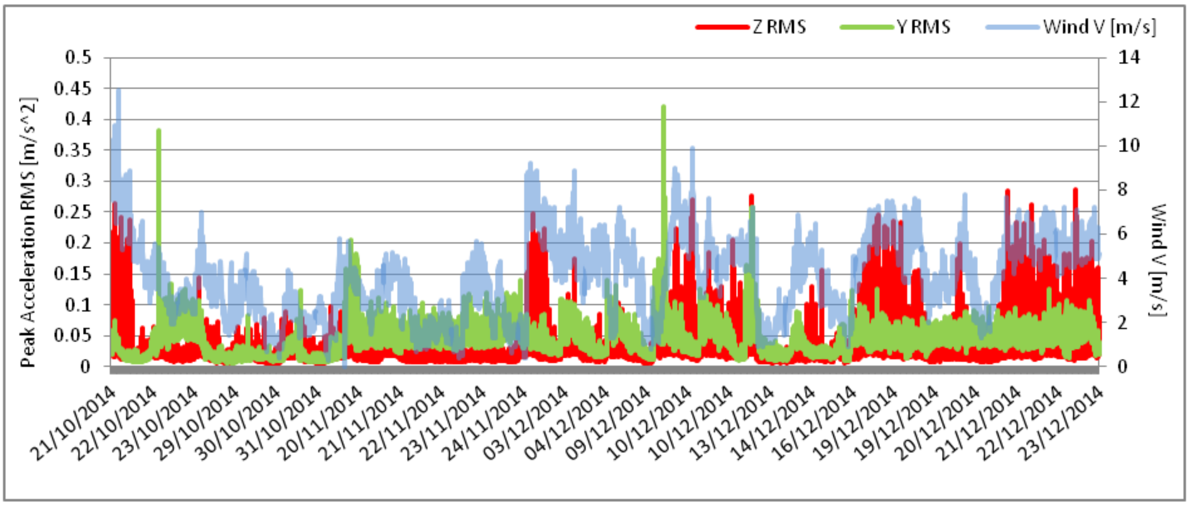

Figure 79: Displays Peak RMS acceleration recorded at the LSBU T610 office external wall compared to recorded LSBU wind speeds for winter 2014 - 2015 period.

Peak	X	Z	Y	Wind Speed
X	1.0			
Z	0.4	1.0		
Y	0.5	0.8	1.0	
Wind Speed	0.0	0.5	0.1	1.0

Table 36: Displays correlation (r) between Z axis peak RMS acceleration and wind speed for winter 2014- 2015.

Figure 76 - 79 show a strong correlation between Z axis acceleration levels and measured wind speed. This indicates that the wind turbine, which was operational during these periods, is most likely to be the cause of the observed vibration levels. It should also be noted that the correlation is stronger in the 2013 - 2014 winter period where recorded peak wind speeds consistently exceeded those in the 2014 - 2015 period. This suggests that at lower speeds there is likely to be a threshold wind speed, below which the turbine could operate without contributing towards any excessive vibration within the Tower Block office levels.

RMS acceleration levels were then binned into 1m/s categories and assessed as displayed in Figure 80. Figure 80 averaged RMS acceleration values per wind speed bin do not raise concern for human discomfort or likelihood of complaint as averaged levels are far below minimum thresholds outlined in BS6841:1987 and ISO2631. However, when averaged Peak acceleration levels are analysed an odd disparity in acceleration and wind speed bin is demonstrated as levels flitter and fluctuate in a seemingly inverse manner to RMS acceleration levels.

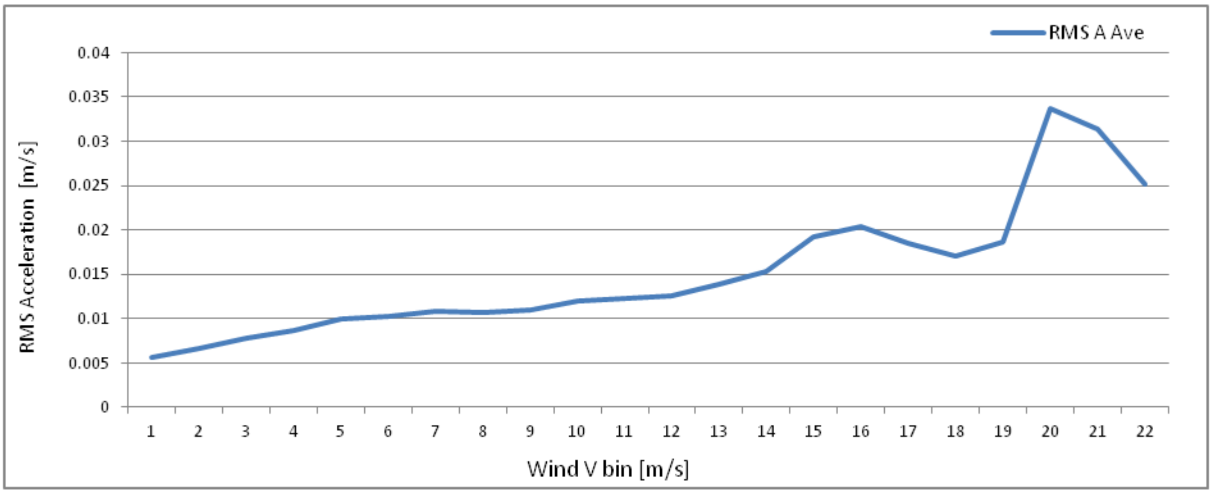

Figure 80: Displays averaged RMS acceleration levels per wind speed bin recorded in 2014-2015. A proportionate increase to wind speed in demonstrated.

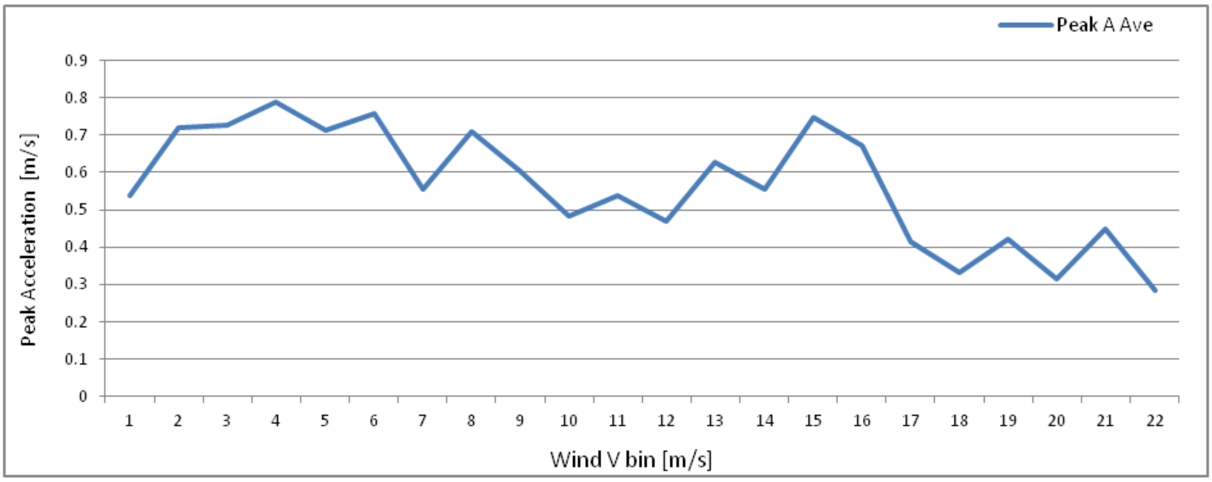

Figure 81: Displays averaged Peak acceleration levels per wind speed bin recorded in 2014-2015. No strong correlation is present attributed to unknown gust speeds due to averaging of results over the 10 minute wind speed measurement interval.

This was further investigated by plotting Peak acceleration as a function of wind speed as presented in Figure 82, which shows that in spite of a clear trend of increasing RMS acceleration level per wind speed Peak acceleration levels do not adhere to this trend or, in this case, make sense. Wind direction was then plotted against Peak acceleration to see if the direction correlated to Peak levels which, as Figure 82 demonstrates, it did not. Wind direction was consistently recorded to flitter between south west and west-south westerly directions.

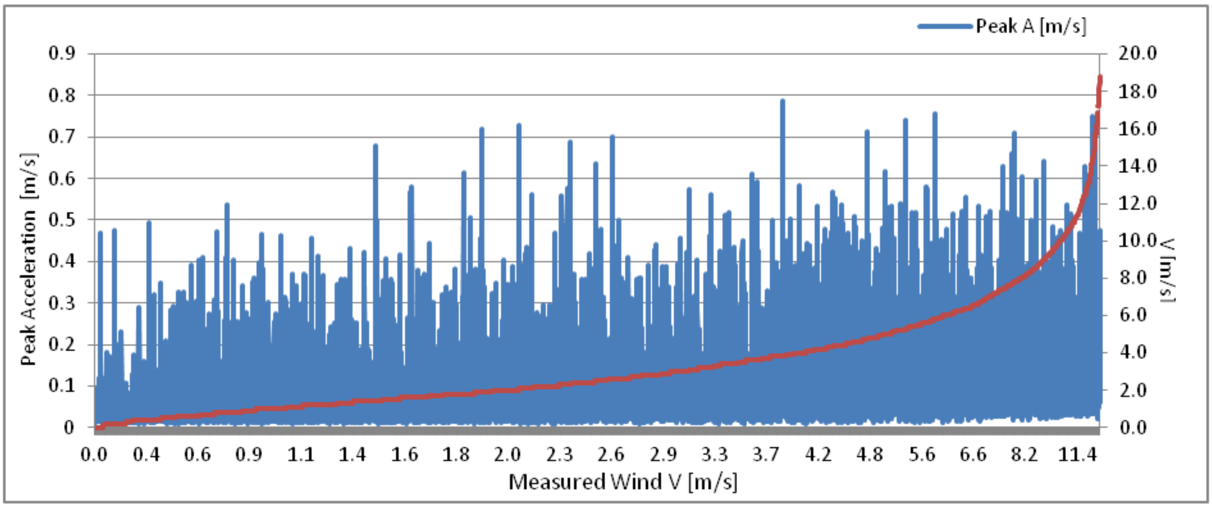

Figure 82: Displays peak acceleration levels plotted as a function of wind speed. Peak levels would usually be expected to be in coherence with wind speed but due to stronger gust speeds being absorbed into averaged wind speeds levels the correlation is lost.

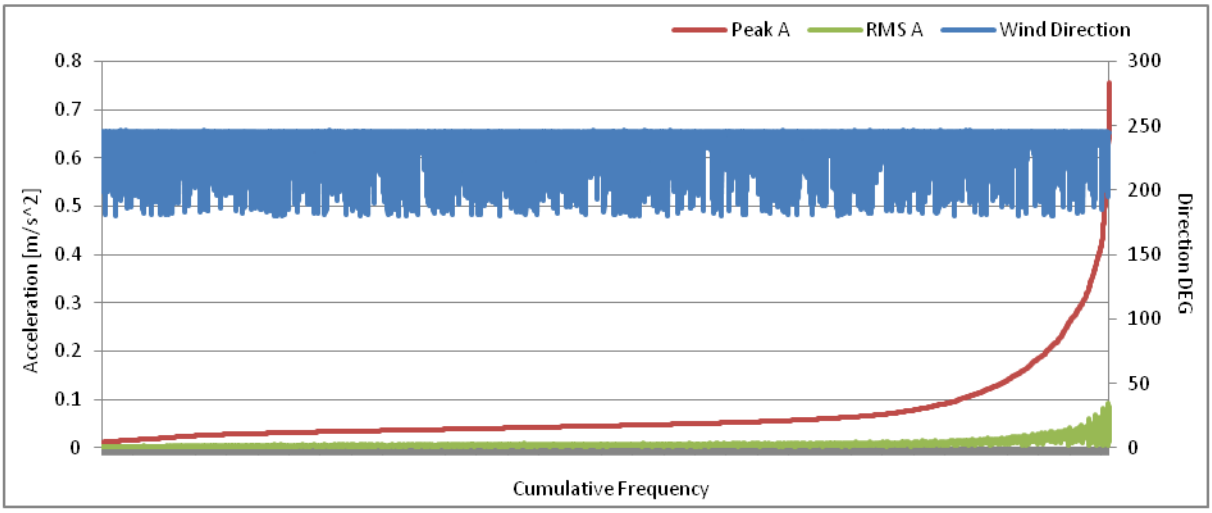

Figure 83: Displays wind direction plotted as a function of Peak and RMS acceleration for 2013-2014. No correlation is seen.

The problem with the Peak acceleration measurements are attributed to a couple of known issues relevant to the measurement periods. The installed anemometry can only offer a maximum resolution of 10 minute averaged recordings. This was considered too long a measurement period to capture the fluctuating nature of the wind and therefore it was agreed to capture 5minute synchronised vibration measurements and to assess all recordings taken within each wind speed period. The problem lies in that these time periods will discriminate against transient or impulsive phenomenon. When it comes to vibration measurements it is true that this 5 minute window will give scope for peak levels to be absorbed into a lower RMS or VDV value but the Peak information is simultaneously logged and extractable for analysis. However, the 10 minute wind speed periods do not allow any 'peak' wind speed logging thus condemning any high speed gusts to be diluted and absorbed into a lower mean wind speed. This was an unfortunate limitation of the weather monitoring instrumentation.

This would explain the wildly fluctuating Peak per wind speed readings observed in Figure 82; a low averaged RMS level, well within the thresholds outlined in BS6841:1987 and ISO2631, could contain measured, short lived, problematic peak levels. But when these results are aligned with an equally averaged wind speed the same corresponding peaks in wind speed, likely to be caused by the knock on effects of higher speed gusts of wind, would be absorbed and averaged out over the time period therefore a higher peak level could be associated with a lower wind speed. These levels should most likely be attributed to a gust of high speed wind, but without a higher resolution of wind speed data, this is just conjecture.

These measurements are adequate enough to underline a problem that needs to be addressed, but is not useful in determining a threshold wind speed or to derive any operational suggestions for the turbine. All that could be summarised from the findings thus far are that the turbine is directly causing peak vibration levels likely to cause complaint and discomfort and no greater details of optimisation could be offered than to shut it down. Ideally a higher resolution anemometer would be installed in an effort to capture higher resolution data to be synchronised to higher resolution vibration data and to re-investigate Peak acceleration per wind speed bins. Unfortunately, due to a lack of resources it was not possible to install such a system but efforts were made to implement a more effective investigation. We could not raise the wind speed resolution but could the vibration. Therefore, for the following winter 1 minute interval vibration data was recorded.

The intention was to get a deeper insight into the fluctuations in Peak acceleration per averaged wind speed period. By assessing 10 vibration levels for every 1 wind speed measurement it is hoped to filter the anomalies to establish consistent Peak acceleration level to the averaged wind speed, define a baseline background acceleration level and observe peak acceleration levels for any likely gusts that may have occurred within the wind speed period (even if the accompanying wind speed is an unknown). The principal behind the method is that if a low average wind speed is recorded and 9 out of the 10 vibration levels are of a proportionally low level (with only one high peak) then they can most likely be deemed an accurate representation for the recorded speed, with the 1 outlier more than likely to be the result of a higher 'gust' wind speed and therefore omitted from the result. Vice versa, if a high wind speed is recorded and the more frequently occurring peak vibrations are proportionally high then this can be viewed as appropriate correlation and the minority lower peak values can be cast as the produce of lower wind speeds and omitted. Therefore the following procedure will be applied to a total of 4608 results logged, results will be:

- 1 minute vibration and 10 minute wind speed measurements are synchronised. Due to technological limitations, 1 minute was the shortest interval available for automatic logging. A shorter duration result would have been more desirable in order to capture a higher resolution representation of vibration activity.
- Maximum and minimum peak values are logged to show what vibration would be experienced at times of high gusts and lulls in wind activity.
- The mode of peak values is determined to represent the typical vibration activity associated with the recorded wind speed.
- Values outside of a ten percentage bandwidth are eliminated. A ten percent bandwidth was chosen as representative of the most frequently occurring or 'typical' vibration levels experienced within the measured wind speed time frame. Various bandwidths were investigated as shown in APPENDIX G and it was found that raising this bandwidth has the effect of lowering the acceleration values by incorporating far lower values than the mean. As it is our intention to find the likely levels of vibration associated with wind speed (and therefore the rotational speed of the turbine blades) and relate them to likelihood of discomfort or complaint from occupants it would be detrimental to under estimate these acceleration values.
- The remaining values centred around the dataset mode are summed and then averaged.

For the purposes of this report this procedure will be referred to by the authors procedural acronym pet-name: 'MAPS' method (Mode. Averaged. Percentage band. Summed). The results of the MAPS method are displayed in Figure 85 along with maximum and minimum peak acceleration results for comparison and discussion.

Firstly wind direction was plotted against recorded wind speeds to ensure that, as observed in the previous winter's data, the erratic results could not be attributed to this. Once again it was observed that no wind direction held no bearing over vibration levels as displayed in Figure 84.

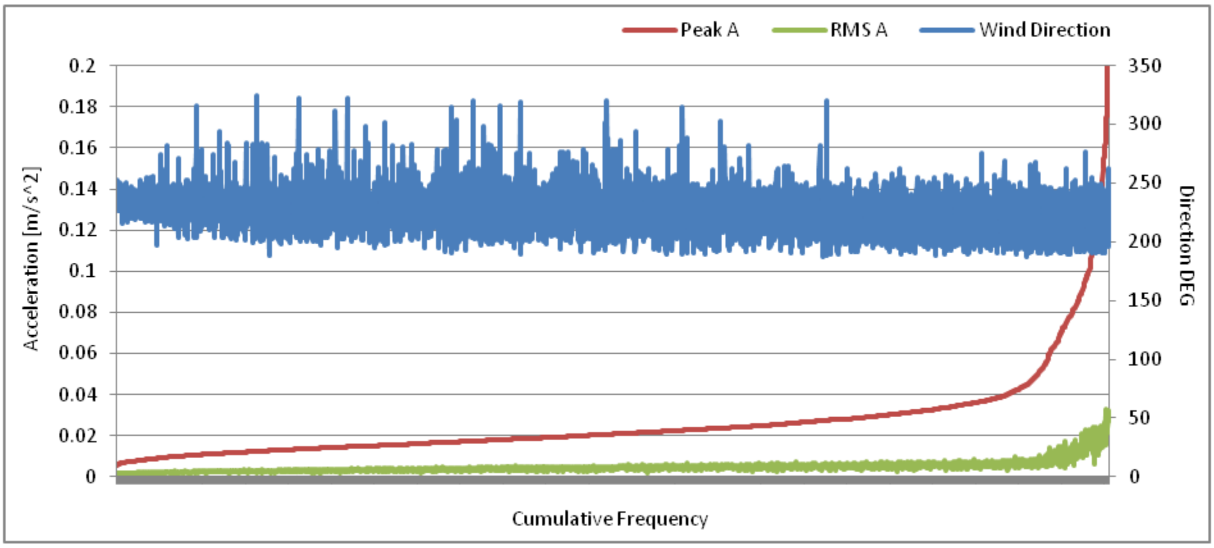

Figure 84: Displays wind direction plotted as a function of acceleration for 2014-2015. No correlation is observed.

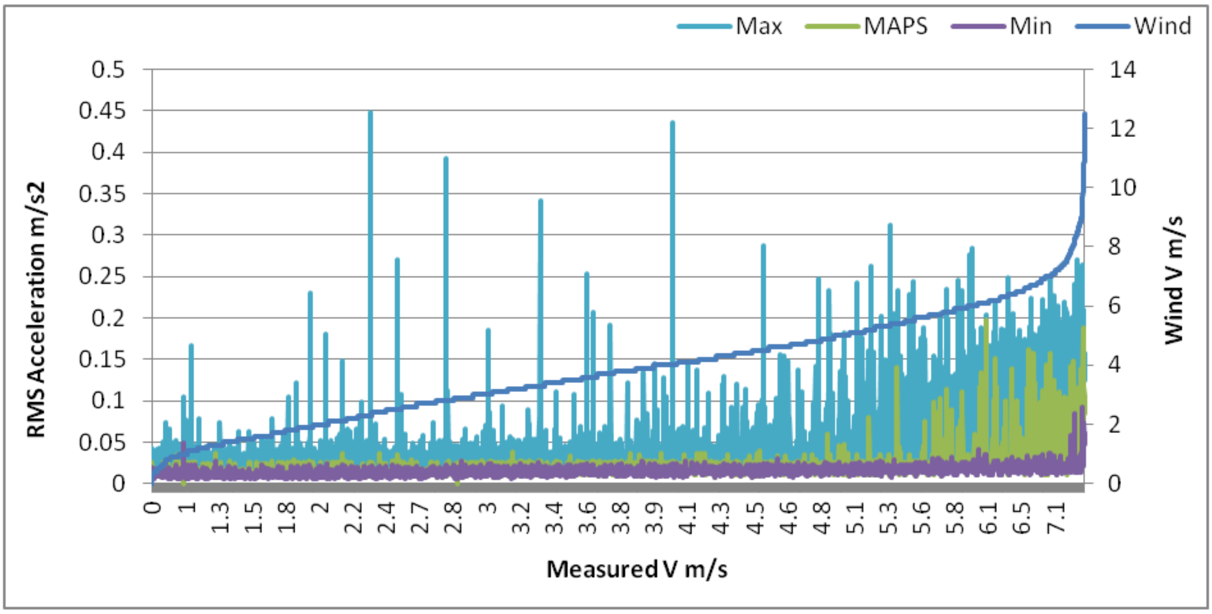

Figure 85: Displays the MAPS peak results calculated using higher resolution 1 minute interval vibration data with the same, low resolution 10 minute wind speed data. Data is compared with maximum and minimum peak levels plotted as a function of wind speed.

As is seen from Figure 85 the MAPS Peak line follows a more realistic trend as a function of wind speed than the maximum or minimum peak levels do for the same period. There are still a few fluctuations in results, but overall a more refined model of increasing peak levels per wind speed increase is presented. There are still some wild fluctuations present in Figure 85; maximum levels plotted are still somewhat erratic in places but minimum levels barely fluctuate or show any sign of correlation with wind speed. It is therefore assumed that the maximum levels represent intermittent, short lived gusts of wind, lost in averaging. While minimum results represent other environmental activity within the office; occupants, heating, ventilation etc.

It is regrettable that the winter, over which these results were monitored, proved to be, on average, calmer than the previous year, as the data set is lacking in wind speeds over 12 m/s, a speed that was often exceeded in the previous winter. Stronger vibration levels were previously observed at higher wind speeds and a better ruling of suggested cut-out speeds could be offered with a more extensive and varied data set. It is clear, however from these results, that as wind speed approaches 7 m/s peak acceleration starts to exceed levels of 0.2 m/s, a threshold of 'low probability of adverse comment' as defined by BS6841:1987 and ISO2631. It is therefore assumed that any speeds in excess of this will raise vibration levels into more detrimental bands of discomfort.

This utilised MAPS method can only, for the moment without further data, prove to give an estimate of the wind regime in relation to vibration levels using the available data. As maximum recorded peak levels suggest, higher wind speeds (or gusts) were regularly observed that need to be quantified before any, more precise, guidelines are offered. However, from these preliminary results it is suggested that the wind turbine, as it stands without appropriate isolation or damping, should be limited to 7 m/s wind speeds to prevent a risk of discomfort from office occupants on the 6th floor of the LSBU tower block.

Another interesting factor to consider is that not only were the results in the office significantly higher than those measured at the turbine mount but it was only the occupants on the 5th and 6th floors who reported any disruptive vibration and even on these levels it was only occupants whose offices lay directly beneath the turbine position. To investigate why, a more in-depth analysis of the building structure along with third octave acceleration results from the turbine mount and T610 office was conducted.

Results were organised into wind speed bins to assess if the frequency signature changes with increasing speed. It was found at the turbine mount that the signature did not differ a great deal spectrally but amplification in 10 Hz, 12.5 Hz, 16 Hz, 31.5 Hz and 50 Hz bands were observed as shown in Figure 86. The 10Hz resonance is attributed to the turbines blade passing frequency of 10 Hz at 200 RPM.

The blade passing frequency of the turbine system needs to briefly be reiterated. The turbine is rated at an RPM of 200 RPM, measured at a wind speed of 5-6 m/s. It is important to note that this is the rated speed and not an upper cap, governed RPM or full RPM. It can and will rotate at faster speeds in stronger winds although having an in-built blade-pitch mechanism to lower blades angle of attack in extreme weather conditions. At 200 RPM the blade passing frequency would be 10 Hz, which would contribute towards the amplified 10 Hz band measurements observed at greater wind speeds. There is also the 12.5 and 16 Hz band resonant peaks to account for, which lay very close to the turbines rated blade passing frequency. In fact 12.5 Hz and 16 Hz would equate to a 250 RPM and 320 RPM, respectively. Both of these figures are likely and achievable for this system. The 12.5 Hz resonance is observed at both the turbine mount and T610 measurement positions but due to the relatively low transmission levels is not likely to be problematic,. The 16 Hz band however, could prove troublesome when considering the structural make up of Tower Block. The section of Tower Block we are considering is essentially a concrete box. It's longest side, from the turbine mounted plant room to the lower level building, is approximately 30 m long using 3600 m/s (Engineering Toolbox, 2015) as the measured speed of sound in concrete we can estimate it's natural frequency to be approximately 30 Hz. Unfortunately this happens to be very close to the second harmonic of the 16 Hz, high speed, blade passing frequency. As is depicted in Figure 88 the peak of the 1st mode of the 30 m side of the tower block falls right on the ceiling of the 5th floor and floor of the 6th. This could possibly explain the observed vibration on those levels.

This problem could further be exacerbated by the tower's latitudinal dimensions. The floors of tower block are also concrete and measure approximately 17.5 m wide which has a 1st mode natural frequency of: 54.3 Hz. Which could be excited by the 50 Hz band resonance observed at measurement positions, especially as it also coincides to be the third harmonic of the fundamental 16 Hz high speed blade passing frequency. The situation could potentially be worsened by the typical 5 m to 7 m parallel walls found in the offices lying directly beneath the turbine as the 1/2 wavelength of 16 Hz band and 3/2 wavelength of 50 Hz band are 5.22 m and 6.68 m, respectively, in air. If these vibrations were transmitted into the air, a standing wave resonance could further cause disturbance issues.

Figure 88 depicts Tower Block's layout and dimensions, Figure 86 and Figure 87 depict the resonant peaks measured at the turbine mount and T610 positions. A narrowband plot of acceleration would be more desirable to highlight the turbine's blade pass resonances and there transmitted effect into T610. Unfortunately, this functionality was not possible using the vibration meters available.

Appropriate isolation and damping has been offered in chapter 7.1., the installation of which, would overtly diminish the structural borne vibration discussed and eliminate any strong likelihood of occupational discomfort.

It would be desirable to obtain more quantitative evidence to confirm the structural resonances and their correlation to measured results at the turbine mount and T610 office space. This could be achieved via FEM of the structure, which would be outside the scope of this thesis. Further measurements to find the structures resonant frequencies could also be conducted using heavy weight impact hammers and accelerometer arrays. This was, unfortunately, also not possible due to access and budget restrictions as the building is occupied. Tests at other point in the building would not be an option as the results would only hold true over the entirety of the structure if it were a homogenous system, which we have already shown not likely to be the case as vibration issues were only reported in one specific area.

The MAPS method discussed and utilised within this chapter, although not a substitute for appropriate equipment set up, may be a useful tool for smaller scale sites where less expensive and more readily available anemometry equipment is available.

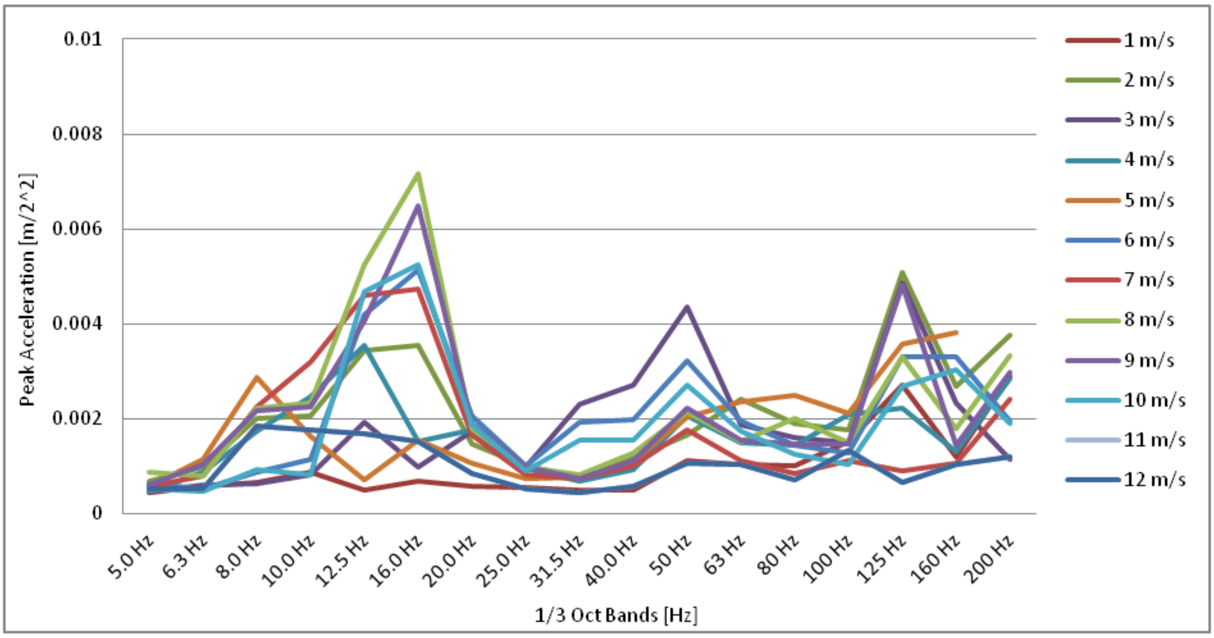

Figure 86: Displays X axis resonances observed at the LSBU turbine mount over 1 - 12 m/s wind speeds.

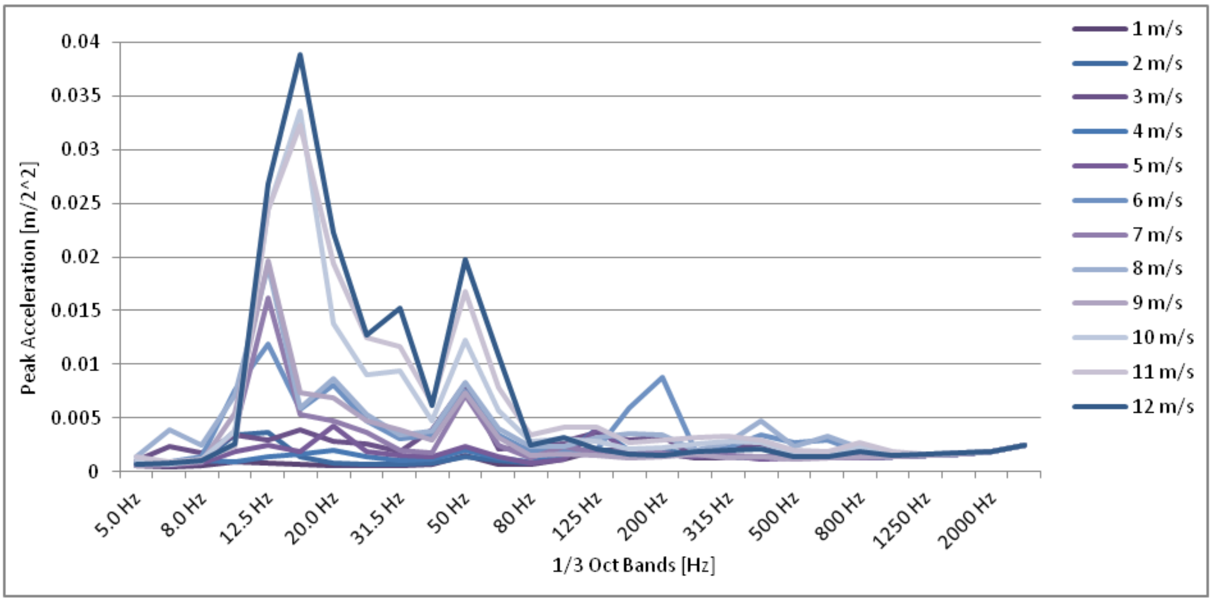

Figure 87: Displays resonance measured on the 6th floor of the tower block at increasing wind speeds.

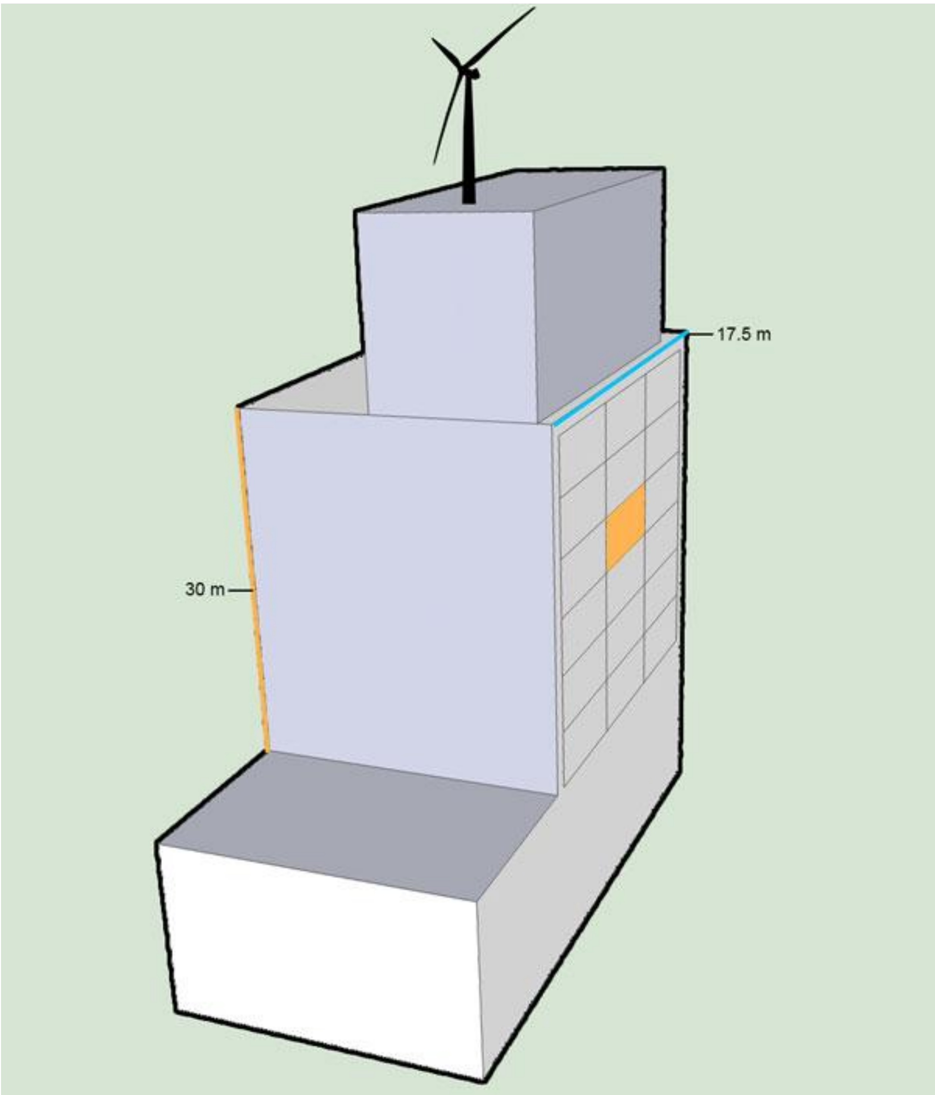

Figure 88: Displays the tower block dimensions in relation to the turbine, the T610 measurement office is depicted in orange.

4.4 LSBU turbine electrical power generation

It had been the intention of the author to install a purchased Bluetooth transmitter into the LSBU installed SMA Windy boy 6000A, which would have allowed Bluetooth communication between an external laptop and the inverters internal data logging system to remotely extract two weeks' worth of 5 minute interval electrical generation data. This could then be synchronised with LSBU recorded weather data to compose an accurate, site specific power curve for the installed Proven 6kW wind turbine. This could then be compared with the manufacturers marketing figures. Unfortunately, permission was denied to install the Bluetooth transmitter unless undertaken by the inverter installation company, so as not to negate a pre-existing maintenance contract. Permission was also not granted to hire in a member of the installation team to install the device before the already arranged annual site visit. In between this time period the maintenance company has ceased trading and the inverter has stopped working[13]. LSBU is currently in the process of setting up a new maintenance contract with an external company to service the turbine installation.

It was, however, possible for the author to take manual readings from the inverters external LCD. Unfortunately it was neither practical nor possible to climb up to the roof top to check the display every 5 minutes. The author therefore regrets that a detailed site specific power curve, power coefficient for the turbine or power output per wind speed bin to the manufacturers provided curve will not be possible for the purposes of this thesis. However, a week by week output will be compared to theoretical power output levels obtained by methods outlined below. This will aid in demonstrating the turbines performance, efficiency and suitability to the urban environment it has been placed within.

Wind speed and inverter output data will be evaluated over a two year period between 01/01/2013 to 01/01/2015. Firstly the LSBU recorded wind speed data is collected and organised into wind speed bins by frequency. The total amount of data collected is presented in Table 37.

A total of 103135 data points were recorded out of a possible 105120, showing a 2% loss of data over the two year period. The missing data is attributed to seldom time lapses but as can demonstrated in Table 37 these gaps are not concentrated in any particular month so a good overall impression of the local wind regime has been maintained. This wind data is then used with the turbine manufacturers power curve, Rayleigh and Weibull data to calculate the yield. The measured and predicted results are displayed in Table 38.

[13] Information correct as of 08/01/15.

2013	Data Available	Data Collected	Missing	Missing %
Jan	4464	4431	33	1
Feb	4032	3966	66	2
Mar	4464	4020	444	10
Apr	4320	4278	42	1
May	4464	4446	18	0
Jun	4320	4293	27	1
Jul	4464	4449	15	0
Aug	4464	4188	276	6
Sep	4320	4170	150	3
Oct	4464	4458	6	0
Nov	4320	4314	6	0
Dec	4464	4390	74	2
TOTAL	52560	51403	1157	2.2
2014	**Data Available**	**Data Collected**	**Missing**	**Missing %**
Jan	4464	4453	11	0
Feb	4032	3947	85	2
Mar	4464	4451	13	0
Apr	4320	4290	30	1
May	4464	4238	226	5
Jun	4320	4227	93	2
Jul	4464	4419	45	1
Aug	4464	4434	30	1
Sep	4320	4266	54	1
Oct	4464	4364	100	2
Nov	4320	4227	93	2
Dec	4464	4416	48	1
TOTAL	52560	51732	828	1.6

Table 37: Displays total 10 minute interval atmospheric data recorded over a two year period.

		Power Curve Yield kWh	Rayleigh kWh	Weibull kWh	Inverter O/P kWh	Ave Wind Speed m/s
2013	Jan	455	237	641	221	3.2
	Feb	629	398	413	271	3.8
	Mar	419	388	81	246	3.8
	Apr	554	342	489	233	3.6
	May	613	367	474	180	3.7
	Jun	306	274	67	188	3.4
	Jul	188	142	53	96	2.7
	Aug	255	189	93	46	3.0
	Sep	239	146	82	80	2.8
	Oct	313	227	99	157	3.2
	Nov	477	376	362	232	3.7
	Dec	272	187	95	120	3.0
	TOTAL	**4720**	**3273**	**2950**	**2070**	
2014	Jan	313	233	378	175	3.2
	Feb	392	360	99	273	3.7
	Mar	251	141	100	161	2.7
	Apr	312	241	376	244	3.2
	May	302	218	107	153	3.1
	Jun	300	228	86	180	3.1
	Jul	357	297	82	189	3.4
	Aug	272	209	352	137	3.0
	Sep	187	123	61	85	2.6
	Oct	277	174	85	150	2.9
	Nov	190	118	59	110	2.6
	Dec	514	425	143	241	3.9
	TOTAL	**3667**	**2766**	**1929**	**2098**	

Table 38: Displays the predicted and measured energy yield over a two year period against average wind speeds for each month.

The cells highlighted in red in Table 38 show a significant drop in energy yield not consistent with wind speed or predictions. This is due to an electrical installation being carried out in the inverter control room which required the inverter to be shut down for certain periods over the end of August and beginning of September.

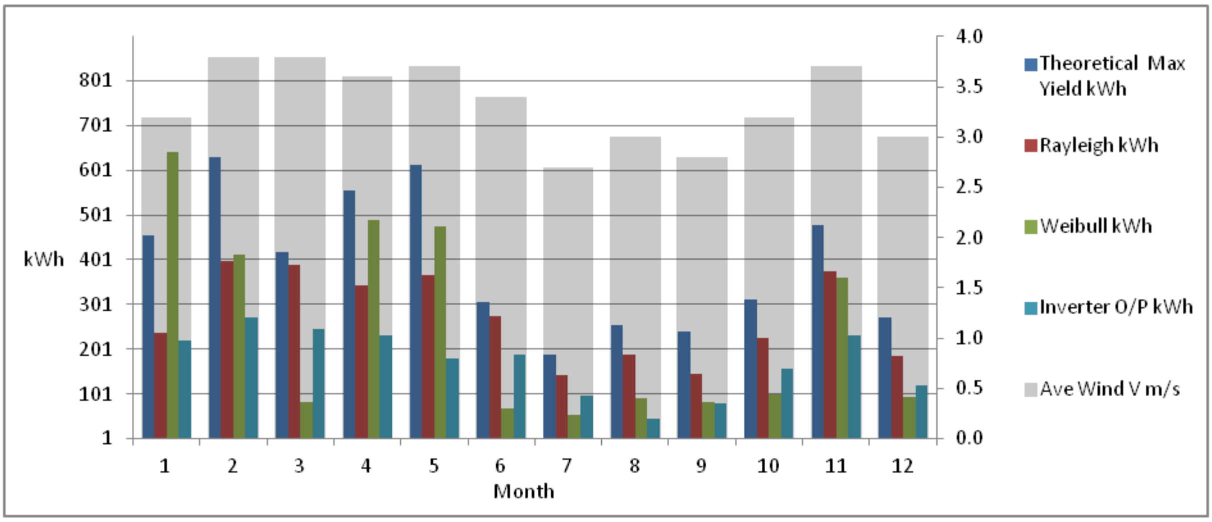

Figure 89: Displays monthly energy yield output, predicted and measured at the LSBU site for 2013.

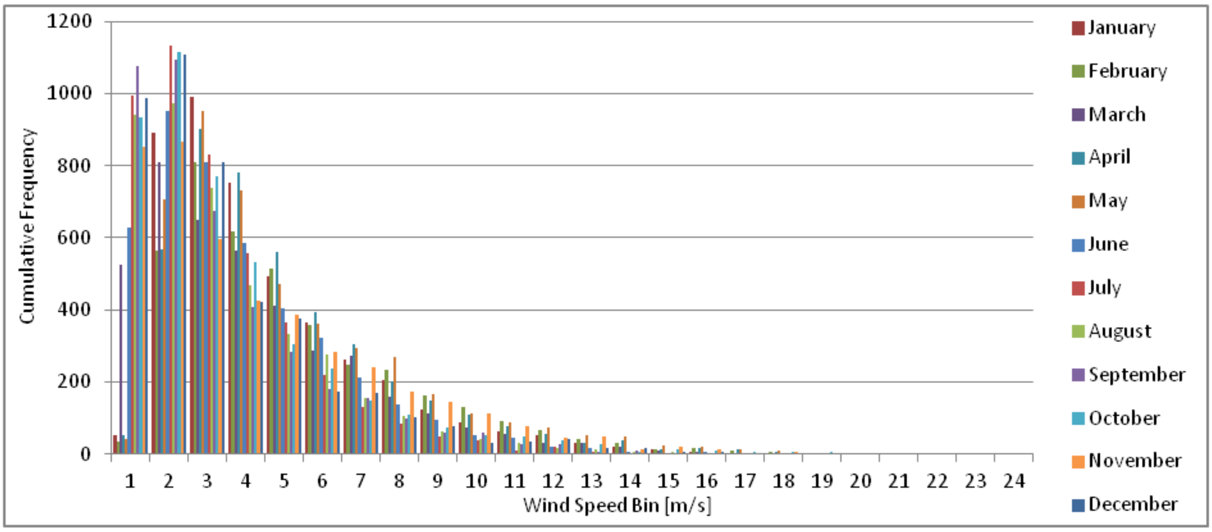

Figure 90: Displays 2013 annual wind speed distribution for each month at the LSBU turbine site.

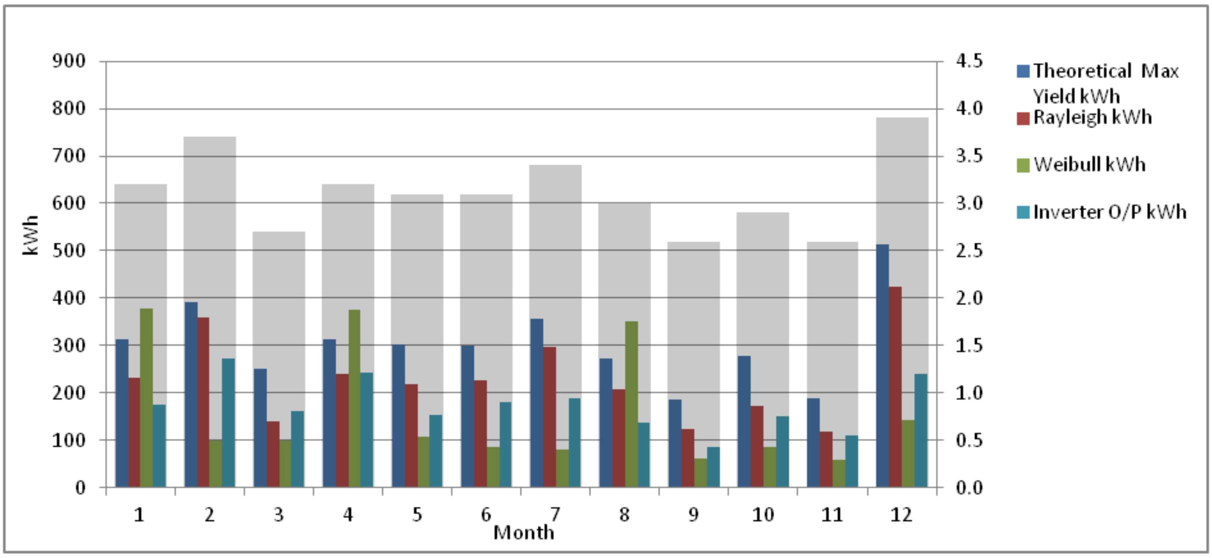

Figure 91: Displays monthly energy yield output, predicted and measured at the LSBU site for 2014.

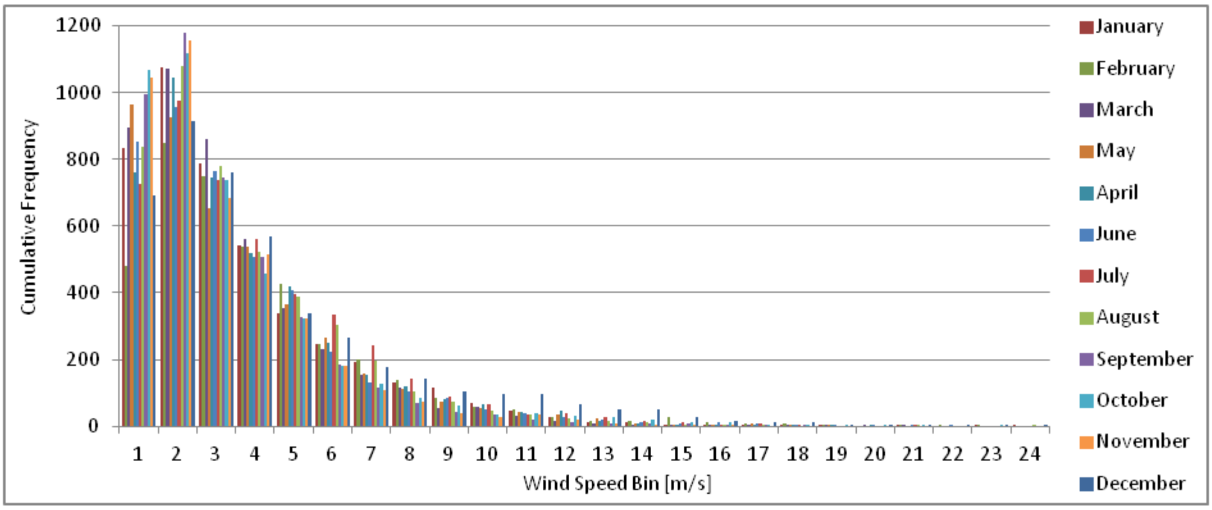

Figure 92: Displays 2014 annual wind speed distribution for each month at the LSBU turbine site.

When looking at Table 38 in spite of similar average wind speeds measured for each corresponding month of the year there are significant differences in predictions as well as recorded output. When further compared to Figure 89 to Figure 92 it becomes that apparent that in spite of similar average wind speeds, wind speed distribution differs from month to month. 2014's distribution demonstrates a higher concentration of low wind speeds including many under the cut in frequency (3 m/s) of the installed Proven 6Kw turbine. This would explain the lower yield for 2014. It also demonstrates the need for more information than just average wind speed when making an accurate energy yield prediction for a turbine installation.

From Figure 93 and Figure 94 we can further see that the Weibull curve is a better fit to actual recorded data with a slightly more peaked curve demonstrating a narrower distribution over lower speeds. The Rayleigh curve is not too dissimilar but deviates more from the actual recorded data distribution curve.

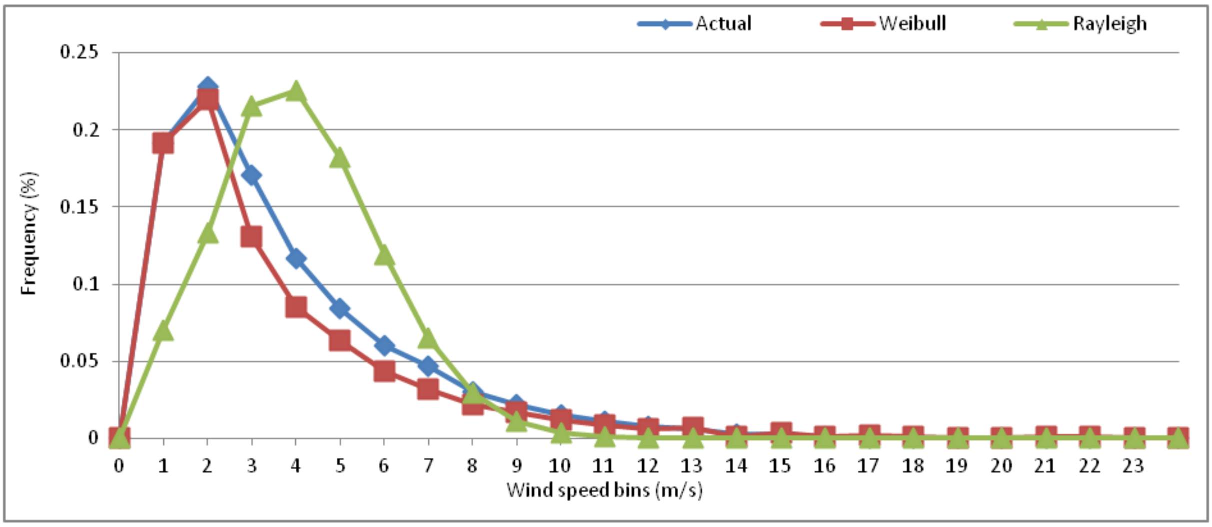

Figure 93: Displays measured, Weibull and Rayleigh predicted wind speed distributions at LSBU in 2013.

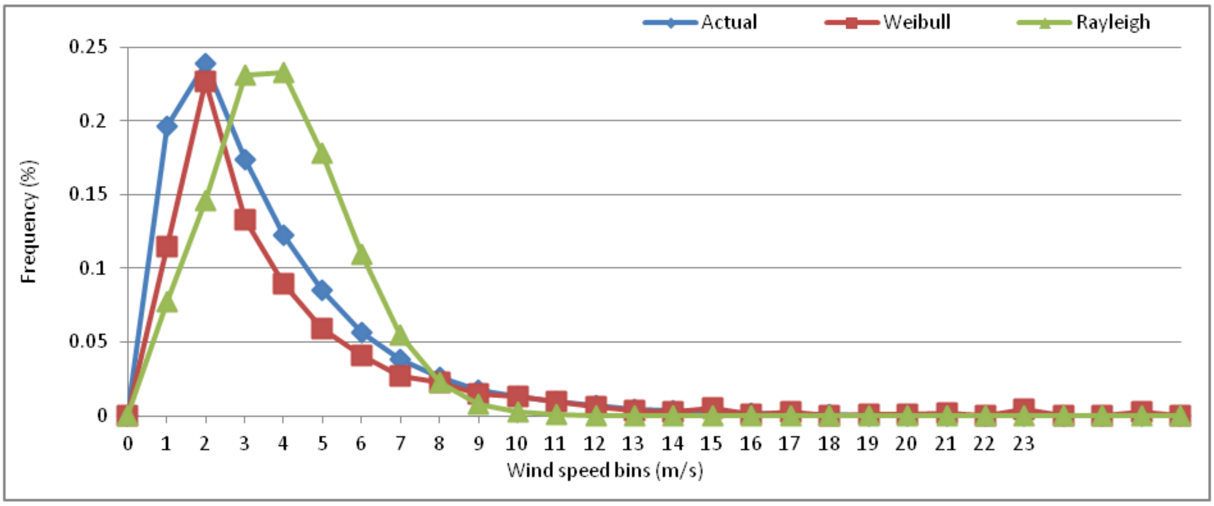

Figure 94: Displays measured, Weibull and Rayleigh predicted wind speed distributions for 2014.

A shift towards higher wind speed bins is demonstrated with its peak over the 3-5 m/s bins as opposed to the Weibull and actual data peaking over 2-3 m/s bins. This has a dramatic effect on the energy yield predictions for two main reasons:

1. Power in the wind is proportional to V^3 (as previously covered in Equation 6) i.e. the shift from 3 m/s to 4m/s may only increase speed by a factor of 0.33 but it will increase power by a factor of 2.35.
2. This shift crosses the installed Proven 6kW turbines cut in speed of 3 m/s. Therefore each over estimation of wind speeds above this cut in speed will lead to a direct over estimation of electrical generation.

It was previously discussed in Chapter 2 that the Weibull distribution is the most applicable and adopted function for wind energy as confirmed by Carta, Ramirez et al (2008) as it is a flexible and simplistic model with only two parameters (shape and scale). It was also shown that the Rayleigh method also had potential as a full time series wind data is not required and distribution predictions based on mean wind speed alone. Our results show that in our particular case the Weibull curve was a much better fit to recorded data and therefore energy predictions were also far closer to recorded data. Figure 93 and 94 show a shift in the Rayleigh peak over the turbines cut in speed, which therefore over estimates the turbine's production capabilities. As the Rayleigh method relies on average mean wind speeds rather than time series data it is possible therefore that two sites with the same mean wind speed could produce different yields. This is because the power in the wind is proportionate to V^3 and the average of the cube of different wind speeds could vary to the cube of the average wind speed. It is therefore advisable that the Weibull method with a full time series atmospheric data be used when estimating a wind regime and yield potential in an urban site where wind speeds are likely to be low due to local topography.

LSBU recorded energy yield is far lower than the manufacturers marketing material claim of 6 - 12 MWh as is the Weibull, Rayleigh and theoretical values estimated.

	Proven 6kW at 5.5 m/s kWh	Theoretical Max Yield kWh	Rayleigh kWh	Weibull kWh	Inverter O/P kWh
2013	6000	4720	3273	2950	2070
2014	6000	3667	2766	1929	2017
2013	**Capacity Factor %**	79	55	49	35
2014	**Capacity Factor %**	61	46	32	34

Table 39: Displays, the LSBU turbine site's predicted and measured output compared to manufacturer marketing figures.

The reasons for the significantly diminished levels displayed in Table 39 could be down to a few reasons such as:

- Electrical connections: Within the generator, the grid or inverter.
- Anemometry errors: The 3D ultra sonic anemometry used on the CEREB building lists an accuracy of up to +- 1 % where as the anemometer used on the LSBU tower block specifies up to +-3 %.
- Air density: Power in the air is proportional to air density and any fluctuations taken within measurements will effect expected outputs. Unfortunately, density data was found to be corrupt and not deemed reliable enough for inclusion in results.
- Idealised estimation: Manufacturers display their product in the best possible light; figures may come from idealised scenarios or theoretical outputs based on constant rotational speeds.

The final point would be the most significant contributor to the difference in energy levels as manufacturer power performance figures are measured in line with IEC61400-12-1:2005 'Wind Turbines - Part 12-1: Power performance measurements of electricity producing wind turbines', which recognises that even smaller wind turbines may not be able to fit into a wind tunnel so therefore proposes a testing procedure is conducted over a range of wind speeds, above what we have demonstrated the site to experience on a flat terrain with less turbulence. Manufacturer data shows that their power curves are calibrated to an average wind speed of 5.5 m/s, which is significantly more than the measured 3.7 m/s when considering the V^3 relationship with power.

The knock on, economic outcomes for these results will be further discussed and summarised in chapter 6.1.1.

Chapter 5 Strata Case Study

This chapter presents the collated atmospheric, energy performance, noise and vibration data measured at the Strata turbine site.

5.1 Atmospheric

Using the same CFD techniques, as discussed in Chapter 4.1, assuming a south westerly prevailing wind the flow results depicted in Figure 95 and Figure 96 were obtained for the Strata site.

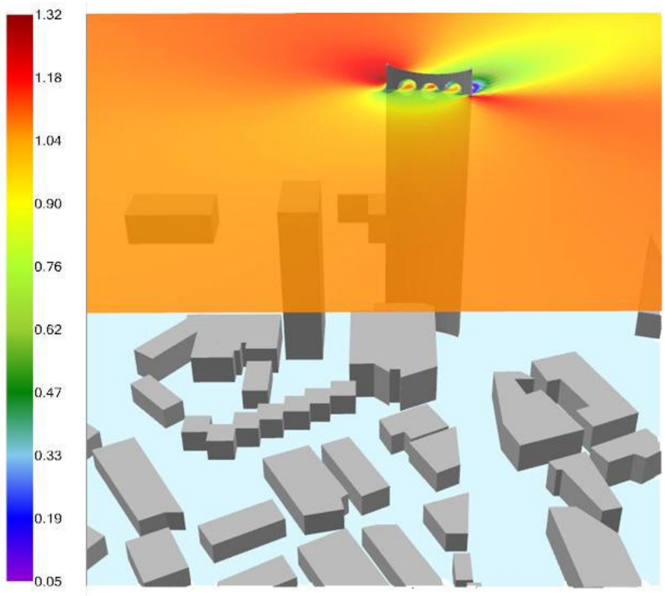

Figure 95: Displays CFD simulation of the predominant south-westerly wind across the Strata turbines. As is evident a clear, uninterrupted flow can be expected.

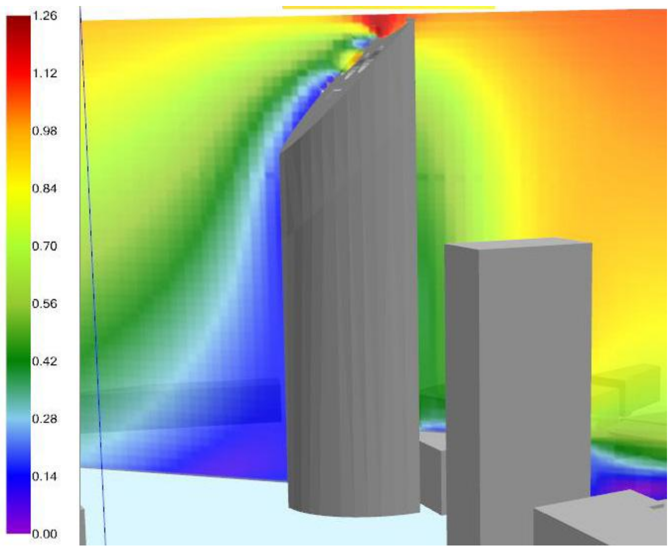

Figure 96: Displays CFD simulation of the predominant south-westerly wind around the Strata tower. As the Strata turbines tower above the surrounding buildings a clear wind flow can be expected from the south west.

As is clear from Figure 95 and Figure 96, the Strata's height puts it well above any disruptive obstacles in the immediate area with a predicted mean wind speed coefficient of 1 in Urbawind demonstrating a clear, uninterrupted wind resource leading up to the three circular venturis where the turbines are situated. Unfortunately as the structure is facing North the prevailing wind would meet the turbines at a 22.5 degree angle side on to the structure slowing the wind speed down to a mean coefficient of 0.75.

The venturi can direct the wind and increase speeds across the blades, the aerodynamic design of which is dependent on many factors that would be beyond the scope of this text but one crucial aspect of its design is symmetry as the rotor hubs are located in the centre of the circular openings. The venturi was designed to fit the Strata's pre-designed shape which did not lend itself to increasing wind speeds. Therefore the engineers focused the venturi design on directing wind flow towards the turbines and minimising turbulent flow (Ramboll, Norwin, 2008). This was achieved by ensuring optimum blade placement within the structure, rounding inlets and exits and specifying a cylindrical shape for the enclosure. Figure 96 displays an Urbawind simulation of the venturi that does demonstrate some increase in wind speed around the rotor hub, but further suggested design alterations and enhancements will be discussed in Chapter 7.

It was regrettable that logging equipment was not installed by the Strata owners in time for this thesis, but extrapolated data from the LSBU site, verified and confirmed through CFD analysis, has proved suitable and useful in predicting the Strata wind regime. Equation 5's log wind profile law with roughness class 4 was utilised; the results are shown in Figure 97, Figure 98, Figure 99, Figure 100 and Table 41. An average wind speed of 5.3 m/s was calculated. The assumption that a class 4 roughness is a true representation of the surrounding topography is made. Referring back to Table 8 there are two roughness classes presented to represent the city environment, class 3.5 and 4. Although class 4's use is intended for large cities such as London it is noted that the turbines sites are not directly within the heart of London where the topography is not as stark and varied. Results may likely fall somewhere between the two classes. Table 40 presents the expected error in extrapolated results dependent on roughness class at varying heights from the Tower Block to the Strata hub height.

The frequency distribution graph in Figure 100 shows that lower winds up to 7 m/s make up 70 % of the estimated wind regime at the Strata site. When referencing the manufacturer power curve in APPENDIX K we see that the 18 kW rated turbines are rated at 18 kW between 14 - 20 m/s. At the average expected wind speed of 5.3 m/s the instantaneous power rating would be approximately 1 kW, therefore an expected range of instantaneous power ratings of between 0.4 and 4 kW can be expected for 70 % of the time.

How this expected wind regime will directly affect the power generation capabilities of the Strata turbine system will be discussed in section 5.4.

Height [m]	Log profile law		Error
	Class 4	Class 3.5	%
150	5.3	5.0	7.7
140	5.2	4.9	7.4
130	5.2	4.8	7.1
120	5.1	4.7	6.7
110	4.9	4.7	6.3
100	4.8	4.6	5.8
90	4.7	4.5	5.3
80	4.6	4.4	4.6
70	4.4	4.2	3.8
60	4.2	4.1	2.9
50	4.0	3.9	1.7
40	3.7	3.7	0.0

Table 40: Demonstrates the error in surface roughness classes applicable in the urban environment

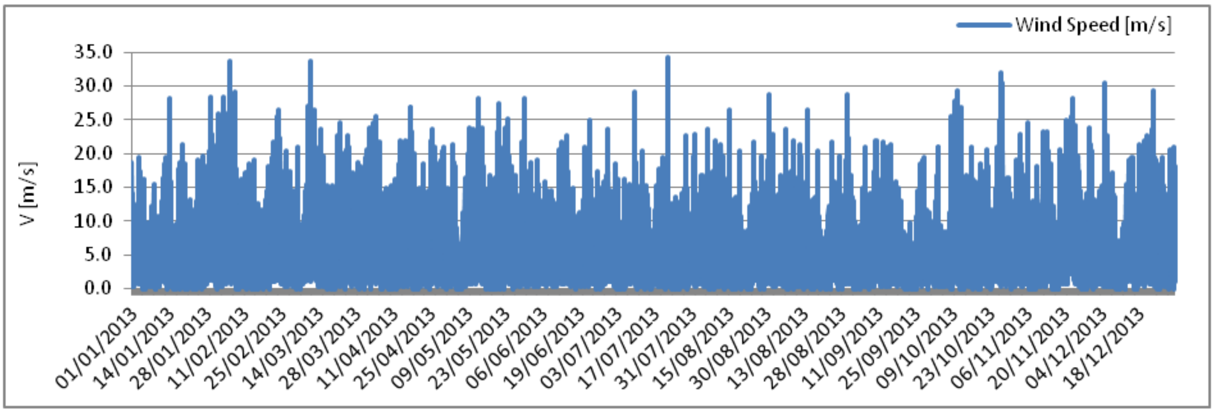

Figure 97: Displays wind speeds extrapolated from the LSBU Towel Block site data for 2013

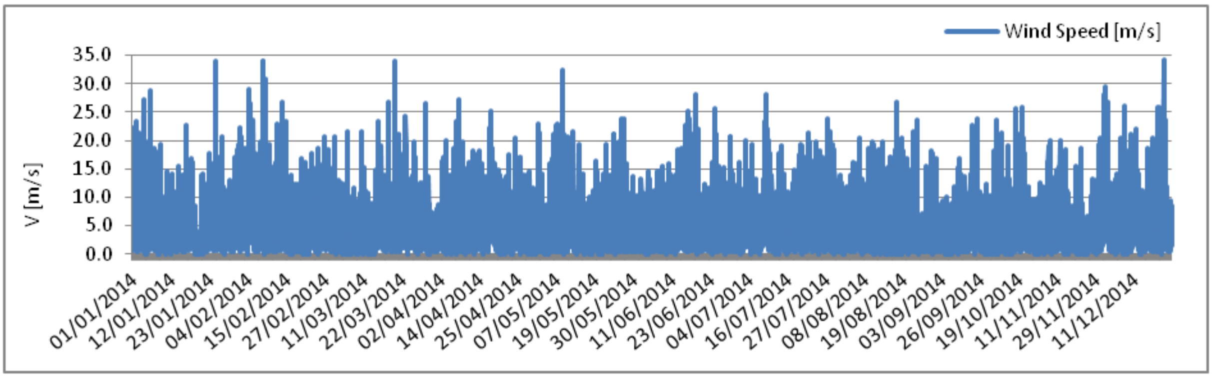

Figure 98: Displays wind speeds extrapolated from LSBU site data for 2014

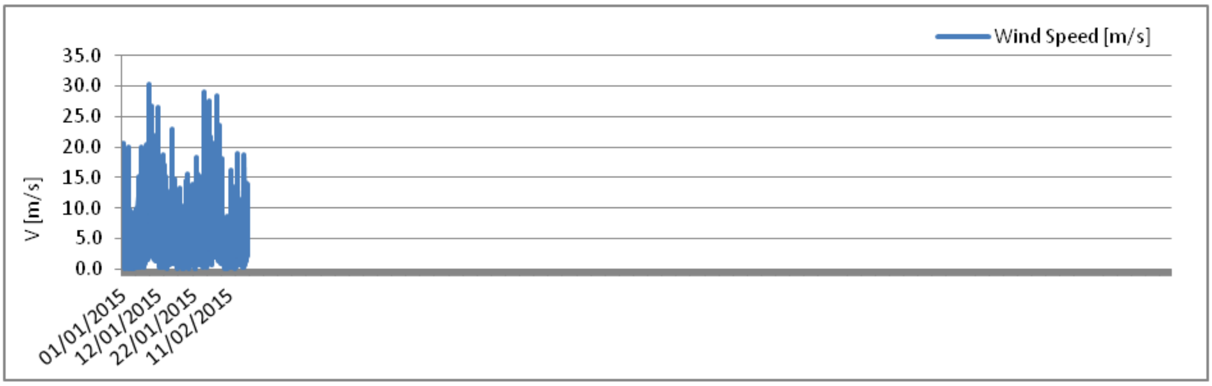

Figure 99: Displays wind speeds extrapolated from LSBU site data for 2015 [up until February].

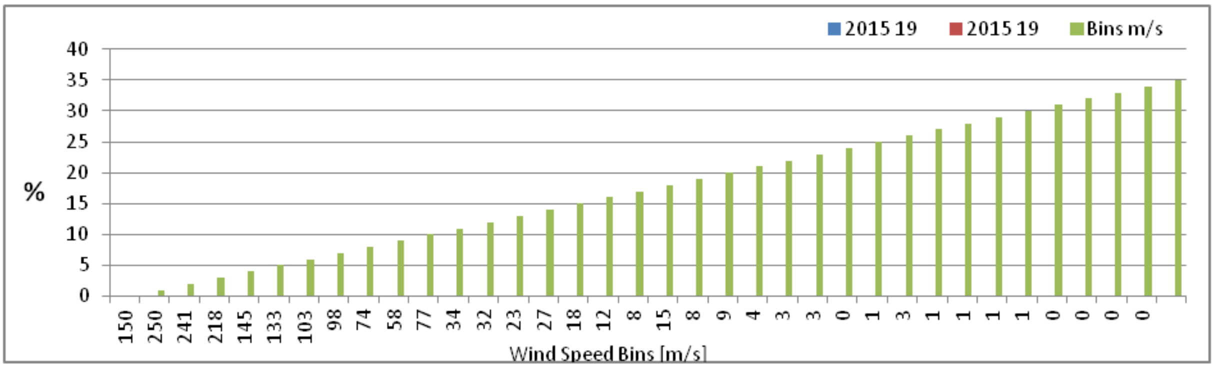

Figure 100: Displays wind speed frequency distribution (%) extrapolated from LSBU data for 2013 - 2015.

Bins m/s	2013 %	2014 %	2015 %
0	0.92	1.06	1.07
1	10.06	10.71	8.47
2	14.57	15.30	14.12
3	13.57	14.11	13.62
4	11.37	12.56	12.32
5	9.44	9.28	8.19
6	7.48	7.42	7.51
7	6.03	6.35	5.82
8	4.87	4.58	5.54
9	4.00	3.94	4.18
10	3.65	2.97	3.28
11	3.54	3.08	4.35
12	2.06	1.80	1.92
13	1.61	1.31	1.81
14	1.47	1.12	1.30
15	1.20	0.93	1.53
16	0.82	0.72	1.02
17	0.68	0.47	0.68
18	0.62	0.46	0.45
19	0.42	0.45	0.85
20	0.42	0.35	0.45
21	0.34	0.25	0.51
22	0.32	0.27	0.23
23	0.15	0.10	0.17
24	0.12	0.14	0.17
25	0.06	0.04	0.00
26	0.04	0.07	0.06
27	0.04	0.06	0.17
28	0.02	0.01	0.06
29	0.05	0.03	0.06
30	0.03	0.01	0.06
31	0.01	0.01	0.06
32	0.00	0.00	0.00
33	0.01	0.01	0.00
MAX	34.3	34.3	30.4
AVE	5.3	5.0	5.6

Table 41: Displays frequency distribution of Strata site wind speed in bins between 2013 - 2015 using data extrapolated from the LSBU site.

Weibull and Rayleigh probability density functions were used to further assess their applicability in the urban environment. The Weibull and MMLM was again shown to correlate most closely with measured data[14]. If we were to have used the NOABL (geographically nearest) database for our extrapolated Strata predictions we would have been basing our results on an average wind speed of 6 m/s at a 49 m height. This would extrapolate to 8.3 m/s when raised to the Strata's hub height of 140 m using Equation 5, far higher than our predicted 5.3 m/s. This represents a 1.4 x difference in speed and therefore (by the wind V^3 proportionality) a 2.75 x increase in estimated power. It is unfortunate that site specific wind data was not available for the Strata building but this example does reiterate the need for applicable data sets. Known problems initially raised over design and installation plans by the turbine manufacturer highlighted that the turbines would face directly south in an area with a prevailing south-westerly wind, which coupled with a lack of yaw mechanism restricts their power extraction capabilities. It was also discussed that the building and venturi shape may shadow the turbines from south-westerly winds. This was assessed using CFD analysis and Figure 101 shows an approximate 10 % reduction in wind speed is predicted. If the building's orientation had been offset +25 degrees then a greater yield could be expected.

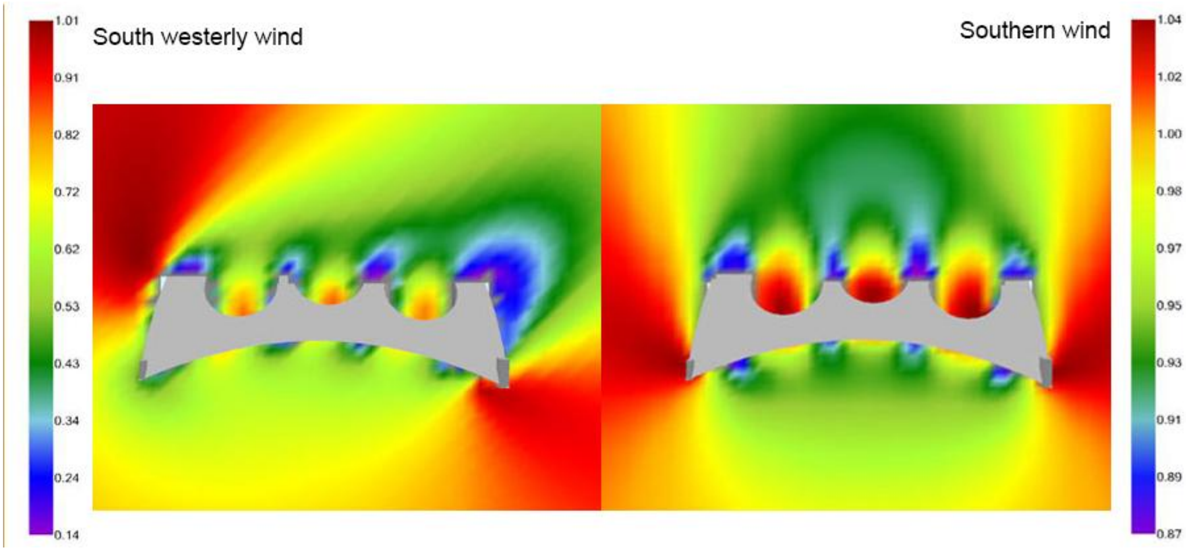

Figure 101: Displays differing wind speed predictions around the Strata venturi from southern and south-westerly winds.

5.2 Noise

The following section will see a review of collected noise measurements captured in the procedures laid out in section 3.3.1. Background, operational and environmental noise mapping results were collected for the Strata site.

[14] Although this is seemingly expected as the results were calculated from the same data as the LSBU site the log wind profile law raised speeds substantially above cut in speeds of the Strata turbines, which then need to be assessed to a new power curve.

5.2.1 Background

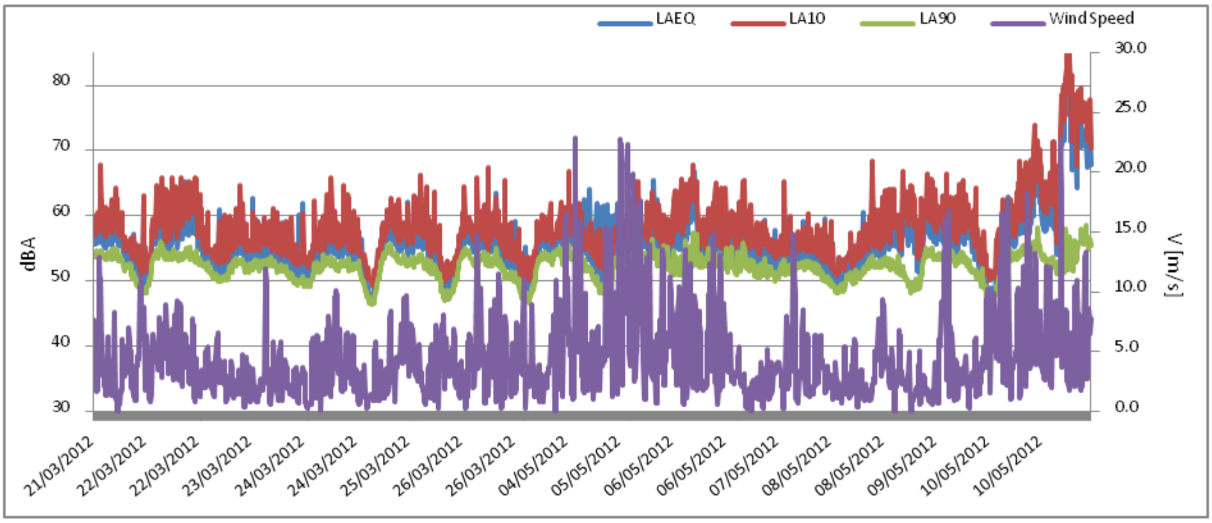

Figure 102: Displays background L_{Aeq} levels plotted against wind speed recorded at the Strata building.

	L_{Aeq}	L_{A10}	L_{A90}	Speed
L_{Aeq}	1			
LA_{10}	1.0	1		
L_{A90}	0.7	0.7	1	
Speed	0.2	0.2	0.2	1

Table 42: Displays the correlation (r) between L_{Aeq}, L_{A10}, L_{A90} and wind speed at the Strata building.

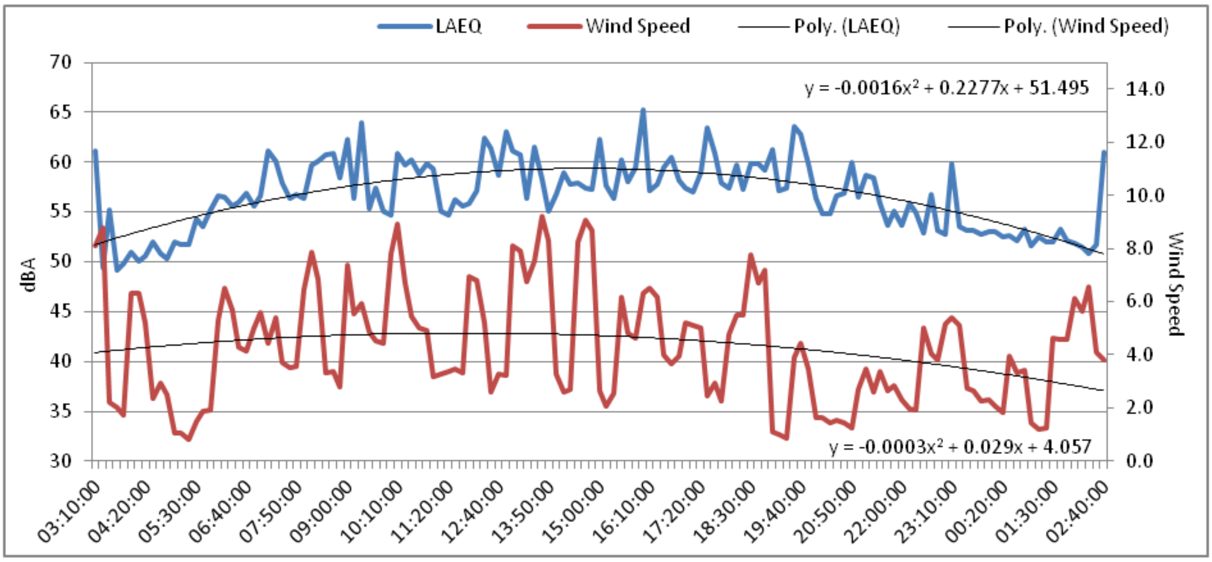

Figure 103: Displays a 24 comparison of background wind speed and L_{Aeq} results at the Strata building.

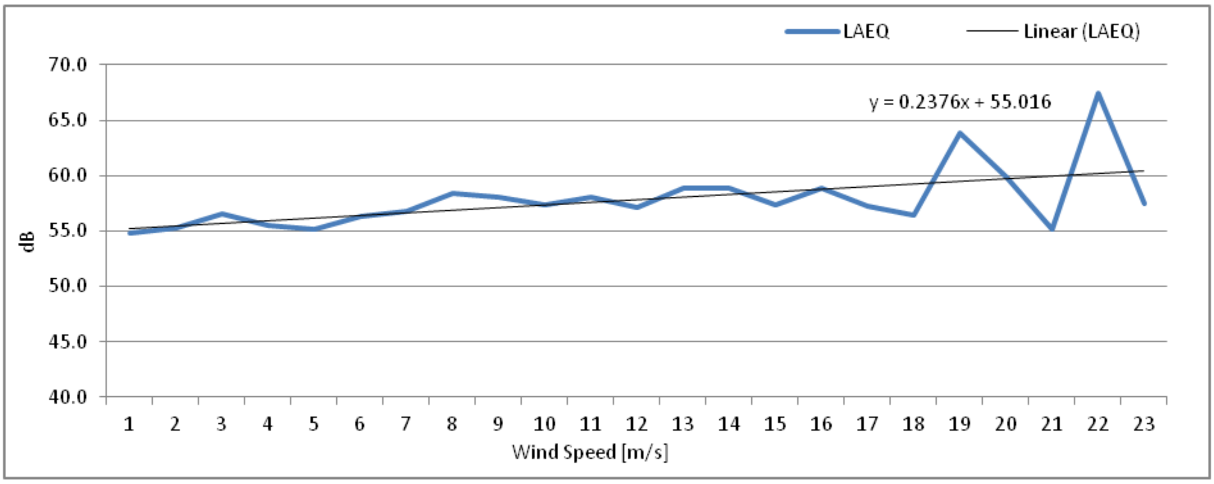

Figure 104: Displays the average L_{Aeq} levels recorded as a function of wind speed at the Strata building.

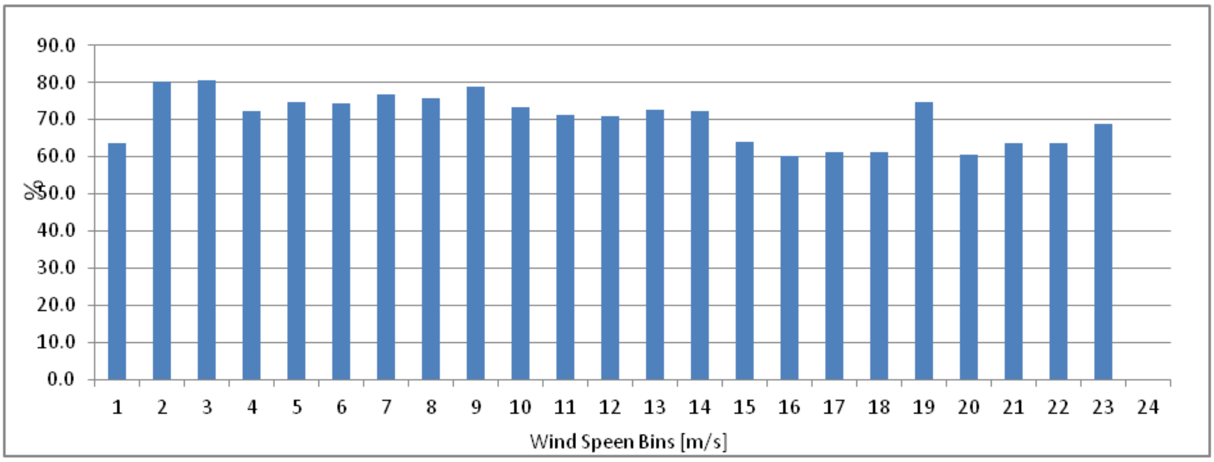

Figure 105: Displays wind speed frequency distribution at the Strata building.

5.2.2 Operational (at turbine)

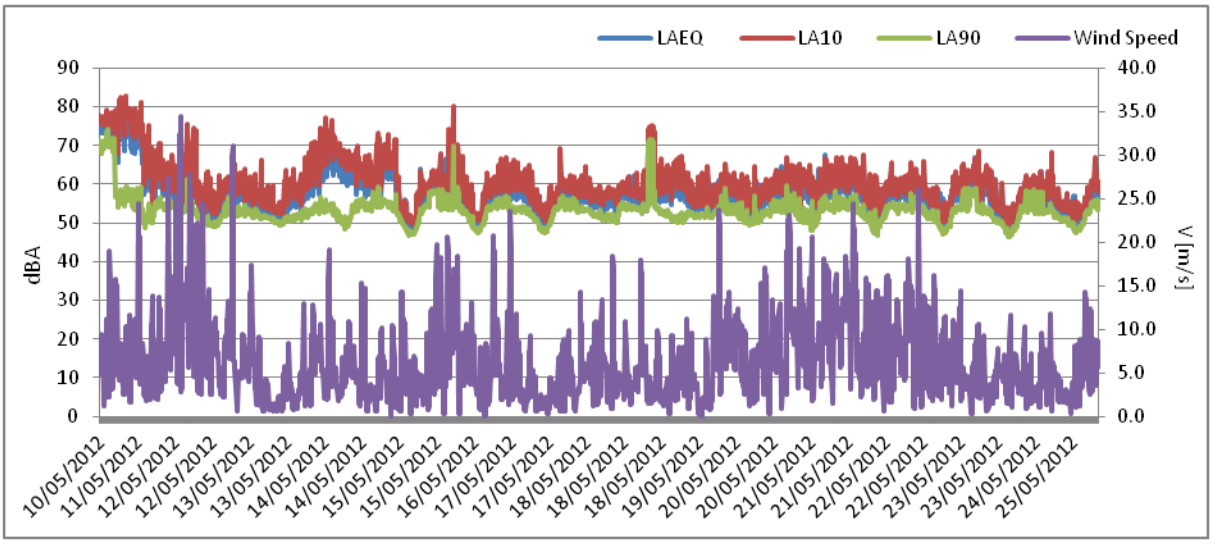

Figure 106: Displays the operational L_{Aeq} levels plotted against wind speed at the Strata building.

	L_{Aeq}	L_{A10}	L_{A90}	Wind Speed
L_{Aeq}	1.0			
L_{A10}	1.0	1.0		
L_{A90}	0.7	0.7	1.0	
Wind Speed	0.1	0.1	0.1	1.0

Table 43: Displays the correlation (r) between L_{Aeq}, L_{A10}, L_{A90} and wind speed results collected at the Strata building.

	Ave	Mode
L_{Aeq}	58.0	56.0
Wind Speed	6.1	1.9

Table 44: Displays the average and most frequently occurring wind speeds estimated at the Strata site compared against recorded average and most frequently occurring L_{Aeq} levels.

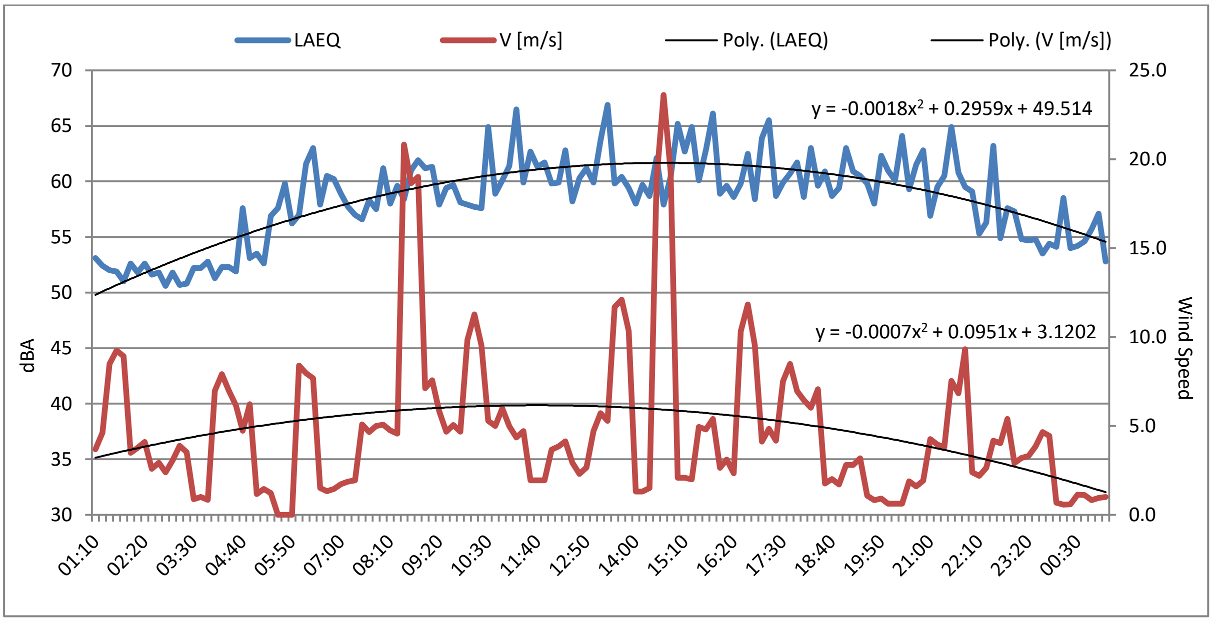

Figure 107: Displays a typical day of operational measurements and accompanying trend lines for L_{Aeq} and predicted wind speed measurements at the Strata building.

	L_{Aeq}	V[m/s]
L_{Aeq}	1	
V[m/s]	0.152	1

Table 45: Displays the correlation (r) data for Figure 107 of wind speed and L_{Aeq} results at the Strata site.

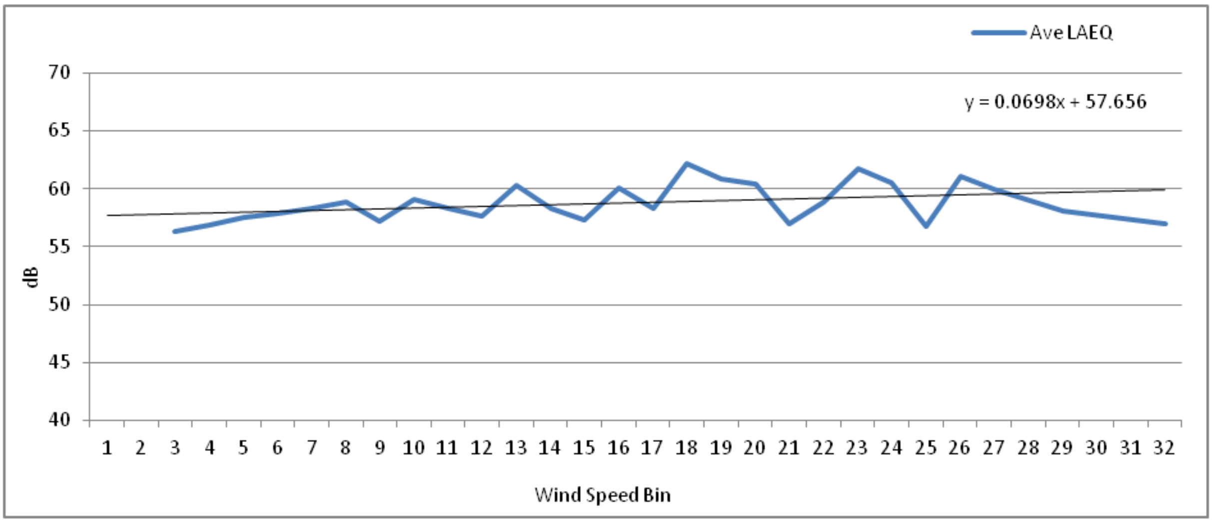

Figure 108: Displays average operational noise levels as a function of wind speed at the Strata building.

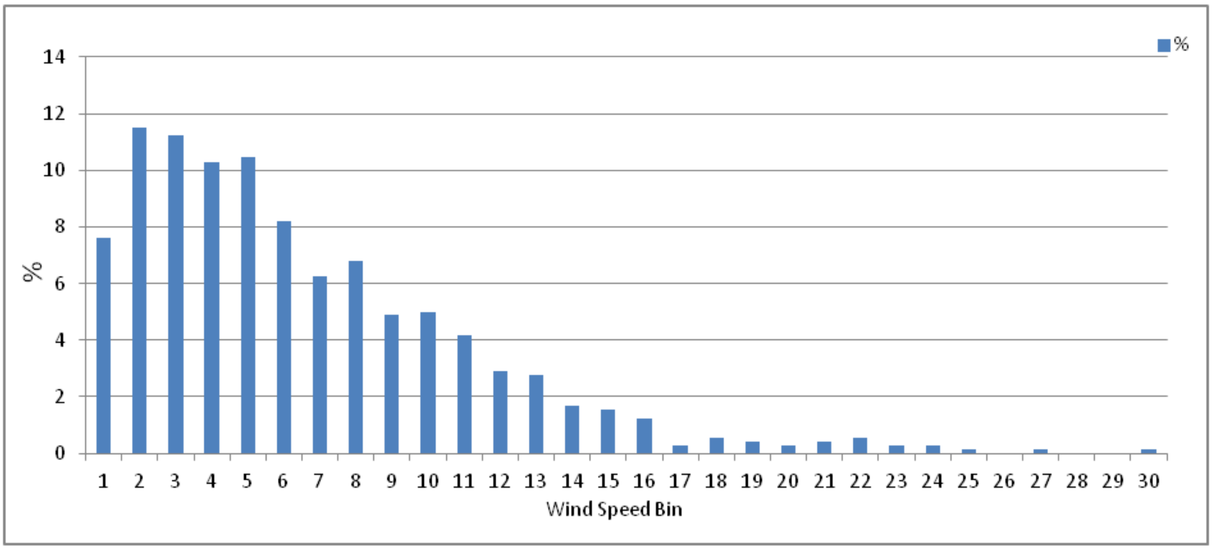

Figure 109: Displays the predicted operational wind speed frequency distribution data in wind speed bins at the Strata building.

Please refer to APPENDIX G for background and operational frequency distribution tables compared to averaged L_{Aeq} noise levels per wind speed bin. These results will be discussed along with an environmental survey of the area in the following section.

5.2.3 Environmental mapping

The following L_{Aeq}, L_{A90} and LA_{10} environmental noise measurements were measured between 10/5/2013 and 30/5/2013. The methodology is as previously mentioned in section 3.3.1.

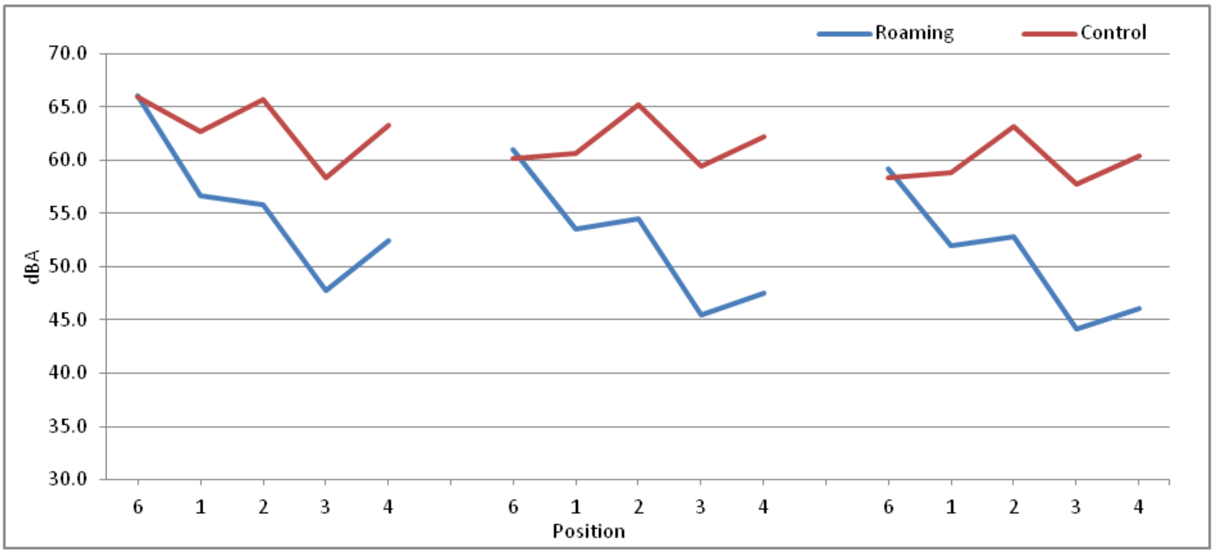

Figure 110: Displays roaming and control measurement results recorded as part of an environmental noise assessment around the Strata site.

	Roaming	Control
Roaming	1	
Control	0.5	1

Table 46: Displays a strong correlation (r) between roaming and control measurement results.

POSITION	AVE L_{Aeq}	AVE L_{A10}	AVE L_{A90}
1	54.1	57.4	45.7
2	54.4	56.2	42.9
3	45.8	47.5	42.9
4	48.7	51.2	40.4
5	61.5	65.0	52.4
6	62.1	65.8	52.2

Table 47: Displays the average L_{Aeq}, L_{A90} and L_{A10} measurements taken at each position displayed in Figure 111 as part of the Strata environmental noise survey.

Figure 111: Displays the environmental measurement positions. 5 is the control position and 1, 2, 3, 4, 6 are roaming positions.

A strong correlation is shown between the control and roaming positions with levels diminishing with distance from the control position. This shows that the hustle and bustle of the dense urban environment surround the Strata area presents a significantly higher aural environment than in the nearest residential areas (Positions 1 - 4). When looking at the projected Strata wind speeds against recorded background L_{Aeq} levels it is clear that there is no real correlation, see Figure 104, which shows an approximate 0.25 dB per wind speed bin. When compared to Figure 102 and Table 42 wind speed fluctuations to not strongly correspond to observed fluctuations in noise level. When analysing a 24 hour period from the one week noise data (as depicted in Figure 23) a distinct repetitive 24 hour noise pattern is observed, which does not correspond to the fluctuations in wind speed. This further suggests that other, background, environmental noise sources dominate the aural environment at the Strata rooftop. Directly beneath the turbine level is a plant room, HVAC and elevator control room, which along with local emergency services, bars, clubs, traffic within the heavily built up area could contribute to the noise pattern observed. This is further confirmed when a strong correlation is observed in compared L_{Aeq} to L_{A10} and L_{A90} data. However, on occasion, results do stray from this pattern and an unusually high levels are observed. This is also observed when focusing in on average L_{Aeq} levels per wind speed band as highlighted in Figure 112. Third octave analysis was conducted to further investigate as shown in Figure 113 for non-operational, background measurements taken at the Strata turbine position.

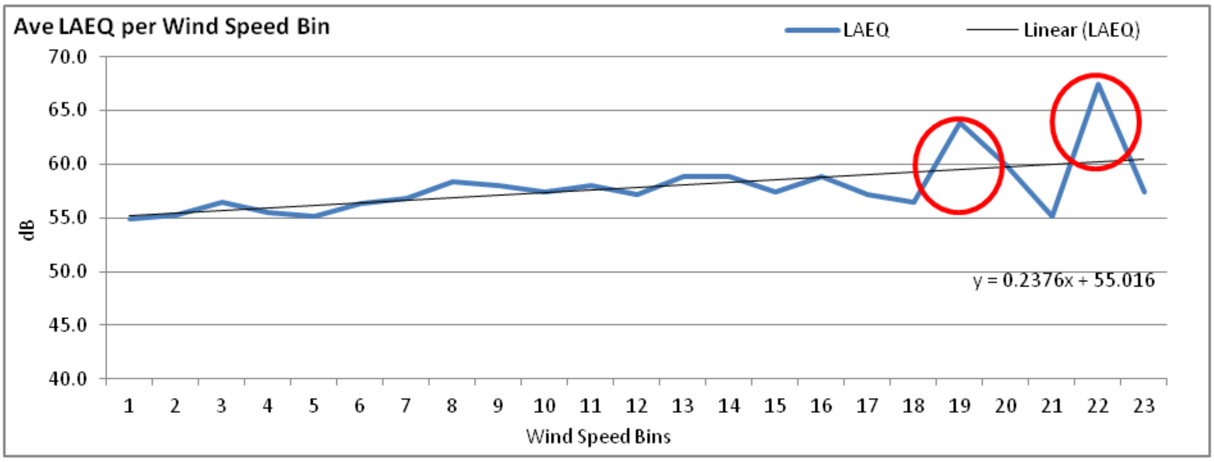

Figure 112: Highlights unexpected discrepancies in average L_{Aeq} results per wind speed bin measured at the Strata site.

It is clear from looking at wind speed bins 19 and 22 that a different frequency signature is observed with a significant increase in low frequency content. These two series correspond to possible outliers in the average L_{Aeq} per wind speed graph presented in Figure 112.

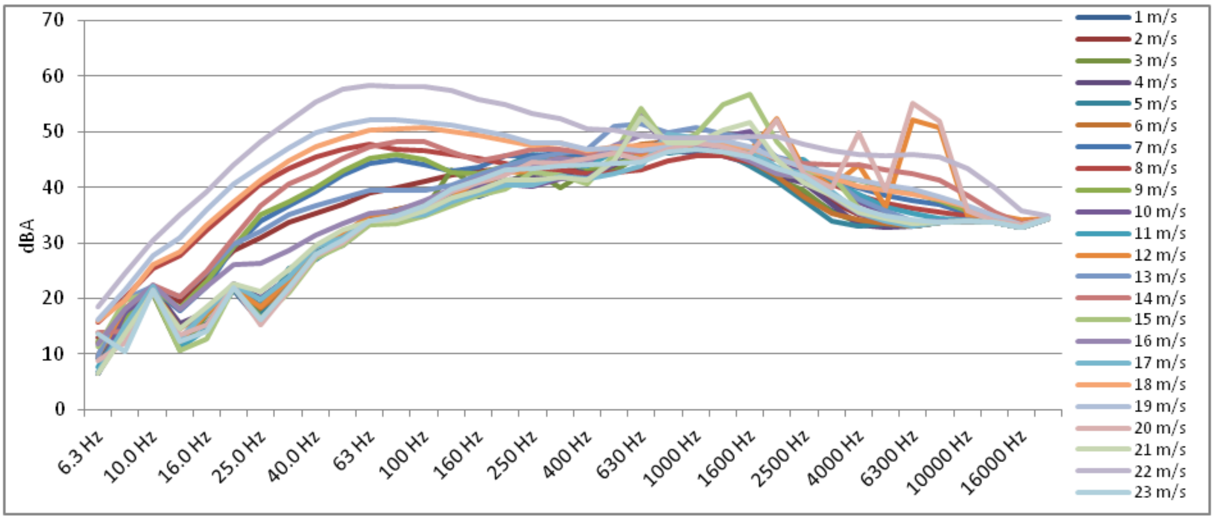

Figure 113: Displays the difference in $^{1}/_{3}{}^{rd}$ octave noise levels recorded at the Strata turbine per increasing wind speed. An increase in low frequency content in observed at higher speeds.

This boost is around the 63 - 125 Hz octave bands; a range which would include the Strata turbines BPF of 83.3 Hz[15]. This would suggest that maybe the turbines had intermittently been in operation through the arranged background measurement period. If not, it would be a curious coincidence.

A full comparison of background and operational third octave results was then conducted. Some sample results are displayed in Figure 114 - Figure 116. Please refer to APPENDIX P for all measured wind speed bin 1/3rd octave graphs.

[15] Please refer to earlier addressed Equation 1 to calculate BPF.

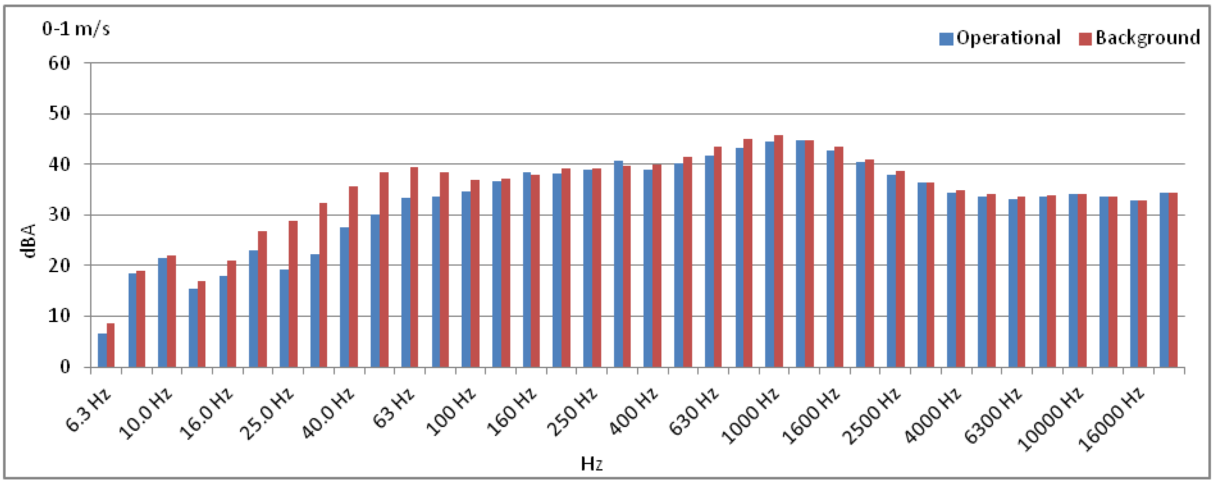

Figure 114: $^{1}/_{3}{}^{rd}$ Octave L_{Aeq} analysis of measured noise at the Strata turbine for 0-1 m/s wind speed bin.

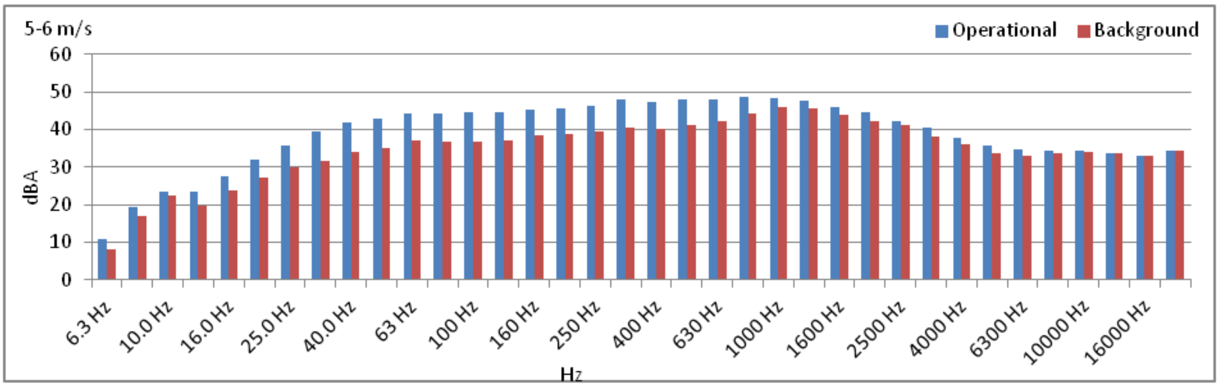

Figure 115: $^{1}/_{3}{}^{rd}$ Octave L_{Aeq} analysis of measured noise at the Strata turbine for 5-6 m/s wind speed bin.

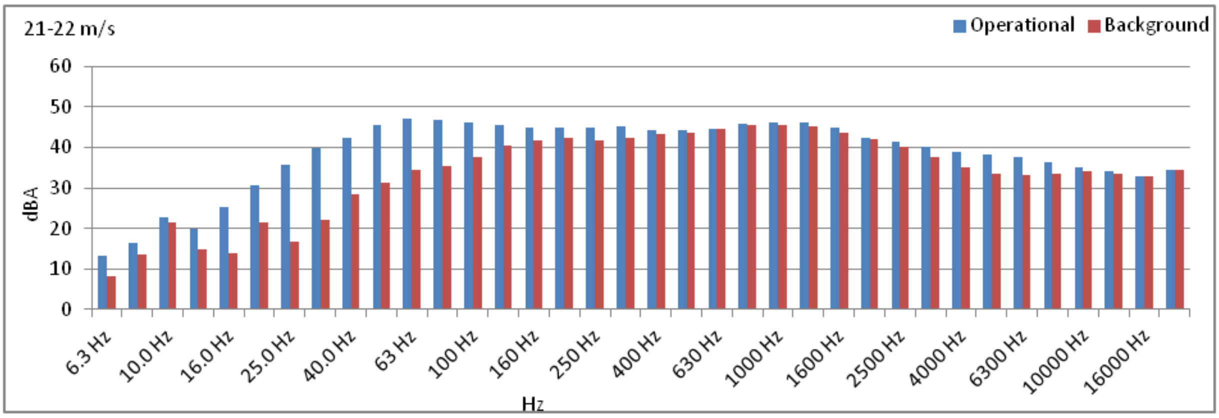

Figure 116: $^{1}/_{3}{}^{rd}$ Octave L_{Aeq} analysis of measured noise at the Strata turbine for 21-22 m/s wind speed bin.

As is clear from Figure 114 - Figure 116 operational third octave analysis in each wind speed above 4 m/s displays a boost in low frequency content centred around the Strata turbines BPF of 83.3 Hz. No observed change in frequency content below 4 m/s is due to this being below the Strata turbines cut in speed. This does suggests that the observed boost around the same frequencies in the background results are probably due to turning turbine blades.

It was organised with the Strata building managers that the turbines would be completely shut down while background measurements were being conducted. However, it is possible that they were mistakenly switched on. The Strata building has a bespoke mechanical arm that extends from below the turbine control platform, out and 360 degrees around the building, therefore a safety mechanism to shut down the turbines is in place when the windows cleaning arm is deployed. The turbines are then reset by a member of the window cleaning or building management team after the mechanical arm has been stowed. This habitual starting of the turbines could possibly explain why the turbines were temporarily turning during the background measurements and in turn explain the turbine signature frequency spectrum appearing within the background results. Conversely, this also could explain the lack of low frequency content found in some operational results taken at wind speeds above the cut in speed of 4 m/s. An investigation into other possible sources of the low frequency noise would, ideally, be appropriate. As previously discussed the control level below the turbine venturi contains the Strata HVAC and elevator systems but unfortunately, due to access restrictions, further inquires could not be conducted.

Accepting the operational turbine's spectral signature as the background intruding frequency spectrum requires a background data re-analysis with this frequency signature filtered out. The updated data is displayed in Table 48 and Figure 117 - Figure 119.

Bin	Range	Freq	Ave L_{Aeq}	Std Dev
1.0	0 < V < 1	151	54.6	2.9
2.0	1 < V < 2	320	54.6	2.9
3.0	2 < V < 3	236	54.5	2.6
4.0	3 < V < 4	252	54.5	2.6
5.0	4 < V < 5	146	54.0	2.7
6.0	5 < V < 6	122	54.5	2.8
7.0	6 < V < 7	91	54.7	2.8
8.0	7 < V < 8	37	55.2	2.6
9.0	8 < V < 9	38	54.5	2.8
10.0	9 < V < 10	43	55.1	3.4
11.0	10 < V < 11	21	54.9	2.6
12.0	11 < V < 12	19	55.0	3.5
13.0	12 < V < 13	10	56.1	2.9
14.0	13 < V < 14	10	55.7	2.5
15.0	14 < V < 15	6	56.2	1.4
16.0	15 < V < 16	4	58.2	2.6
17.0	16 < V < 17	6	56.3	1.5
18.0	17 < V < 18	4	55.3	0.4
19.0	18 < V < 19	2	59.7	1.8
20.0	19 < V < 20	1	60.6	0.0
21.0	20 < V < 21	2	55.1	0.0
23.0	22 < V < 23	5	55.2	0.6
	TOTAL	**1526**		
	Ave V[m/s]	**4.0**		

Table 48: Displays extrapolated wind speed frequency and measured average L_{Aeq} levels per wind speed bin for the Strata site. The data displayed has been updated with erroneous $^{1}/_{3}{}^{rd}$ octave signatures, attributed to turning blades, extracted.

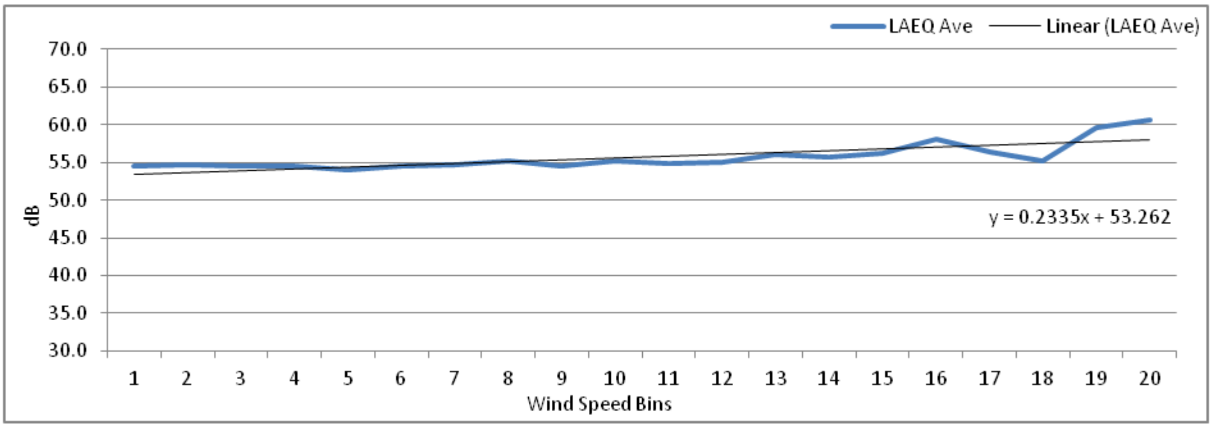

Figure 117: Displays a more consistent trend in L_{Aeq} level per wind speed bin after erroneous 1/3rd octave signatures have been extracted.

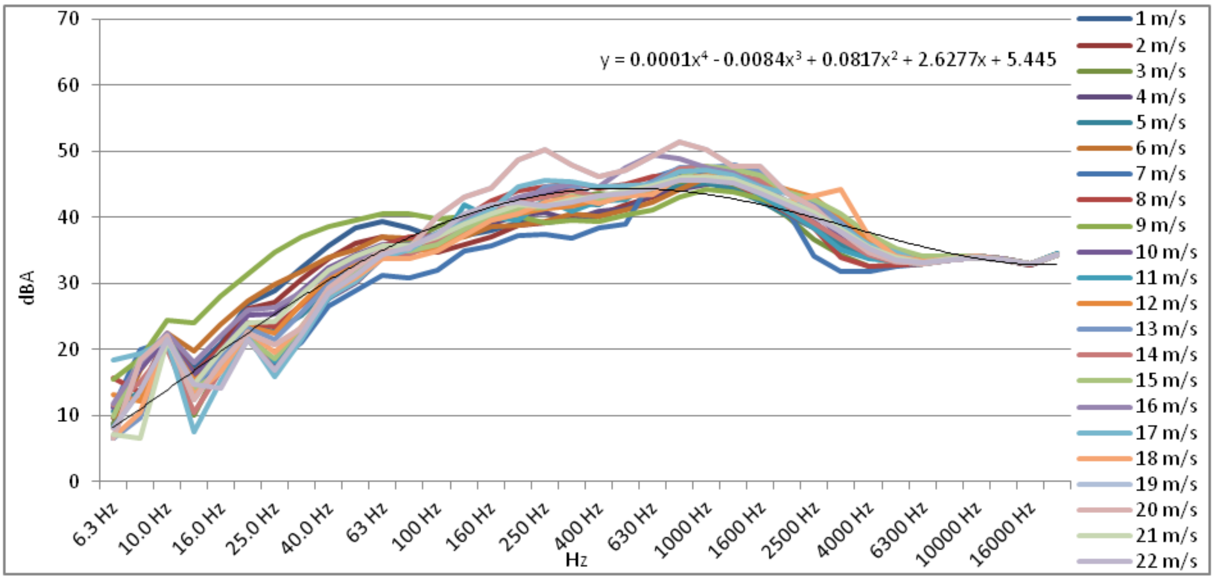

Figure 118: Displays background measured 1/3rd octave L_{Aeq} levels per wind speed bin at the Strata site with extraneous frequency signatures removed.

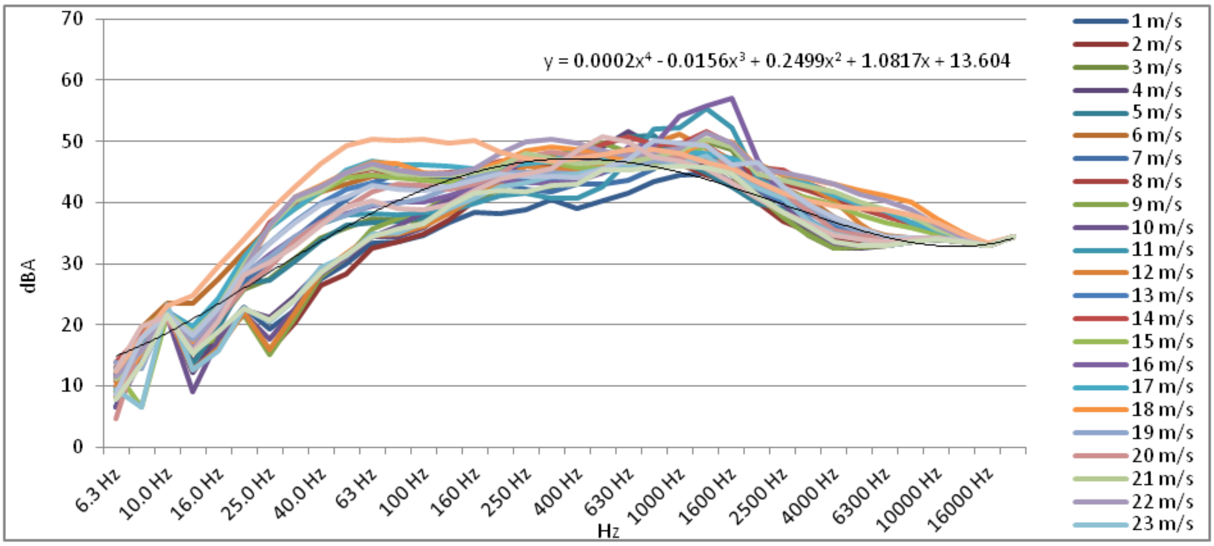

Figure 119: Displays operational, measured 1/3rd octave L_{Aeq} levels per wind speed bin at the Strata site with extraneous frequency signatures removed.

This provides a much more uniformly consistent set of data for both background and operational results.

Background and operational L_{Aeq} data per wind speed was then compared to see if a baseline turbine noise level per wind speed was obtainable. Once the turbine specific sound pressure levels are achieved it is then possible to calculate the turbines apparent sound power level per wind speed bin ($L_{WA,k}$). The turbines $L_{WA,k}$ can then be inputted into environmental noise software CadnaA to simulate the turbine noise propagation into the surrounding area. This will aid assessing any likelihood of complaint. This process was completed in accordance with guidelines set out in IEC 61400-11, the first step of which is to correct for background noise utilising Equation 21.

$$Ls = 10log\left[10^{(0.1\,.Ls+n)} - 10^{(0.1\,.Ln)}\right]$$

Equation 21: Demonstrates how to calculate the isolated turbine sound pressure level where Ls = Equivalent isolated sound pressure level of the wind turbine, Ls+n = Equivalent sound pressure level of the wind turbine plus the background, Ln = Equivalent background noise level.

$$L_{WA,k} = L_{Aeq,c,k} - 6 + 10log\left[\frac{4\pi R^2}{S}\right]$$

Equation 22: used to calculate the turbines apparent sound power level using corrected dBA sound pressure levels obtained using Equation 21 in accordance with IEC 61400-11 where LAeq,c,k = Background corrected A-weighted sound pressure level at the relevant wind speed bin, R = distance from the rotor hub to the microphone and S = reference area.

IEC 61400-11 puts some stipulations on using these equations. If the difference between operational and background turbine noise levels is greater than 6 dBA then both Equation 21 and Equation 22 can be used. If the difference is only between 3-6 dBA then a correction value of 1.3 dBA will be used, the results marked with an asterisk (*) within the report and the result could not be used with Equation 22. If the difference is less than 3 dBA then the operational turbine noise is presumed less than the measured background noise level at that wind speed bin and should not be reported or used for any further equation.

The data collected, as displayed in Table 49 only has one wind speed bin that qualifies to be used with both equations (Bin 21), with the rest of the bins falling into 3-6 dBA and less than 3 dBA categories.

As discussed earlier in Chapter 3.3.1 the author had no option but to install the microphone within the Strata turbine venturi. Far from ideal in many ways including the venturi being reflective. As previously mentioned in Chapter 3.3.1 a directivity factor as included in Equation 23 can be utilised to assess level increase due to close proximity reflective surfaces. Equation 22 as recommended in IEC 61400-11 does not allow for this inclusion. Due to this circumstantial difference and as the author intends on estimating noise propagation into the surrounding area using extrapolated equivalent sound power levels IEC 61400-11 stipulations on Equation 21 have been bypassed and Equation 22 substituted for a more traditional acoustical formulae.

IEC 61400-11 is more suited to rural, quiet, areas where background noise would predominantly consist of atmospheric sources i.e. wind. It is therefore more applicable to accept that turbine noise less than the background atmospheric noise is likely to always be masked. The author is evaluating noise levels within a densely populated, built up environment, which is always subject to change and development. Also, the turbine technology evaluated at the Strata building may further be utilised in other, quieter areas. Therefore a full analysis will be pursued. Table 49 displays the calculated turbine levels and equivalent sound power levels using Equation 21 and Equation 23.

$$L_{w,k} = SPL + 20Log(r) - 10Log(Q) + 11$$

Equation 23: Used to calculate the turbine equivalent sound power level (Lw) using a directivity index to account for the reverberant venturi where Lw,k = Equivalent Sound Power Level, SPL = Sound Pressure Level, r = distance and Q = directivity factor.

It is also important to note that in spite of the operational an background average L_{Aeq} levels being within a 3 dB range some of their third octave components demonstrate a greater difference and present a possible threat of tonal presence. Table 50 and 51 show the 1/3 octave level differences between the turbines operational and background measurements. Cells highlighted in red show where the equivalent isolated turbine sound pressure level is substantially higher than the background level (approximately +3 dB). The 6-7 m/s wind speed bin has been chosen to perform this analysis as the Strata sites average wind speed was estimated at 6.1 m/s in Table 49.

Bin	BKG Ave a	OP Ave b	b - a	Ls	$L_{WA, k}$
1	54.6	56.3	1.7	51.5	66.5
2	54.6	56.8	2.2	52.8	67.9
3	54.5	57.6	3.1	54.6	69.7
4	54.5	57.9	3.4	55.3	70.4
5	54.0	58.3	4.2	56.2	71.3
6	54.5	58.9	4.5	57.0	72.1
7	54.7	57.3	2.5	53.7	68.8
8	55.2	59.0	3.8	56.7	71.8
9	54.5	58.4	3.9	56.1	71.2
10	55.1	57.7	2.5	54.1	69.2
11	54.9	60.3	5.4	58.8	73.9
12	55.0	58.3	3.3	55.6	70.7
13	56.1	57.3	1.2	51.0	66.1
14	55.7	60.1	4.4	58.1	73.2
15	56.2	58.4	2.1	54.3	69.3
16	58.2	62.1	4.0	59.9	75.0
17	56.3	60.8	4.5	58.9	74.0
18	55.3	60.4	5.2	58.9	73.9
19	59.7	57.0	-2.7	56.3	71.4
20	60.6	58.8	-1.8	55.8	70.9
21	55.1	61.8	6.6	60.7	75.8
23	55.2	56.8	1.6	51.7	66.8

Table 49: Displays the equivalent Strata turbine average sound pressure and power levels per wind speed bin.

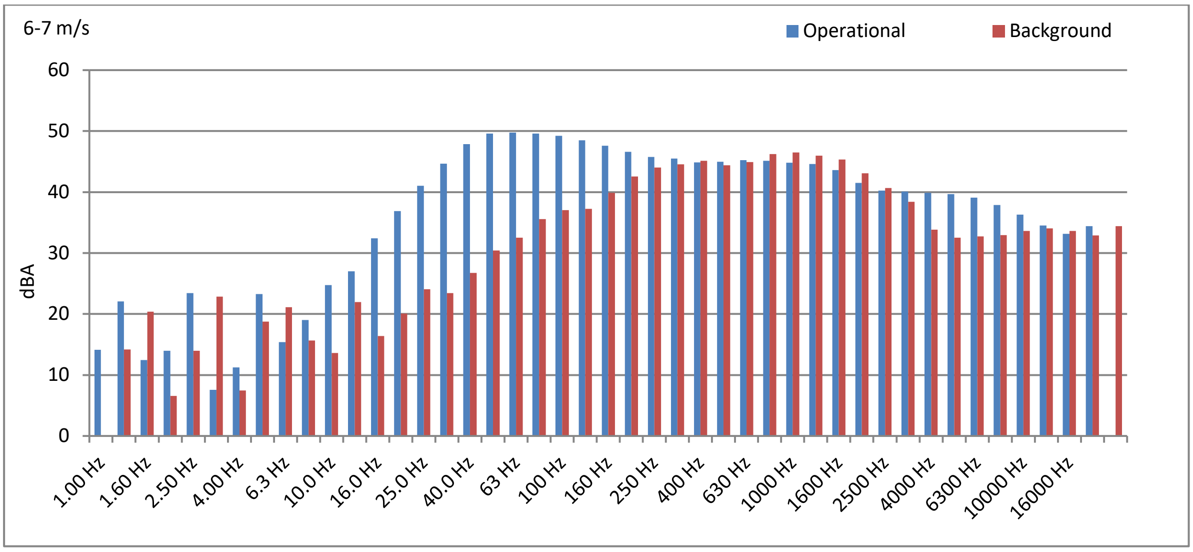

Figure 120: Displays 1/3 octave operational and background measurements in the 6-7m/s wind speed bin.

1/3 Oct Band	Operational a	Background b	a-b	L_S	$L_{WA,k}$
25.0 Hz	41.0	23.4	**17.6**	41.0	56.0
31.5 Hz	44.7	26.8	**17.9**	44.6	59.7
40.0 Hz	47.9	30.4	**17.4**	47.8	62.9
50 Hz	49.6	32.5	**17.1**	49.5	64.6
63 Hz	49.8	35.6	**14.2**	49.6	64.7
80 Hz	49.6	37.0	**12.6**	49.4	64.4
100 Hz	49.2	37.3	**12.0**	49.0	64.0
125 Hz	48.5	39.9	**8.7**	47.9	63.0
160 Hz	47.6	42.6	5.1	46.0	61.1
200 Hz	46.6	44.0	2.6	43.2	58.2
250 Hz	45.7	44.6	1.2	39.5	54.6
315 Hz	45.5	45.1	0.4	35.0	50.0
400 Hz	44.9	44.4	0.5	35.3	50.3
500 Hz	45.0	44.9	0.1	28.6	43.7
630 Hz	45.2	46.2	-1.0	39.3	54.4
800 Hz	45.1	46.5	-1.4	40.8	55.9
1000 Hz	44.8	46.0	-1.1	39.5	54.6
1250 Hz	44.6	45.4	-0.8	37.4	52.5
1600 Hz	43.6	43.1	0.5	34.1	49.1
2000 Hz	41.5	40.7	0.9	34.1	49.1
2500 Hz	40.3	38.4	1.9	35.7	50.8
3150 Hz	40.1	33.9	**6.2**	38.9	54.0
4000 Hz	39.9	32.5	**7.4**	39.0	54.1
5000 Hz	39.7	32.8	**6.9**	38.7	53.7
6300 Hz	39.1	32.9	**6.2**	37.9	53.0
8000 Hz	37.9	33.6	4.2	35.8	50.9
10000 Hz	36.3	34.1	2.3	32.4	47.5
12500 Hz	34.5	33.7	0.9	27.2	42.3
16000 Hz	33.2	32.9	0.3	20.8	35.9
20000 Hz	34.4	34.4	0.0	8.0	23.1

Table 50: Displays the level difference between operational and background 1/3 octave measurements in the 6-7m/s wind speed. Equivalent sound pressure and sound power levels are also provided.

The levels displayed in Table 50 were then converted into the 1/1 octave levels displayed in Table 51 and put into CadnaA to simulate sound propagation from the operational Strata turbine in to the local and generate a visual noise map. These levels were then compared to background noise levels recorded at street level in Chapter 5.2.1.

1/3 Oct Band	$L_{w,k}$	$L_{w,k}$ 1/1 Oct
25.0 Hz	62.1	
31.5 Hz	65.7	71.1
40.0 Hz	68.9	
50 Hz	70.6	
63 Hz	70.7	75.4
80 Hz	70.5	
100 Hz	70.1	
125 Hz	69.0	73.6
160 Hz	67.1	
200 Hz	64.3	
250 Hz	60.6	66.2
315 Hz	56.1	
400 Hz	56.4	
500 Hz	49.7	62.1
630 Hz	60.4	
800 Hz	61.9	
1000 Hz	60.6	65.3
1250 Hz	58.5	
1600 Hz	55.2	
2000 Hz	55.2	60.5
2500 Hz	56.8	
3150 Hz	60.0	
4000 Hz	60.1	64.7
5000 Hz	59.8	
6300 Hz	59.0	
8000 Hz	56.9	61.8
10000 Hz	53.5	
TOTAL	73.0	78.6

Table 51: 1/1 Octave sound power for 6-7m/s bin for use in CadnaA software.

	Measured		CadnaA	Measured		CadnaA	Measured		CadnaA
P	**1**			**2**			**3**		
	1/3	**1/1**		**1/3**	**1/1**		**1/3**	**1/1**	
25 Hz	56.1			54.6			44.6		
31.5 Hz	55.5	21.7	-22	54.8	22.0	-23	42.3	8.9	-30
40 Hz	57.2			59.0			43.3		
50 Hz	59.6			59.1			45.9		
63 Hz	56.0	35.5	-4.6	57.5	35.9	-5.3	43.4	22.3	-11.6
80 Hz	51.7			54.1			40.1		
100 Hz	48.8			49.5			40.7		
125 Hz	45.7	35.8	-0.1	49.1	37.3	-0.9	43.1	30.7	-1.8
160 Hz	46.1			46.9			42.1		
200 Hz	48.0			47.1			38.0		
250 Hz	47.7	43.4	-6.5	46.9	42.2	-7.3	36.9	33.5	-7
315 Hz	45.7			43.3			36.9		
400 Hz	44.4			41.5			36.6		
500 Hz	44.5	46.2	-5	41.5	43.6	-5.9	34.8	37.0	-5.6
630 Hz	44.8			42.9			34.6		
800 Hz	45.6			45.8			33.1		
1.0 kHz	45.9	50.3	6.5	47.9	51.6	5.8	33.9	38.5	6
1.25 kHz	44.9			46.4			34.2		
1.6 kHz	43.1			45.3			34.1		
2.0 kHz	40.8	47.3	3	43.6	49.6	2.2	34.5	40.4	2.5
2.5 kHz	38.9			40.6			34.6		
3.15 kHz	37.1			37.4			35.5		
4.0 kHz	36.6	42.5	2.5	36.0	41.5	1.4	37.9	41.3	1.8
5.0 kHz	36.5			32.5			29.9		
6.3 kHz	36.6			27.9			20.0		
8.0 kHz	36.8	40.4	-18.9	24.6	29.2	-21.3	16.2	20.9	-20.4
10.0 kHz	36.9			22.2			12.1		
12.5 kHz	36.9			20.1			9.6		
16.0 kHz	36.9	35.0		15.8	15.3		8.2	6.9	
20.0 kHz	36.9			11.5			8.4		
L_{Aeq}	**53.6**		**10**	**54.5**		**9.2**	**45.5**		**9.3**

Table 52: Displays measured background noise levels at street level positions 1 - 3 compared to CadnaA simulated levels from the operational Strata turbine at the same positions.

	Measured		CadnaA	Measured		CadnaA	Measured		CadnaA
P	**4**			**5**			**6**		
	1/3	**1/1**		**1/3**	**1/1**		**1/3**	**1/1**	
25 Hz	53.2			59.9			60.5		
31.5 Hz	54.1	18.2	-26	63.2	29.9	-23	63.8	30.4	-22
40 Hz	50.6			67.3			67.8		
50 Hz	50.8			65.3			65.8		
63 Hz	48.6	27.3	-8.7	64.3	42.1	-5.4	64.8	42.7	-4.5
80 Hz	45.1			59.0			59.5		
100 Hz	44.4			56.7			57.1		
125 Hz	43.3	32.4	-1.3	53.9	43.7	-1	54.4	44.2	0
160 Hz	43.2			54.1			54.5		
200 Hz	47.1			55.7			56.2		
250 Hz	41.3	40.3	-7.8	54.2	50.4	-7.4	54.6	50.9	-6.3
315 Hz	41.3			52.2			52.6		
400 Hz	41.0			51.6			52.1		
500 Hz	39.2	41.5	-6.3	53.1	54.1	-6	53.5	54.5	-4.9
630 Hz	39.4			52.6			53.1		
800 Hz	39.9			53.0			53.4		
1.0 kHz	39.7	44.1	5.3	53.5	57.7	5.6	54.0	58.2	6.6
1.25 kHz	38.3			52.2			52.6		
1.6 kHz	37.5			50.7			51.1		
2.0 kHz	35.9	41.8	1.7	48.9	55.0	2.1	49.3	55.4	3.1
2.5 kHz	32.9			46.4			46.8		
3.15 kHz	30.6			43.8			44.2		
4.0 kHz	28.1	34.2	0.7	41.4	47.6	1.1	41.7	47.9	2.7
5.0 kHz	24.5			38.8			39.1		
6.3 kHz	20.4			37.3			37.6		
8.0 kHz	16.6	21.5	-22.8	36.6	39.3	-21.8	36.9	39.6	-18.5
10.0 kHz	14.2			30.3			30.5		
12.5 kHz	12.4			26.8			27.0		
16.0 kHz	10.5	9.0		24.8	22.6		25.0	22.9	
20.0 kHz	9.0			17.7			17.8		
L_{Aeq}	**47.5**		**8.7**	**60.4**		**9.1**	**61.0**		**10.2**

Table 53: Displays measured background noise levels at street level positions 4 - 6 compared to CadnaA simulated levels from the operational Strata turbine at the same positions.

Table 52 and Table 53 displays the simulated noise levels from the operational strata turbine at street level positions recorded in the surrounding area. It is clear from the results that no threat of annoyance from the turbine is likely within the surrounding area as calculated results at each frequency band would be so significantly lesser than the background levels measured that they would be completely masked.

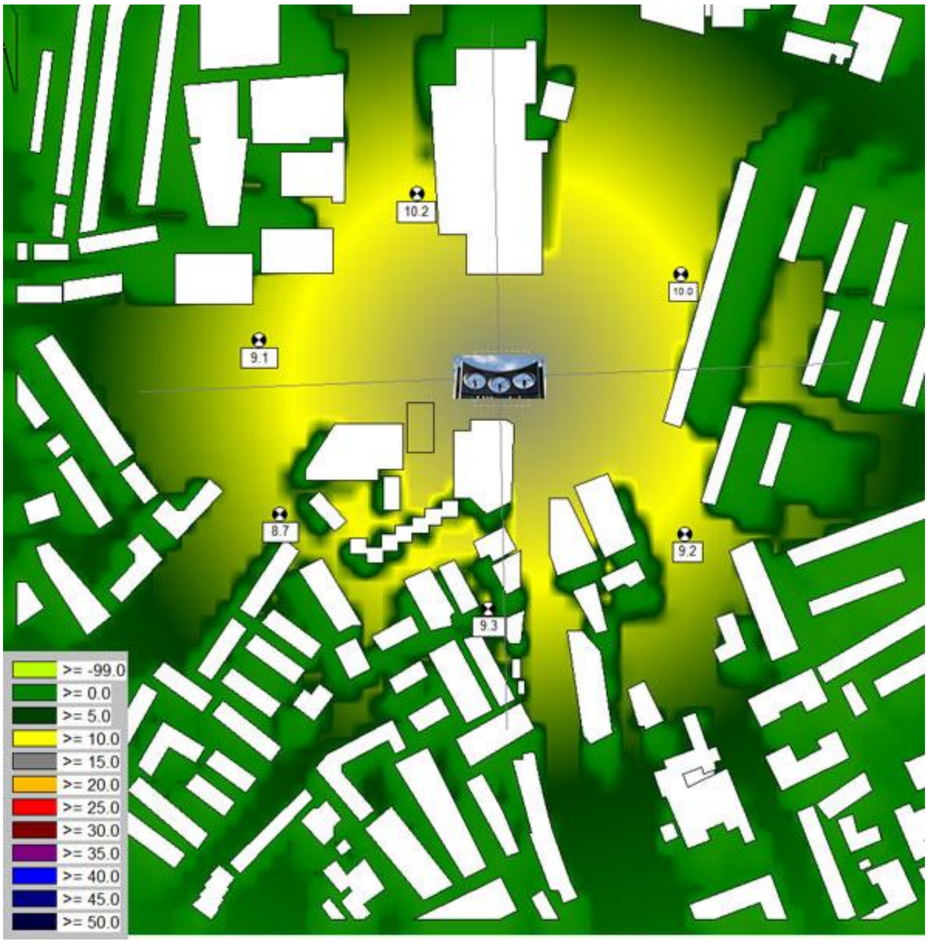

Figure 121: Displays CadnaA calculated noise levels surrounding the Strata tower with receiver points set up at the same position to measurements positions displayed in Error! Reference source not found.. Noise levels of ess than 15 dBA from the turbine are shown at all positions.

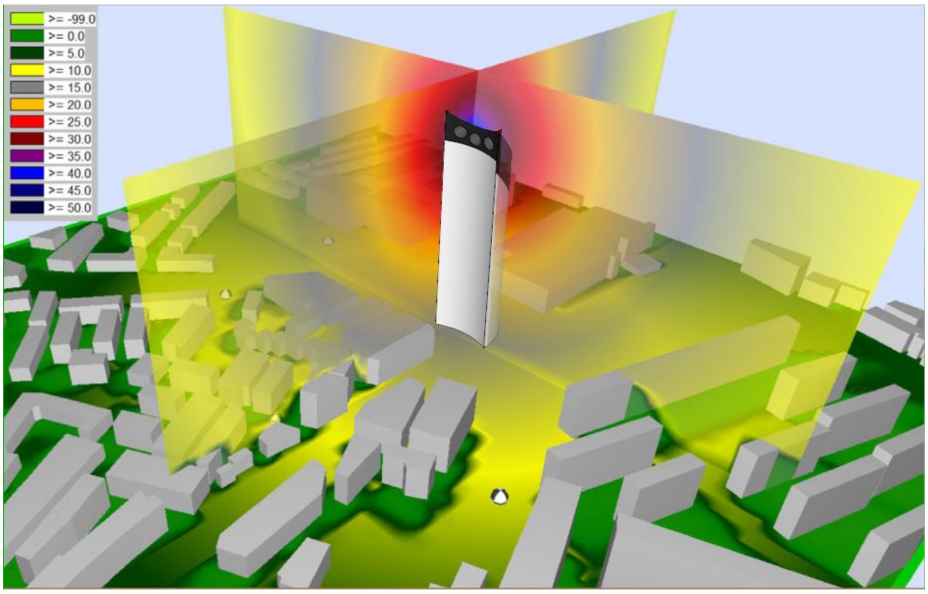

Figure 122: Displays a 3D graphic of sound propagation from the Strata tower into it's surrounding area. Due to the towering height above the local residential areas extremely low noise levels of less than 15 dBA are observed at the nearest buildings.

It has been shown that noise levels from the operational turbine will not be cause for complaint at street level or from the Strata towers nearest residential neighbours. However, as the Strata tower is itself a residential building assessment of any internal levels must be carried out to assess the likelihood of any complaint from the Strata's occupants.

There are two main, direct pathways the operational turbine noise could travel into the nearest residential apartments to be investigated.

- Directly through the structure of the building itself to the floors below
- Out of the venturi, down and through the external glazing of the structure

When investigating sound radiating through the structure of a building it is important to know the internal layout, architecture and structural make up of the building. Any sound striking a wall, floor or any panel will cause, to differing extents, the panel to vibrate in sympathy of the frequency of sound and therefore transmit the sound waves on the other side of the panel. The mass, stiffness, damping, air gaps between panels and frequency content of the sound will affect the sounds transmission through the panel.

The Strata turbines are mounted upon an inertia base of 550 mm thick concrete. Given a known stiffness and density of concrete to be 19 N/m and 2600 kg/m^3, respectively, then we can calculate the inertia base critical frequency of 34.5 Hz by the relationship displayed in Equation 24.

$$f_c = \frac{k}{t}$$

Equation 24: Where Fc = critical frequency (Hz), k = stiffness (N/m), t = thickness (m).

The Strata turbines known blade passing frequency is 8.3 Hz, well below the inertia base critical frequency. Therefore. no coincidence dip phenomenon is expected.

The turbines inertia base is fixed upon a 34.3 x 10.6 m concrete level of 0.45 m thickness. Given a known density of 2600 kg/m^3 for concrete a superficial mass (or surface density) is calculated of 1170 kg/m^2. Therefore an estimate of sound reduction per frequency band can be calculated utilising Equation 25.

$$R = 20Log(fm) - 48$$

Equation 25: Where R = Sound reduction (dB), f = frequency (Hz), m = superficial mass (kg/m2).

The results displayed in Table 54 demonstrate that a significant reduction in sound levels can be expected due to the extensive concrete mass between the turbines and lower maintenance level.

Freq Hz	$L_{w,k}$ 1/1 Oct	R	
	a	b	a-b
31.5	71.1	43.3	27.8
63	75.4	49.4	26.0
125	73.6	55.3	18.3
250	66.2	61.3	4.9
500	62.1	67.3	-5.2
1000	65.3	73.4	-8.0
2000	60.5	79.4	-18.8
4000	64.7	85.4	-20.7
8000	61.8	91.4	-29.6
TOTAL	78.6		
m	1170	kg/m^2	
t	0.45	(m)	
ρ	2600	kg/m^3	
F resonant	1.4	Hz	

Table 54: Displays R values for the Strata turbine concrete maintenance level.

It is important to note that there is a further level between the calculated maintenance level and the top residential, which is of similar construction. If this extra level is to be viewed as a multiple leaf partition system then the natural frequency of the system can be found and evaluated using Equation 26.

$$f_0 = 60\sqrt{\frac{(m_1 + m_2)}{m_1 m_2 d}}$$

Equation 26: Where f0 = natural frequency (Hz) of multiple leaf partition system, m1 and m2 are the relevant masses (kg/m2) of each partition and d = distance (m) between the partitions.

As the lower level is of similar make up a natural frequency of 1.4 Hz is predicted, far below the turbines natural frequency.

The theoretical sound reduction levels demonstrated in Table 54 presume a solid, isolated partition separating the turbines and the lower level. Obviously in a real world scenario there are stair wells, access points and elevator shafts interrupting the partition as well as doors, air gaps and any structural coupling between beams, supports and walls. There would therefore be a certain amount of sound transmission expected via direct sound paths, as well as indirect and flanking paths.

Similarly, noise levels from the turbine entering the apartment via flanking paths outside the building, and in through the glass exterior facades, can be calculated using Equation 27. This will be known after calculating the reduction in levels due to separating external distances. A +6dB penalty is added to Equation 27 as the external level is taken within a reverberant venturi.

$$L_2 = L_1 - R + 10Log(S) - 10Log(A)$$

Equation 27: Where L2 = Internal noise level (dB), L1 = sound level at the turbine. In relation to R = sound reduction of the partition (dB), S = surface area of partition (m2), A = absorption in the receiving room.

The use of this equation involves known absorption values for the internal surfaces. Unfortunately due to access restrictions this exact information is unknown, however educated assumptions can be made in reference to marketing material and floor plans provided by Brookfield Multiplex. Figure 123 shows internal marketing images of the living space and bedroom. To assess the likelihood of complaint, calculations for both areas will be carried out with particular attention toward the bedroom as this would be occupied in quieter times of the day and require the lowest noise criteria.

Theoretical results for direct sound transmission through the concrete level separating the turbines and lower apartments are displayed in Table 91 and Table 92 displays the theoretical results for outside to inside the apartment.

The top, penthouse apartments are at 117 m height, 21 m below the 138 m turbine hub height therefore 21 m is used to calculate propagation to the external facade with a directivity of 2 to compensate for the reflective venturi. The glass walls are used in calculation as they represent the weakest partition / transmission path for sound. The bedroom windows come fitted with heavy draping, providing greater absorptive qualities than bare glass. Therefore the bedroom has been assessed with drapes closed and open. Closed values are highlighted in **BLUE**.

As is clear from Table 55calculated internal levels are extremely low for both rooms. As they are they would meet the National Planning policy Framework (formerly PPG24) NEC A[16] with noise source levels below 45 dB.

[16] 'Noise need not be considered as a determining factor in granting planning permission...'.

Figure 123: Displays the penthouse apartment floor plan and internal decor needed to estimate internal absorptive values.

Results also adhere to the WHO environmental health criteria 12 - Noise:1980 guidelines of levels not exceeding 35dBA and indoor noise criteria of 30 dBA L_{Aeq} for continuous noise. They also adhere to the ETSU-R-97 35-40 dB $L_{A90\text{-}10min}$ indoor noise level range.

All sound power levels used for noise calculation emanate from the L_{Aeq} levels taken at the average wind speed of 6.1 m/s at the Strata site. Wind speeds of under 7 m/s are estimated for 77 % of the time, but on occasion it is noted that wind speeds of over 20 m/s have been observed. Therefore, a calculation of sound power levels for higher wind speed bands are calculated to offer a worst case scenario using the levels in Table 56.

Hz	63	125	250	500	1000	2000	4000	8000
Direct Transmission								
Living Room								
$L_{Turbine}$	75.4	73.6	66.2	62.1	65.3	60.5	64.7	61.8
Lin	35.5	27.9	17.6	9.2	7.5	-3.1	-5.4	-14.3
Bed Room								
$L_{Turbine}$	75.4	73.6	66.2	62.1	65.3	60.5	64.7	61.8
L_{in}	39.4	31.7	22.2	13.9	10.5	-1.2	-4.7	-13.7
L_{in}	39.8	32.2	20.3	9.8	5.5	-5.5	-7.6	-16.6
External Transmission								
Living Room								
$L_{Turbine}$	75.4	73.6	66.2	62.1	65.3	60.5	64.7	61.8
L_{out}	40.9	39.2	31.8	27.7	30.9	26.1	30.3	27.4
L_{in}	32.2	24.5	14.2	5.8	4.1	-6.5	-8.7	-17.7
Bed Room								
$L_{Turbine}$	75.4	73.6	66.2	62.1	65.3	60.5	64.7	61.8
L_{out}	40.9	39.2	31.8	27.7	30.9	26.1	30.3	27.4
L_{in}	34	26.4	16.9	8.6	5.2	-6.6	-10	-19
L_{in}	34.5	26.8	14.9	4.5	0.2	-10.8	-13	-21.9

Table 55: Displays calculated internal noise levels due to direct transmission and external, propagated noise levels at the Strata apartments in closest proximity to the operating turbines. All relevant surface area, material make up and absorptive values for internal surfaces, needed to utilise Equation 20 along with theoretical results for direct sound transmission and flanking external levels transmitted through the lower office windows are displayed in 0. Levels are calculated with and without drawing the bedroom drapes. Drawn levels are highlighted in blue.

Hz	$L_{w,k}$
31.5 Hz	71.1
63 Hz	75.4
125 Hz	73.4
250 Hz	66.0
500 Hz	69.3
1000 Hz	78.8
2000 Hz	77.9
4000 Hz	55.5
8000 Hz	46.9
TOTAL	**83.4**

Table 56: Sound power levels for the 21 m/s wind speed bin as part of a 'worst case scenario' calculation.

	Direct Transmission			**External Flanking**			
Hz	Living room Window Internal	Bedroom Window Internal	Bedroom Drapes Internal	Apartment External	Living room Window Internal	Bedroom Window Internal	Bedroom Drapes Internal
63	35.6	39.4	39.9	41.0	32.2	34.1	34.5
125	27.6	31.4	31.9	39.0	24.3	26.1	26.6
250	17.3	22.0	20.0	31.6	14.0	16.6	14.7
500	16.4	21.1	17.1	34.9	13.1	15.8	11.7
1000	20.9	23.9	18.9	44.3	17.5	18.6	13.6
2000	14.3	16.2	11.9	43.5	10.9	10.8	6.6
4000	-14.6	-13.9	-16.9	21.1	-18.0	-19.3	-22.2
8000	-29.2	-28.5	-31.5	12.5	-32.6	-33.9	-36.8

Table 57: Displays worst case scenario results using the sound power levels for the 21 m/s wind speed bin in Table 56 Levels are shown both with and without drawing the bedroom drapes.

Table 57 displays the calculated worst case scenario results. The used sound power levels used represent those measured at the 21 m/s wind speed bin, an event that only occurred for 2 % of the measurement period.

Internal levels are still estimated to be within National Planning Policy Framework, WHO environmental health criteria and ETSU-R-97 guidelines and therefore are not a likely threat to sleep disturbance of noise annoyance from apartment occupants.

It should also be noted that the levels discussed so far presume closed windows. During the summer months if the top apartment residents where to open their windows then there would be no transmission loss and levels would approach 45 dB, which relates to NEC B according to the National Planning Policy Framework.

As previously mentioned access was not granted to conducted internal noise level surveys within the apartments. Therefore, a noise survey was conducted to overlap with one week of the operational turbine noise survey on the apartment level within a closed room, a storage cupboard, on the same floor level. The results are depicted in Figure 124. Figure 124 displays an unusually flat noise level curve hovering around 38 dBA. As previously estimated for the residential apartments on the same level the operational turbine noise would be well below this. A 1/3rd Octave analysis of the sound is depicted in Figure 125.

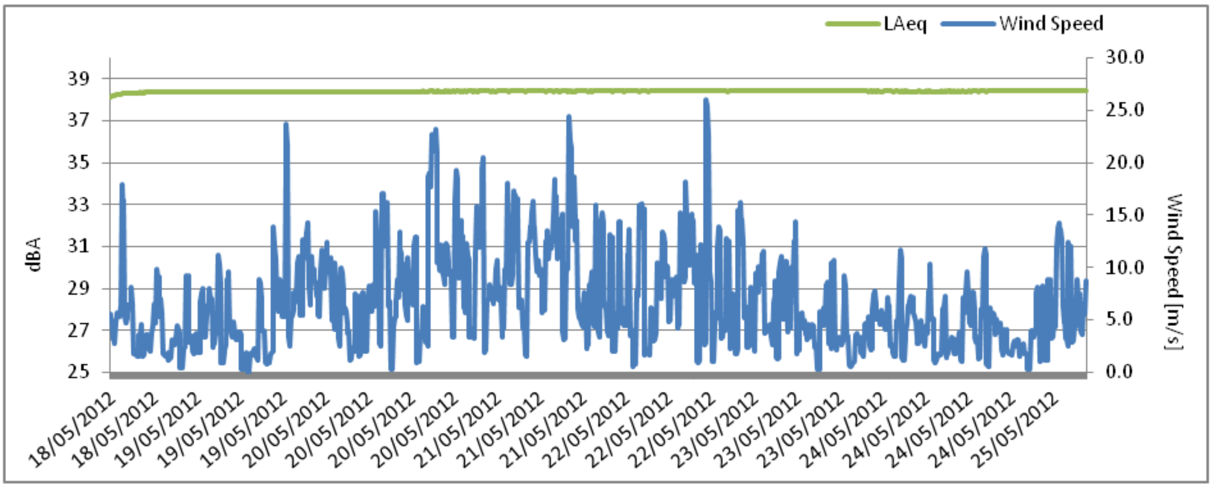

Figure 124: Displays Internal noise levels recorded on the Strata's top residential level, plotted over time against extrapolated, recorded wind speeds.

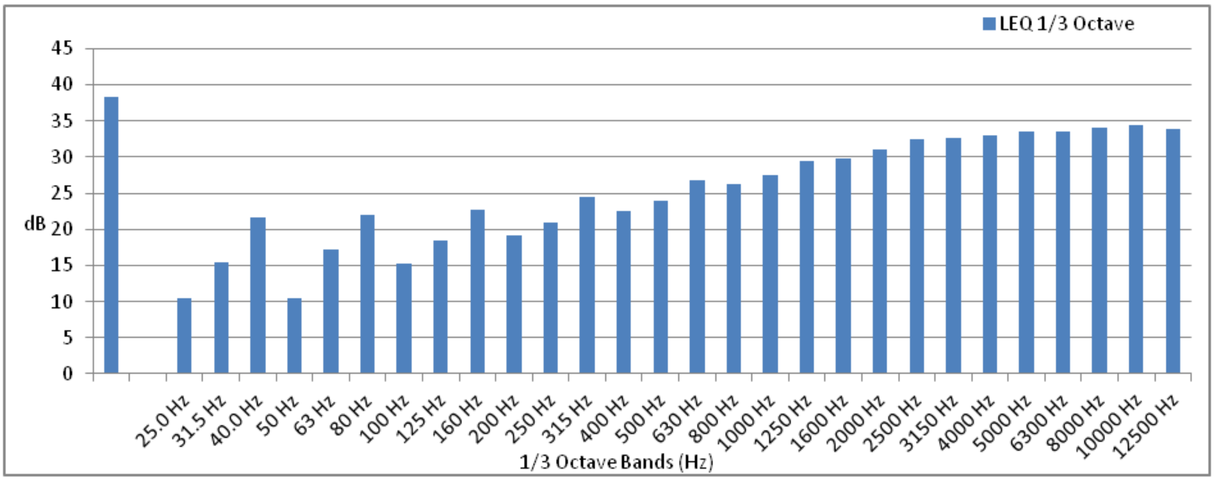

Figure 125: Displays 1/3rd octave L_{Aeq} operational Strata turbine measurements taken at the residential level.

This clear, unchanging frequency signature along with a constant unchanging noise level suggests that this is due to other factors, most likely the electrical wiring and plumbing running through the storage cupboards, which would likely be the main cause of this steady noise level. As these measurements are unchanging and dominated by local environmental factors they do not offer much in the assessment of the residential apartments aural environment other than to say that the external turbine is not a contributing factor at this level in this instance.

5.3 Vibration

5.3.1 Strata tower turbine mounting background vibration

Background vibration measurements were conducted at the Strata turbine mount between 4/5/2012 and 11/5/2012. 5 minute X,Y & Z axis RMS acceleration levels are shown in Figure 126. Methodology, positioning, weightings and units are as previously discussed in chapter Strata vibration measurement setup 3.4.1.

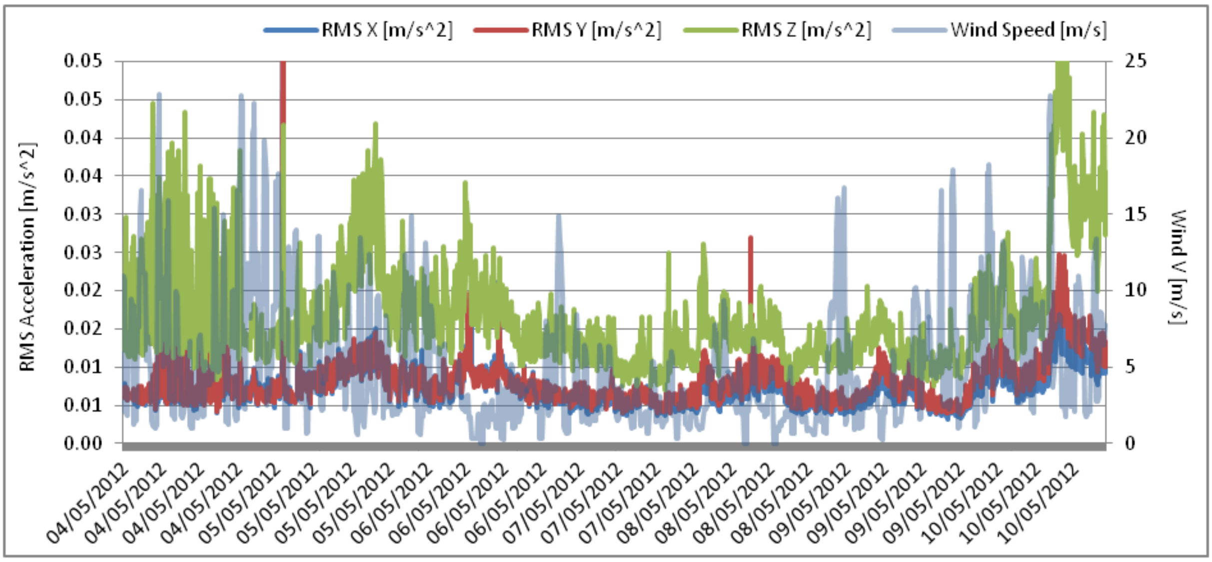

Figure 126: Displays 1 week background vibration levels at non-operational Strata turbines

	X Axis	Y Axis	Z Axis	Wind Speed
X Axis	1.0			
Y Axis	0.9	1.0		
Z Axis	0.6	0.7	1.0	
Wind Speed	0.0	0.0	0.1	1.0

Table 58: Displays no significant correlation (r) between acceleration and wind speed.

It is clear from Figure 126 and Table 58 that wind speed demonstrates no direct effect on the turbine structures vibration levels, however, regular fluctuations in acceleration are perceived. Although not at high enough amplitude to warrant any concern for residential discomfort it would be of interest to investigate the source of this vibration. The results are further discussed and compared to operational results later in this chapter.

5.3.2 Strata tower operational vibration measurements (turbine)

Vibration measurements were conducted while the Strata turbines were operational at the turbine mount between 11/5/2012 and 18/5/2012. 5 minute X,Y & Z axis RMS acceleration levels are shown in Figure 127. Methodology, positioning, weightings and units are as previously discussed in chapter Strata vibration measurement setup 3.4.1.

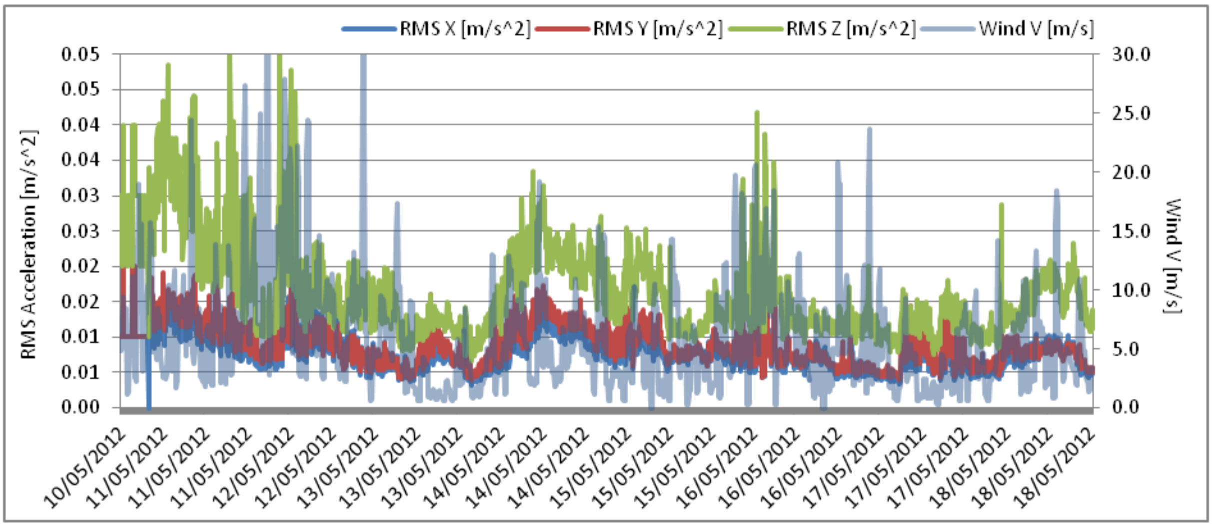

Figure 127: Displays 1 week vibration levels on the inertia base of the Strata turbine whilst the turbines are operational.

	X Axis	Y Axis	Z Axis	Wind V
X Axis	1.0			
Y Axis	0.9	1.0		
Z Axis	0.8	0.8	1.0	
Wind V	0.2	0.1	0.2	1.0

Table 59: Displays a slight correlation (r) between wind speed and Z axis acceleration levels when compared to the background, non-operational results. However, this still does not demonstrate a strong relationship between wind speed and turbine vibration.

Figure 127 and Table 59 demonstrates that even when the turbines are operating there is still no significant relationship between wind speed and Z axis acceleration levels. As presented in Figure 126 there are fluctuating levels in RMS acceleration recorded at the turbines which do not coincide with an increase in wind speed or turbine movement. The measurements are far below[17] any levels likely to cause complaint or discomfort and are likely caused by other mechanical factors within the building. The lowest threshold defined in BS6841:1987 and ISO2631 is 0.315 m/s^2. This level is defined as 'not uncomfortable' and any levels below this are not deemed a threat to discomfort. Low end VDVs of 0.1 - 0.2 are defined as having a 'low probability of adverse comment'. Levels recorded at the Strata turbines are shown to be far lower than these guidelines[18] so no cause for concern.

The vibration data was then sorted into wind speed bins and analysed to assess the systems response to increasing wind speed while operational and stalled (presented as Figure 128 to Figure 131, background and operational average RMS Acceleration levels per wind speed bin are

[17] By at least a factor of 10. Please refer to chapter 3.4 for acceptable vibration limits.
[18] by a factor of -10 on average.

documented in Chapter 3. When assessing these figures some interesting trends appear, vibration levels seem to fluctuate independently of wind speed both when the turbines were spinning and stalled. Third octave analysis was conducted to assess any foreign frequency signature that could be attributed to any external or internal mechanisms as seen in Figure 129.

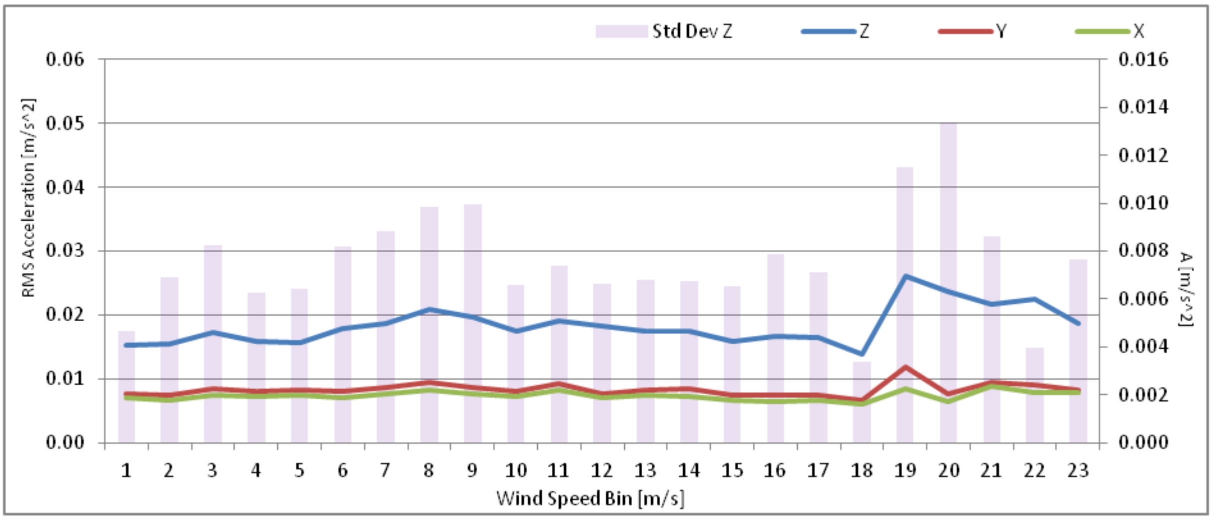

Figure 128: Background average RMS Acceleration [m/s^2) per wind speed against Z axis standard deviation.

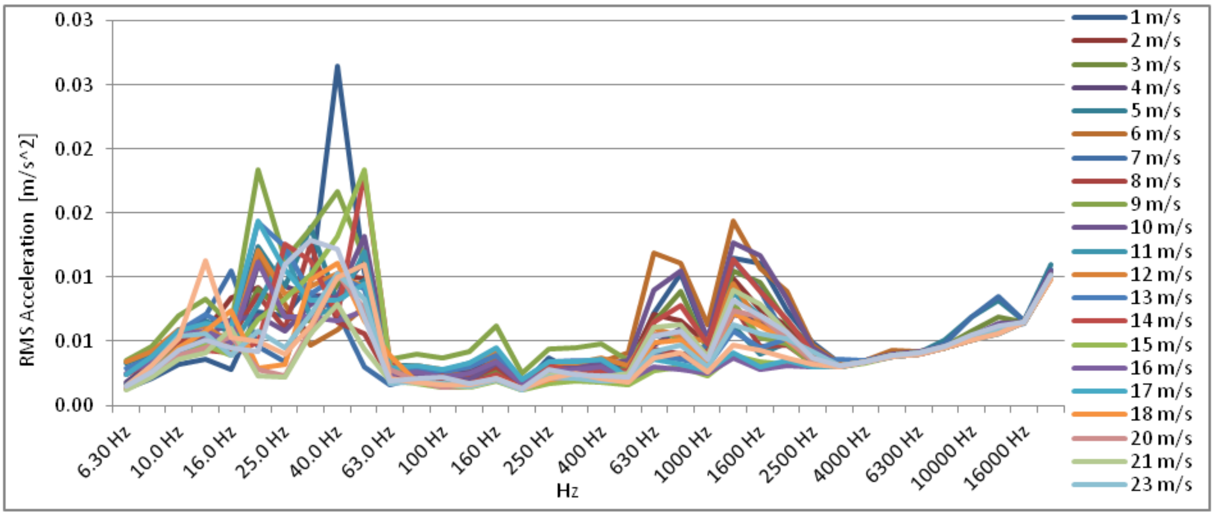

Figure 129: Background 1/3 octave analysis of the Strata turbine, taken at the inertia base. Z axis levels are compared across all recorded wind speeds.

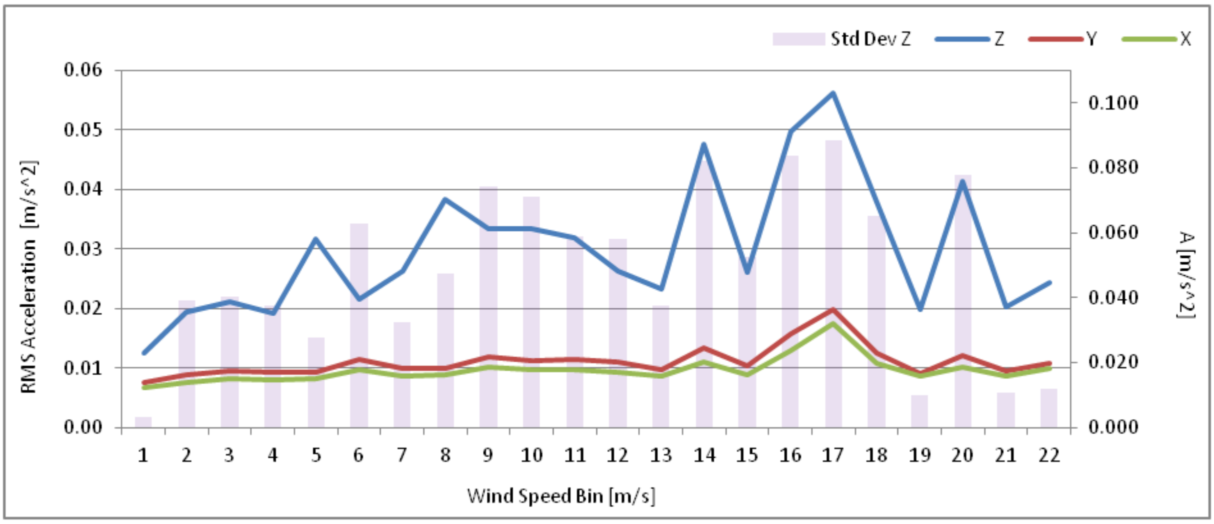

Figure 130: Operational average RMS Acceleration [m/s2] per wind speed against Z axis standard deviation.

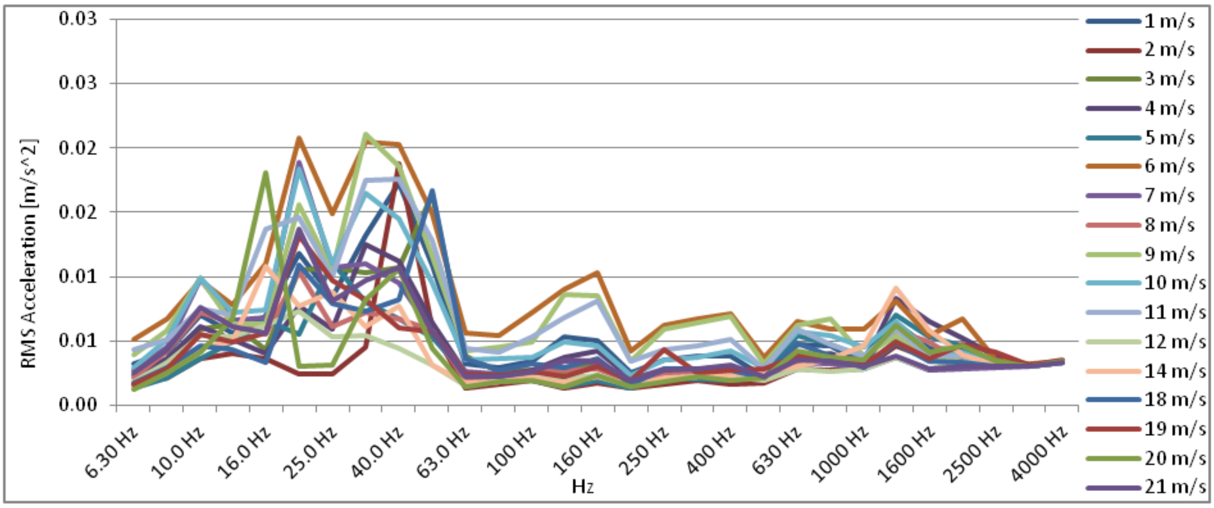

Figure 131: Displays operational 1/3 octave analysis of the Strata turbine Z axis RMS acceleration, measured at the inertia base.

As can be seen from Figure 129 and Figure 131, the frequency characteristics of the results are identical and of a similar amplitude in spite of whether the turbine blades were spinning or not. The Castle House Turbine Design Study (Norwin, 2008) prepared by the turbine manufacturers quotes the overall turbine system to have a natural frequency between 14-16 Hz which ties in with the measured peaks displayed in Figure 129 and Figure 131. The 630 Hz and 1600 Hz peaks tie in with the natural resonance of the steel beam (material width and thickness) to which the accelerometer was affixed, see Figure 38.

These 1/3rd octave results suggest that the turbine structure and inertia base was excited at its natural frequency but at levels below those stated in ISO2631's guideline for comfort and only marginally peaking the average human perception threshold of 0.02 m/s^2.

As before, simultaneous vibration monitoring was conducted at the residential level to assess any structural transmission and likelihood of complaint. The results are presented in Figure 132. As is displayed the resonances observed around the systems natural frequency were not transmitted to the lower residential floors reiterating the assumption that residential complaints would not be likely.

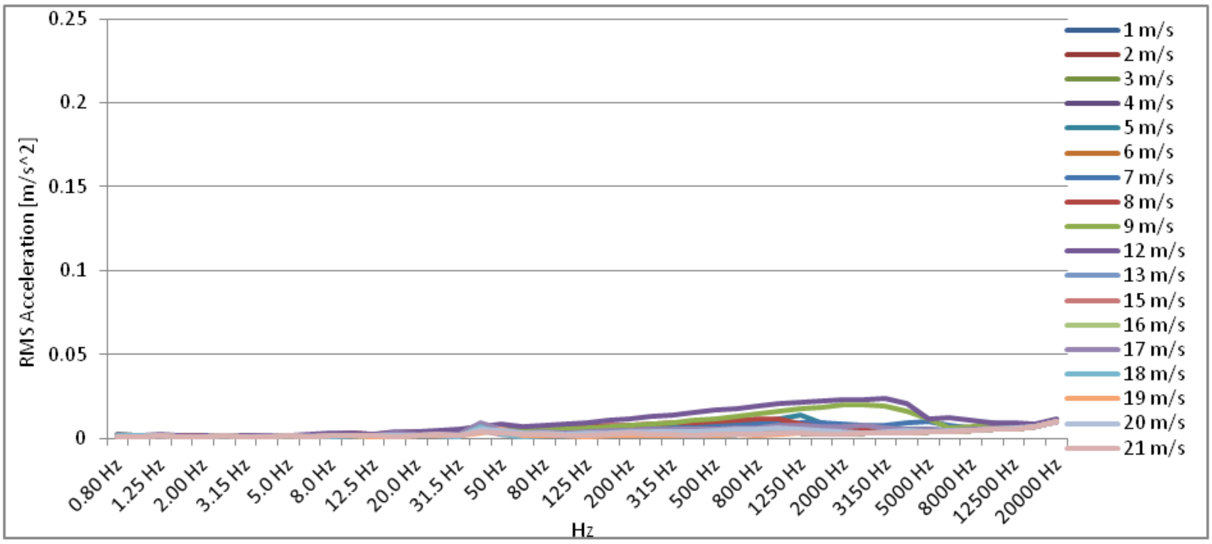

Figure 132: Displays 1/3rd octave RMS acceleration [m/s^2] vibration results measured simultaneously at the lower residential levels as those displayed in Figure 131.

5.4 Strata tower theoretical electrical power generation

To reiterate, no logging equipment was operational, so extrapolated LSBU wind speeds for 2013 and 2014 are relied upon to estimate the potential Strata energy output and compare to the manufacturers claims. Following the same methodology conducted at LSBU to compare measured and Weibull predicted outputs with a theoretical Strata case study should give an interesting juxtaposition of two different turbine installations in the same urban environment. Methodology and process is as outlined in section 4.4.

Table 60 displays the data collected over the test periods and Table 61 shows the predicted energy yield using this data.

	Data Available	Data Collected	Missing	Missing %
2013	52560	51202	1358	3
2014	52560	51451	1109	2

Table 60: Displays collected wind data for 2013 and 2014.

	Norwin 18kW at 6.2 m/s kWh Lower	Norwin 18kW at 6.2 m/s kWh Upper	Theoretical Max Yield kWh	Rayleigh kWh	Weibull kWh	Ave Wind V m/s
2013	45000	100000	14313	13868	12734	5.2
2014	45000	100000	12463	11689	11521	5
2013	**% Efficiency**	**Lower**	95	92	85	
2014	**% Efficiency**	**Lower**	83	78	77	
2013	**% Efficiency**	**Upper**	43	42	38	
2014	**% Efficiency**	**Upper**	37	35	35	

Table 61: Displays predicted energy yield for the Strata site compared to manufacturers marketing figures, turbine efficiency and average wind speed for 2013 and 2014. The manufacturers estimate covered a range of 45 - 100 MWh per year, therefore predicted yield is evaluated against both extremes.

Figure 133 to Figure 136 presents the Strata site's predicted energy output and wind speed distribution curves. As can be seen, the Rayleigh predictions are shown to be higher than the Weibull due, in part, to the Rayleigh's higher wind speed peak compared to the lower wind speed concentration of the Weibull, which peters out where manufacturers power coefficients start to rise (around 6 m/s).

It is clear from Figure 134 and Figure 136 that the Rayleigh curves crest over-estimates the concentration of wind speeds whilst the Weibull curve slightly under estimates these same speeds when compared to collected data. As the Weibull curve best fits the distribution curve of collected wind speed data it would be more realistic to take the Weibull prediction as a good estimation of annual energy yield at the Strata site.

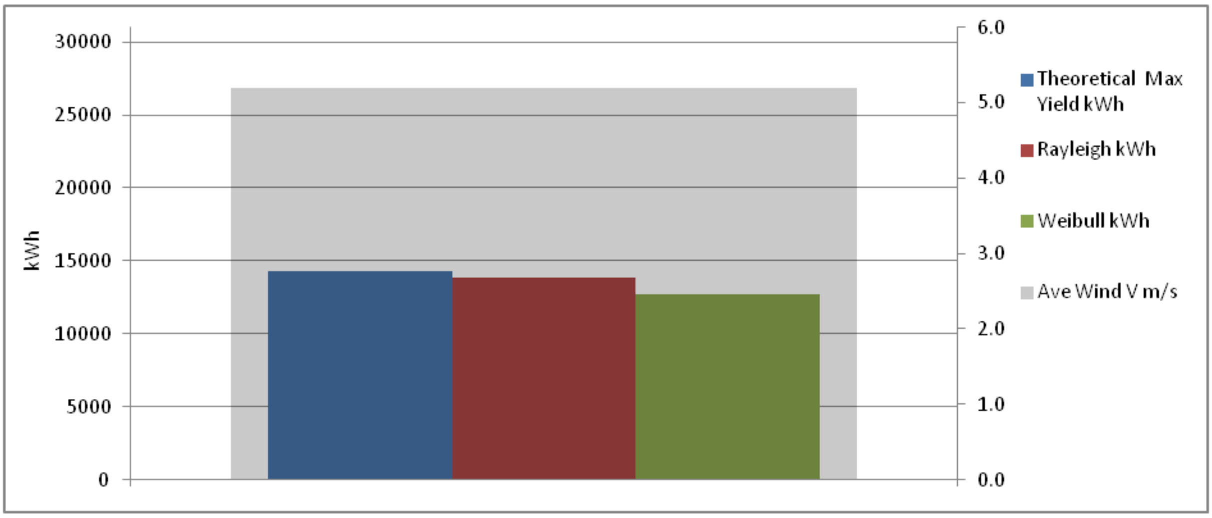

Figure 133: Displays predicted energy yield at the Strata site for 2013

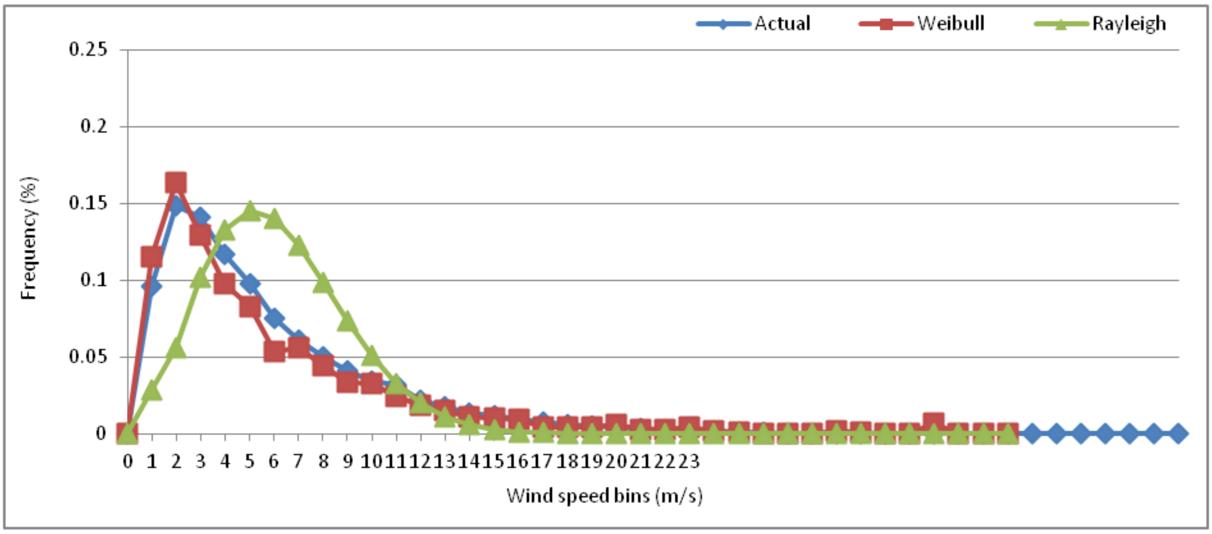

Figure 134: Displays measured, Weibull and Rayleigh predicted wind speed distributions for the Strata in 2013.

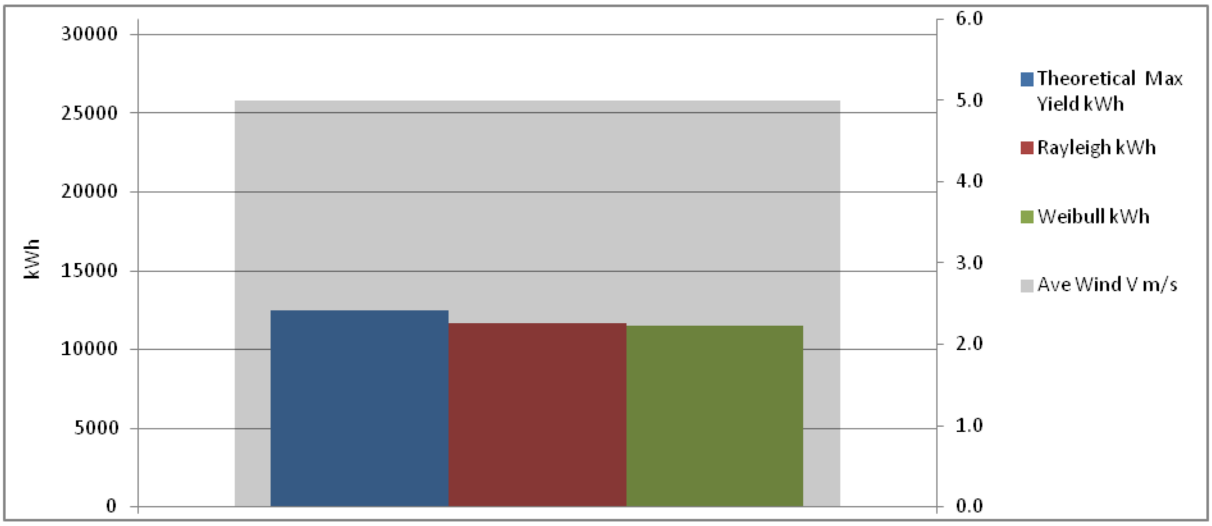

Figure 135: Displays Energy yield predictions for 2014 at the Strata site.

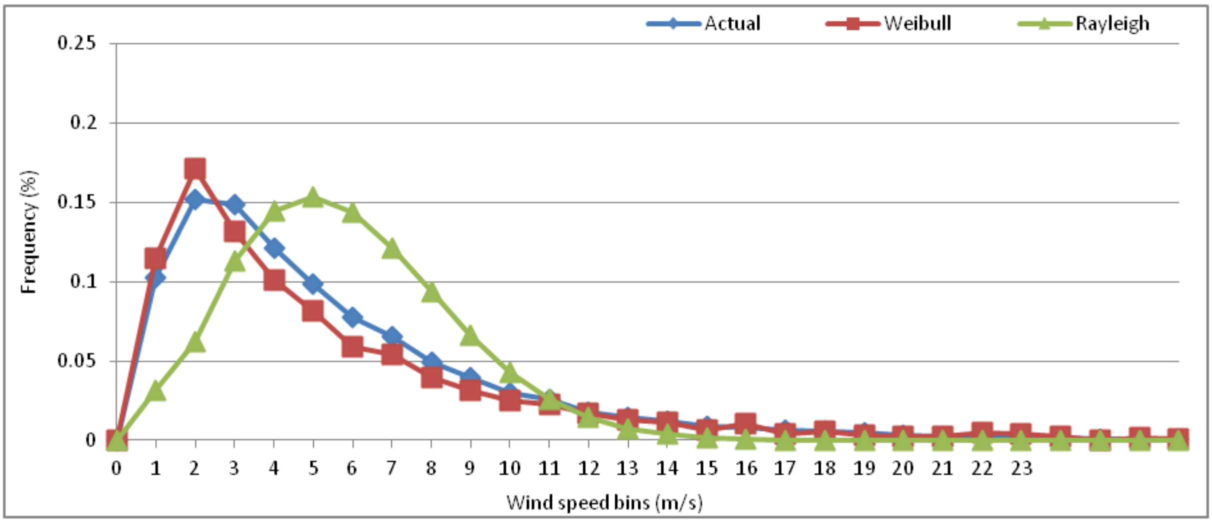

Figure 136: Displays measured, Weibull and Rayleigh predicted wind speed distributions for the Strata in 2014.

Table 61 shows that the manufacturers lower end predictions were not too far off from the more suitable Weibull predictions; a 15 - 23 % difference is calculated[19]. This difference becomes wider when compared to the upper end estimations; a 62 - 65 % difference is calculated

The manufacturer predictions of 45 to 100 MWh p.a. is based on an average wind speed for London of 6.21 m/s. This was derived from NOABL archived average wind speeds recorded at Heathrow's average wind of 4.7 m/s at a 10 m height, which is extrapolated to 140m height, roughness class 3 to give 6.21 m/s (Norwin, 2008). This is higher than the authors estimate of 5.2 and 5 m/s and for 2013 and 2014 which are attributed to a couple of things:

1. The roughness class 3 used by the manufacturer gives a roughness length of 0.4, more suitable for villages, small towns, agricultural land, rough and uneven terrain. A roughness class of 4 (roughness length 1.6) was used in the authors calculations to allow for the dense urban topography within the Elephant and Castle area. This point, on its own, should have far elevated the authors calculations above the manufacturers expectations if it were not for point 2.
2. Heathrow is a rural, open plane with less disturbed wind flow and higher wind speeds. Heathrow's average wind speed is 4.7 m/s which extrapolates to 6 m/s at 49 m height whereas the average recorded wind speed at 49 m at the LSBU site was 3.5 m/s.

The manufacturer is not UK based therefore it is understandable why the NOABL database was relied upon, but does highlight the need for site specific wind speed data for accurate estimations of energy generation as the manufacturer estimates appear over optimistic.

It should be noted that in the manufacturer 'Turbine Design Study' (Norwin, 2008) the following points are noted:

1. There may be a 'blockage effect of the wind due to the presence of the building'. This could diminish wind speeds at the turbines.
2. '25% of the time the wind direction is in the acceptable interval where the turbines are allowed to operate'. Due to the lack of yaw mechanism the turbines cannot furl into the wind. They are fixed facing winds from the south[20] therefore using wind roses from the NOABL database it is calculated that a prevailing wind from the south would occur ~25 % of the time.
3. 'The reduction of power output due to skew winds when the wind direction is more from the side elaborates to an average of 10% loss'. The venturi and building shape has been taken into consideration as having potential to block the wind and reduction wind speeds at the turbine.
4. 'It is assumed that the turbine is running both day and night'. This was added in case noise levels became too obtrusive for residents at night, therefore meaning the turbines would only be operational during the day. As estimated from noise measurements made at the Strata

[19] It is important to note that manufacturer estimations of 45-100 MWh is for all three turbines. Investigations thus far have been on just one so figures have been adjusted accordingly.
[20] Not ideal for an area with a predominantly south-westerly prevailing wind.

site and evaluated in section 5.2.2, this would most likely not be an issue and therefore the turbines could run 24 hours a day.

Figure 137 confirms the manufacturers concerns as measured wind direction data in the area results in the displayed wind rose, which clearly depicts a predominantly south-westerly prevailing wind. The difference is building response to wind direction is displayed in Figure 138 and Figure 139, confirming the manufacturers estimations of a reduced wind flow at the turbines influenced by the venturi and building shape when wind is not directly from the south. The extrapolated LSBU data was therefore scaled accordingly to simulate this effect. These results and points will be further discussed in chapter 6.1.2.

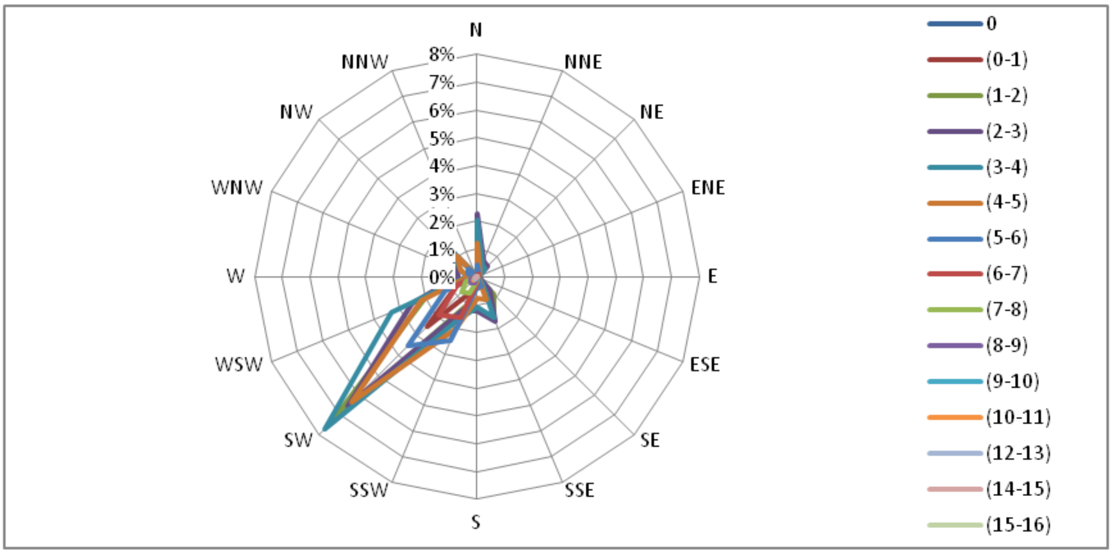

Figure 137: Displays a Strata wind rose depicting the predominantly south-westerly prevailing wind resource.

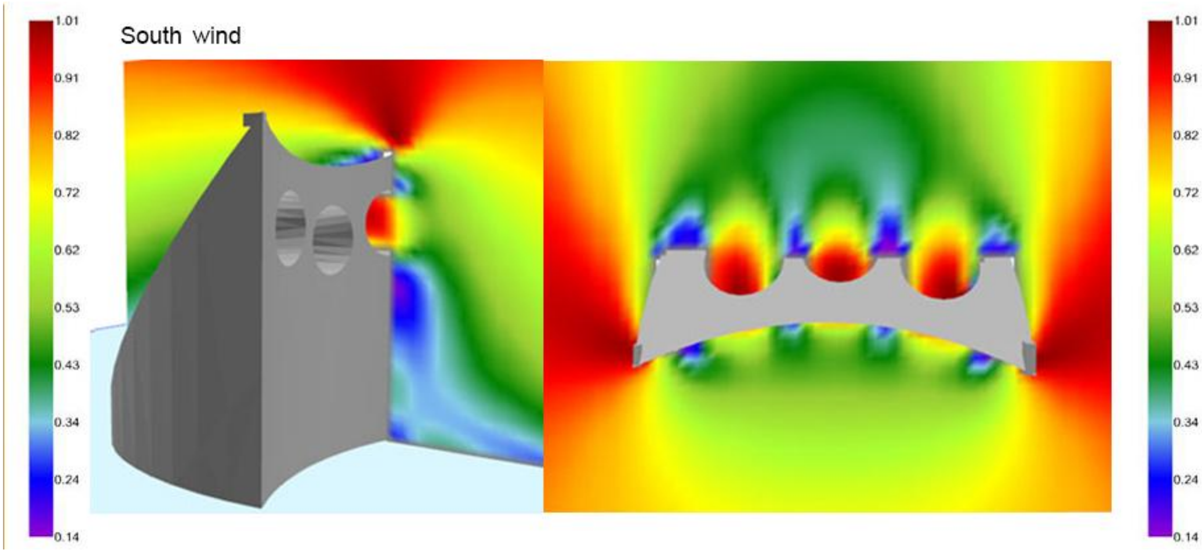

Figure 138: Displays wind flow around the Strata venturi with a southerly prevailing wind.

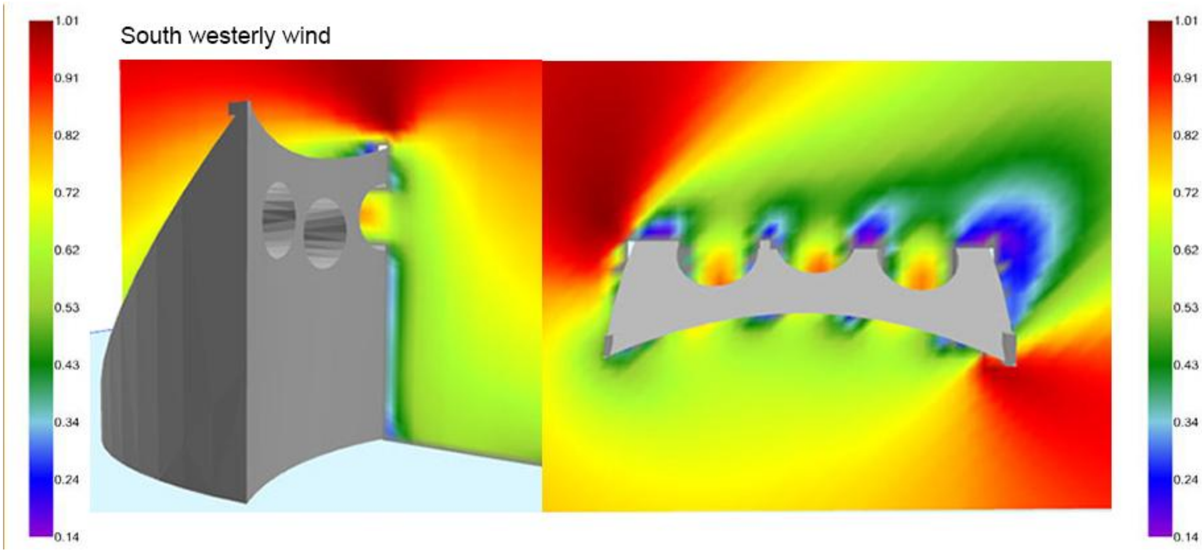

Figure 139: Displays wind flow around the Strata venturi with a south-westerly prevailing wind.

Chapter 6 Wind Energy Economics & London Guidance Compliance

The research conducted in this thesis began in response to policy 4A.9 of the mayor of London's 'London Plan' (GLA, 2004) and proposal 3 of the 'Energy Strategy' in 2004 that required that 'all new major developments to generate a proportion of the site’s electricity or heat needs from renewables' and that all new planning applications should 'generate at least 10 % of the site’s energy needs (power and heat) from renewable energy on the site'. This is all part of an attempt to reduce London's CO_2 emissions by 50 % by 2050.

The Strata in Elephant and Castle was the first major development to comply with three 18kW turbines installed to meet these demands; the first time wind turbines had been integrated into the fabric of a builds architecture. In 2012 LSBU installed a Proven 6kW turbine on campus which is expected to produce 6 MWh per annum. It is estimated that it would provide 0.75 - 1.25 % of the electrical needs of the Tower Block. Both installations will now be analysed from an energy production standpoint to assess each systems degree of compliance with the 'London Plan' (GLA, 2004) and 'Energy Strategy' (GLA, 2004). For the purposes of this analysis a CO_2 emission factor of 0.527 kg/kWh is used as defined by DEFRA (Defra, 2014). The economics of each system will also be assessed, a comparison price per kWh will be demonstrated, which can be calculated as depicted in Equation 28. This will be compared with current utility prices over the lifespan of the system and a return on investment (ROI) will be predicted using Equation 29. The installations will also be judged on merit as investments using Equation 30 to derive the NPV (Net Present Value) and IRR (Internal Rate of Return).

$$\pounds_{kWh} = \frac{Total\ System\ Cost}{Yield_{p.a}\,.Lifespan}$$

Equation 28: To calculate the price per kWh of a renewable energy system. Total system costs should include equipment and installation costs as well as expected maintenance.

$$ROI = \frac{Annual\ value\ of\ electricity\ yield}{Cost\ of\ the\ System}$$

Equation 29: Calculates a renewable system's annual return on investment.

$$Pv = \left(\frac{Fv}{(1+r)^n}\right)$$

Equation 30: Calculates Present Value where Pv = Present Value, Fv = Future Value, r = interest rate and n = term (years).

The figures derived using Equation 29 can be evaluated to financial returns expected from a government gilt, bonds or other missed investment opportunities. There are limits to these quick economic assessments as they do not consider insurance costs, interest lost from cash investments, the rise in utility charges per kWh or a depreciation in currency over time, therefore a more detailed financial assessment can be forecast using a economic procedure known as discounting.

Discounting allows the inclusion of other economic factors like maintenance costs, grid tariff inflation and the time value of money, which is the depreciating value of currency over time. This is calculated via opportunity costs, which are the lost economic gain by investing in one scheme over another (i.e. property instead of stocks etc). Interest rates from debt accrued from a turbine installation are usually used to represent the discounting or diminishing value of currency over time. In the case of the LSBU and Strata turbine installations, where this information is not known, figures will be drawn from current available investment rates with a comparable risk profile to renewable energy systems. A 30-year UK gilt treasury stock with a 2.32 % coupon is used for the purposes of the LSBU example and a 15 year gilt yield of 1.58 % for the Strata to reflect the installations relative life expectancies.

The costs of electricity purchased from the local grid supplier is then calculated over the expected turbine life span including any expected inflation in electricity costs. A 4% annual increase of utility price per kWh is presumed, reflective of the trend set in recent years (British Gas, 2014). The costs of utility provided electricity is then recalculated using the diminished value of currency due to inflation, which represents the value of the electricity purchased in today's monetary value terms. These figures are then set against the turbine installation costs and any expected maintenance costs, which can be added per year.

The UK government does not currently offer bursary or grant incentives for renewable systems but does offer a 'Feed-In-Tariff' (FIT); a price per kWh of electricity generated and/or exported. Therefore a comparison of expected yield in kWhs per year multiplied by the government FIT rate will be applied for each system. This can then be subtracted from the final discounted cost of the system[21]. FIT was much higher when installed (41 p/KWh) The current (2015) FIT rate of 14.45 p/kWh[22] for installed capacity between 1.5 kW and 100 kW is used. The discounted cost of the installation is then calculated using either the rate of interest of debt, loan repayments or (in this case) investment rates. After these parameters have been calculated over the turbines expected lifespan a comparison can be drawn from the discounted cost of the installation and the discounted cost of the electricity purchased from the utility company. If the discounted installation costs are lower than the discounted purchased electricity then the installation is a financially profitable investment showing a net saving over the time period. The LSBU installed Proven 6kW turbine has a life expectancy of 25-30 years. Therefore for the purposes of an economic forecast as optimistic 30 year life span will be used. The Strata installation has a limited lifespan of 15 years, which will be used for its economic overview.

[21] It is assumed that both installations are eligible for the government backed 'Feed-In-Tariff' and are both certified under the Micro generation Certification Scheme in order to benefit from these incentives.
[22] Prices correct as of 01/04/15. The author feels it is important to note that the FIT at time of the Strata installation was far greater at 34.5 pence per kWh but as the turbines have not generated any electricity there is no need to take this into consideration. Theoretical figures assume the turbines to be a new installation generating energy from this year forth.

6.1.1 LSBU site

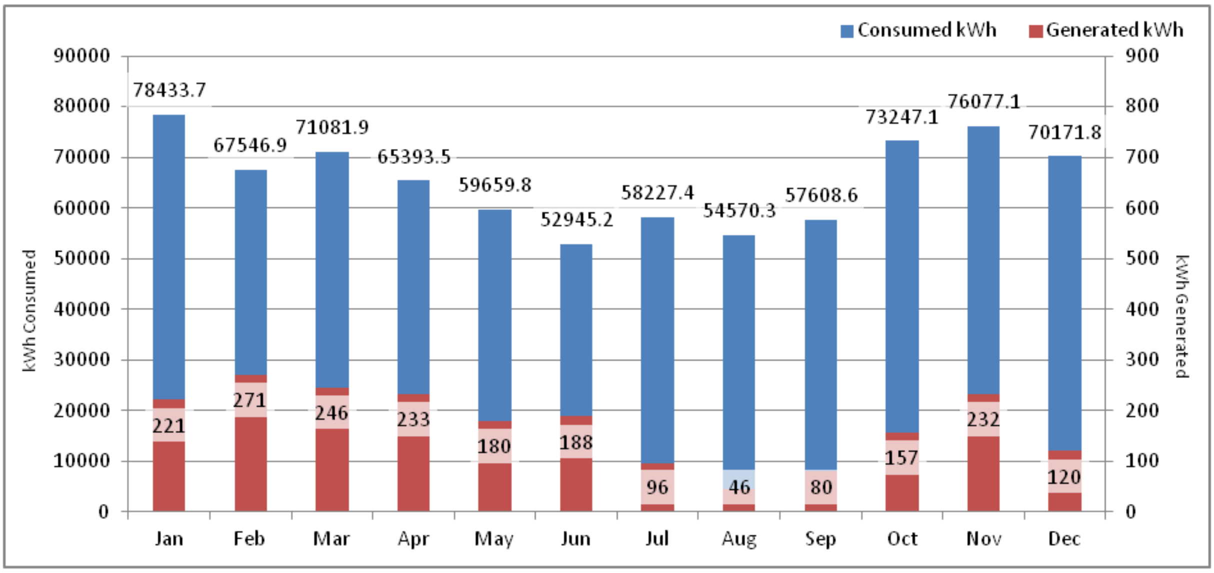

Figure 140: Depicts the electrical consumption against electrical generation for LSBU Tower Block 2013.

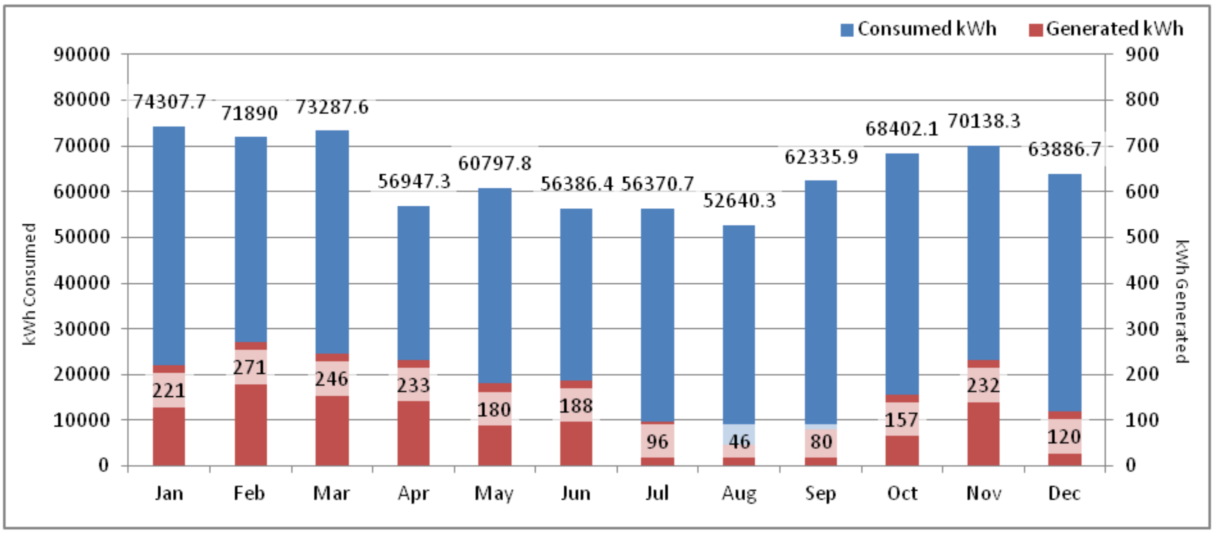

Figure 141: Depicts the electrical consumption against electrical generation for the LSBU Tower Block 2014.

As can be seen from Figure 140, Figure 141 and Table 63 - Table 64 the LSBU turbine produced a total of 2070 kWh and 2098 kWh of energy per year compared to the tower blocks electrical consumption of 784963.3 kWh and 767390.8 kWh for the 2013 and 2014 year periods. This equates to 0.3 % of the tower blocks needs and only saved the university a total of £550.34 out of a £204,805.31 spent of electricity over the 2013-2014 period. It has saved 1.09 out of 413.68 tonne CO_2 emissions. This installation would not meet the requirements of the Mayor's policy 4A.91 or London's 'London Plan'. Comparing the installed cost of £25,000 against an energy yield of 2098 kWh over a 30 year period gives an LSBU price per kWh of £0.40 and the systems ROI of 1.16 %. The LSBU installation is also evaluated from an NPV, IRR investment point of view, which is depicted in Table 62. This assessment further re-iterates the minimal output/annual return would not entice investors.

The LSBU installation economic value is further assessed using the discounting method as shown in Table 65. As is clear from Table 65 the price of electrical generation from the LSBU turbine is far greater than the same amount purchased from the utility company over its life span; £24,835.46 as opposed to £10,525.87.

	Rate	-5.796	%
Amount	**Year**	**0.94204**	**PV**
-25000	0	1	-25000
290	1	0.9420	307.84
290	2	0.8874	326.78
290	3	0.8360	346.89
290	4	0.7875	368.23
290	5	0.7419	390.89
290	6	0.6989	414.94
290	7	0.6584	440.47
290	8	0.6202	467.57
290	9	0.5843	496.33
290	10	0.5504	526.87
290	11	0.5185	559.29
290	12	0.4885	593.70
290	13	0.4602	630.23
290	14	0.4335	669.00
290	15	0.4084	710.16
290	16	0.3847	753.86
290	17	0.3624	800.24
290	18	0.3414	849.47
290	19	0.3216	901.74
290	20	0.3030	957.22
290	21	0.2854	1016.11
290	22	0.2689	1078.63
290	23	0.2533	1144.99
290	24	0.2386	1215.44
290	25	0.2248	1290.22
290	26	0.2117	1369.60
290	27	0.1995	1453.87
290	28	0.1879	1543.32
290	29	0.1770	1638.28
290	30	0.1668	1739.07
		NPV	**1.25**

Table 62: Displays NVP/IRR analysis for the LSBU turbine site.

CO_2 F: 0.527					
2013	**Month**	**Consumed kWh**	**Electric Sum tCO_2**	**Generated kWh**	**Electric Sum tCO2**
	Jan	78433.7	41.33	221	0.12
	Feb	67546.9	35.60	271	0.14
	Mar	71081.9	37.46	246	0.13
	Apr	65393.5	34.46	233	0.12
	May	59659.8	31.44	180	0.09
	Jun	52945.2	27.90	188	0.10
	Jul	58227.4	30.69	96	0.05
	Aug	54570.3	28.76	46	0.02
	Sep	57608.6	30.36	80	0.04
	Oct	73247.1	38.60	157	0.08
	Nov	76077.1	40.09	232	0.12
	Dec	70171.8	36.98	120	0.06
	TOTAL	784963.3	413.68	2070	1.09
	kWh £	0.126		% 0.3	
	TOTAL £	£98,905.38		£260.82	

Table 63: Depicts a monthly break down of electrical consumption and generation from the LSBU Tower Block for 2013 including electrical bills and CO2 emissions.

CO_2 F	0.527				
2014	**Month**	**Consumed kWh**	**Electric Sum tCO_2**	**Generated kWh**	**Electric Sum tCO_2**
	Jan	74307.7	39.16	175	0.09
	Feb	71890	37.89	273	0.14
	Mar	73287.6	38.62	161	0.08
	Apr	56947.3	30.01	244	0.13
	May	60797.8	32.04	153	0.08
	Jun	56386.4	29.72	180	0.09
	Jul	56370.7	29.71	189	0.10
	Aug	52640.3	27.74	137	0.07
	Sep	62335.9	32.85	85	0.04
	Oct	68402.1	36.05	150	0.08
	Nov	70138.3	36.96	110	0.06
	Dec	63886.7	33.67	241	0.13
TOTAL	**kWh**	767390.8	404.41	2098	1.11
	kWh £	0.138		% 0.3	
	TOTAL £	£105,899.93		£289.52	

Table 64: Depicts a monthly break down of electrical consumption and generation from the LSBU Tower Block for 2014 including electrical bills and CO_2 emissions.

Annual Generation		2098	kWh				
Year	Discounting	Utility Electricity			Proven 6kW		
	Factor	Cost	Discounted	Costs	Discounted	(FIT)	Discounted
	2.32%	4%	(DF)		Costs	£0.145	Income
0	1	0	0	£25,000.00	£25,000.00	0	0
1	0.98	£283.23	£276.66	£0.00	£0.00	£304.21	£297.15
2	0.95	£294.56	£281.05	£600.00	£572.48	£304.21	£290.26
3	0.93	£306.34	£285.51	£0.00	£0.00	£304.21	£283.52
4	0.91	£318.60	£290.04	£600.00	£546.23	£304.21	£276.95
5	0.89	£331.34	£294.65	£0.00	£0.00	£304.21	£270.52
6	0.87	£344.59	£299.32	£600.00	£521.18	£304.21	£264.25
7	0.85	£358.38	£304.07	£0.00	£0.00	£304.21	£258.11
8	0.83	£372.71	£308.90	£600.00	£497.27	£304.21	£252.13
9	0.81	£387.62	£313.80	£0.00	£0.00	£304.21	£246.28
10	0.79	£403.12	£318.78	£600.00	£474.47	£304.21	£240.56
11	0.77	£419.25	£323.84	£0.00	£0.00	£304.21	£234.98
12	0.75	£436.02	£328.98	£600.00	£452.71	£304.21	£229.53
13	0.74	£453.46	£334.20	£0.00	£0.00	£304.21	£224.21
14	0.72	£471.60	£339.51	£600.00	£431.95	£304.21	£219.00
15	0.70	£490.46	£344.90	£0.00	£0.00	£304.21	£213.92
16	0.69	£510.08	£350.37	£600.00	£412.14	£304.21	£208.96
17	0.67	£530.48	£355.93	£0.00	£0.00	£304.21	£204.11
18	0.66	£551.70	£361.58	£600.00	£393.24	£304.21	£199.38
19	0.64	£573.77	£367.32	£0.00	£0.00	£304.21	£194.75
20	0.63	£596.72	£373.15	£600.00	£375.20	£304.21	£190.23
21	0.61	£620.59	£379.07	£0.00	£0.00	£304.21	£185.82
22	0.60	£645.42	£385.09	£600.00	£357.99	£304.21	£181.51
23	0.58	£671.23	£391.20	£0.00	£0.00	£304.21	£177.30
24	0.57	£698.08	£397.41	£600.00	£341.58	£304.21	£173.18
25	0.56	£726.00	£403.72	£0.00	£0.00	£304.21	£169.17
26	0.54	£755.04	£410.13	£600.00	£325.91	£304.21	£165.24
27	0.53	£785.25	£416.64	£0.00	£0.00	£304.21	£161.41
28	0.52	£816.66	£423.25	£600.00	£310.96	£304.21	£157.66
29	0.51	£849.32	£429.97	£0.00	£0.00	£304.21	£154.01
30	0.49	£883.30	£436.79	£600.00	£296.70	£304.21	£150.43
					31,310.01		6,474.54
	TOTAL		10,525.87		24,835.46		

Table 65: Depicts economic value of the LSBU turbine installation over it's projected 30 year life span at the current production rate.

6.1.2 Strata site

The same analysis for the LSBU site was performed for the Strata installation.

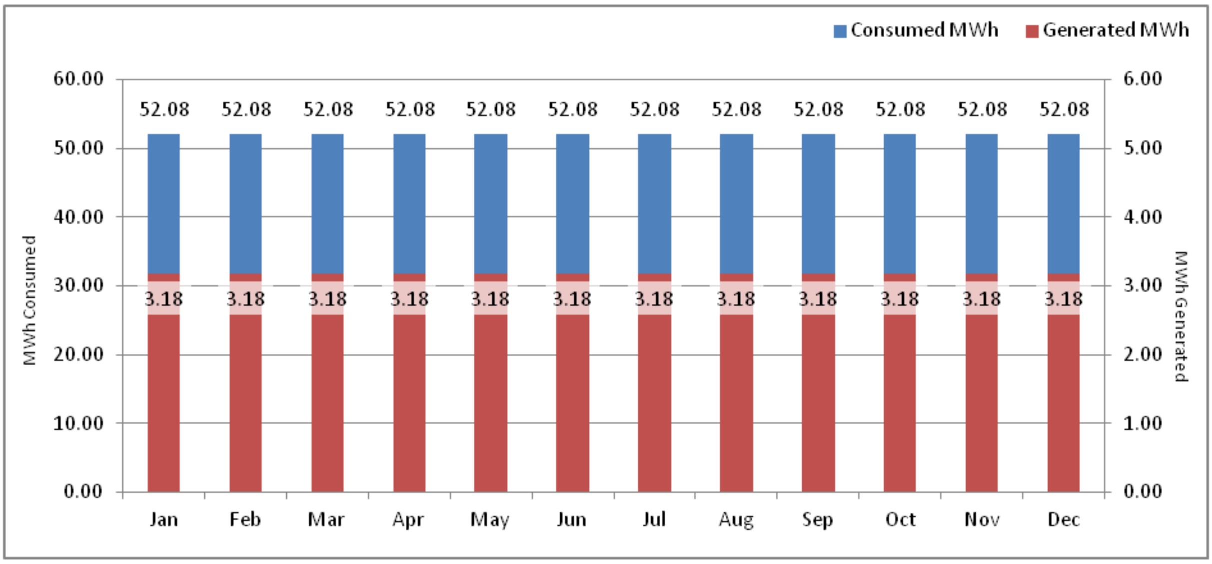

Figure 142: Depicts the Strata tower's electrical consumption against generation data for 2013.

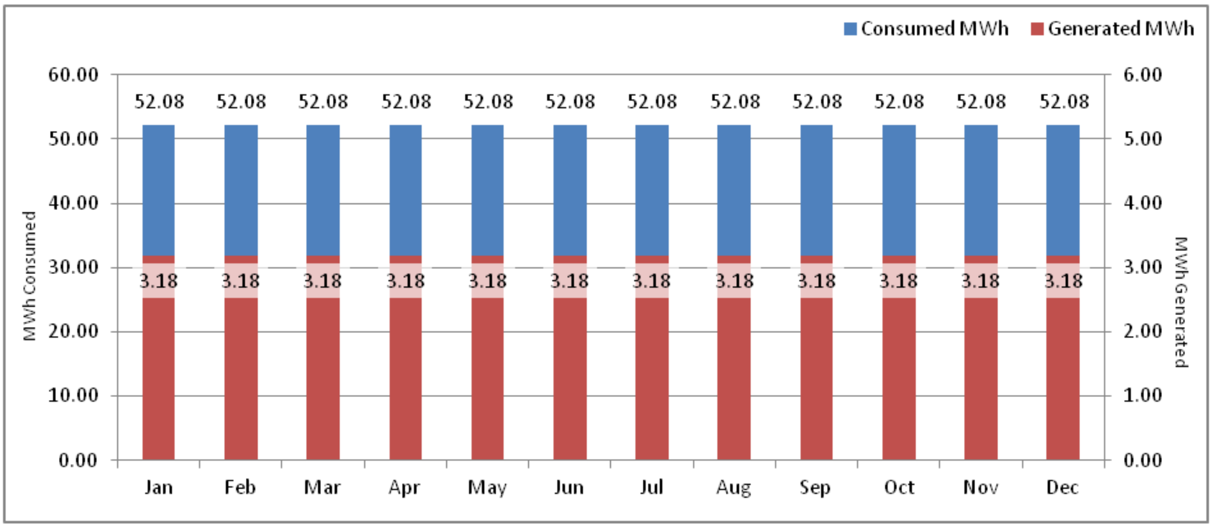

Figure 143: Depicts the Strata tower's electrical consumption against generation data for 2014.

The Strata installation is expected to produce 50 MWh per year, 8 % of the buildings energy needs per the requirements of the Mayor's policy 4A.9 or London's 'London Plan'. It is observed from Figure 142, Figure 143 and Table 68 that this figure is not quite met. A total theoretical output of 38.2 MWh and 35.6 MWh for 2013 and 2014, respectively was generated providing 6.1 % and 5.5 % of the Strata's needs. This culminates in a reduction of CO_2 emissions of 20.31 and 18.21 tonne.

The greater output of electrical generation must be weighed up against the installations short life expectancy of 15 years and high installation costs of approximately £1,000,000. An energy yield of 38.2 MWh per year over 15 years set against the installation costs gives an equivalent price per kWh of: £1.75 per kWh and a system ROI of 0.5 %.

The Strata installation economic value is further assessed using the discounting method, which is shown in Table 69. As is clear from Table 69 the price of electrical generation from the Strata turbine is far greater than the same amount purchased from the utility company over its life span; £930,385.97 as opposed to £90,071.20.

The Strata installation is also evaluated from an NPV, IRR investment point of view, which is depicted in Table 67. This assessment further re-iterates the large installation costs along with the short life span would not entice investors[23].

	Rate	**-21.863**	**%**
Amount £	**Year**	**0.78137**	**PV**
-1000000	0	1	-1000000
5539	1	0.7814	7088.83
5539	2	0.7361	9072.31
5539	3	0.6934	11610.77
5539	4	0.6532	14859.51
5539	5	0.6154	19017.25
5539	6	0.5797	24338.34
5539	7	0.5461	31148.29
5539	8	0.5144	39863.69
5539	9	0.4846	51017.69
5539	10	0.4565	65292.61
5539	11	0.4301	83561.71
5539	12	0.4052	106942.56
5539	13	0.3817	136865.45
5539	14	0.3595	175160.87
5539	15	0.3387	224171.49
		NPV	**11.37**

Table 66: Depicts the Strata output return in NPV/IRR analysis.

In spite of the Strata's high energy generation capabilities it's high installation costs, highlighted in Table 67, and short life span results in a total loss of £840,314.77. However, in spite of this the installation would, almost, adhere to the required 8% production figure demanded by the Mayor's policy 4A.9 and London's 'London Plan'. And initial predictions were good enough to grant planning permission for the Strata towers 400+ residential apartments, including 5 penthouse apartments worth figure in excess of £1.75M each. So from this point of view it is worth every penny.

[23] From a purely turbine installation investment point of view.

	LSBU	STRATA
COSTS	£25,000.00	£1,000,000.00
Yield [per annum] kWh	2,098.00	38,200.00
£/kWh	£0.40	£1.75
ROI	1.16 %	0.50 %

Table 67: Comparative costs and economic values for the LSBU and Strata turbine sites.

CO_2 F		0.527		
Annual Consumption (MWh)		625		
2013 Weibull Yield (MWh)		38.20		
Month	**Consumed MWh**	**Electric Sum tCO_2**	**Generated MWh**	**Electric Sum tCO_2**
Jan	52.08	27.45	3.18	1.68
Feb	52.08	27.45	3.18	1.68
Mar	52.08	27.45	3.18	1.68
Apr	52.08	27.45	3.18	1.68
May	52.08	27.45	3.18	1.68
Jun	52.08	27.45	3.18	1.68
Jul	52.08	27.45	3.18	1.68
Aug	52.08	27.45	3.18	1.68
Sep	52.08	27.45	3.18	1.68
Oct	52.08	27.45	3.18	1.68
Nov	52.08	27.45	3.18	1.68
Dec	52.08	27.45	3.18	1.68
TOTAL MWh	625	329.38	38.20	20.13
kWh (pence)	12.6		% 6.1	
TOTAL £	£78,750.00		£4,813.55	
2014 Weibull Yield (MWh)		35		
Jan	52.08	27.45	2.88	1.52
Feb	52.08	27.45	2.88	1.52
Mar	52.08	27.45	2.88	1.52
Apr	52.08	27.45	2.88	1.52
May	52.08	27.45	2.88	1.52
Jun	52.08	27.45	2.88	1.52
Jul	52.08	27.45	2.88	1.52
Aug	52.08	27.45	2.88	1.52
Sep	52.08	27.45	2.88	1.52
Oct	52.08	27.45	2.88	1.52
Nov	52.08	27.45	2.88	1.52
Dec	52.08	27.45	2.88	1.52
TOTAL MWh	625	329.38	34.56	18.21
kWh (pence)	13.8		% 5.5	
TOTAL £	£86,250.00		£4,769.71	

Table 68: Depicts a monthly break down of electrical consumption and generation from the Strata Tower for 2013 - 2014 including electrical bills and CO_2 emissions.

Annual Generation	38200	kWh					
Year	**Discounting**	**Utility Electricity**		**Proven 6kW**			
	Factor	**Cost**	**Discounted**	**Costs**	**Discounted**	**Income (FIT)**	**Discounted**
	1.58%	**4%**	**(DF)**		**Costs**	**£0.145**	**Income**
0	1	0	0	£1,000,000.00	£1,000,000.00	0	0
1	0.98	£5,157.00	£5,075.52	£0.00	£0.00	£5,539.00	£5,451.48
2	0.97	£5,363.28	£5,195.14	£600.00	£581.19	£5,539.00	£5,365.35
3	0.95	£5,577.81	£5,317.58	£0.00	£0.00	£5,539.00	£5,280.58
4	0.94	£5,800.92	£5,442.90	£600.00	£562.97	£5,539.00	£5,197.14
5	0.92	£6,032.96	£5,571.18	£0.00	£0.00	£5,539.00	£5,115.03
6	0.91	£6,274.28	£5,702.48	£600.00	£545.32	£5,539.00	£5,034.21
7	0.89	£6,525.25	£5,836.88	£0.00	£0.00	£5,539.00	£4,954.67
8	0.88	£6,786.26	£5,974.44	£600.00	£528.22	£5,539.00	£4,876.39
9	0.87	£7,057.71	£6,115.25	£0.00	£0.00	£5,539.00	£4,799.34
10	0.85	£7,340.02	£6,259.37	£600.00	£511.66	£5,539.00	£4,723.51
11	0.84	£7,633.62	£6,406.89	£0.00	£0.00	£5,539.00	£4,648.88
12	0.83	£7,938.96	£6,557.89	£600.00	£495.62	£5,539.00	£4,575.43
13	0.81	£8,256.52	£6,712.45	£0.00	£0.00	£5,539.00	£4,503.14
14	0.80	£8,586.78	£6,870.65	£600.00	£480.09	£5,539.00	£4,431.99
15	0.79	£8,930.26	£7,032.57	£0.00	£0.00	£5,539.00	£4,361.96
					1,003,705.08		**73,319.10**
	TOTAL		**90,071.20**		**930,385.97**		

Table 69: Depicts economic value of the Strata turbine installation over a projected 15 year life span at the estimated production rate potential.

Chapter 7 Optimisation & Proposed future work

This chapter aims to address potential avenues of research to follow the author's research conducted so far. Optimisation recommendations to enhance or rectify outlined issues will also be presented.

7.1 LSBU Vibration Isolation Design

As measured vibration levels discussed in section 4.3 could be cause for complaint the following isolation and damping recommendations for the LSBU turbine are offered as a potential remedy. Isolation is advised between the turbine support beams and tank room concrete beam as shown in Figure 144. Appropriate selection of isolation material is important to avoid exciting natural frequencies of the system.

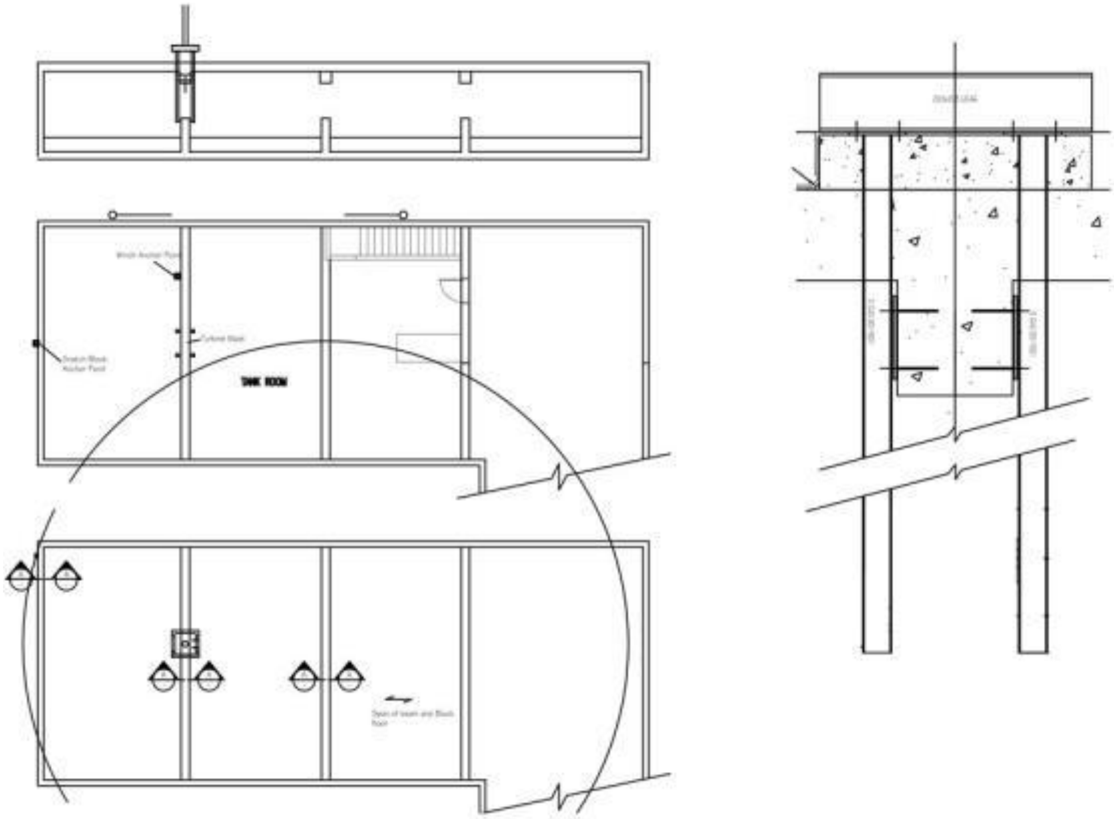

Figure 144: Displays the LSBU plant room plans with the turbine mounting position.

The Proven 6 kW turbine has an operating RPM range of 100-200 RPM with a minimum cut in speed of 3 m/s and an automatic blade pitch control to turn the blades out of the wind at high speeds to limit its RPM to 200. Effective isolation to cover this range will be investigated.

The lowest driving frequency of the system is related to the turbines RPM, in this case 100 and 200 RPM. As the turbine is a three blade system this translates to a driving frequency (f) of: 5 Hz at 100 RPM and 10 Hz at 200 RPM using Equation 1.

The level of isolation (i.e. amount of vibration reduction required) to achieve must be determined. If an isolator with a high efficiency of ~90 % or transmissibility of 0.1 is utilised this will give our mass spring system a natural frequency of 1.5 Hz at 100 RPM and 3 Hz at 200 RPM for zero damping, see Equation 31..

$$\frac{f}{f_0} = \sqrt{\frac{1}{T} + 1}$$

Equation 31: Transmissibility equation for zero damping where: f = driving frequency, f_0 = natural frequency, T = Transmissibility.

Applying Equation 31 it can be seen that a frequency ratio of 3.32 is achieved with this level of isolation efficiency. This is well above resonance, the mass controlled region as shown in Figure 145 . Vibration amplitude at these frequencies reduce at a rate of 6 dB per octave band of increasing frequency. An expected 20 dB decrease in vibration level can be expected in accordance with equation 33 .

$$dB_{reduction} = 20log_{10}\left(\frac{1}{T}\right)$$

Equation 32: Vibration reduction in dB related to Transmissibility (T)

The installed turbine system has a mass of 930 kg and requires 4 isolating pads. Therefore four isolating pads with a stiffness of approximately 20.65 kN/m each is calculated utilising .

$$k = 4\pi^2 {f_0}^2 m$$

Equation 33: Equation to calculate stiffness (k) where f0 = natural frequency and m = mass (Kg).

The turbine requires a certain amount of power to be present in the wind to start turning, therefore having a cut in speed. As the turbine is not in constant motion and will start and stop at various speeds (effectively raising and lowering the systems frequency ratio) it is imperative to assess appropriate damping for the suggested isolators to prevent accidental amplification at the systems resonant frequency.

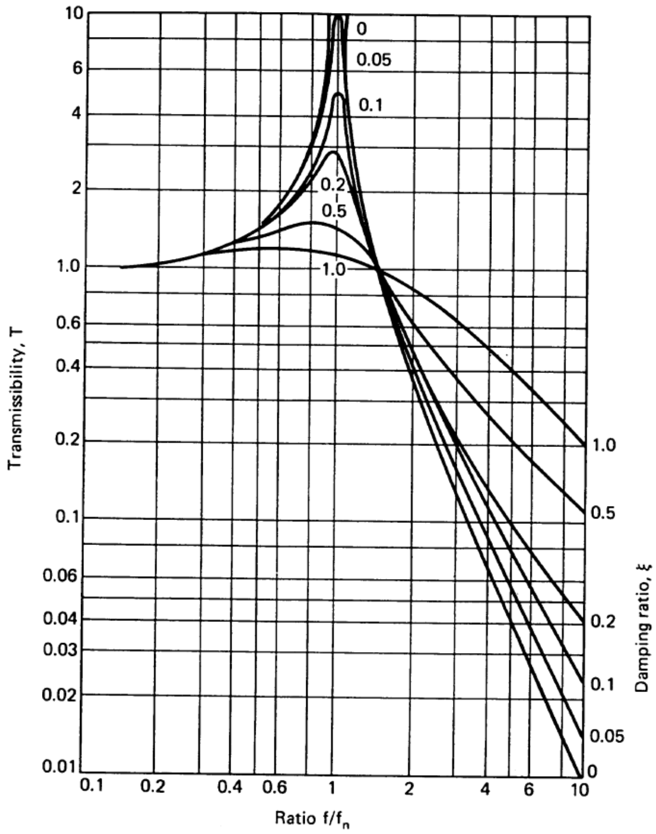

Figure 145: Graph of transmissibility and frequency ratio for varying degrees of damping

Damping is a form of friction, converting kinetic energy into heat. In a closed, frictionless system vibration without any damping would continue forever. As damping is introduced and increased the vibration will die down and halt. The time taken for vibration to decay is called the rate of decay. The rate of decay is inversely proportional to the amount of damping introduced to the system, up until a point.

From figure 145 we see the resonance peak is diminished with damping but at a cost: a broader range of frequencies (higher) can be transmitted. Varying levels of damping is assessed for the suggested LSBU turbine isolation in Table 70. It is shown that as damping increases the transmissibility is significantly diminished at the systems resonance, yet augmented at the system's frequency ratio. A damping of 0.1 is suggested as transmissibility is only slightly compromised for the systems frequency ratio, providing a resonant amplification value of 5.1 is acceptable.

The suggested isolation and damping material characteristics will achieve a satisfactory decoupling of the turbine-roof top system allowing for the operational 100 RPM rotational speed of the turbine as well as providing adequate start-up damping as the turbine starts and stops turning.

DAMPING	T f/f_0 3.32	T f/f_0 1
0.01	0.10	50.01
0.05	0.11	10.05
0.1	0.12	5.10
0.2	0.16	2.69
0.5	0.33	1.41
1	0.56	1.12

Table 70: Comparison of the effects of damping on Transmissibility at the turbine system frequency ratio and at systems natural frequency.

7.2 LSBU Turbine Elevation

In chapter 4.1 it was shown through CFD simulations (depicted in Figure 51) that increasing the LSBU turbine height by 10 m would yield a clearer, less interrupted wind flow with an expected 40 % increase in local wind speeds leading to a 2.75 multiple increase in power generation. This combined with a further increase of via Equation 5 due to the increased height will now be used to extrapolate the data from section 4.1 to produce a new electrical generation prediction compared to those shown and measured in section 4.4.

The updated results are compared to those in Table 71. As is clear a substantial gain in energy production could be realised if the turbine were able to be elevated an extra 10 m. This is not only due to the increased wind speeds but the clearer resource seen above the urban topography allowing the frequency distribution of wind speed to shift across the turbines cut in speed allowing the turbine to convert power in the wind previously unobtainable. Frequency distribution curves are compared in Figure 146 and Figure 147, Rayleigh and Weibull curves are compared in APPENDIX V.

	Manufacturer kWh	Rayleigh kWh	Weibull kWh	Ave Wind V m/s
2013 + 10 m	8067	6494	12671	4.9
2013	2910	3273	2950	3.3
2014 + 10 m	7430	5707	10162	4.7
2014	2640	2766	1929	3.2

Table 71: A comparison of predicted power generation at the LSBU turbine site using pre-discussed results and extrapolated results gained from a + 10 m elevation.

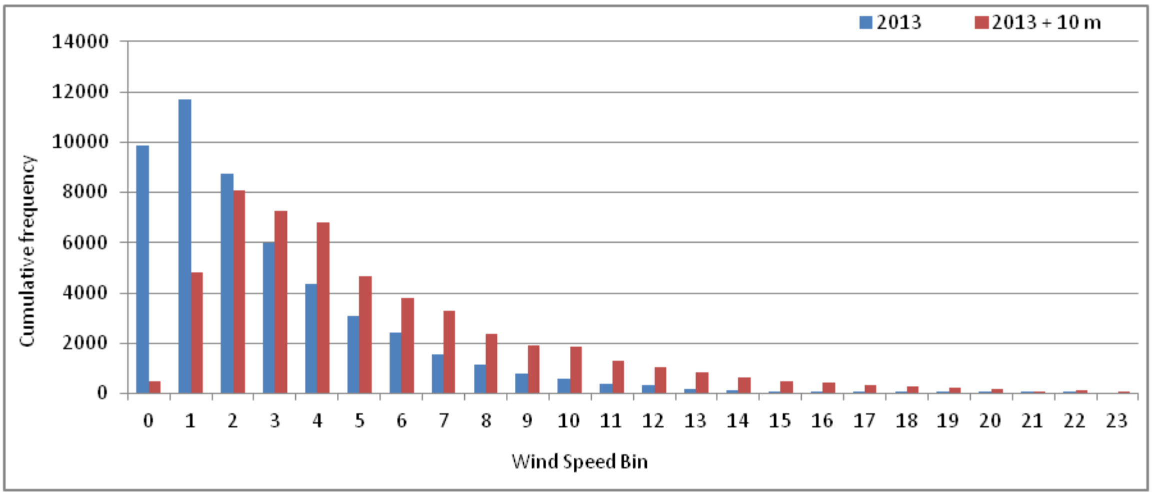

Figure 146: Compares wind speed frequency distribution for the LSBU site for 2013 data and 2013 data with an extrapolated + 10 m height increase.

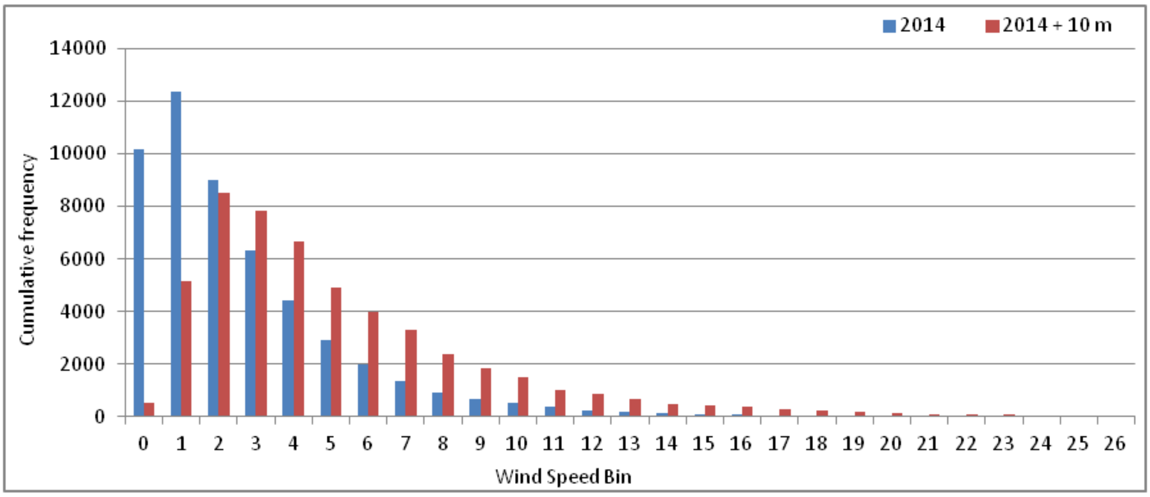

Figure 147: Compares wind speed frequency distribution for the LSBU site for 2014 data and 2014 data with an extrapolated + 10 m height increase.

7.3 LSBU Specific Power Curve

The author originally intended to produce an LSBU specific power curve from collected data to compare to manufacturer provided data. Unfortunately this was not possible due to planning permission to install inverter logging equipment was refused. The logging equipment has been purchased and awaits permission to be installed. The author therefore suggests that some further work could include the logging of inverter power generation data to be synced with wind speed data to generate the site specific power curve, which would help determine how relative manufacturer data can be when estimating a turbine sites potential within the urban environment.

7.4 Strata Orientation

It was previously discussed in chapter 5.1 through CFD analysis displayed in Figure 101 that an approximate 10 % reduction in wind speed is observed at the Strata turbines due to the orientation of the building towards the south rather than to meet the prevailing south westerly wind. The author will now demonstrate the potential power generation increase that could have been achieved if the building were rotated 25 degrees clockwise.

Table 72, Figure 148 and Figure 149 compares the existing average wind speeds and energy yield against expected gains due to the Strata re-orientation. On average a 3.5 MWh increase per annum is predicted, attributed to the 10 % increase in wind speeds raising the sites average wind speed and increasing higher wind speed frequency at the site. Using 2013's data as an example, this increase would raise the Strata's potential yield from 38.2 MWh to 48.7 MWh, which when input to Table 67 and Table 68 in section 6.1.2 would reap an increase to 7.8 % of electrical needs and a lowered energy price of £1.37 per kWh This would only be 0.2 % shy of the Mayor's policy 4A.9's target of 8 % and all for free if architectural focus had been on optimum turbine placement rather than centring the penthouse view on St. Paul's cathedral. Comparisons of resultant Weibull and Rayleigh distribution curves are included in APPENDIX W.

	Manufacturer kWh	Rayleigh kWh	Weibull kWh	Ave Wind V m/s
2013 + 25 DEG	16192.8	17587.2	17429.2	5.7
2013	14312.5	13867.6	12734.3	5.2
2014 + 25 DEG	14306.4	15104.0	15873.0	5.4
2014	12462.8	11689.0	11521.0	4.9

Table 72: Compares extrapolated energy yield predictions with adjusted Strata orientation against existing site predictions for both 2013 and 2014 measured wind speed data.

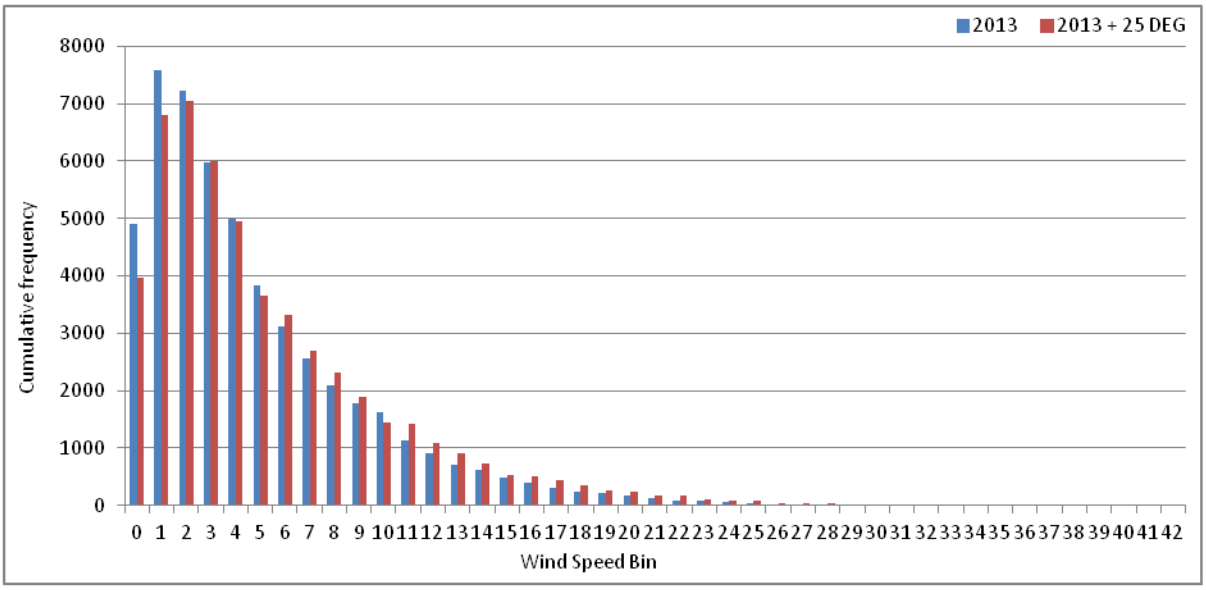

Figure 148: Compares wind speed frequency distribution at the existing Strata site with expected gains from a + 25 deg re-orientation towards the south-westerly prevailing winds, extrapolated from 2013 data.

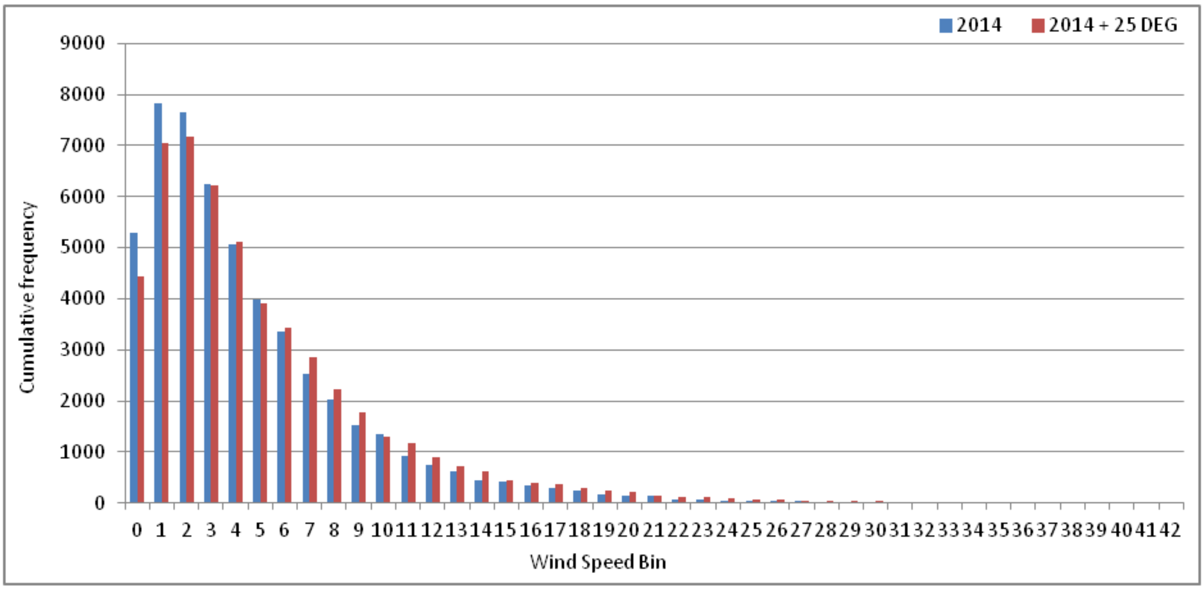

Figure 149: Compares wind speed frequency distribution at the existing Strata site with expected gains from a + 25 deg re-orientation towards the south-westerly prevailing winds, extrapolated from 2014 data.

Chapter 8 Conclusions

This study was instigated from London's need to reduce CO_2 emissions via the employment of renewable energy sources. Being a densely populated, urban area the London's topography does not lend itself to traditional turbine placement, hence more bespoke methods are required for successful integration. Two such sites are displayed in south London's Elephant and Castle: the Strata tower's BIWTs (three 18 kW HAWTs) and LSBUs Tower Block mounted 6 kW HAWT.

A literature review has shown there to be an existing body of research into noise, vibration and wind regime concerns associated with UWTs that demonstrates they can have a potentially detrimental effect on energy yield thus questioning their practicality within the urban environment.

It has been shown that hitherto no studies have specifically focused on the urban potential for BIWTs. As their integration is bespoke, typically determined by the architecture, it is unknown whether existing guidelines for roof mounted wind turbines could be directly applied. It is probable that each installation would merit its own assessment and analysis procedure.

The purpose of this study has been to investigate the differences between roof mounted and BIWTs in order to quantify and assess the aforementioned concerns with the hope of demonstrating how a successful UWT installation can be achieved.

In order to achieve an efficient BIWT a multifaceted approach is presented, comprised of: (i) local noise surveys to inform acceptable turbine operating ranges, (ii) acoustic modelling of manufacturer provided data and/or acoustic testing of the proposed turbine across all applicable wind speed ranges, (iii) vibration assessment of the turbine system, housing and any lower residential floors to (iv) the obtainment of site specific wind data to inform architectural design, turbine selection and placement and (v) CFD modeling of local topography and the turbine mount and/or enclosure.

It is imperative to assessment the potential for any local residential annoyance due to turbine generated noise pollution in the built environment. Key turbine noise issues have been highlighted and investigated for both installations. For the LSBU site it has been shown through measurement and simulation that any turbine generated noise propagated into the Tower Block is within regulations, therefore not likely to disturb any occupants although it has been shown that may faintly be detected through an open window in the upper levels. Noise levels at the nearest residential buildings are slightly in breach of established guidance but only at wind speeds above 6 m/s; a speed only recorded for 13 % of the time over a 2 year period. Below 6 m/s wind speeds other, pre-established environmental noise sources have been shown to dominate the existing aural environment.

For the Strata site it has been demonstrated that turbine generated noise is of great enough distance from local residential areas at to the street level that any noise would have diminished far below existing environmental noise levels. The isolation of the turbine venturi and lower maintenance level has also been shown to effectively reduce any structurally transmitted noise to levels far below regulation standards. Noise propagating from outside, detracting around the tower and into residents via the external facade has also shown to be of negligible level to cause any likelihood of complaint. It has therefore been shown that the Strata BIWT can comply with all relevant guidance.

An investigation into the likelihood of annoyance via turbine induced vibration was also undertaken for both sites. The LSBU site proved an interesting case as in spite of initial turbine mount measurements being far below levels likely to be perceived or cause complaint as laid out in BS 6472-1:2008 and BS 6841:1987, physical and visual manifestations of the turbine vibration were being observed on the 5th and 6th floors of the LSBU Tower Block.

The typical use of vibration measurements synchronised to the anemometry time interval, although useful in determining problems, was shown to be lacking in ability to quantify acceptable wind speed ranges due to impulsive gusts being associated with lower averaged wind speeds.

Therefore, in order to get a deeper insight into the fluctuations in Peak acceleration per averaged wind speed period the high resolution MAPS method was developed and utilised to present a more representative trend of peak vibration as a function of wind speed to determine operational limits.

Via the MAPS method, high-resolution sampling within an office of complaint amplified levels were recorded within 10, 12.5, 16 and 31.5 Hz 1/3 octave bands as wind speed approaches and exceeds 7 m/s. Further analysis explains the observed increase to likely be due to amplified resonance of the turbine tower via the turbines blade passing frequency around this wind speed as well as an unfortunate coincidence of high gust-speed blade passing frequency and structural resonance of the tower block itself. Initial site inspections did not foresee such a rare phenomenon and due to the extremely high ratio of structural to turbine mass no isolation or damping was suggested or installed. Effective isolation design is offered in chapter 7.1 to reduce any structurally transmitted vibrations to levels far below cause for complaint.

Vibration measurements recorded at the Strata site demonstrated that no likely cause for complaint would arise at any residential level within the range of monitored wind speeds. All measurements more than adequately met BS 6472-1:2008 and BS 6841:1987 guidelines.

This demonstrates that vibration must be appropriately considered for any UWT placement to ensure no structural natural frequencies are excited and to prevent any vibration transmission via appropriate mounting, isolation or damping where necessary.

Atmospheric measurements were recorded at LSBU to assess the local wind resource available to both sites. These measurements confirm that site specific, hub-height data is intrinsically essential in order to accurately estimate energy yield. As demonstrated in Table 73 the publicly available NOABL database gave 6 m/s as the average wind speed at LSBU hub-height for 2014 compared to the measured 0.8 m/s recorded at the LSBU CEREB site, different again to the 3.47 m/s average recorded at hub height next to the LSBU turbine. This not only demonstrates the need for site specific data but further highlights how important it is to specifically mirror the hub position to avoid any topographical interference.

NOABL Heathrow	CEREB	LSBU
6 m/s	0.8 m/s	3.47 m/s

Table 73: Compares measured average wind speed figures from the LSBU sites with the average data available from the UK database NOABL for 2014.

A 2 year set of wind data was extrapolated to predict the Strata site's expected energy yield using the log profile law in Equation 5, which was shown to be more suitable for turbine heights over 100 m within a rough surface area. This was juxtaposed to the Weibull prediction method, which was show to be a better fit to the urban environment as it allows for a higher standard deviation in wind speed fluctuations per wind speed bin via the shape and scale factors.

CFD simulations have proved a useful tool in potential turbine site evaluation to facilitate the local wind flow assessment across specific roof mounted and BIWT structures to inform optimal turbine placement. CFD assessment further allows for potential sites to be evaluated with varying parameters to maximise the energy capture potential. Results indicate that if pre-installation CFD analysis had been employed and optimisation tips adhered to the LSBU site could see a four-fold increase in energy yield and the Strata site a 4.5 MWh per annum increase as figures show in Table 74.

Site	Existing kWh pa	Post-Optimisation kWh pa	Ave Wind Speed increase m/s
LSBU	2950	12671	1.5 m/s
STRATA	11521	15873	0.5 m/s

Table 74: Compares existing site energy yield with estimated yields post-optimisation proposals via the utilisation of CFD simulation.

This increased in yield would increase each sites ROI and generated percentage of electrical needs to the figures displayed in Table 75. While the ROI is still not an attractive investment on its own for the Strata site the percentage of electrical needs does go up to a fraction under the 8 % required by GLA's policy 4A.9.

As it stood, predicted yield figures presented by the Strata planning committee was enough to be granted planning permission, therefore rendering the turbine installation a sound investment in spite of its initial installation cost.

	ROI Existing	ROI Post-Optimisation	% Electrical Needs Existing	% Electrical Needs Post-Optimisation
LSBU	1 %	6.9 %	0.3 %	1.7 %
STRATA	0.5 %	0.6 %	6.1 %	7.6 %

Table 75: Compares ROI and percentage of electrical needs data for each site pre and post site optimisation.

The LSBU site, as it stands, neither provides a substantial percentage of building electrical needs nor presents a sound investment but if advised optimisation were to be heeded a healthy IRR of 6.1% could be reaped and its price per kWh reduced from 28.2 pence to 6.5 pence, therefore making it viable, clean alternative to fossil fuelled electricity.

Both study sites have demonstrated strengths and weaknesses; while neither site poses a noise threat, structural borne vibration was an issue for LSBU. Energy wise the Strata site has a huge potential albeit at a substantial set up cost where as the current LSBU site is under-achieving. Nevertheless, by employing appropriate, vibration installation design, CFD modelling and noise propagation simulation techniques in advance it has been shown that both site's downfalls could have been avoided to produce two unobtrusively effective electrical generation sites.

This thesis has highlighted key factors to consider at the planning stage of turbine placement, intrinsic within the urban environment. With these factors in mind detrimental installation mistakes can be avoided to make wind turbines an effective and feasible method of urban green energy production to contribute towards lowering London's carbon footprint.

Chapter 9 References

- Abohela, I et al. (2013). Effect on roof shape, wind direction, building height and urban configuration on the energy yield and positioning of roof mounted wind turbines. Renewable Energy, 50(February): 1106-1118.
- Abohela, I. (2012) Effect of Roof Shape, Wind Direction, Building Height and Urban Configuration on the Energy Yield and Positioning of Roof Mounted Wind Turbines. Ph.D. Thesis, Newcastle University, Newcastle, UK, 2012.
- Abohela, I. (2011) Effect of Roof Shape on Energy Yield and Positioning of Roof Mounted Wind Turbines. 12th Conference of International Building Performance Simulation Association, Sydney, Australia 14-16 November 2011.
- Abohela, I. (2009). The Integration of Wind Turbines in Architectural Design. Paper presented at the Third Ain Shams University International Conference on Environmental Engineering.
- Abohela, I et al. (2011) Urban Wind Turbines Integration in the Built Form and Environment. In: FORUM Ejournal 10 ,June 2011, Newcastle, UK (pp 23-39)
- Alberts D.J., (2005), Addressing Wind Turbine Noise, Michigan (U.S.A), Lawrence Technology University
- Anderson, D. C., Whale, J., Livingston, P. O., & Chan, D. (2008). Rooftop Wind Resource Assessment using a Three-Dimensional Ultrasonic Anemometer. Retrieved on 20-01-2010, from http://www.ontario-sea.org/Storage/26/1798_A_Wind_Resource_Assessment_on_a_Rooftop_Using__3D_Ultrasonic_Anemometer.pdf
- Asfour, O. S. and Gadi, M. B. (2008) 'Using CFD to investigate ventilation characteristics of vaults as wind-inducing devices in buildings', Applied Energy, 85, (12), pp. 1126-1140.
- AWS Scientific, Inc. (1997) Wind Resource Assessment Handbook: fundamentals for Conducting a Successful Wind Monitoring Program, Albany: AWS Scientific, Inc. [Online]. Available from: http://www.nrel.gov/wind/pdfs/22223.pdf [Accessed: 10 October 2011].
- AYHAN, D. (2012) A technical review of building-mounted wind power systems and a sample simulation model. Renewable and Sustainable Energy Reviews, 16, 1040-1049.
- Bahaj, A. S., Myers, L., & James, P. A. B. (2007). Urban energy generation: Influence of micro-wind turbine output on electricity consumption in buildings. Energy and Buildings, 39(2), 154-165.
- Balcombe, P et al. (2013) Motivations and barriers associated with adopting microgeneration energy technologies in the UK. In: Renewable and Sustainable Energy Reviews 22 March 2013, Amsterdam, The Netherlands (pp 655 - 666)
- Balduzzi, F (2012) Micro electric turbines in the built environment: Influence of the installation site on the potential energy yield. Renew. Energy 2012, 45, 163–174.
- Blackmore, P. (2010) Building-mounted micro-wind turbines on high-rise and commercial buildings. Watford: BRE.
- Blackmore, P. (2008) Siting micro-wind turbines on house roofs. Watford: BRE.
- Booker, J.D. (2010) A compact, high efficiency contra-rotating generator suitable for wind turbines in the urban environment. Renewable Energy Volume 35 2027 - 2033.

- British Gas (2015) [Online] Available from: http://www.britishgas.co.uk/products-and-services/gas-and-electricity/our-energy-tariffs/Tariffs-A-Z.html [Accessed: 28th February 2015].
- British Standards, (2003), BS61400-11: 2003 – Wind turbine Generator Systems Acoustic Noise Measurement Techniques, London, BSI
- British Standards, (1997), BS4142: 1990 – Method for Rating Industrial Noise Affecting Mixed Residential and Industrial Areas, London, BSI
- British Standards, (1992), BS6472: 1992 - Evaluation to Human Exposure to Vibrations in Buildings, London, BSI
- British Wind Energy Association (2011a) BWEA Small Wind Turbine FAQ [Online] Available from: http://www.bwea.com/small/faq.html [Accessed 15 October 2011].
- British Wind Energy Association (2007b) Harnessing the energy of the wind [Online] Available from: http://www.bwea.com/edu/extract.html [Accessed 24 September 2014].
- British Wind Energy Association (2007c) UK Wind Speed Database [Online] Available from: http://www.bwea.com/noabl/ [Accessed 2 October 2014].
- Bussel, G.J.W., Mertens, S.M., (2005) Small wind turbines for the built environment, EACWE4 — The Fourth European & African Conference on Wind Engineering J. N´aprstek & C. Fischer (eds); ITAM AS CR, Prague, 11-15 July, 2005, Paper #210.
- Cace J, Horst E, Syngellakis K. Guidelines for small wind turbines in the built environment. Bristol, UK; 2007. Available at:http://www.urbanwind.net.
- Cace, J. (2007) Wind Energy Integration in the Urban Environment. Pendleton: Intelligent Energy of Europe
- Cace, J., Horst, E. t., Syngellakis, K., Niel, M., Clement, P., Heppener, R., et al. (2007). Urban Wind Turbines, Guide Lines for Small Wind Turbines in the Built Environment. Retrieved on 25-01-2016, from http://www.urbanwind.net/pdf/SMALL_WIND_TURBINES_GUIDE_final.pdf.
- Campos-Arriaga, L. (2009). Wind energy in the built environment: a design analysis using CFD and wind tunnel modelling approach. Unpublished PhD, University of Nottingham.
- Carpman N. (2011) Turbulence intensity in complex environments and its influence on small wind turbines. M.Sc. Dissertation. Department of Earth Sciences, Uppsala University; 2011.
- Carta, J. A., Ramírez, P., and Velázquez, S. (2008) A review of wind speed probability distributions used in wind energy analysis: Case studies in the Canary Islands. Renewable and Sustainable Energy Reviews [Online] Available from: http://www.sciencedirect.com/science/article/pii/S1364032108000889 [Accessed 7 October 2012].
- Celik, A. N et al (2007). An investigation into micro wind energy systems for their utilization in urban areas and their life cycle assessment. Proceedings of the Institution of Mechanical Engineers, Part A: Journal of Power and Energy, 221: 1107-1117.
- Chong, W. T. (2012) Early development of an energy recovery wind turbine generator for exhaust air system. International Conference on Applied Energy (ICAE 2012) 5–8 July 2012, Suzhou, China. Applied Energy.

- Chong Wen Tong, et al (2016) Performance assessment of a hybrid solar-wind-rain eco-roof system for buildings. Malaysia: Department of Mechanical Engineering, Faculty of Engineering, University of Malaya.
- Chong, W.T. (2012) Performance investigation of a power augmented vertical axis wind turbine for urban high-rise application. Renewable Energy Volume 51 (2013) pp 388 - 397.
- Chung, M et al. (2008) Comparison of Traffic Noise Predictions of Arterial Roads using Cadna-A and SoundPLAN Noise Prediction Models, Victoria, Australian Acoustical Society.
- Ciang, C et al (2008). Structural health monitoring for a wind turbine system: a review of damage detection methods. Measurement Science and Technology 19.12.122001.
- Clifford, M. J., Everitt, P. J., Clarke, R., & Riffat, S. B. (1997). Using computational fluid dynamics as a design tool for naturally ventilated buildings. Building and Environment, 32(4), 305-312.
- Cochran, B., & Damiani, R. (2008). Integrating Wind Energy into the Design of Tall Buildings – A Case Study of the Houston Discovery Tower. Retrieved on 27-01-2010, from http://www.cppwind.com/support/papers/papers/windenergy/Building-Integrated_Turbines.pdf
- Dayan, E. (2006). Wind energy in buildings: Power generation from wind in the urban environment - where it is needed most. Refocus, 7(2), 33-38.
- Day, A.R. (2007) Economics of Wind Power. Energy Resources Utilisation and Economics, London: London South Bank University.
- Day, T. (2007) The Economics of Wind power, London, London South Bank University.
- Deisadze, L. (2013) Vertical Axis Wind Turbine Evaluation and Design. Worcester: Worcester Polytechnic Institute.
- Denon, R., Cochran, B., Banks, D., & Wood, G. (2008). Harvesting Wind Power from Tall Buildings. Retrieved on 20-01-2010, from http://www.ctbuh.org/Portals/0/Repository/T8_DenoonWood.357b6d8b-96e3-4988-b1d6-240cbafe12e3.pdf
- Department of Energy and Climate Change, (2010). Impact Assessment of Feed-in Tariffs for Small-Scale, Low Carbon, Electricity Generation. London.
- Department of Trade & Industry, (1996), ETSU-R-1997 - The Assessment and rating of Noise from Wind Farms, ETSU for the DTI
- Department of Trade & Industry, (1996), ETSU-R-1997 - The Assessment and rating of Noise from Wind Farms, ETSU for the DTI.
- Devine-Wright, P. (2005) Beyond Nimbyism: Towards An Integrated Framework For Understanding Public Perceptions Of Wind Energy. Wind Energy, 2005. 8(2): P. 125-139.
- Drew, D. R., Barlow, J. F., Cockerill, T. T. (2013) Estimating the potential yield of small wind turbines in urban areas: A case study for Greater London, UK. Journal of Wind Engineering and Industrial Aerodynamics 115, 104-111.
- Dutton, A. G., Halliday, J. A., & Blanch, M. J. (2005). The Feasibility of Building Mounted/Integrated Wind Turbines (BUWTs): Achieving their Potential for Carbon Emission

Reductions: Energy Research Unit, Rutherford Appleton Laboratory, Science & Technology Facilities Council.

- Engineering Toolbox 2015, accessed 20 May 2015, <http://www.engineeringtoolbox.com/sound-speed-solids-d_713.html>
- European Commission. Horizon 2020 Programme. Available online: http://ec.europa.eu/programmes/horizon2020/ (accessed on 7 February 2016).
- Francisco, T (2015) On Roof Geometry for Urban Wind Energy Exploitation in High-Rise Buildings. Computation Volume 3 pp 299-325.
- Franke, J., Hellsten, A., Schlünzen, H. and Carissimo, B. (2007) Best Practice Guideline for the CFD Simulation of Flows in the Urban Environment, Action 732. Brussels: COST
- Gipe, P (2009) Noise from Small Wind Turbines: An Unaddressed Issue.Wind Works Article. URL: http://www.wind-works.org/articles/noiseswt.html [Accessed 2 December 2015]
- Glauert, K.H., (1935) The Lancester-Betz limit, Journal of Energy, Volume 3, No 6, 1935.
- Greater London Authority, (2006), Climate Change is top priority of London Plan Review [online] Press Release May 2006, available from Greater London Authority, (2006), Climate Change is top priority of London Plan
- Greater London Authority, (2004), Green Light to Clean Power, The Mayor’s Energy Strategy [online] PDF, available from: www.london.gov.uk/mayor/strategies/energy/download.jsp [Accessed 5/11/2012]
- Greening, B. (2013) Environmental impacts of micro-wind turbines and their potential to contribute to UK climate change targets. Energy Volume 59 pp 454-466.
- Grieser, B. (2013) Economics of Small Wind Power Plants in Urban Settings: An Empirical Investigation for Germany. AAchen: Institute for Future Energy Consumer.
- Grover, D. (2013) The British Feed-in Tariff for small renewable energy systems: Can it be made fairer? Leeds: Centre for Climate Change Economics and Policy.
- Gwani, M. et al (2015) FEASIBILITY AND OPTIMIZATION ANALYSIS OF A STAND-ALONE WIND-PV HYBRID ENERGY SYSTEM WITH OMNI- DIRECTION-GUIDE-VANE IN MALAYSIA; AN APPLICATION OF HOMER. International Journal of Technical Research and Applications. July 2015, Lucknow, India (PP. 22-28)
- Heath, M.A., Walshe, J.D., Watson, S.J., (2007). Estimating the Potential Yield Wind Turbines 271-287.
- H'ng, Y. (2016) Direct Measurements of Turbulence and Flow Characteristics of a Vertical Axis Wind Turbine Using the Eddy Covariance Method. Iranica Journal of Energy and Environment 7(2): pp 84-93
- Hodgson, E. V. F., (2004), Residential Wind Turbines and Noise Emissions, [online] PDF, available from: www.wind.appstate.edu/reports/ResidentialWindTurbinesandNoiseEmissions.pdf [Accessed 13/04/2015]
- International Standards, (1993), ISO9613-1:1993 – Attenuation of sound during propagation outdoors, Geneva, Switzerland, ISO

- International Electrotechnical Commission, (2005), IEC61400-12-1:2005 'Wind Turbines - Part 12-1: Power performance measurements of electricity producing wind turbines', Geneva, Switzerland, IEC
- Islam, M. R, (2011). Assessment of wind energy potentiality at Kudat and Labuan, Malaysia using Weibull distribution function. Energy, 36, 985-992.
- Islam A et al (2013). Effect of roof shape, wind direction, building height and urban configuration on the energy yield and positioning of roof mounted wind turbines, Renewable Energy, Volume 50. Available at: (http://www.sciencedirect.com/science/article/pii/S0960148112005381)
- Justus, C. G., and A. S. Mikhail, 1976, “Height Variation of Wind Speed and Wind Distribution Statistics,” Geophysical Research Letters, 3: pp. 261-264.
- Kalmikov A (2010). Wind power resource assessment in complex urban environments: MIT campus case-study using CFD analysis. In: AWEA 2010 WINDPOWER Conference. Dallas, USA; 2010.
- King, K (2009) Wind Speed and Energy Yield Analysis of Small Wind Turbines on a 45m High-rise Building in the Built Environment. Loughborough, Leicestershire: Loughborough University.
- Kitson, M., & Moran, H. (2006). Taking the Built Environment to New Heights. Retrieved on 16-02-2016, from http://www.fluent.com/about/news/newsletters/06v15i2/a5.pdf.
- Knopper, L et al (2011) Health effects and wind turbines: A review of the literature, Environmental Health, 10:78
- Lack, C. A. (2010). Urban Wind Turbines. Barcelona: Tallinn University of Technology.
- Lane, S et al (2013). An assessment of a three-beam Doppler lidar wind profiling method for use in urban areas. Journal of Wind Engineering & Industrial Aerodynamics: Journal of the International Association for Wind Engineering, 119: 53-59.
- Lang, C (2014) The windy city: Property value impacts of wind turbines in an
- urban setting. Energy Economics Volume 44 pp 413-421.
- Lassig, J (2016) Determining the Location of Wind Turbines on Roof Building with the Help of Wind Tunnel. IOSR Journal of Mechanical and Civil Engineering. Volume 13, Issue 3 Ver. V (May-Jun. 2016), PP 08-13
- Lazar, I et al (2014). Analysis of Factors Affecting Wind-Energy Potential in Low Built-Up Urban Environments, Conference: Air and Water Components of the Environment, University Cluj Napoca, Cluj-Napoca, Romania
- LEICESTER, P.A., GOODIER, C.I. and ROWLEY, P., (2011). Evaluating the impacts of community renewable energy initiatives. IN: Proceedings of the ISES Solar World Congress, 28th August- 2nd September 2011, Kassel, Germany.
- Ledo, L. (2011). Roof mounting site analysis for micro-wind turbines. Renewable Energy Volume 36 (2011) 1379 - 1391.
- Lowson, M. (1993) Assessment and Prediction of Wind Turbine Noise. Department of Trade and Industry W/13/00284/REP. Department of Trade and Industry.
- Lubitz, W. (2011) Impact of ambient turbulence on performance of a small wind turbine. Wind Energy Applications. World Renewable Energy Congress. Sweden.

- Lu, L.; Ip, K.Y. Investigation on the feasibility and enhancement methods of wind power utilization in high-rise buildings of Hong Kong. Renew. Sustain. Energy Rev. 2009, 13, 450–461.
- Merton Council (2008) The history of the Merton Rule [Online] Available from: http://www.merton.gov.uk/living/planning/planningpolicy/mertonrule/the_history_of_the_merton_rule.htm [Accessed 2 October 2012].
- Mertens, S., (2002) Wind description for roof location of wind turbines, Global Conference and exhibition on Wind Energy, Paris, 2002
- Mertens, S (2002) Wind energy conversion in the built environment. Delft, Netherlands: Delft University of Technology.
- Mertens, S. (2006) Wind Energy in the Built Environment. Concentrator Effects of Buildings. Bretwood: Multi-Science.
- Miles, C (2006) Survey of Urban Wind Energy Technology. Reading: Sustainability and the Built Environment
- Millward-Hopkins, J.T et al (2012). The predictability of above roof wind resource in the urban roughness sublayer. Wind Energy, 15(2): 225-243
- Mohammadi, S., Vries, de, B., & Schaefer, W. F. (2014). Modelling the allocation and economic evaluation of PV panels and wind turbines in urban areas. 12th International Conference on Design & Decision Support Systems in Architecture and Urban Planning (DDSS2014), 24-27 August 2014, Eindhoven, The Netherlands. (pp. 333-351). (Procedia Environmental Sciences; Vol. 22). Elsevier. DOI: 10.1016/j.proenv.2014.11.032
- Moorhouse et al., (2007), Research into Aerodynamic Modulation of Wind Turbine Noise: Final Report, Commissioned by DEFRA, Manchester, University of Salford
- Muir, S. (2008) Urban Wind Turbines. MSc dissertation, London: London South Bank University.
- Neophytou M.K.A. & Britter R.E., (2005), Modelling the Wind Flow in Complex Urban Topographies: a Computational-Fluid-Dynamics Simulation of the Central London Area, 5th GRACM International Congress on Computational Mechanics, Cyprus
- Norwin, Ramboll (2008), Castle House - Wind Turbine Project. Preliminary Design Study, Denmark. Norwin A/S
- Ntinas, G.K (2014) Airflow patterns around obstacles with arched and pitched roofs: Wind tunnel measurements and direct simulation. Eur. J. Mech. B Fluid. 2014, 43, 216–229.
- Parcell, C. (2007) Urban Turbines. MSc dissertation, London: London South Bank University.
- Parliamentary Office of Science and Technology, (2006) Carbon footprint of electricity generation. [Online] Available from: http// www.parliament.uk/documents/upload/postpn268.pdf. [Accessed: 28th February 2015].
- Philips, R et al (2007). Micro-wind turbines in urban environments - An assessment. 1st edition, BRE Trust, Watford, UK.
- Ragheb, M. (2014) Wind Turbines In the Urban Environment. Chicago: University of Illinois
- Rogers et al., (2006), Wind Turbine Acoustic Noise, white paper, Renewable Energy Research Laboratory, U.S.A, University of Massachusetts

- Sagrillo, M., (2004), Residential Wind Turbines and Noise, [online] Press Release April 2004. Available from http://archive.awea.org/smallwind/sagrillo/ms_noise_0404.html [Accessed 03/10/2012]
- Sáenz-Díez Muro, J. C et al (2010). Two-dimensional model of wind flow on buildings to optimize the implementation of mini wind turbines in urban spaces. International Conference on Renewable Energies and Power Quality (ICREPQ 2010), March 23-25, 2010, Granada, Spain.
- Santiago, J.L (2007) CFD simulation of airflow over a regular array of cubes. Part I: Three-dimensional simulation of the flow and validation with wind-tunnel measurements. Bound. Lay. Meteorol. 2007, 122, 609–634.
- Sarl, A (2012). Urban Wind Turbines Technology Review. Gouzon: European Commission.
- Seguro, J. V., and Lambert, T. W. (2001) Discussion on modern estimation of the parameters of the Weibull wind speed distribution for wind speed energy analysis [Online] Available from: http://www.sciencedirect.com/science/article/pii/S016761050000088X [Accessed 7 October 2011].
- Stankovic, S., Campbell, N. and Harries, A. (2009) Urban wind energy. London: Earthscan.
- Smith B. J. et al., (1996), Acoustic and Noise Control, 2nd Ed, Harlow, Longman Group UK Ltd
- Smith, J (2010) Effects of Turbulence Intensity on the Performance of Small Wind Turbines. Small Wind Conference, Stevens Point, WI, USA. June 14-15, 2010.
- Spera, D. A., (2009) Wind Turbine Technology: Fundamental Concepts of Wind Turbine Engineering. 2nd ed. New York: ASME.
- Sunderland K. M., Mills G., and Conlon M. F, (2013) Estimating the wind resource in an urban area: A case study of micro-wind generation potential in Dublin, Ireland. Journal of Wind Engineering and Industrial Aerodynamics, vol. 118, pp. 44-53, 2013.
- Sunderland, K et al (2010). Estimating the yield of micro wind turbines in an urban environment: A methodology. Conference Papers, Universities Power Engineering Conference (UPEC), August 31, 2010, Dublin, Ireland.
- Syngellakis, K., & Traylor, H. (2007). An introduction to wind resource assessment in the urban environment. Chineham: European Commission's Intelligent Energy Europe Agency.
- Syngellakis, K. and Traylor, H. (2008) Urban Wind Resource Assessment in the UK [Online]Available from: http://www.urban-wind.org/pdf/Reports_UrbanWindResourceAssessment_UK.pdf [Accessed 7 October 2015].
- Tabrizi, A.B.; Whale, J.; Lyons, T.; Urmee, T. Performance and safety of rooftop wind turbines: Use of CFD to gain insight into inflow conditions. Renew. Energy 2014, 67, 242–251.
- Taylor, J et al (2013) Noise levels and noise perception from small and micro wind turbines. Renewable Energy, 55 . pp. 120-127. ISSN 1879-0682
- Taylor, J (2011). The characteristics and perception of small wind system noise, PhD Thesis, University of Nottingham.
- Thresher, R et al. Wind Energy Technology: Current Status and R&D Future. Physics of Sustainable Energy Conference University of California at Berkeley March 1–2, 2008.

- Toja-Silva, F.; Colmenar-Santos, A.; Castro-Gil, M. Urban wind energy exploitation systems: Behavior under multidirectional flow conditions—Opportunities and challenges. Renew. Sustain. Energy Rev. 2013, 24, 364–378.
- Tominaga, Y., Mochida, A., Yoshie, R., Kataoka, H., Nozu, T., Yoshikawa, M., Shirasawa, T., (2008) AIJ guidelines for practical applications of CFD to pedestrian wind environment around buildings. Journal of Wind Engineering and Industrial Aerodynamics, Volume 96, Issues 10-11, October-November 2008, 1749-1761
- Tong, W. (2010) Wind Power Generation and Wind Turbine Design. Boston: WIT Press.
- Troen, I. and E.L. Petersen (1989). European Wind Atlas. Risø National Laboratory, Roskilde. 656 pp.
- Turner, B, D. (1994) Workbook of atmospheric dispersion estimates: an introduction to dispersion modelling, second edition: CRC Press.
- Van Den Berg, F (2011). An Overview Of Residential Health Effects In Relation To Wind Turbine Noise, Fourth International Meeting On Wind Turbine Noise, Rome, Italy, 12-14 April 2011.
- Wagner, S. Bareiss, R. Guidati, G (1996), Wind Turbine Noise, Germany, University of Stuttgart.
- Wayne, K et al (2002) Psycho-acoustic characters of relevance for annoyance of wind turbine noise. Journal of Sound and Vibration, 2002. 250(1): p. 65-73.
- Windeur. (2010) Urban Wind Turbines Technology Review [Online]. Available from:
- WINEUR. (2007) Wind Energy Integration in the Urban Environment: Report on Resource Assessment. European Commission
- Urbanwind Online. http://www.urbanwind.net/pdf/technological_analysis.pdf [Accessed: 18th June 2012].
- World Health Organization, (1999), Guidelines for Community Noise, Geneva, World Health Organization.

APPENDIX A London Urban Turbines

Existing urban turbine systems in London show the successes and pitfalls that have been achieved in the urban environment along with the diversity of their application.

Unsuccessful urban turbine installations in London		
Strata tower, Elephant & Castle	3 x 18 kW turbines. 140 m hub-height, 8.5 m rotor diameter each with a predicted output of 16.6 - 33.3 MWh p.a. The turbines have not been operational since early 2012, currently producing nothing due to maintenance issues.	
Propeller park, A406 Neasden	4 x 6 kW turbines. 9 m hub-height, 5.5 m rotor diameter. These turbines each have a predicted output of 6 - 11 MWh per annum and were Intended to power the business park utility services but are currently shut down due to no movement.	
David Cameron's House	David Cameron installed a small turbine on his west London home in 2007 to promote urban renewable sources. It was quoted to provide 30 % of Mr Cameron's electricity needs. It was decommissioned, following objections from local neighbours, after a week due to structural implications.	

Successful urban turbine installations in London		
London array, Thames estuary	175 x 3.6 MW rated wind turbines. 147 m (85 m above sea level), 120 m rotor diameter. 21 TWh p.a. - enough to power nearly 500,000 homes.	
LSBU campus, Southwark	1 x 6 kW turbine. 49 m hub-height, 5.5 m rotor diameter. The turbine currently produces approximately 2 MWh p.a.	
Ricoh eco-billboard, M4	96 x PV panels and 5 x wind turbines are installed upon the Ricoh advertising board producing approximately 4536 kWh p.a. - enough to power a medium sized family home for a year.	
Ford, Dagenham	2 x 1.8 MW capacity turbines are installed at the Dagenham site. They are 85 m hub-height, 70 m rotor diameter turbines producing 6.3 MWh electricity p.a. - enough to power 100 % of their diesel engine factory.	

APPENDIX B Risk Assessment

All projects come with certain. As this research has relied upon site access, data access and the use of equipment over long periods of time certain risks had to be considered, allowed for and overcome to successfully complete the work. These issues will be discussed in the following sections.

Site access

Maintenance levels and the turbine venturi are controlled areas within the Strata, away from the security controlled residential levels throughout the rest of the building.

Therefore, advanced notice and access permission must be granted to enter the building, restricted areas and then to set up and monitoring equipment. All monitoring equipment and installations had to meet health and safety requirements of the building management company. Provisions were made with Brookfield Multiplex to ensure site access for a period of 2 years commencing from February 2012 as long as these site specific health and safety regulations and procedures were met.

Fortunately access was only denied on a very few occasions when maintenance work was being carried out.

The LSBU turbine is located upon a plant room on the roof top level of the university tower block. General access is restricted due to health and safety reasons but provisional access was granted by the university for the purpose of conducting my research after a method statement was written and signed off.

Reports of vibration had been noted in a sixth floor office. Access to this office had kindly been granted to set up monitoring equipment.

Document access

Architectural plans and installation notes, blueprints for each site and turbine technology was essential to fully understand the structural configuration of each site. This allowed for accurate vibration, noise propagation analysis and troubleshooting.

Brookfield Multiplex kindly supplied all installation plans and notes from Norwin regarding the bespoke turbine materials, set up and installation as well as manufacturer performance and testing data.

As part of the initial project framework agreement between LSBU and Brookfield Multiplex access was granted to atmospheric data from installed sensors. Unfortunately logging equipment was never installed so site specific data to correlate to noise and vibration data was not available.

LSBU Estates and Facilities department were able to provide a handover pack from Embrace Energy, the turbine installation contractors. This included manufacturer performance data, mechanical and installation plans. Permission to access LSBU architectural plans was sought but unfortunately LSBU are digitising and archiving the plans so they are unavailable.

Technical risk

Atmospheric data is simultaneously collected from the university CEREB (Centre for Efficient and Renewable Energy in Buildings) building rooftop and the hub height tower block anemometry. This data is logged remotely onto a server, which is linked to the LSBU building management system website. This allows for remote access to recorded 10 minute interval data at all times.

Unfortunately in November 2013 the LSBU building management system became inaccessible and the CEREB data logging server license expired early 2014 so all access was blocked. Fortunately temporary access has been granted to extract all missing data.

The Tower block anemometer fell victim to sabotage. Evidence of gnawing or pecking was found on a very damaged data logger, due to which data at this site was not logged for two weeks during November 2014 until a replacement could be installed.

There is always technical risk of equipment failure but regular calibration, servicing and appropriate usage can contribute towards avoiding these issues. Fortunately the only equipment failure experienced has been of flash memory cards needing to be replaced throughout the course of my measurements.

APPENDIX C LSBU Anemometer Installation Health & Safety Plan

HEALTH & SAFETY PLAN

Project Name: Tower Block Anemometer Mast Installation

Project Location: Tower Block Roof Top, LSBU, Borough Road, London SE1 OAA

Mr Ben Dymock

PhD Researcher in Acoustics

Department of Urban Engineering

FESBE

London South Bank University

Borough Road

London SE1 0AA

T: 07742313249

E: dymockb@lsbu.ac.uk

SECTION 1 – PRELIMINARIES

1 Health & Safety General Statement

It is this department's intention that its work will be carried out in accordance with the relevant statutory provisions and all reasonably practicable measures taken to avoid risks to its employees or others who may be affected.

Management and supervision staff have responsibility for implementing this policy throughout the department and must ensure that Health and Safety considerations are always given priority in planning and day to day supervision work.

All employees are expected to co-operate with the department in carrying out this policy and must ensure that their own work, so far as reasonably practicable, is carried out without risk to themselves or others.

The Acoustics Group has appointed the Director of Studies as having particular responsibility for Health and Safety to whom reference should be made in the event of any difficulty arising in the implementation of the policy.

The management and staff of the department will monitor the operation of this policy. To assist them in this respect the department has appointed Steve Dance as safety supervisor to visit the site and to give advice on the requirements of the relevant statutory provisions and safety matters generally.

The organisation and details of this document will be freely available from each site supervisor and project manager as and when required.

2 Management Structure

Stephen Dance	Director of Studies, Person Responsible for Health and Safety, Project Manager (office) (Mobile phone no 07817597080)
Ben Dymock	Researcher, Project Manager (Mobile phone 07742313249)
Michael Massey	Site Manager, Maintenance Engineer. (Phone: 02078156864)

3 Legislation and Standards

All works are to be carried out in accordance with the Health and Safety at Work Act 1974, Electricity at Work Regulations 1989 and BS 7671 (I.E.E. Wiring Regulations 16th Edition), Part P of the Building Regulations and Engineering Recommendation G83/1.

The materials and workmanship shall be to the satisfaction of the site manager and shall be the best of their respective kinds and in all instances shall comply with the current British Standards and codes of practice.

Materials purchased for delivery to site will be accompanied by the relevant Health and Safety information by virtue of regulation 13 (2) (b) of the Health and Safety at Work Act 1974.

All plant on site will be used for the purpose for which it is intended by trained and experienced personnel. Plant on site will be free of defects and regularly maintained.

4 Information to Personnel

Any persons entering the site for the first time will initially be briefed by the site supervisor on site rules, risks on site, site safety plan and on-site welfare.

Further on site tool box meetings will be held as work progresses. This is to ensure that all relevant personnel are made aware of processes and work practices to be carried out.

5 Communication and Co-operation

The project manager will be in contact with the site supervisor, Michael Massey, with regard to site operations and the agreed programme of work.

Any relevant information arising whilst installation work is carried out, will be reported to the Project Manager/site supervisor.

There will be a free flow of information on relevant Health and Safety matters between on-site operatives and the site supervisor at all times.

The Health and Safety Plan will be available from the project manager.

The site supervisor will ensure that workers to the site are briefed on site rules, Health and Safety and methods of working. All workers will be under full time supervision while on site.

Operatives and workers on site installing, commissioning, loading, unloading, etc. will be made aware of any relevant information and instructions which may be provided by suppliers of materials e.g. C.O.S.H.H. sheets, Health and Safety Plan.

6 First Aid

The site supervisor and project manager, will keep a first aid kit to be used in the event of an accident. All operatives on site will be made aware of the location of the first aid kit.

7 Site Emergency Procedures

At all times the site supervisor will know the locations of working for the work party. The work party will be in possession of a mobile telephone. In the event of fire or dangerous occurrences all staff on site will evacuate to the nearest open area adjacent to the place of work. The site supervisor will be informed of the incident by mobile telephone.

HOSPITAL ACCIDENT & EMERGENCY UNIT ADDRESS

St Thomas Hospitial

Lambeth Palace Road, London, SE1 7EH

Tel: 0207 188 7188

In the event of a serious accident where hospital treatment is required, the site supervisor's mobile telephone shall be used to contact the emergency services.

The Site Safety Supervisor will be made aware of any accidents that occur on site so that the relevant investigation, reporting and remedial action can take place as necessary.

8 Fire Precaution

Processes will be selected to minimise the risk of fire.

The site supervisor will keep suitable fire extinguishers in the event of a fire. All operatives on site will be made aware of the location of extinguishers and how to use.

9 Noise

Processes will be selected to minimise the affect of noise. Working hours will be between 8.00am and 5.00pm, Monday to Friday. Work to be carried outside of these hours would be approved beforehand.

10 Reporting of R.I.D.D.O.R.

The Installations Manager / Site Safety Supervisor will investigate any incident and complete any reports required under R.I.D.D.O.R. Regulations 1995.

11 Site Storage Facilities

All equipment relevant to the proposed installation will be stored within the Acoustics lab on Keyworth street.

12 COSHH

The Acoustics Group does not plan to use any items subject to COSHH (Control of Substances Hazardous to Health) as part of this project.

16 Site Rules

Please see copy of company site rules attached at the end of this document.

17 Arrangements for Monitoring

Health and Safety records will be kept and reviewed regularly by the Site Safety Supervisor.

18 Project Completion

On completion of system commissioning, a completion certificate will be issued. The department's representative will be asked to sign the completion certificate to indicate acceptance of the installations.

Full documentation including test and commissioning documents will be submitted to Michael Massey upon completion of the project.

19 Project Review

On completion of works, a review will be carried out of the standards achieved on-site compared with the job specification and department standards.

20 Construction Design and Management Regulations

On the advice from the project planning supervisor, this project is not subject to the requirements of the Construction Design and Management Regulations. Therefore, there is no requirement to appoint a planning supervisor or to notify H.S.E.

SECTION 2 - PROJECT DESCRIPTION AND METHOD STATEMENT

This Method Statement should be read in conjunction with the installation instructions for the mounting environmental monitoring anemometer and wind vane.

Project Ref:	**1008**
Project Name:	**Tower Block Monitoring Anemometer**
Location:	**Tower Block, Borough Road, London, SE1 OAA**

1 Project Description

Installation of monitoring instrumentation and mast on the tower block roof top (supervised private access). Installed anemometry equipment will be used to collect site specific wind data. The project is to be a temporary installation, existing for a period of 12-18months.

2 Existing Environment

All properties to be worked on are in the ownership of LSBU. The roof top, plant room and site are to remain occupied during the works. Safe and continuous access is to be provided and maintained to all areas throughout the duration of the project.

3 Theft and Security

Access to the roof area is supervised by the site operator. The public top floor is only accessible to the employees of the University. The instrumentation and equipment will not be left unattended in any public area.

4 Equipment to be Used

- Better Generation Power Predictor 2 - battery powered
- Better Generation 12m Extension cable.
- 8 x (1m L, 32mm D) Aluminium alloy mast pole sections.
- 32mm tube aluminium alloy tripod.
- Steel guy wire (1900mPa).
- Stainless steel wire rope clips/grips.
- Stainless steel turnbuckles.
- 2" Wire guy hooks.

5 Method Statement for Wind Monitoring Installation

Fit of Anemometry Instrumentation/Mast (1 day only)

1. Accompanied by the site supervisor
2. Access the roof top: climb ladder onto the roof top.
3. Assemble mast pole sections with all assembly equipment.

4. Attach power predictor monitor.
5. Run and secure extension cables from monitor to mast base.
6. Secure guy hooks to mast.
7. Secure connecting brackets to existing rails/ground stakes.
8. Connect guy wires between all grounded brackets and mast brackets.
9. Hoist the mast while tightening guy wire/turnbuckles.
10. Once vertically raised: adjust turnbuckles to desired tension.

System will be installed in the shortest duration possible to minimise disruption to other employees.

SECTION 2 - RISK ASSESSMENT

Management of Health and Safety at Work Regulations 1992

Regulation 3

1 Work Activity

Electrical Services

Installation of Anemometry Instrumentation.

2 Work Location

Tower Block roof top of Borough Road building, LSBU, London.

3 People Affected

Operatives, LSBU employees, general public.

4 Hazard Rating

Hazard Severity Rating

3 = Major = Fatality, major injury or illness causing long term disability

2 = Serious = Injury or illness causing short term disability

1 = Minor = Other injury or illness

Likelihood of Occurrence Rating

3 = High = Certain or near certain

2 = Medium = Frequently

1 = Low = Seldom

Hazard	Hazard Rating	Occurrence Rating	Hazard x Occurrence = Risk Rating

1. Falls from heights	3	1	3
2. Falling objects	2	1	2
3. Fire	3	1	3
4. Chemicals/Substance	N/A	N/A	N/A
5. Electricity	3	1	3
6. Dust	N/A	N/A	N/A
7 . Fumes	N/A	N/A	N/A
8. Noise	1	1	1
9. Manual Handing	1	1	1
10. Lighting Levels	1	1	1
11. Temperature Levels	N/A	N/A	N/A
12. Lifting Equipment	2	1	2
13. Confined Spaces	N/A	N/A	N/A
14. Contact with moving machinery	N/A	N/A	N/A
15. Vermin Infestation	N/A	N/A	N/A

5. Prioritisation

Risk Rating	Priority
1	No Action
2	Low Priority Action
3 or 4	Medium Priority Action
6	High Priority Action
9	Urgent Action

Hazard	**Actions to Be Taken**
1.	Hand rails on upper tower block roof level, hand rails on ladder to access roof, restricted access by unauthorised personnel and times, avoid working in high winds, do not work at times when surfaces are slippery, ensure structural elements are able to take the required loading, do not work at night

2. Multiple cable ties to by used to secure equipment cables, appropriate PPE to be worn, tools to be carried safely to areas, tools to be tethered or fixed object as appropriate.
3. Multiple guy wires, guy hooks, guy clips and turnbuckles to be used to secure mast and tripod to the roof top.
4. Fire extinguisher to be available on site, good working practices to limit risk.
5. Use low voltage site tools, or battery operated equipment where appropriate, clearly label equipment as per standard guidelines and standards. LSBU electricity checked tools only to be used.
6. N/A
7. N/A
8. Use personal protective equipment, use alternative work method such as not working in high winds on the roof top
9. Ensure all lifting personnel are instructed in safe manual handling techniques, reduce handle loads to below 25kg per person, for heavy loads use more than one person
10. Provide additional temporary lighting if necessary, do not work at night

Project Name: **Tower Block Anemometer Mast Installation**

Project Location: **Tower Block Roof Top, LSBU, Borough Road, London SE1 OAA**

Director of Studies	**Site Supervisor**
Acoustics Group	Estates and Facilities
London South Bank University	London South Bank University
Name ……. ....………	Name …………………...………………………
Signed ………………………………………	Signed ……………………………………………
Date ………………………………………..	Date ……………………………………………..

GENERAL SAFETY RULES AND POLICY STATEMENT

FOR ALL STAFF AND CONTRACTORS

Before You Start Work

- Read and understand the Company's safety rules and those for the site
- Know where you are going
- Always report to your site office/site supervisor when you start work
- Look out for safety signs
- Look out for danger

When You Are Working

- Know what the job entails and your role in it
- Do not wear a personal stereo or trainers on-site
- Always wear a hard hat on-site
- Always wear protective boots on-site
- Always wear goggles, gloves and ear defenders when required
- Remember you are responsible for your own safety and the safety of others
- If you do not know, ask your supervisor
- Do not work on live circuits
- Make sure the power is off before you plug equipment into extension leads
- Read labels and signs
- Check equipment carefully before you use it
- Always label faulty equipment, make sure nobody uses it and report it to your supervisor
- Keep your eyes open for hazards
- Do not take short cuts
- Check all ladders and tower scaffold etc., are secure before climbing or descending
- Do not leave tools in hazardous positions
- Arrange safe working area with regard to the safety of the occupiers/site at all times.
- Protect floor covering when using vice/bender/drilling/cutting.
- Confirm all electrical circuits are isolated before commencement.
- Keep locked if possible and control access to fuse boards.
- Use PPE, eye shields on all drilling operations.

- When using steps or ladders, do not work above or near occupier/operatives. Remove steps or ladders to safe place when not in use.
- Observe the location of free ends of cables during installation.
- When pulling through cables, control cable drums to prevent surplus cable causing tripping hazards.
- During testing and commissioning, control areas to prevent occupier/operatives coming into contact with live exposed equipment.
- Do not smoke

On completion of installation works:

- Remove waste materials to agreed collection point and clear location as required.
- Remove tools and equipment from site.
- Inform site supervisor that agreed work has been completed.

When You Leave Work

- Tidy away tools and extension leads, equipment etc.
- Dispose of waste materials property in accordance with the Company's instruction
- Be conscious of hazards that exist when leaving the site

General Policy

- Sites are designated as ‘no smoking areas’, smoking is only permitted in designated areas stated by the client.
- Due to the possible danger to both Operatives and Clients whilst working with electricity, any employee found to have consumed alcoholic beverage during working hours (including lunch times) will be instantly dismissed.
- The wearing of excessive jewellery, especially rings, has proved to be dangerous in our trade, therefore in the interests of safety our electricians are required to wear one ring only.

APPENDIX D Air Density with Altitude

As the project compares two individual turbine sites at varying heights, atmospheric variables must be considered for fair analysis.

Power in the wind (W):

$$W = \frac{1}{2}\rho A V^3$$

Density (ρ):

$$\rho = \frac{pM}{RT}$$

Pressure (p):

$$p = p0\left(1 - \frac{Lh}{T0}\right)^{\frac{gM}{RL}}$$

Temperature (T):

$$T = T0 - Lh$$

Where:

p_0 = atmospheric pressure at seas level = 101.3 kPa

T_0 = Temperature at sea level = 288.15 K (15 C)

g = earth's gravitational acceleration = 9.8 m/s^2

L = temperature lapse rate = 0.0065 K/m

R = idea gas constant = 8.31 J/(mol.k)

M = molar mass of dry air = 0.0289 kg/mol

h = height above sea level - metres

Therefore we see the deviation from sea level density at both altitudes is minimal:

Sea Level	**Strata (140 m)**	**LSBU (49 m)**
1.225 kg/m^3	1.202 kg/m^3	1.214 kg/m^3

Table 76: Air density at altitude

APPENDIX E Monthly Tower Block Wind Speed Distribution

2013

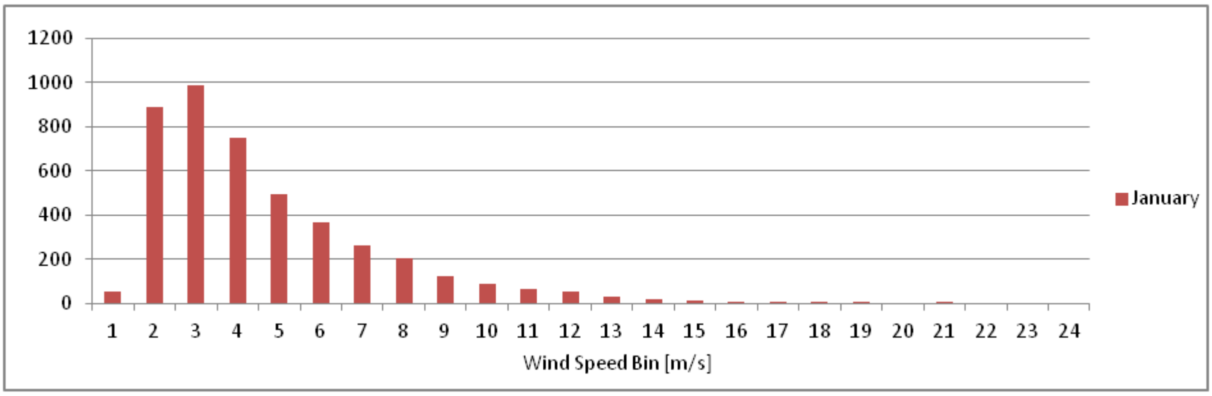

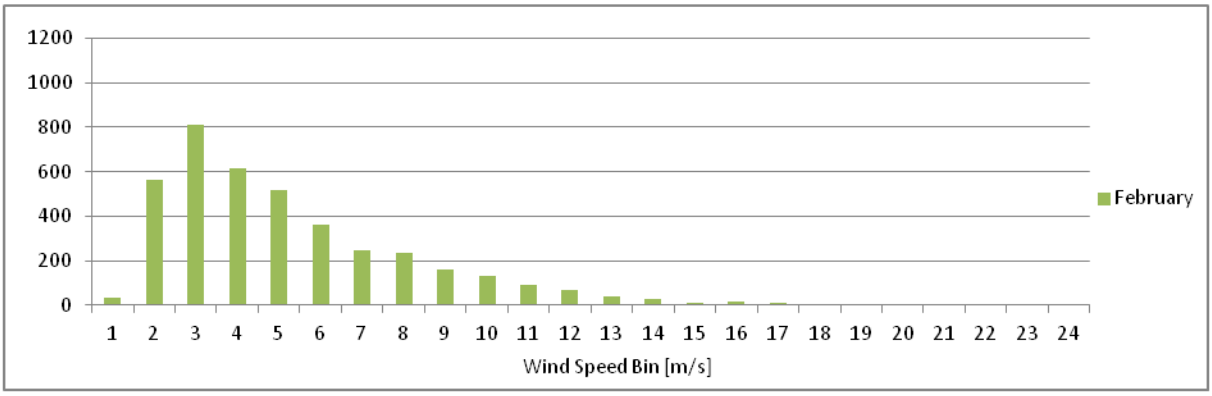

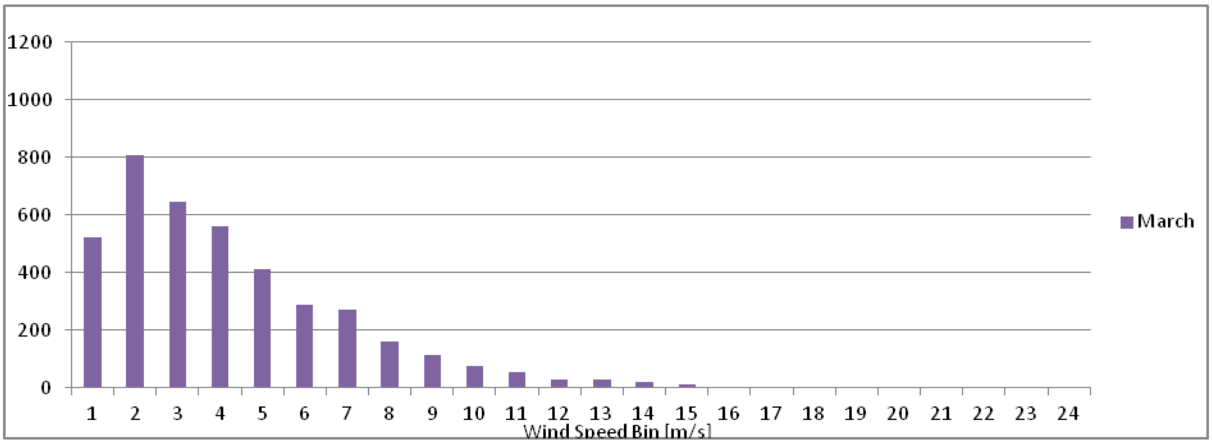

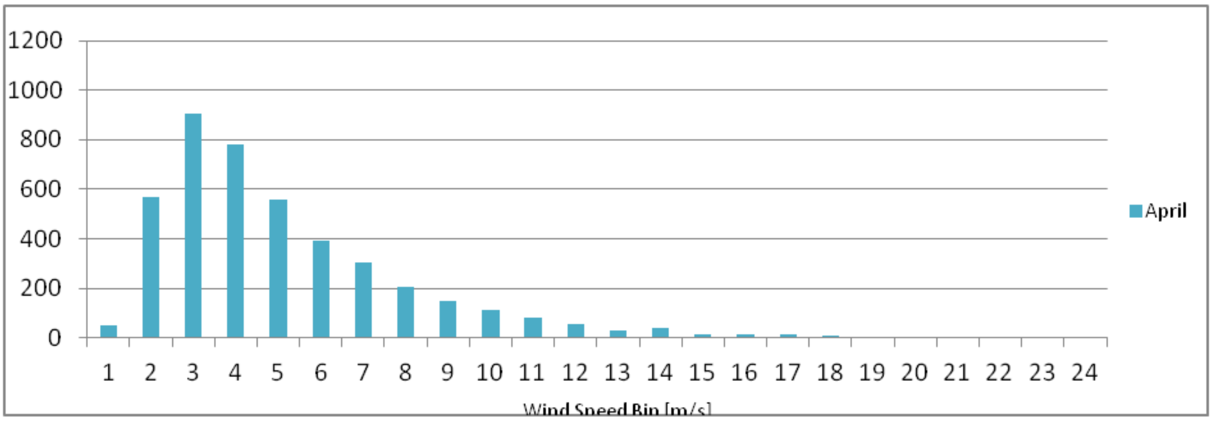

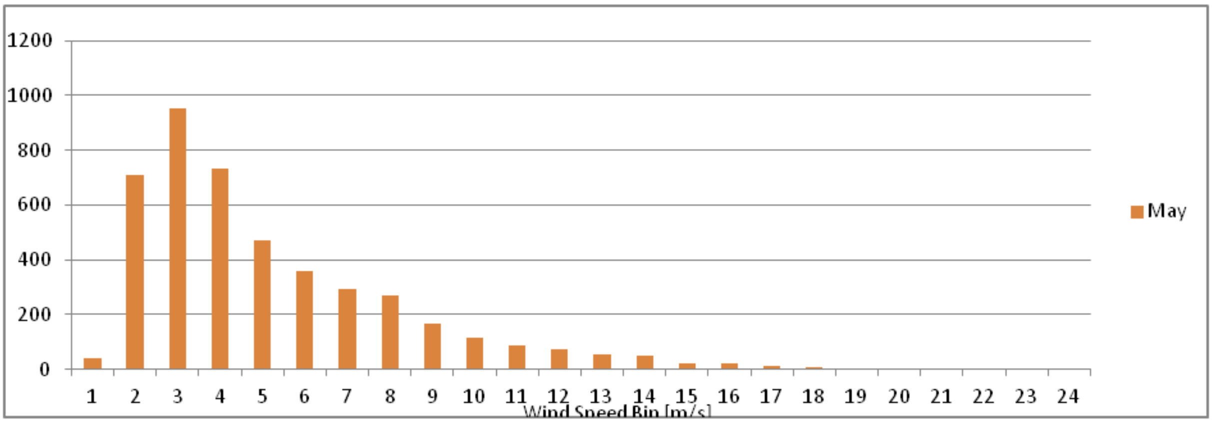
1200
1000
800
600
400
200
0
1 2 3 4 5 6 7 8 9 10 11 12 13 14 15 16 17 18 19 20 21 22 23 24
Wind Speed Bin [m/s]
May

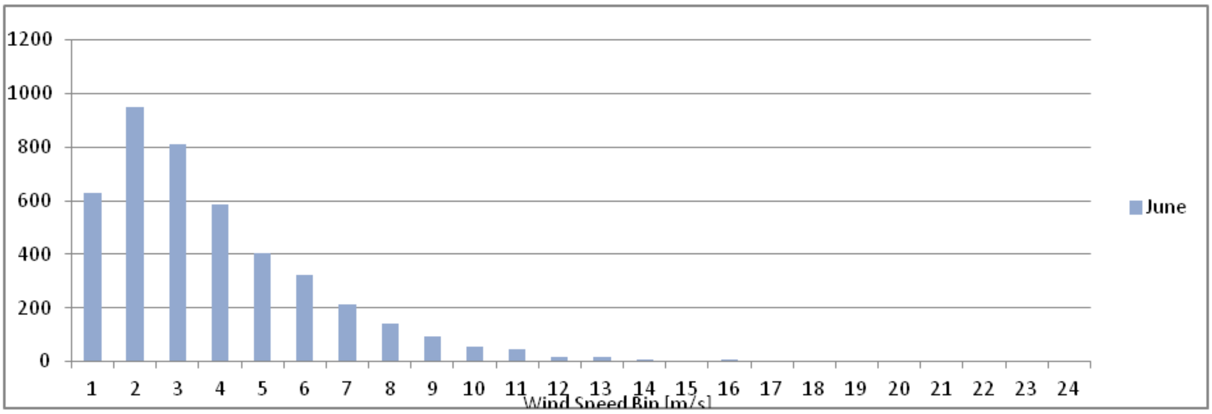
1200
1000
800
600
400
200
0
1 2 3 4 5 6 7 8 9 10 11 12 13 14 15 16 17 18 19 20 21 22 23 24
Wind Speed Bin [m/s]
June

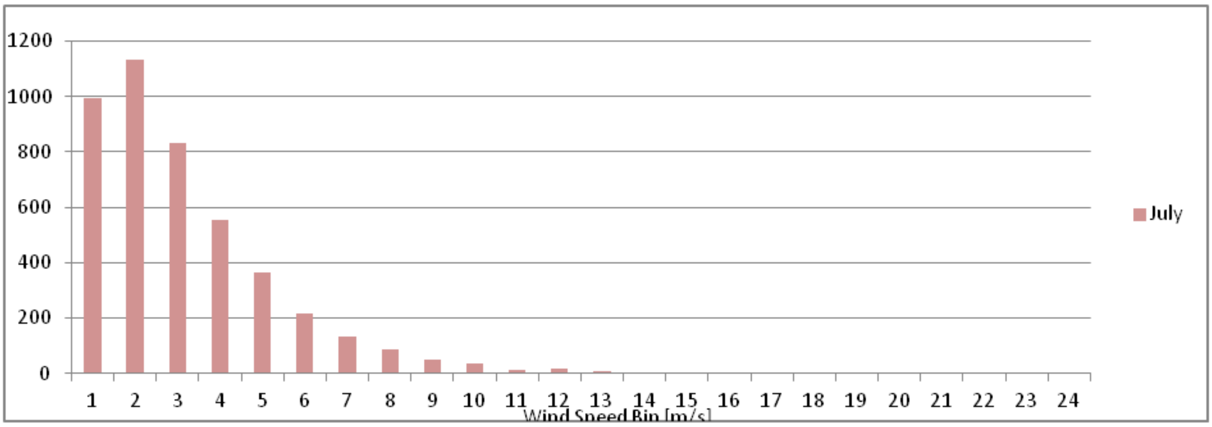
1200
1000
800
600
400
200
0
1 2 3 4 5 6 7 8 9 10 11 12 13 14 15 16 17 18 19 20 21 22 23 24
Wind Speed Bin [m/s]
July

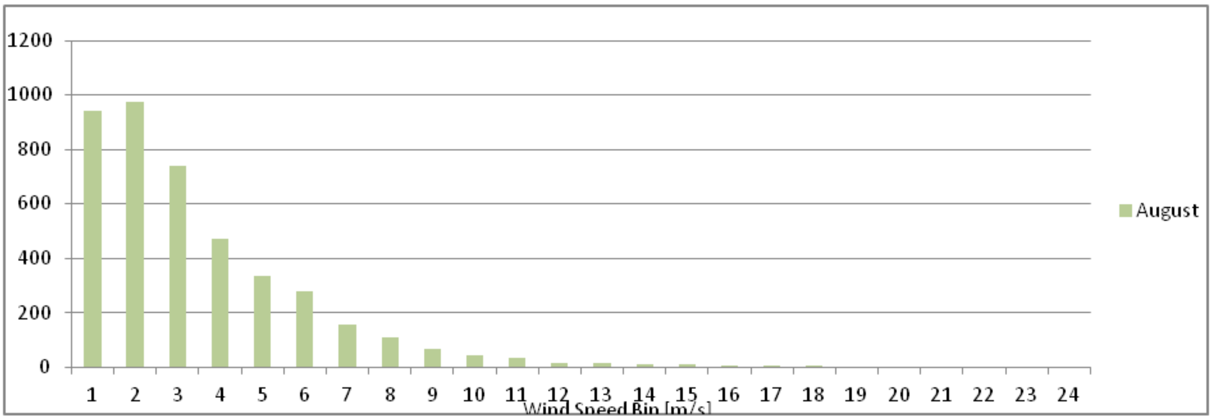
1200
1000
800
600
400
200
0
1 2 3 4 5 6 7 8 9 10 11 12 13 14 15 16 17 18 19 20 21 22 23 24
Wind Speed Bin [m/s]
August

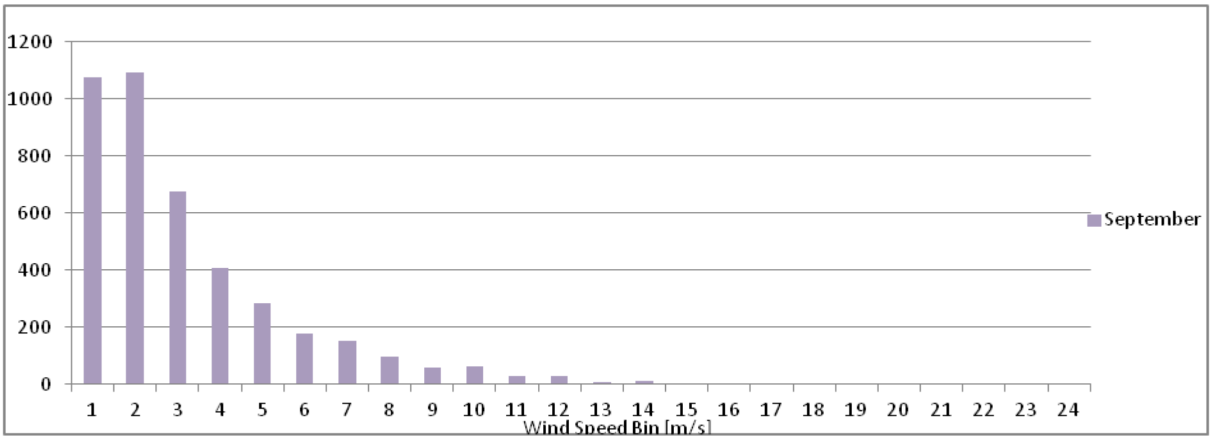

1200
1000
800
600
400
200
0
1 2 3 4 5 6 7 8 9 10 11 12 13 14 15 16 17 18 19 20 21 22 23 24
Wind Speed Bin [m/s]
September

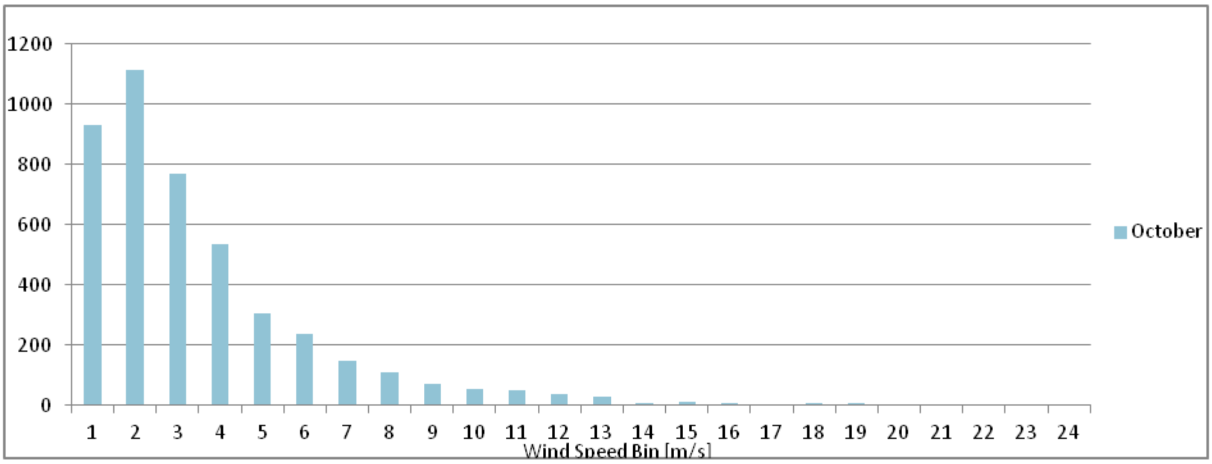

1200
1000
800
600
400
200
0
1 2 3 4 5 6 7 8 9 10 11 12 13 14 15 16 17 18 19 20 21 22 23 24
Wind Speed Bin [m/s]
October

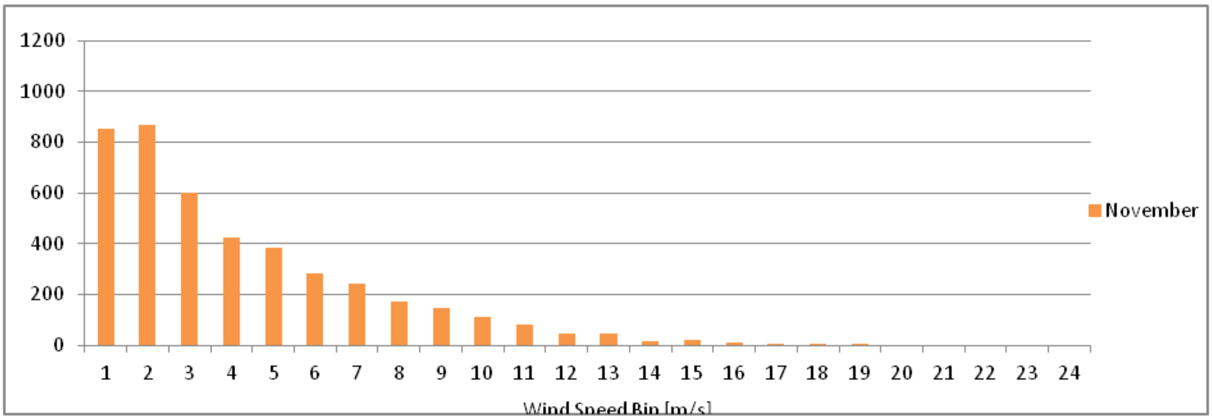

1200
1000
800
600
400
200
0
1 2 3 4 5 6 7 8 9 10 11 12 13 14 15 16 17 18 19 20 21 22 23 24
Wind Speed Bin [m/s]
November

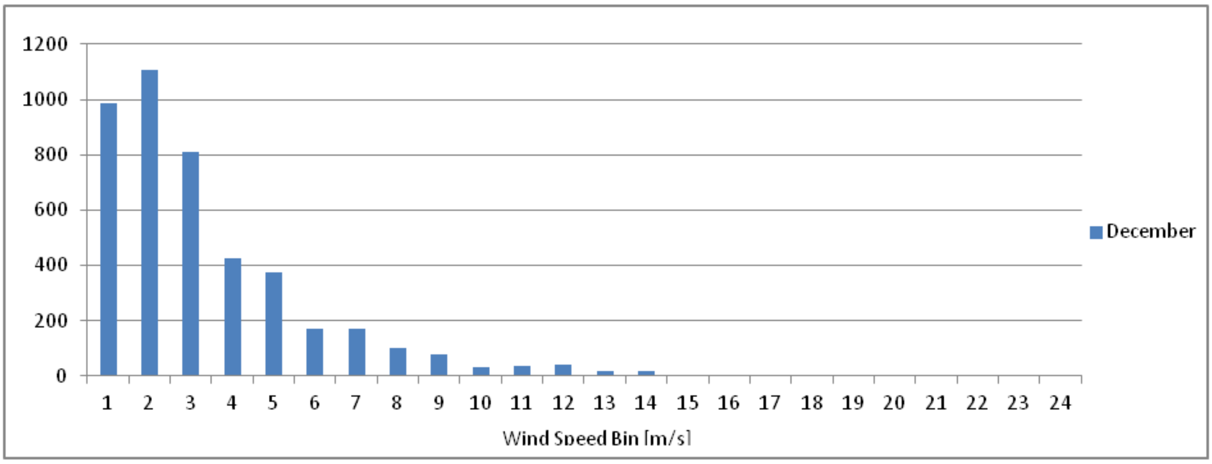

1200
1000
800
600
400
200
0
1 2 3 4 5 6 7 8 9 10 11 12 13 14 15 16 17 18 19 20 21 22 23 24
Wind Speed Bin [m/s]
December

2014

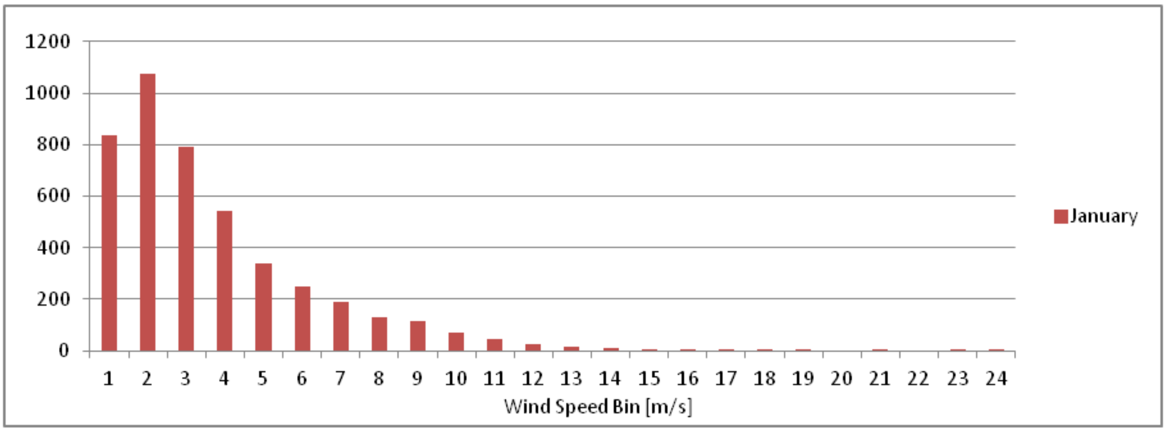
1200
1000
800
600
400
200
0
1 2 3 4 5 6 7 8 9 10 11 12 13 14 15 16 17 18 19 20 21 22 23 24
Wind Speed Bin [m/s]
January

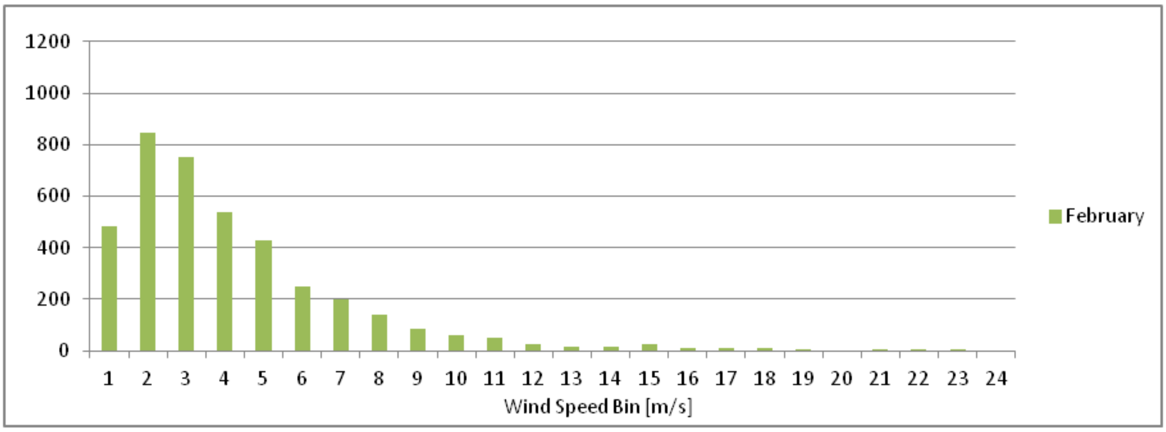
1200
1000
800
600
400
200
0
1 2 3 4 5 6 7 8 9 10 11 12 13 14 15 16 17 18 19 20 21 22 23 24
Wind Speed Bin [m/s]
February

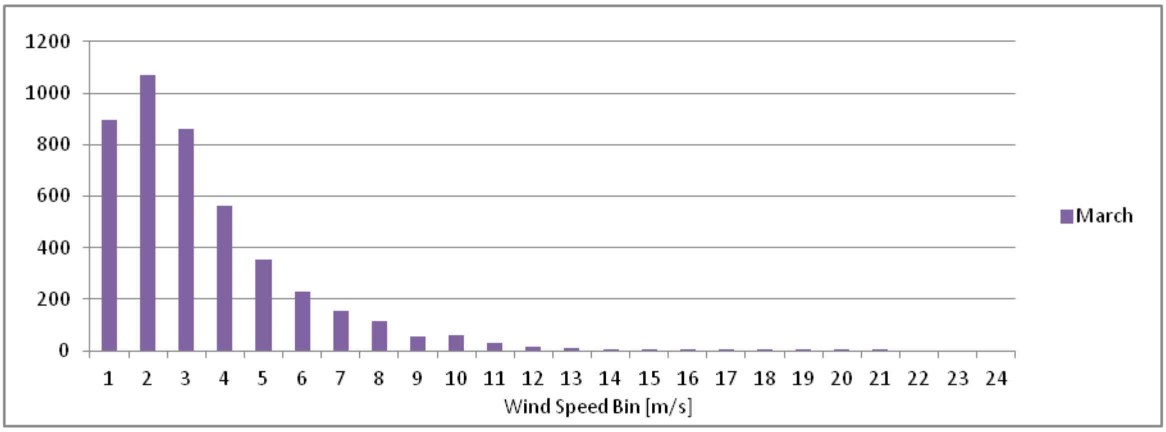
1200
1000
800
600
400
200
0
1 2 3 4 5 6 7 8 9 10 11 12 13 14 15 16 17 18 19 20 21 22 23 24
Wind Speed Bin [m/s]
March

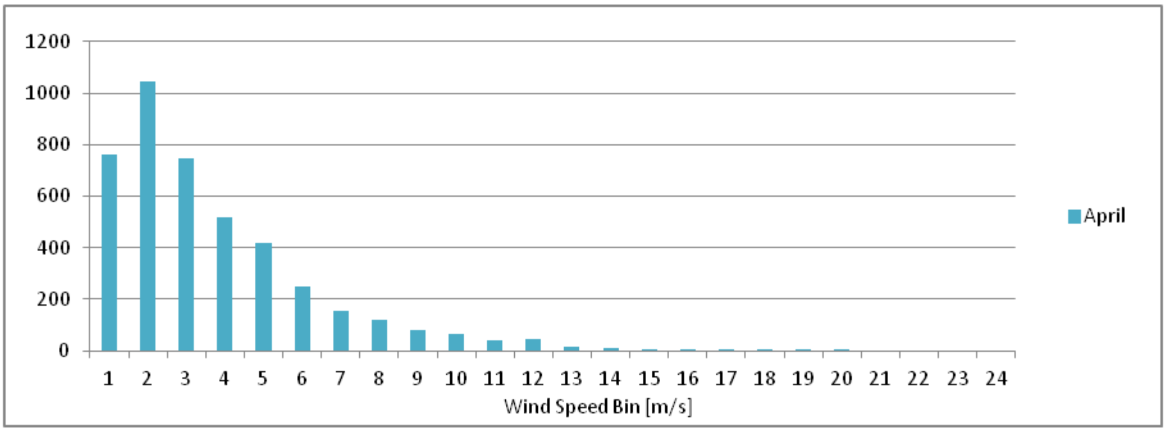
1200
1000
800
600
400
200
0
1 2 3 4 5 6 7 8 9 10 11 12 13 14 15 16 17 18 19 20 21 22 23 24
Wind Speed Bin [m/s]
April

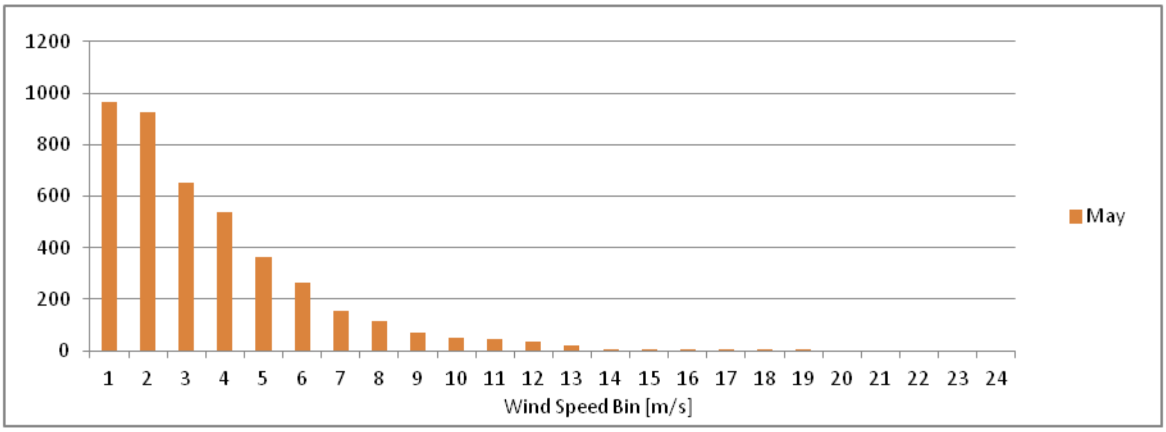
1200
1000
800
600
400
200
0
1 2 3 4 5 6 7 8 9 10 11 12 13 14 15 16 17 18 19 20 21 22 23 24
Wind Speed Bin [m/s]
May

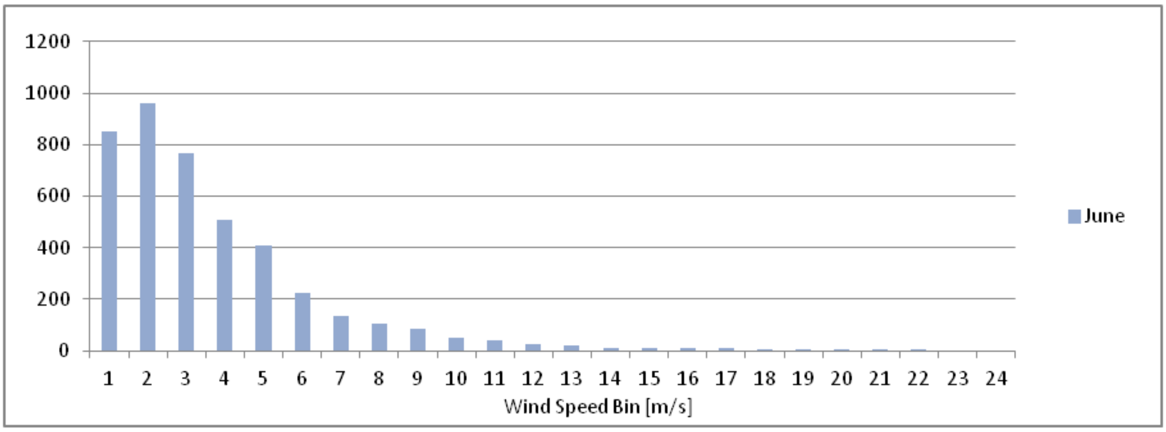
1200
1000
800
600
400
200
0
1 2 3 4 5 6 7 8 9 10 11 12 13 14 15 16 17 18 19 20 21 22 23 24
Wind Speed Bin [m/s]
June

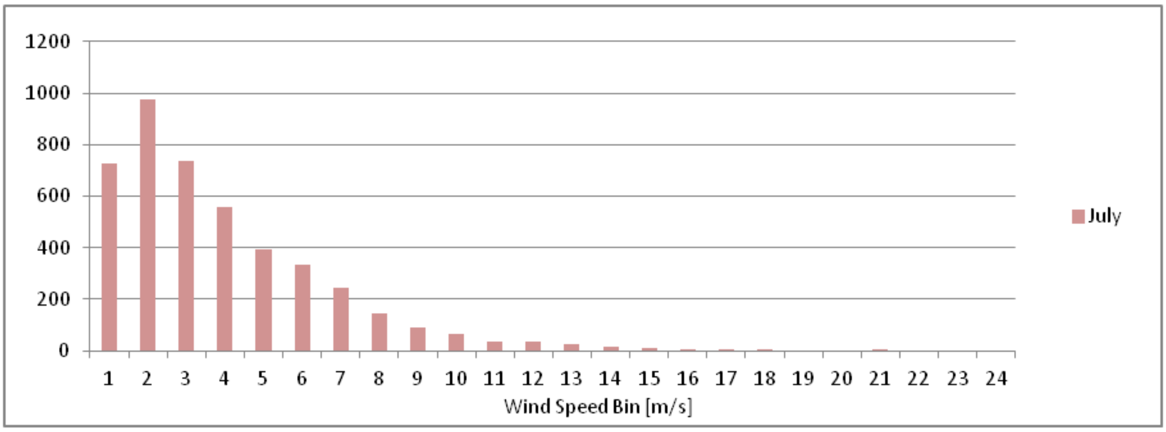
1200
1000
800
600
400
200
0
1 2 3 4 5 6 7 8 9 10 11 12 13 14 15 16 17 18 19 20 21 22 23 24
Wind Speed Bin [m/s]
July

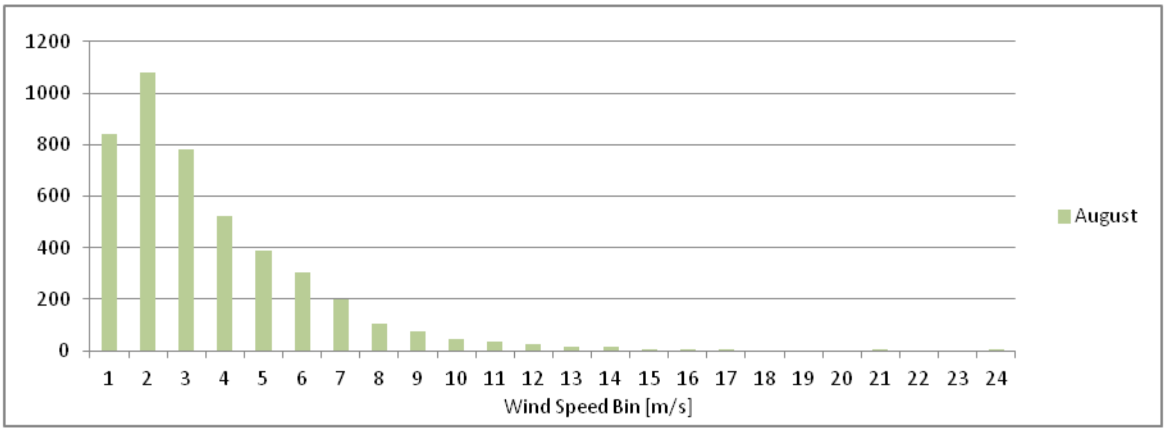
1200
1000
800
600
400
200
0
1 2 3 4 5 6 7 8 9 10 11 12 13 14 15 16 17 18 19 20 21 22 23 24
Wind Speed Bin [m/s]
August

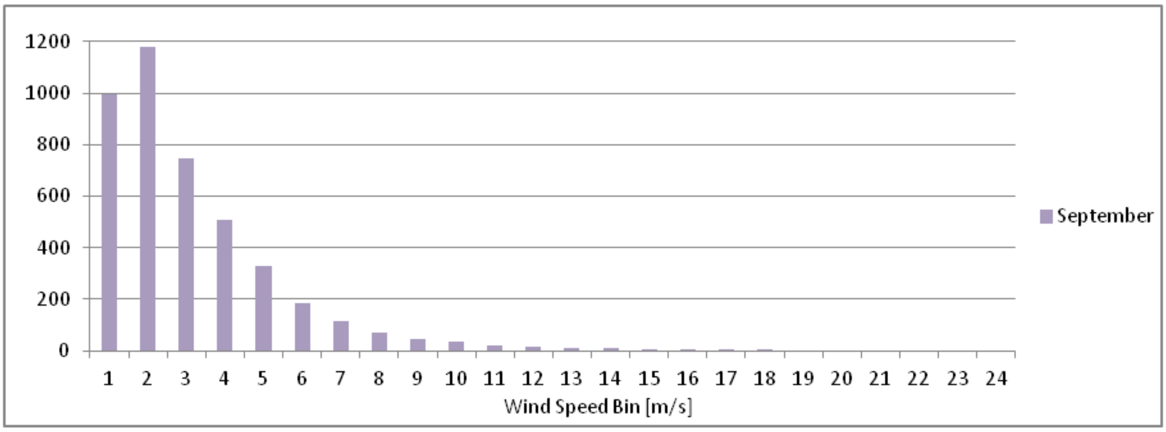
1200
1000
800
600
400
200
0
1 2 3 4 5 6 7 8 9 10 11 12 13 14 15 16 17 18 19 20 21 22 23 24
Wind Speed Bin [m/s]
September

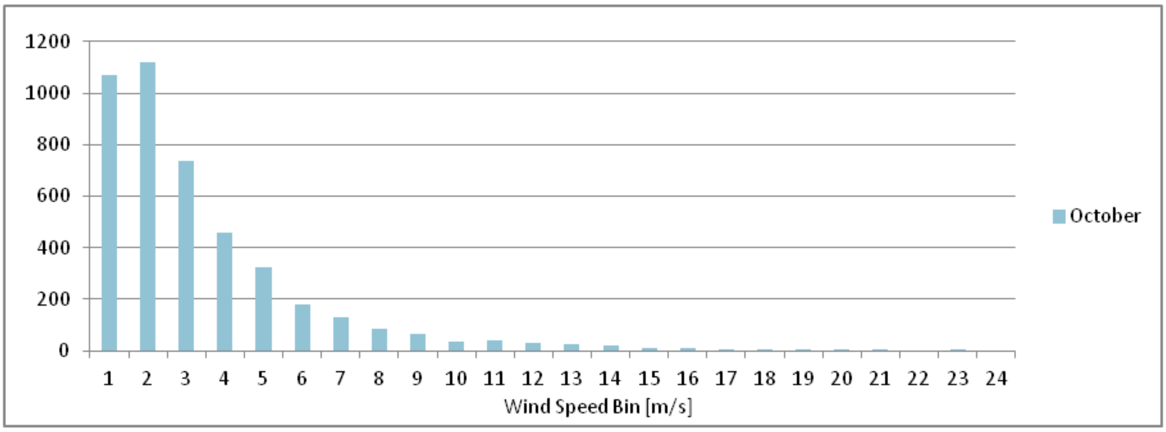
1200
1000
800
600
400
200
0
1 2 3 4 5 6 7 8 9 10 11 12 13 14 15 16 17 18 19 20 21 22 23 24
Wind Speed Bin [m/s]
October

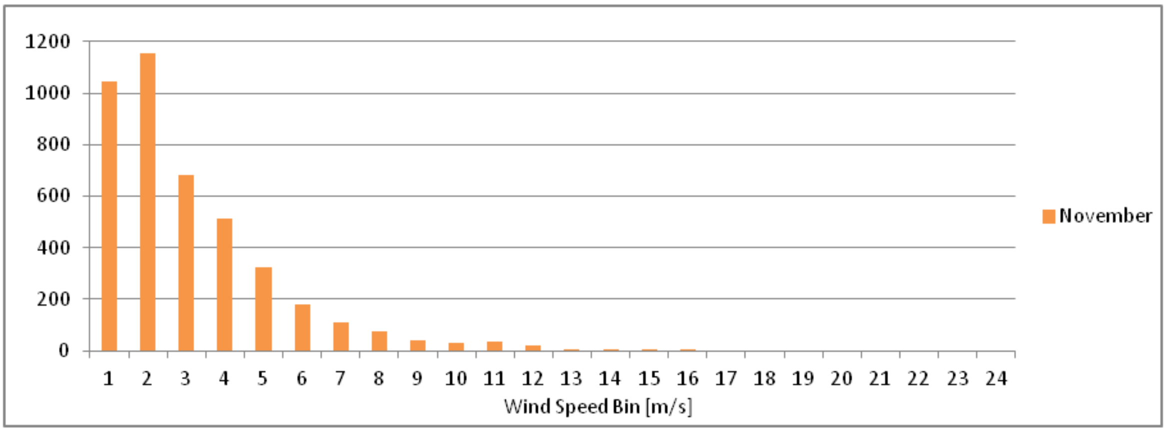
1200
1000
800
600
400
200
0
1 2 3 4 5 6 7 8 9 10 11 12 13 14 15 16 17 18 19 20 21 22 23 24
Wind Speed Bin [m/s]
November

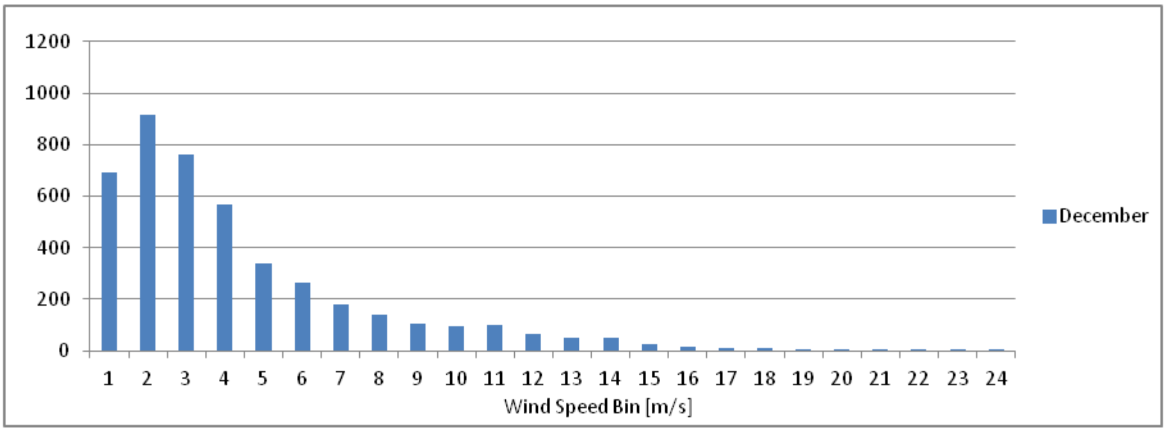
1200
1000
800
600
400
200
0
1 2 3 4 5 6 7 8 9 10 11 12 13 14 15 16 17 18 19 20 21 22 23 24
Wind Speed Bin [m/s]
December

APPENDIX F LSBU Wind Speed Distributions

The following tables display the measured wind speed distributions observed at the LSBU turbine site both for background, non-operational and operational measurement periods. An increase in average L_{Aeq} per wind speed bin is observed when the turbine is operational but the standard deviation of each bins results demonstrate a winder fluctuation of results likely due to other environmental factors.

Background

Bin	Range	Freq	Ave L_{Aeq}	Std Dev
1	0 < V < 1	700	56.73	3.34
2	1< V < 2	189	56.75	3.22
3	2< V < 3	14	60.17	2.13
4	3< V < 4	32	59.57	2.82
5	4< V < 5	3	57.97	2.38
6	5< V < 6	0	0.00	0
TOTAL		938		
Average V [m/s]		0.8		

Table 77: Displays wind speed frequency distribution and averaged L_{Aeq} levels for each wind speed bin.

Operational

Bin	Range	Freq	Ave L_{Aeq}	Std Dev
1	0 < V < 1	6560	61.5	5.2
2	1 < V < 2	1918	64.3	6.7
3	2 < V < 3	378	64.7	5.7
4	3 < V < 4	111	65.6	6.1
5	4 < V < 5	32	67.5	5.2
6	5 < V < 6	17	67.0	3.8
7	6 < V < 7	6	67.6	3.0
8	7 < V < 8	0		
	TOTAL	9022		
	Average [m/s]	0.79		

Table 78: Displays the frequency distribution of operational wind speeds recorded at the LSBU turbine position along with averaged noise levels for each wind speed bin.

APPENDIX G MAPS Bandwidth

The table below presents the resultant effect of modifying the modal bandwidth of the MAPS method in increments of 10 % as discussed in Chapter 4. Although widening the band smoothes out the curve it dilutes the peak acceleration results which may underestimate the typical representation of likely vibration levels per wind speed.

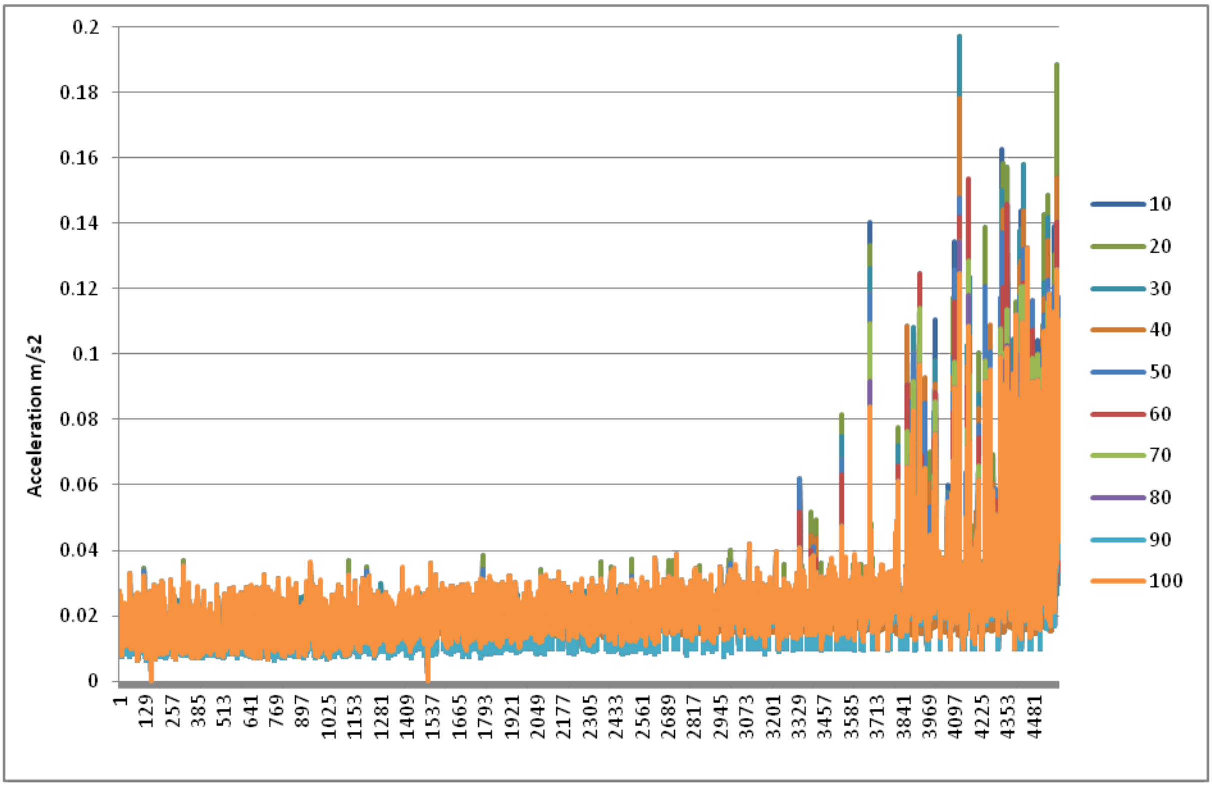

APPENDIX H LSBU Sound Transmission Loss Calculations

Office	External	Area	Hz							
			63	125	250	500	1000	2000	4000	8000
Floor	Carpet	30	0.15	0.01	0.02	0.06	0.15	0.25	0.45	0.07
Ceiling	Tiles	30	0.15	0.15	0.11	0.04	0.04	0.07	0.08	0.08
Wall	Glass	7.5	0.18	0.18	0.06	0.04	0.03	0.02	0.02	0.02
Wall	Plaster board	58.5	0.29	0.29	0.1	0.06	0.05	0.04	0.04	0.04
	R Façade		6.5	12.4	18.4	24.5	30.5	36.5	42.5	48.5
	S Façade	**7.5**								
	A =	**Sα**	**27.3**	**23.1**	**10.2**	**6.8**	**8.9**	**12.1**	**18.4**	**7.0**
		$L_{turbine}$	63.7	64.1	63.5	69.3	78.8	77.9	55.5	46.9
		L_{out}	20.4	18.1	14.5	17.4	23.8	20.0	-5.5	-17.1
		L_{in}	13.9	5.7	-3.9	-7.1	-6.7	-16.5	-48.0	-65.6
ρ glass	2800	**kg/m³**								
t	0.003	**m**								
m	8.4	**kg/m²**								Average

Table 79: Displays predicted external (L_{out}) and internal (L_{in}) sound levels (dB) at the LSBU office in closest proximity to the operational turbine.

Office	Direct	Area	Hz							
			63	125	250	500	1000	2000	4000	8000
Floor	Carpet	30	0.15	0.01	0.02	0.06	0.15	0.25	0.45	0.07
Ceiling	Tiles	30	0.15	0.15	0.11	0.04	0.04	0.07	0.08	0.08
Wall	Glass	7.5	0.18	0.18	0.06	0.04	0.03	0.02	0.02	0.02
Wall	Plaster board	58.5	0.29	0.29	0.1	0.06	0.05	0.04	0.04	0.04
	R Façade		45.8	51.8	57.8	63.8	69.8	75.9	81.9	87.9
	S Façade	**50**								
	A =	**Sα**	**27.3**	**23.1**	**10.2**	**6.8**	**8.9**	**12.1**	**18.4**	**7.0**
		$L_{turbine}$	63.7	64.1	63.5	69.3	78.8	77.9	55.5	46.9
		L_{in}	20.5	15.7	12.6	14.2	16.4	8.2	-22.1	-32.4
ρ concrete	2600	**kg/m³**								
t	0.3	**m**								
m	780	**kg/m²**								Average

Table 80: Displays calculated expected internal noise levels due to direct transmission through the concrete partition separating the LSBU turbine and nearest occupied areas.

Office	External	Area	Hz							
			63	125	250	500	1000	2000	4000	8000
Floor	Carpet	30	0.15	0.01	0.02	0.06	0.15	0.25	0.45	0.07
Ceiling	Tiles	30	0.15	0.15	0.11	0.04	0.04	0.07	0.08	0.08
Wall	Glass	7.5	0.18	0.18	0.06	0.04	0.03	0.02	0.02	0.02
Wall	Plaster board	58.5	0.29	0.29	0.1	0.06	0.05	0.04	0.04	0.04
	R Façade		6.5	12.4	18.4	24.5	30.5	36.5	42.5	48.5
	S Façade	**7.5**								
	A =	**Sα**	**27.3**	**23.1**	**10.2**	**6.8**	**8.9**	**12.1**	**18.4**	**7.0**
		$L_{turbine}$	75.4	73.6	66.2	69.3	78.8	77.9	64.7	61.8
		L_{out}	32.1	27.6	17.3	17.4	23.8	20.0	3.8	-2.2
		L_{in}	25.6	15.2	-1.1	-7.1	-6.7	-16.5	-38.7	-50.7
ρ glass	2800	**kg/m^3**								
t	0.003	**m**								
m	8.4	**kg/m^2**								Worst

Table 81: Displays predicted worst case scenario external (Lout) and internal (Lin) sound levels (dB) at the LSBU office in closest proximity to the operational turbine.

Office	Direct	Area	Hz							
			63	125	250	500	1000	2000	4000	8000
Floor	Carpet	30	0.15	0.01	0.02	0.06	0.15	0.25	0.45	0.07
Ceiling	Tiles	30	0.15	0.15	0.11	0.04	0.04	0.07	0.08	0.08
Wall	Glass	7.5	0.18	0.18	0.06	0.04	0.03	0.02	0.02	0.02
Wall	Plaster board	58.5	0.29	0.29	0.1	0.06	0.05	0.04	0.04	0.04
	R Façade		45.8	51.8	57.8	63.8	69.8	75.9	81.9	87.9
	S Façade	**50**								
	A =	**Sα**	**27.3**	**23.1**	**10.2**	**6.8**	**8.9**	**12.1**	**18.4**	**7.0**
		$L_{turbine}$	75.4	73.6	66.2	69.3	78.8	77.9	64.7	61.8
		L_{in}	32.2	25.2	15.3	14.2	16.4	8.2	-12.8	-17.6
ρ concrete	2600	**kg/m^3**								
t	0.3	**m**								
m	780	**kg/m^2**								Worst

Table 82: Displays calculated expected worst case scenario internal noise levels due to direct transmission through the concrete partition separating the LSBU turbine and the closest occupied areas.

APPENDIX I Strata Wind Speed Distributions

The following tables display the projected wind speed distributions observed at the Strata turbine site compared with measured average L_{Aeq} levels for both background, non-operational and operational measurement periods.

Bin	Range	Freq	Ave L_{Aeq}	Std Dev
1.0	0 < V < 1	156	54.8	3.2
2.0	1 < V < 2	349	55.3	4.0
3.0	2 < V < 3	296	56.5	5.2
4.0	3 < V < 4	300	55.6	3.6
5.0	4 < V < 5	174	55.2	3.8
6.0	5 < V < 6	153	56.4	4.5
7.0	6 < V < 7	118	56.8	4.5
8.0	7 < V < 8	58	58.4	5.2
9.0	8 < V < 9	58	58.1	5.7
10.0	9 < V < 10	59	57.4	6.8
11.0	10 < V < 11	32	58.0	4.8
12.0	11 < V < 12	24	57.1	5.9
13.0	12 < V < 13	18	58.9	4.9
14.0	13 < V < 14	15	58.9	5.7
15.0	14 < V < 15	7	57.4	2.9
16.0	15 < V < 16	6	58.9	2.3
17.0	16 < V < 17	8	57.2	2.1
18.0	17 < V < 18	5	56.5	2.7
19.0	18 < V < 19	4	63.9	7.5
20.0	19 < V < 20	2	60.0	0.9
21.0	20 < V < 21	2	55.1	0.0
22.0	21 < V < 22	1	67.5	0.0
23.0	22 < V < 23	6	57.4	5.5
24.0	23 < V < 24	0	0.0	
	TOTAL	**1851**		
	Ave V [m/s]	**4.3**		

Table 83: Displays frequency of average L_{Aeq} levels per wind speed bin for the Strata building.

Bin	Range	Freq	Ave L_{Aeq}	Std Dev
1	0 < V < 1	165	56.3	4.3
2	1 < V < 2	249	56.8	5.2
3	2 < V < 3	243	57.6	5.2
4	3 < V < 4	222	57.9	5.7
5	4 < V < 5	226	58.3	5.2
6	5 < V < 6	177	58.9	5.2
7	6 < V < 7	135	57.3	4.3
8	7 < V < 8	147	59.0	6.1
9	8 < V < 9	106	58.4	4.6
10	9 < V < 10	108	57.7	5.0
11	10 < V < 11	90	60.3	7.1
12	11 < V < 12	63	58.3	3.4
13	12 < V < 13	60	57.3	3.0
14	13 < V < 14	36	60.1	6.8
15	14 < V < 15	33	58.4	4.1
16	15 < V < 16	27	62.1	6.2
17	16 < V < 17	6	60.8	2.2
18	17 < V < 18	12	60.4	4.4
19	18 < V < 19	9	57.0	1.5
20	19 < V < 20	6	58.8	3.3
21	20 < V < 21	9	61.8	7.8
22	21 < V < 22	12	60.6	5.0
23	22 < V < 23	6	56.8	0.6
24	23 < V < 24	6	61.1	2.7
25	24 < V < 25	3	60.0	1.4
26	25 < V < 26	0		0.0
27	26 < V < 27	3	58.1	0.3
28	27 < V < 28	0		0.0
29	28 < V < 29	0		0.0
30	29 < V < 30	3	57.0	1.6
	TOTAL	2162		
	Ave V [m/s]	6.1		

Table 84: Displays operational wind speed frequency data along with corresponding average L_{Aeq} levels.

APPENDIX J Accelerometer Mounting Types

Figure 150 outlines suggested accelerometer mounting types for use in vibration monitoring. An installed stud mount or the use of cement would have been ideal but under the circumstances a thin, strong, double sided adhesive material with minimal padding was used to secure the accelerometer to the LSBU plant room surfaces, turbine mount and the Strata inertia base.

	Resonance frequency	Temperature	Mass of transducer and stiffness of mounting	Resonance magnification factor Q	Importance of surface preparation
Stud	●	●	●	●	●
Methylcyano acrylate cement	●	●	●	●	◑
Beeswax	◑	○	◑	●	●
Double-sided tape	○	◑	○	○	●
Quick mount	◑	●	◑	◑	◑
Vacuum mounted	◑	●	●	◑	◑
Magnet	◑	●	○	○	●
Hand held	○	○*)	○	○	○

*) Depends entirely on distance between hand and measured surface.
Key: ● high ◑ average ○ poor

Figure 150: Depicts differing accelerometer mounting types and their effectiveness relative to measurement procedure parameters.

APPENDIX K Norwin 18 kW (STRATA) power coefficient & power curves.

Wind Speed (m/s)	Power in Wind (W)	Norwin Power Curve (W)	Norwin Coefficient of Performance, Cp
0	0	0	0.000
1	34	0	0.000
2	274	0	0.000
3	923	0	0.000
4	2188	200	0.091
5	4274	400	0.094
6	7385	2000	0.271
7	11727	4000	0.341
8	17505	6700	0.383
9	24924	9000	0.361
10	34189	11700	0.342
11	45505	13900	0.305
12	59078	15900	0.269
13	75113	17100	0.228
14	93814	18000	0.192
15	115387	18200	0.157729
16	140038	18300	0.130679
17	167970	18300	0.108948
18	199390	18200	0.091279
19	234501	18000	0.076759
20	273511	17000	0.062155
21	316623	0	0
22	364043	0	0
23	415976	0	0
24	472627	0	0
25	534201	0	0

Table 85: Norwin 18 kW manufacturer turbine power curve data

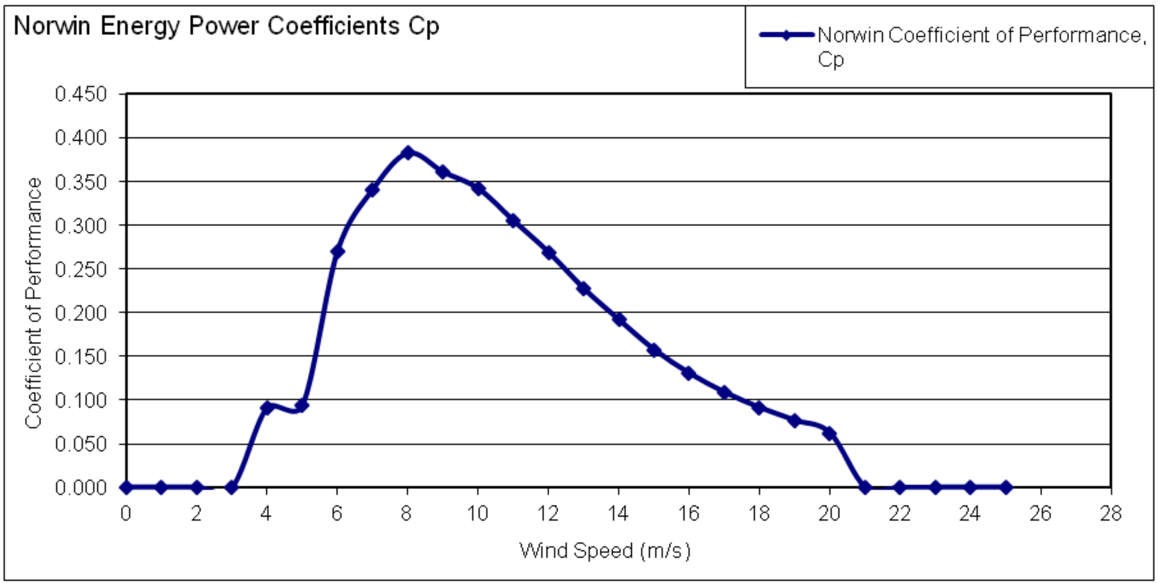

Figure 151: Norwin 18 kW Power Coefficients

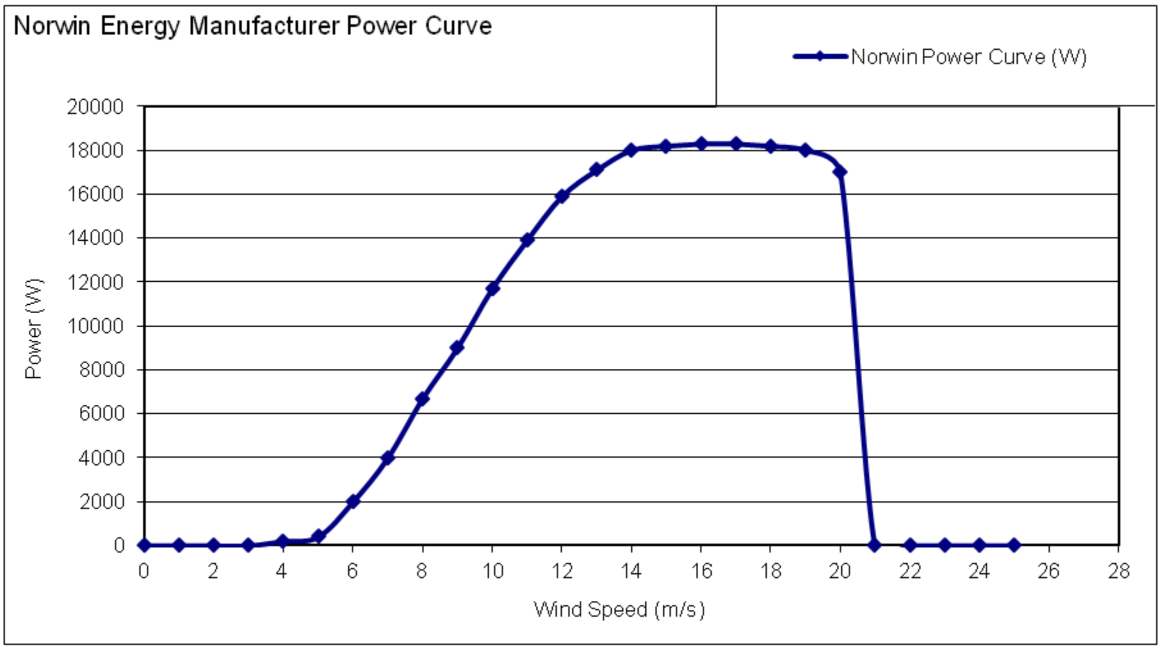

Figure 152: Norwin 18 kW power curve

APPENDIX L Proven 6 kW (LSBU) power coefficient & power curves.

Wind Speed (m/s)	Power in Wind (W)	Proven Power Curve (W)	Proven Coefficient of Performance, Cp
0	0	0	0.000
1	14	0	0.000
2	115	0	0.000
3	386	100	0.259
4	916	450	0.491
5	1789	1000	0.559
6	3092	1500	0.485
7	4910	2050	0.418
8	7329	3000	0.409
9	10435	4000	0.383
10	14314	5000	0.349
11	19052	6000	0.315
12	24735	6200	0.251
13	31449	6250	0.199
14	39279	6150	0.157
15	48311	6000	0.124195
16	58632	6000	0.102334
17	70327	6000	0.085316

Table 86: Proven 6 kW power curve data

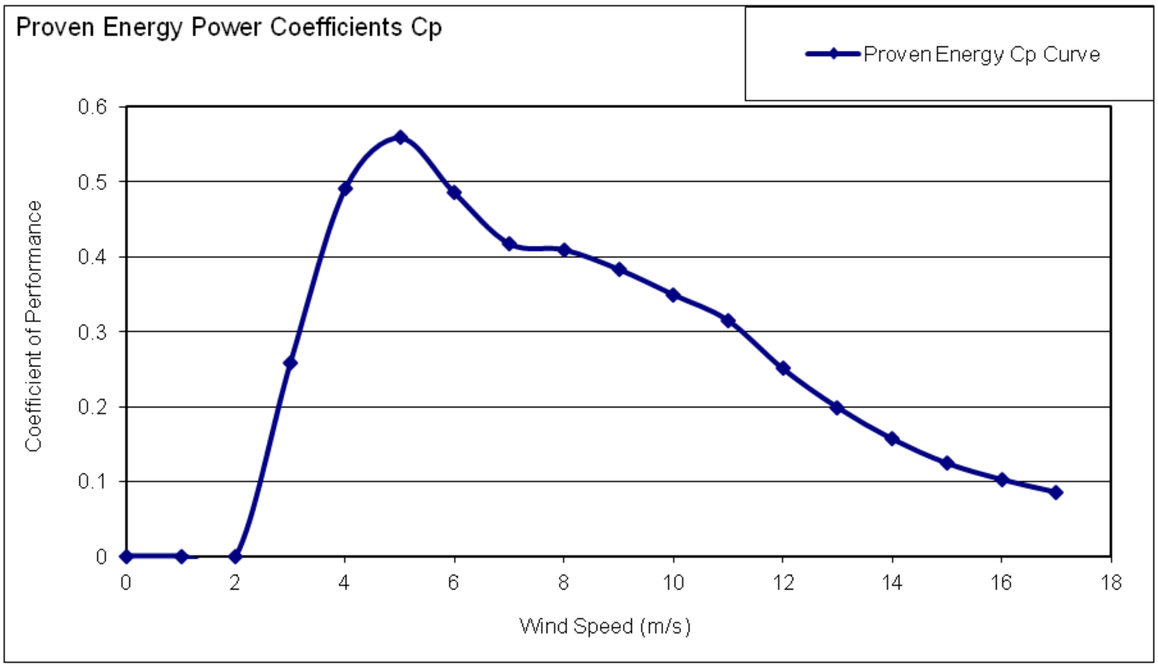

Figure 153: Proven 6 kW power coefficients

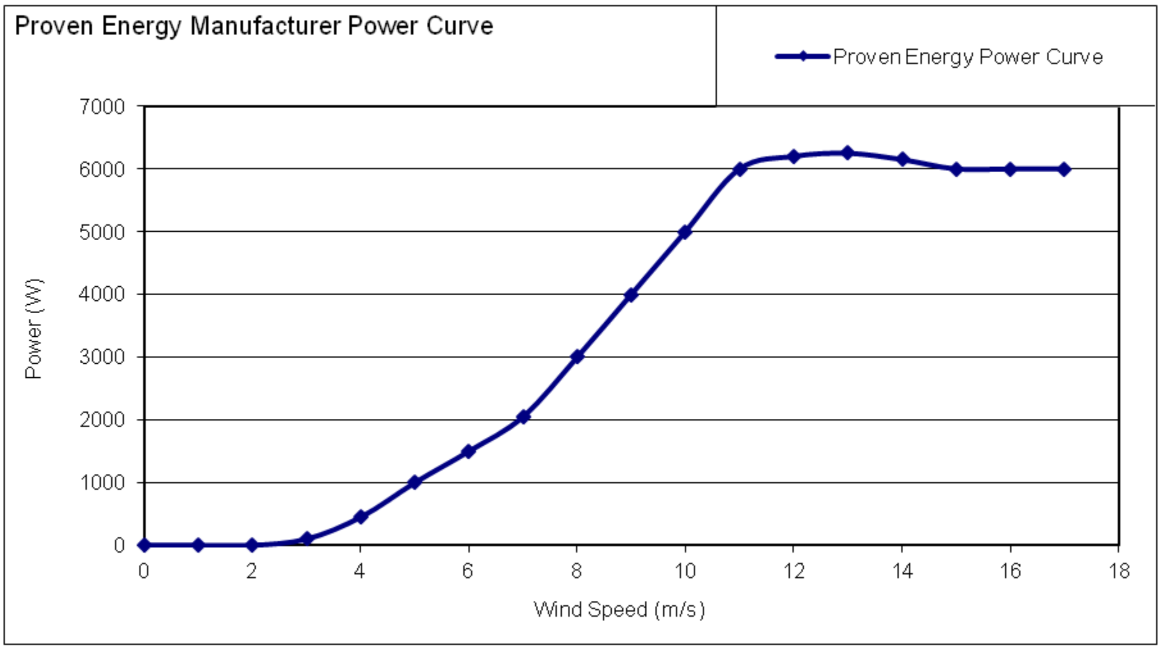

Figure 154: Proven 6 kW power curve

APPENDIX M Wind Speed Frequency distributions LSBU 2013

Year:	2013	MMLM - 10 MINUTE AV. DATA	Total number of missing wind data:	1157	2.2

INTERVAL	WIND SPEED BINS (m/s)	FREQUENCY	MEDIAN WIND SPEED (m/s)	INTERVAL TOTAL, vi (m/s)	Av WIND SPEED, vi (m/s)	ln(vi)	p(vi) ACTUAL	vi^k1	FUNCTION A: vi^k . ln(vi) . P(vi)	FUNCTION B: vi^k . P(vi)	FUNCTION C: ln(vi) . P(vi)	WEIBULL	RAYLEIGH
							o					o	o
0	0 < v ≤ 0.5	9847	0.5	1008.44	0.10	-2.279	0.192	0.1401280131621	-0.061	0.027	-0.437	0.192	0.071
1	0.5 < v ≤ 1.5	11706	1	12084.16	1.03	0.032	0.228	1.0277984045694	0.007	0.234	0.007	0.220	0.134
2	1.5 < v ≤ 2.5	8766	2	20704.44	2.36	0.859	0.171	2.0984577907554	0.308	0.358	0.147	0.131	0.216
3	2.5 < v ≤ 3.5	6004	3	22065.36	3.68	1.302	0.117	3.0724705423288	0.467	0.359	0.152	0.085	0.226
4	3.5 < v ≤ 4.5	4342	4	20150.60	4.64	1.535	0.084	3.7572716462246	0.487	0.317	0.130	0.064	0.182
5	4.5 < v ≤ 5.5	3093	5	18466.80	5.97	1.787	0.060	4.6690720858206	0.502	0.281	0.108	0.044	0.119
6	5.5 < v ≤ 6.5	2395	6	16965.12	7.08	1.958	0.047	5.4107155738371	0.494	0.252	0.091	0.032	0.065
7	6.5 < v ≤ 7.5	1577	7	13545.64	8.59	2.151	0.031	6.3892743243883	0.422	0.196	0.066	0.022	0.030
8	7.5 < v ≤ 8.5	1123	8	10796.48	9.61	2.263	0.022	7.0412960673095	0.348	0.154	0.049	0.017	0.012
9	8.5 < v ≤ 9.5	790	9	8616.88	10.91	2.389	0.015	7.8510851949809	0.288	0.121	0.037	0.012	0.004
10	9.5 < v ≤ 10.5	585	10	7068.28	12.08	2.492	0.011	8.5753184941136	0.243	0.098	0.028	0.009	0.001
11	10.5 < v ≤ 11.5	398	11	5385.48	13.53	2.605	0.008	9.4550963293453	0.191	0.073	0.020	0.006	0.000
12	11.5 < v ≤ 12.5	310	12	4088.80	13.19	2.579	0.006	9.2488377554939	0.144	0.056	0.016	0.007	0.000
13	12.5 < v ≤ 13.5	153	13	3036.52	19.85	2.988	0.003	13.1558849105973	0.117	0.039	0.009	0.002	0.000
14	13.5 < v ≤ 14.5	127	14	1988.96	15.66	2.751	0.002	10.7253580479715	0.073	0.026	0.007	0.004	0.000
15	14.5 < v ≤ 15.5	77	15	1586.96	20.61	3.026	0.001	13.5911193565551	0.062	0.020	0.005	0.001	0.000
16	15.5 < v ≤ 16.5	41	16	782.52	19.09	2.949	0.001	12.7198644817674	0.030	0.010	0.002	0.002	0.000
17	16.5 < v < 17.5	31	17	610.76	19.70	2.981	0.001	13.0731800979089	0.024	0.008	0.002	0.002	0.000
18	17.5 < v < 18.5	16	18	485.28	30.33	3.412	0.000	18.9654466472571	0.020	0.006	0.001	0.000	0.000
19	18.5 < v < 19.5	7	19	188.96	188.96	5.242	0.000	91.8619613664021	0.066	0.013	0.001	0.000	0.000
20	19.5 < v < 20.5	10	20	220.68	22.07	3.094	0.000	14.4164338098403	0.009	0.003	0.001	0.001	0.000
21	20.5 < v < 21.5	3	21	62.80	20.93	3.041	0.000	13.7748772109623	0.002	0.001	0.000	0.001	0.000
22	21.5 < v < 22.5	2	22	88.56	44.28	3.791	0.000	26.2836299311999	0.004	0.001	0.000	0.000	0.000
23	22.5 < v < 23.5	0	23	0.00	23.00	3.135	0.000	14.9400033023762	0.000	0.000	0.000	0.001	0.000
		51403		169998.5			1.000	312.24	4.245	2.652	0.441	0.8537	1.058

Mean V:	3.31	m/s

Weibull factors:		
	(Iterative) k =	0.8624
	k =	2.0000
	c =	3.0989

Proven Power Curve (W)	Measured		Weibull PDF		Rayleigh PDF	
	p(vi) ACTUAL	Energy Yield (kWh)	Weibull	Energy Yield (kWh)	Rayleigh	Energy Yield (kWh)
0	0.192	0.00	0.192	0.00	0.071	0.00
0	0.228	0.00	0.220	0.00	0.134	0.00
0	0.171	0.00	0.131	0.00	0.216	0.00
100	0.117	60.04	0.085	43.87	0.226	116.05
450	0.084	195.39	0.064	147.68	0.182	421.20
1000	0.060	309.30	0.044	224.78	0.119	613.07
1500	0.047	359.25	0.032	249.00	0.065	500.89
2050	0.031	323.29	0.022	229.14	0.030	314.00
3000	0.022	336.90	0.017	258.21	0.012	178.85
4000	0.015	316.00	0.012	249.32	0.004	79.15
5000	0.011	292.50	0.009	233.87	0.001	28.09
6000	0.008	238.80	0.006	198.30	0.000	8.21
6200	0.006	192.20	0.007	222.26	0.000	1.77
6250	0.003	95.63	0.002	48.55	0.000	0.32
6150	0.002	78.11	0.004	123.40	0.000	0.05
6000	0.001	46.20	0.001	39.35	0.000	0.01
6000	0.001	24.60	0.002	55.23	0.000	0.00
6000	0.001	18.60	0.002	48.13	0.000	0.00
6000	0.000	9.60	0.000	4.92	0.000	0.00
6000	0.000	4.20	0.000	0.00	0.000	0.00
6000	0.000	6.00	0.001	28.56	0.000	0.00
6000	0.000	1.80	0.001	36.63	0.000	0.00
6000	0.000	1.20	0.000	0.30	0.000	0.00
	0.000	0.00	0.001	0.00	0.000	0.00
	0.999	**2886.80**	**0.851**	**2441.48**	**1.058**	**2261.66**

	Guestimate Cp = 0.20		
Power in the wind (kW)	Coefficient of Power	Power in Wind with Cp Applied (kW)	Power x Frequency (kW)
0.00	0.20	0.000	0.000
0.01	0.20	0.003	33.513
0.11	0.20	0.023	200.768
0.39	0.20	0.077	464.095
0.92	0.20	0.183	795.558
1.79	0.20	0.358	1106.859
3.09	0.20	0.618	1481.022
4.91	0.20	0.982	1548.560
7.33	0.20	1.466	1646.084
10.44	0.20	2.087	1648.758
14.31	0.20	2.863	1674.782
19.05	0.20	3.810	1516.573
24.74	0.20	4.947	1533.585
31.45	0.20	6.290	962.329
39.28	0.20	7.856	997.677
48.31	0.20	9.662	743.990
58.63	0.20	11.726	480.780
70.33	0.20	14.065	436.024
83.48	0.20	16.696	267.141
98.18	0.20	19.636	137.455
114.51	0.20	22.903	229.030
132.57	0.20	26.513	79.539
152.42	0.20	30.484	60.968
174.16	0.20	34.833	0.000
			18045

APPENDIX N Wind Speed Frequency distributions LSBU 2014

Year:	2014	MMLM - 10 MINUTE AV. DATA ANALYSIS	Total number of missing wind data:	829	1.6

INTERVAL	WIND SPEED BINS (m/s)	FREQUENCY	MEDIAN WIND SPEED (m/s)	INTERVAL TOTAL, vi (m/s)	Av WIND SPEED, vi (m/s)	ln(vi)	p(vi) ACTUAL	vi^k1	FUNCTION A: vi^k . ln(vi) . P(vi)	FUNCTION B: vi^k . P(vi)	FUNCTION C: ln(vi) . P(vi)	WEIBULL	RAYLEIGH
0	0 < v ≤ 0.5	10150	0.5	1103.69	0.11	-2.219	0.196	0.1443093411306	-0.063	0.028	-0.435	0.426	0.078
1	0.5 < v ≤ 1.5	12342	1	12677.59	1.03	0.027	0.239	1.0236820030489	0.007	0.244	0.006	0.227	0.146
2	1.5 < v ≤ 2.5	9008	2	21386.59	2.37	0.865	0.174	2.1262513390082	0.320	0.370	0.151	0.133	0.231
3	2.5 < v ≤ 3.5	6332	3	22477.16	3.55	1.267	0.122	3.0200892282101	0.468	0.370	0.155	0.089	0.233
4	3.5 < v ≤ 4.5	4410	4	21451.84	4.86	1.582	0.085	3.9755071950887	0.536	0.339	0.135	0.059	0.178
5	4.5 < v ≤ 5.5	2914	5	17853.14	6.13	1.813	0.056	4.8619532347304	0.496	0.274	0.102	0.041	0.109
6	5.5 < v ≤ 6.5	1965	6	14815.43	7.54	2.020	0.038	5.8269510184261	0.447	0.221	0.077	0.027	0.055
7	6.5 < v ≤ 7.5	1346	7	11074.18	8.23	2.107	0.026	6.2881089491630	0.345	0.164	0.055	0.022	0.023
8	7.5 < v ≤ 8.5	908	8	8850.40	9.75	2.277	0.018	7.2902278848875	0.291	0.128	0.040	0.015	0.008
9	8.5 < v ≤ 9.5	669	9	6826.04	10.20	2.323	0.013	7.5870479802770	0.228	0.098	0.030	0.013	0.002
10	9.5 < v ≤ 10.5	520	10	5867.59	11.28	2.423	0.010	8.2834364146498	0.202	0.083	0.024	0.010	0.001
11	10.5 < v ≤ 11.5	373	11	4874.51	13.07	2.570	0.007	9.4154843097605	0.174	0.068	0.019	0.006	0.000
12	11.5 < v ≤ 12.5	234	12	3525.24	15.07	2.712	0.005	10.6590041610176	0.131	0.048	0.012	0.004	0.000
13	12.5 < v ≤ 13.5	177	13	2873.15	16.23	2.787	0.003	11.3761325799380	0.108	0.039	0.010	0.003	0.000
14	13.5 < v ≤ 14.5	122	14	1714.46	14.05	2.643	0.002	10.0314695739833	0.063	0.024	0.006	0.005	0.000
15	14.5 < v ≤ 15.5	74	15	1597.59	21.59	3.072	0.001	14.5896915129597	0.064	0.021	0.004	0.001	0.000
16	15.5 < v ≤ 16.5	67	16	1087.54	16.23	2.787	0.001	11.3757806909411	0.041	0.015	0.004	0.003	0.000
17	16.5 < v < 17.5	40	17	1102.75	27.57	3.317	0.001	18.0586784355437	0.046	0.014	0.003	0.000	0.000
18	17.5 < v < 18.5	24	18	504.34	21.01	3.045	0.000	14.2500560988197	0.020	0.007	0.001	0.001	0.000
19	18.5 < v < 19.5	17	19	361.45	21.26	3.057	0.000	14.3963599164566	0.014	0.005	0.001	0.001	0.000
20	19.5 < v < 20.5	16	20	300.45	18.78	2.933	0.000	12.9178446522564	0.012	0.004	0.001	0.002	0.000
21	20.5 < v < 21.5	8	21	335.50	41.94	3.736	0.000	26.0393175962041	0.015	0.004	0.001	0.000	0.000
22	21.5 < v < 22.5	11	22	44.53	4.05	1.398	0.000	3.3870228245192	0.001	0.001	0.000	0.004	0.000
23	22.5 < v < 23.5	4	23	204.95	51.24	3.936	0.000	31.0116580577398	0.009	0.002	0.000	0.000	0.000
24	23.5 < v < 24.5	4	24	143.48	35.87	3.580	0.000	22.7201450856792	0.006	0.002	0.000	0.000	0.000
25	24.5 < v < 25.5	3	25	49.56	16.52	2.805	0.000	11.5517317163412	0.002	0.001	0.000	0.003	0.000
26	25.5 < v < 26.5	1	26	103.19	103.19	4.637	0.000	57.1221941469694	0.005	0.001	0.000	0.000	0.000
		51731		**162910.1**			**1.000**	**237.94**	**3.977**	**2.570**	**0.401**	**1.0914**	**1.064**
				Mean V	3.15	m/s		**Weibull factors:**			(Iterative) k =	0.8724	
											k =	2.0000	
											c =	2.9507	

Proven Power Curve (W)	Measured		Weibull PDF		Rayleigh PDF	
	p(vi) ACTUAL	Energy Yield (kWh)	Weibull	Energy Yield (kWh)	Rayleigh	Energy Yield (kWh)
	0		0		0	
0	0.196	0.00	0.115	0.00	0.078	0.00
0	0.239	0.00	0.227	0.00	0.146	0.00
0	0.174	0.00	0.133	0.00	0.231	0.00
100	0.122	63.32	0.089	46.13	0.233	120.52
450	0.085	198.45	0.059	137.52	0.178	415.38
1000	0.056	291.40	0.041	210.17	0.109	565.72
1500	0.038	294.75	0.027	210.92	0.055	426.13
2050	0.026	275.93	0.022	238.25	0.023	242.68
3000	0.018	272.40	0.015	231.03	0.008	123.73
4000	0.013	267.60	0.013	272.85	0.002	48.29
5000	0.010	260.00	0.010	256.80	0.001	14.90
6000	0.007	223.80	0.006	194.70	0.000	3.73
6200	0.005	145.08	0.004	121.79	0.000	0.68
6250	0.003	110.63	0.003	92.00	0.000	0.10
6150	0.002	75.03	0.005	155.59	0.000	0.01
6000	0.001	44.40	0.001	24.39	0.000	0.00
6000	0.001	40.20	0.003	88.33	0.000	0.00
6000	0.001	24.00	0.000	6.13	0.000	0.00
6000	0.000	14.40	0.001	27.94	0.000	0.00
6000	0.000	10.20	0.001	26.35	0.000	0.00
6000	0.000	9.60	0.002	47.59	0.000	0.00
6000	0.000	4.80	0.000	0.26	0.000	0.00
6000	0.000	6.60	0.004	124.15	0.000	0.00
6000	0.000	2.40	0.000	0.04	0.000	0.00
6000	0.000	2.40	0.000	0.97	0.000	0.00
6000	0.000	1.80	0.003	82.30	0.000	0.00
6000	0.000	0.60	0.000	0.00	0.000	0.00
	0.998	**2586.99**	**0.773**	**2512.94**	**1.064**	**1961.88**

	Guestimate Cp = 0.20		
Power in the wind (kW)	Coefficient of Power	Power in Wind with Cp Applied (kW)	Power x Frequency (kW)
0.00	0.20	0.000	0.000
0.00	0.20	0.000	0.000
0.00	0.20	0.000	0.000
0.10	0.20	0.020	126.640
0.45	0.20	0.090	396.900
1.00	0.20	0.200	582.800
1.50	0.20	0.300	589.500
2.05	0.20	0.410	551.860
3.00	0.20	0.600	544.800
4.00	0.20	0.800	535.200
5.00	0.20	1.000	520.000
6.00	0.20	1.200	447.600
6.20	0.20	1.240	290.160
6.25	0.20	1.250	221.250
6.15	0.20	1.230	150.060
6.00	0.20	1.200	88.800
6.00	0.20	1.200	80.400
6.00	0.20	1.200	48.000
6.00	0.20	1.200	28.800
6.00	0.20	1.200	20.400
6.00	0.20	1.200	19.200
6.00	0.20	1.200	9.600
6.00	0.20	1.200	13.200
6.00	0.20	1.200	4.800
0.00	1.20	0.000	0.000
0.00	2.20	0.000	0.000
0.00	3.20	0.000	0.000
			5270

APPENDIX O LSBU $^{1}/_{3}{}^{rd}$ Octave levels per Wind Speed

The following graphs display the third octave results measured at the turbine monitoring position at the LSBU turbine site. Graphs are ordered by ascending wind speed bin and demonstrate an increase in low frequency content at the cut in speed of 3-4 m/s, which continue to rise with speed.

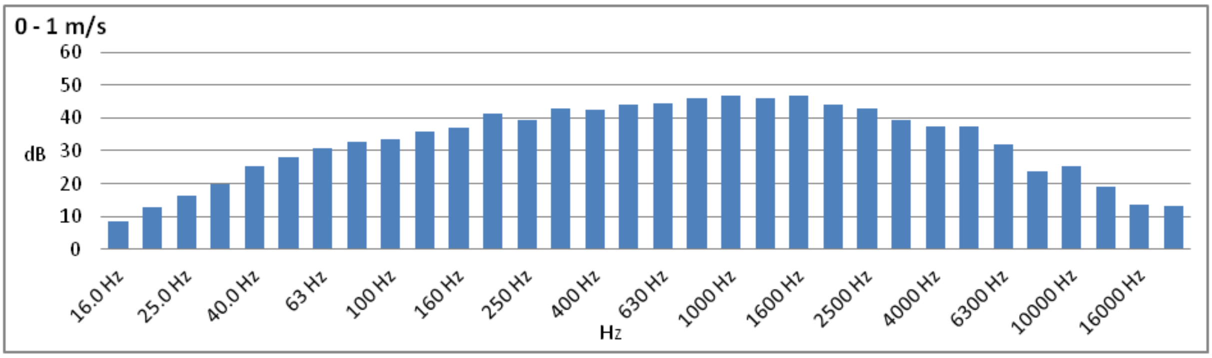

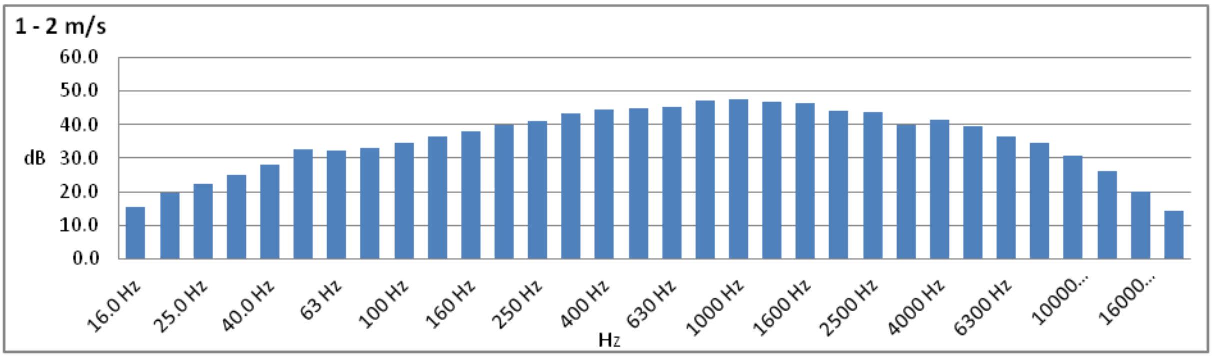

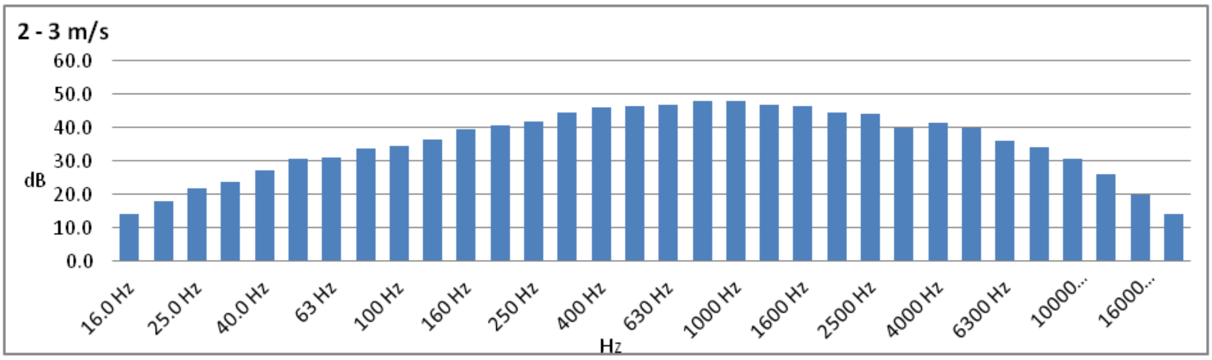

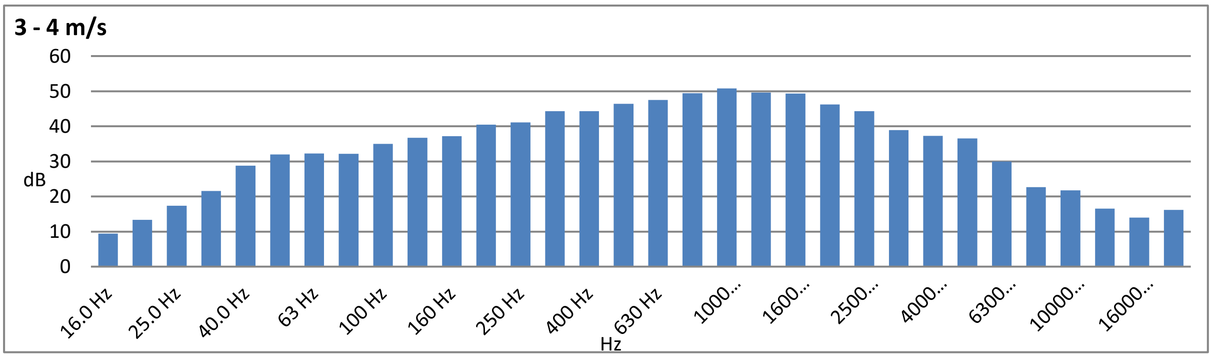

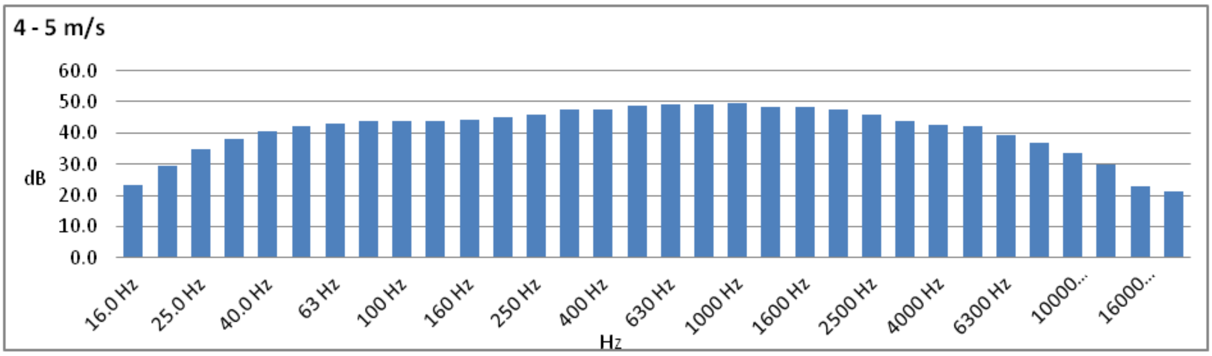
4 - 5 m/s
60.0
50.0
40.0
30.0
20.0
10.0
0.0
dB
16.0 Hz
25.0 Hz
40.0 Hz
63 Hz
100 Hz
160 Hz
250 Hz
400 Hz
630 Hz
1000 Hz
1600 Hz
2500 Hz
4000 Hz
6300 Hz
10000...
16000...
Hz

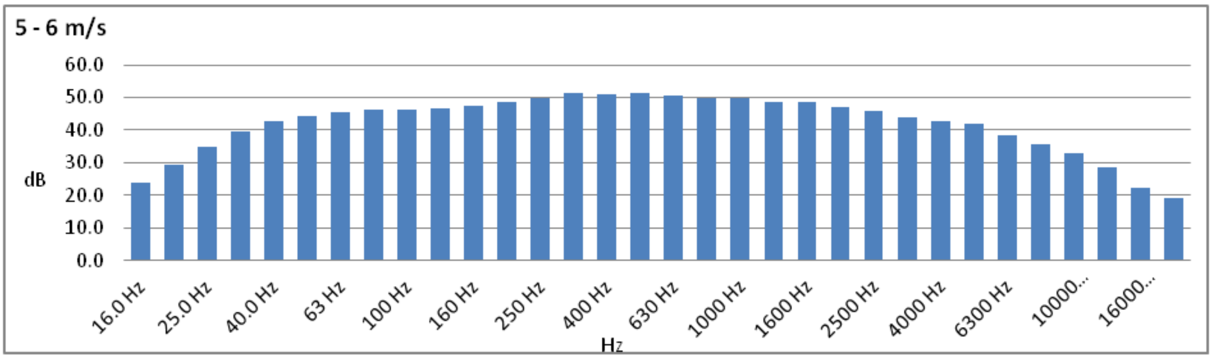
5 - 6 m/s
60.0
50.0
40.0
30.0
20.0
10.0
0.0
dB
16.0 Hz
25.0 Hz
40.0 Hz
63 Hz
100 Hz
160 Hz
250 Hz
400 Hz
630 Hz
1000 Hz
1600 Hz
2500 Hz
4000 Hz
6300 Hz
10000...
16000...
Hz

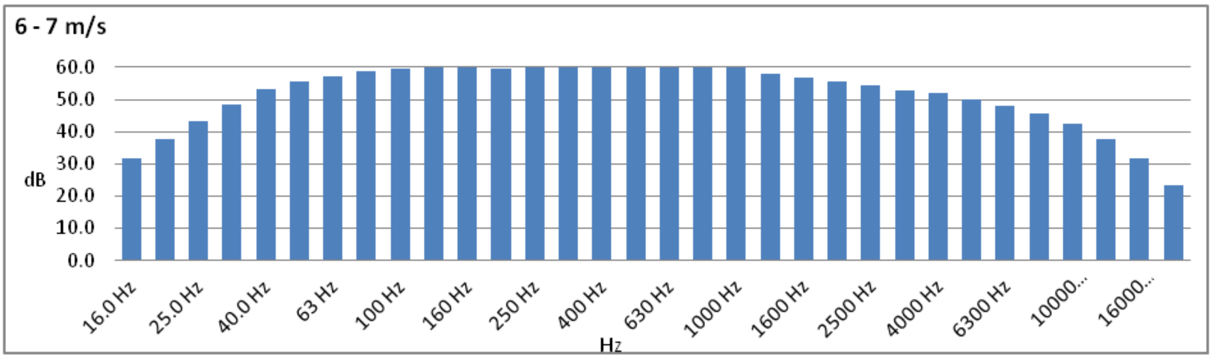
6 - 7 m/s
60.0
50.0
40.0
30.0
20.0
10.0
0.0
dB
16.0 Hz
25.0 Hz
40.0 Hz
63 Hz
100 Hz
160 Hz
250 Hz
400 Hz
630 Hz
1000 Hz
1600 Hz
2500 Hz
4000 Hz
6300 Hz
10000...
16000...
Hz

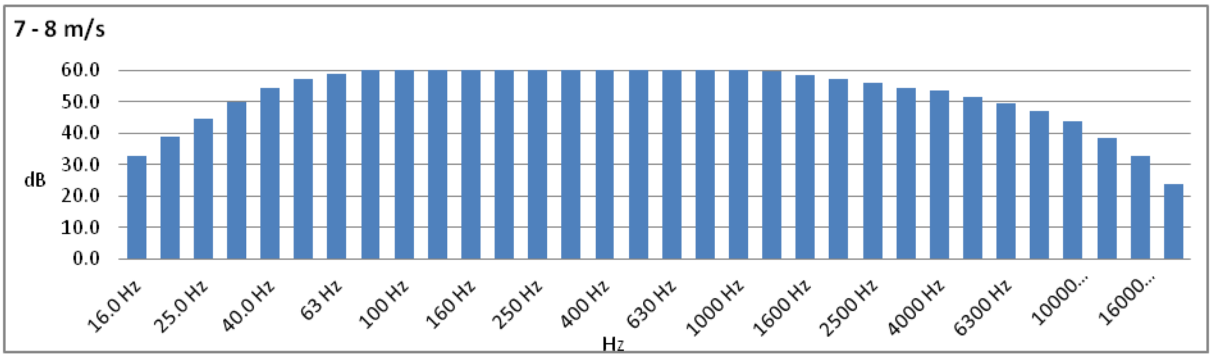
7 - 8 m/s
60.0
50.0
40.0
30.0
20.0
10.0
0.0
dB
16.0 Hz
25.0 Hz
40.0 Hz
63 Hz
100 Hz
160 Hz
250 Hz
400 Hz
630 Hz
1000 Hz
1600 Hz
2500 Hz
4000 Hz
6300 Hz
10000...
16000...
Hz

APPENDIX P **LSBU Environmental t-Test data**

L_{AEQ}	SSW	SW
Mean	61.2	52.0
Variance	16.7	1.8
Observations	121	110
Hypothesized Mean Difference	0	
df	147	
t Stat	23.45071	
P(T<=t) one-tail	7.77E-52	
t Critical one-tail	1.655285	
P(T<=t) two-tail	1.55E-51	
t Critical two-tail	1.976233	

Table 87: Displays t-Test results for SSW - SW L_{Aeq} comparison data for the control position.

Wind Speed	SSW	SW
Mean	5.6	2.0
Variance	0.5	0.9
Observations	121	110
Hypothesized Mean Difference	0	
df	204	
t Stat	32.58581	
P(T<=t) one-tail	4.2E-83	
t Critical one-tail	1.652357	
P(T<=t) two-tail	8.4E-83	
t Critical two-tail	1.971661	

Table 88: Displays t-Test results for SSW - SW wind speed comparison data for the control position.

L_{AEQ}	SSW	SW
Mean	65.17787	59.34484
Variance	39.69848	11.98124
Observations	118	111
Hypothesized Mean Difference	0	
df	184	
t Stat	8.750302	
P(T<=t) one-tail	6.71E-16	
t Critical one-tail	1.653177	
P(T<=t) two-tail	1.34E-15	
t Critical two-tail	1.972941	

Table 89: Displays t-Test results for SSW - SW L_{Aeq} comparison data for the street position.

Wind Speed	SSW	SW
Mean	5.658475	1.956757
Variance	0.539885	0.900295
Observations	118	111
Hypothesized Mean Difference	0	
df	207	
t Stat	32.86548	
P(T<=t) one-tail	2.17E-84	
t Critical one-tail	1.652248	
P(T<=t) two-tail	4.34E-84	
t Critical two-tail	1.97149	

Table 90: Displays t-Test results for SSW - SW wind speed comparison data for the street position.

APPENDIX Q Strata $^{1}/_{3}^{rd}$ Octave levels per Wind Speed

The following graphs display the third octave results measured at the Strata turbine site. The graphs are ordered by ascending wind speed bin and demonstrate an increase in low frequency content at the cut in speed of 3-4 m/s, which continue to rise with speed.

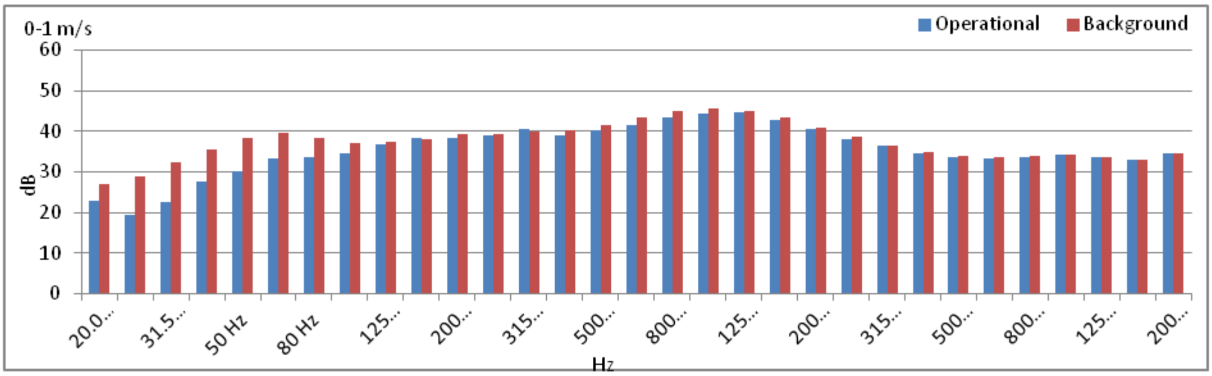

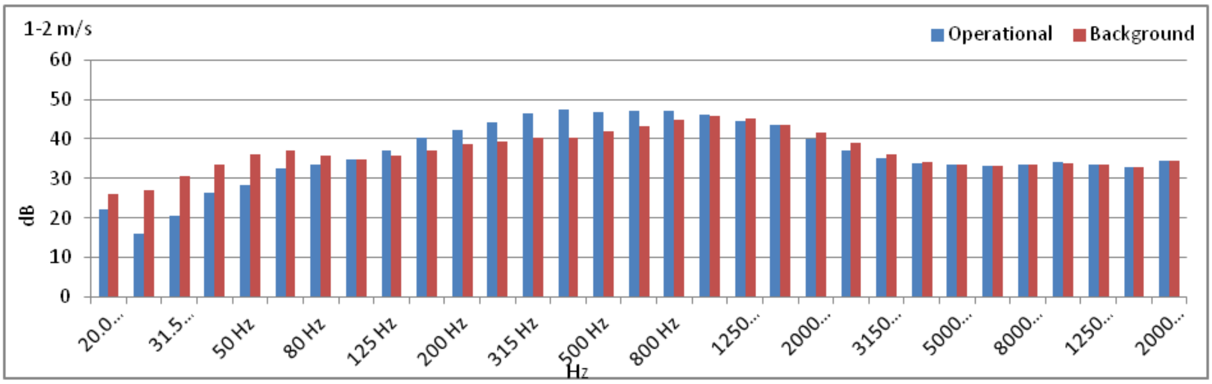

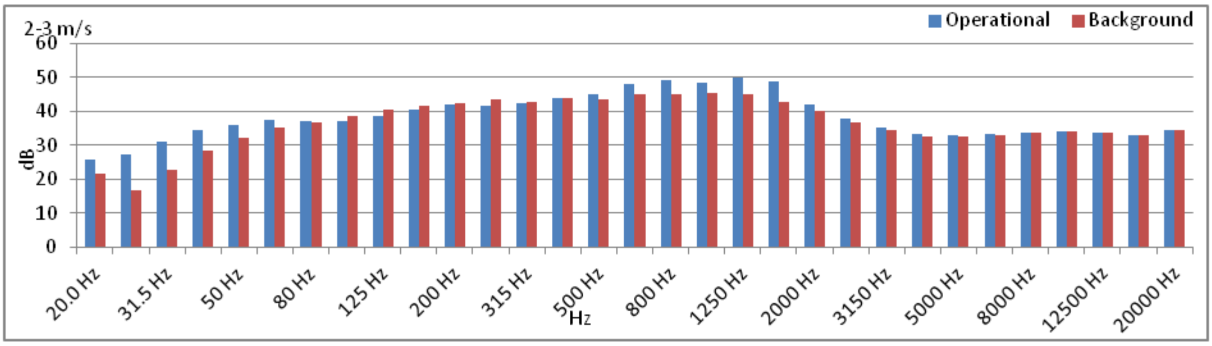

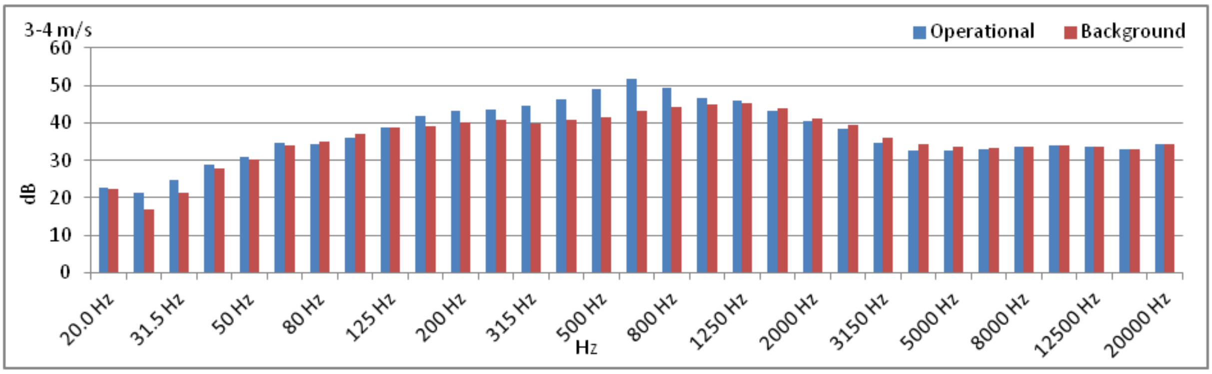

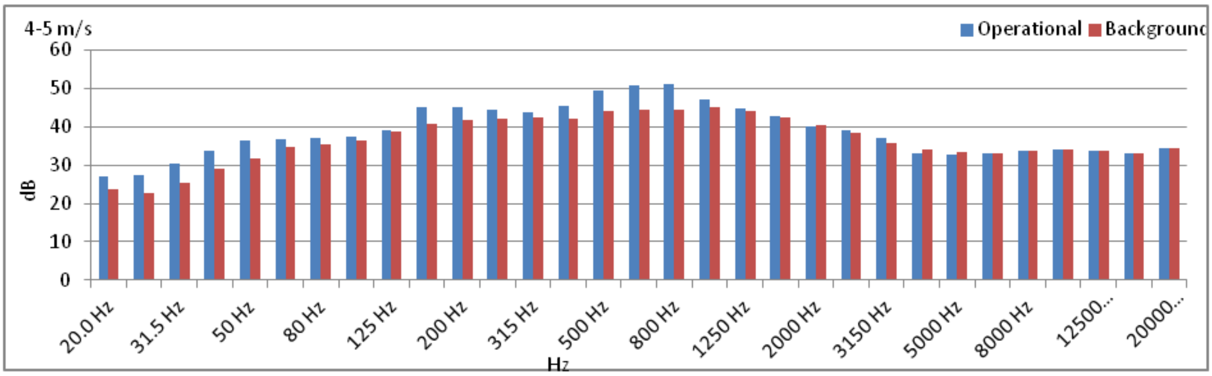
4-5 m/s
Operational
Background
dB
Hz
20.0 Hz
31.5 Hz
50 Hz
80 Hz
125 Hz
200 Hz
315 Hz
500 Hz
800 Hz
1250 Hz
2000 Hz
3150 Hz
5000 Hz
8000 Hz
12500...
20000...

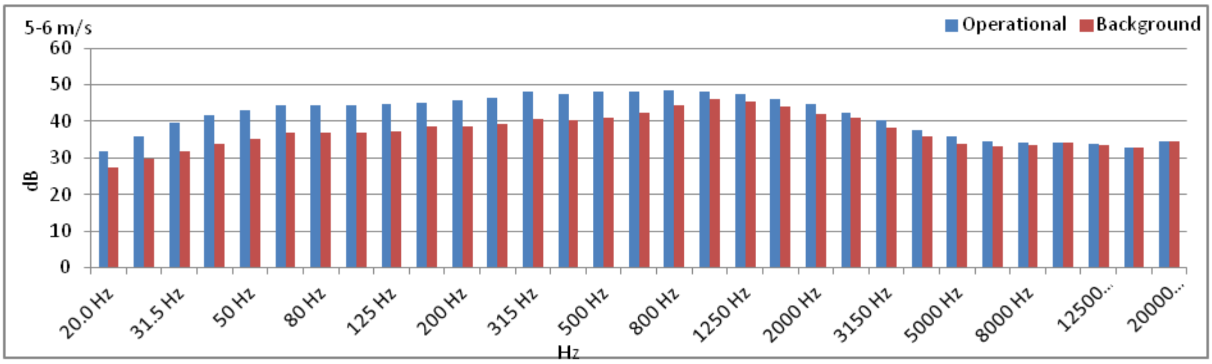
5-6 m/s
Operational
Background
dB
Hz
20.0 Hz
31.5 Hz
50 Hz
80 Hz
125 Hz
200 Hz
315 Hz
500 Hz
800 Hz
1250 Hz
2000 Hz
3150 Hz
5000 Hz
8000 Hz
12500...
20000...

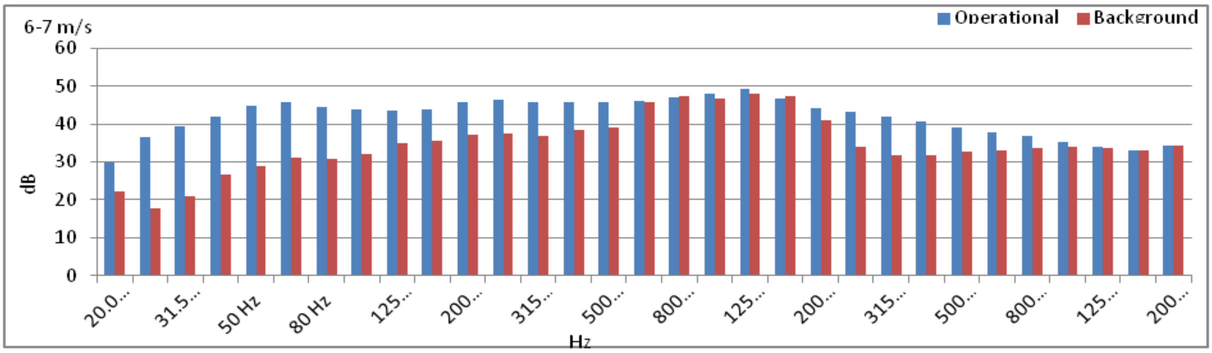
6-7 m/s
Operational
Background
dB
Hz
20.0...
31.5...
50 Hz
80 Hz
125...
200...
315...
500...
800...
125...
200...
315...
500...
800...
125...
200...

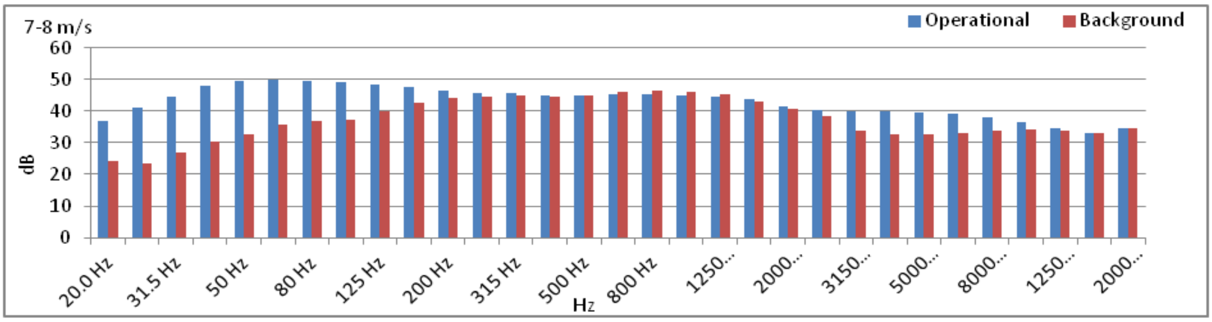
7-8 m/s
Operational
Background
dB
Hz
20.0 Hz
31.5 Hz
50 Hz
80 Hz
125 Hz
200 Hz
315 Hz
500 Hz
800 Hz
1250...
2000...
3150...
5000...
8000...
1250...
2000...

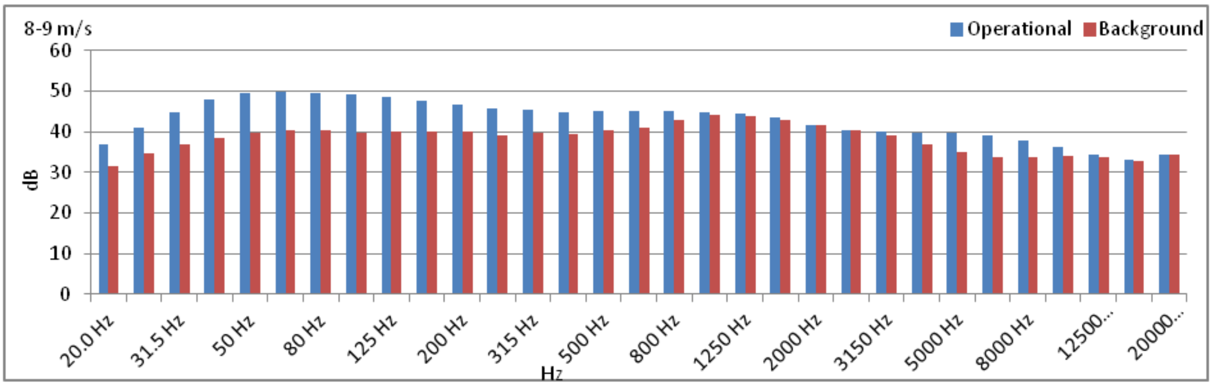
8-9 m/s
Operational
Background
dB
Hz
20.0 Hz
31.5 Hz
50 Hz
80 Hz
125 Hz
200 Hz
315 Hz
500 Hz
800 Hz
1250 Hz
2000 Hz
3150 Hz
5000 Hz
8000 Hz
12500...
20000...

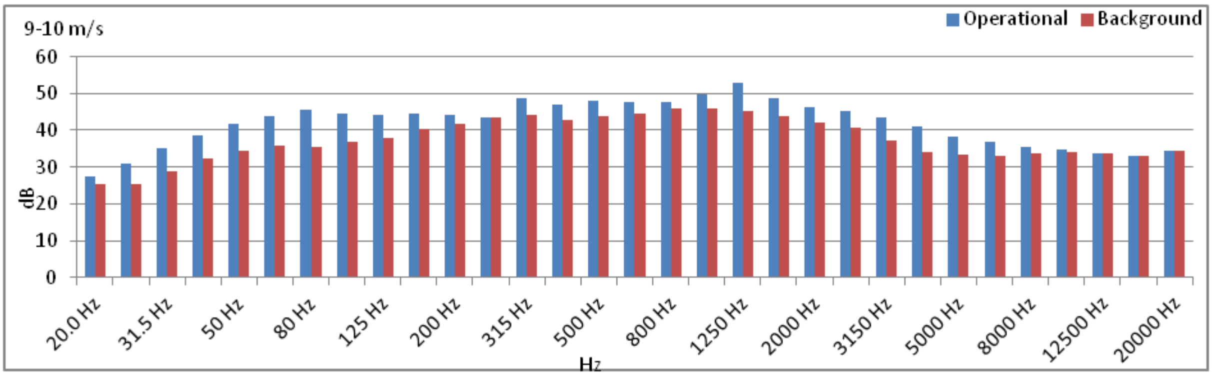
9-10 m/s
Operational
Background
60
50
40
30
20
10
0
dB
20.0 Hz
31.5 Hz
50 Hz
80 Hz
125 Hz
200 Hz
315 Hz
500 Hz
800 Hz
1250 Hz
2000 Hz
3150 Hz
5000 Hz
8000 Hz
12500 Hz
20000 Hz
Hz

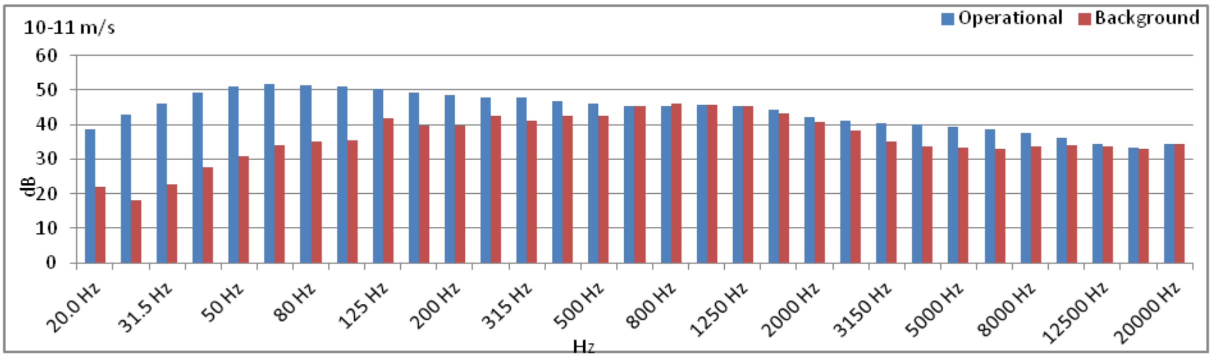
10-11 m/s
Operational
Background
60
50
40
30
20
10
0
dB
20.0 Hz
31.5 Hz
50 Hz
80 Hz
125 Hz
200 Hz
315 Hz
500 Hz
800 Hz
1250 Hz
2000 Hz
3150 Hz
5000 Hz
8000 Hz
12500 Hz
20000 Hz
Hz

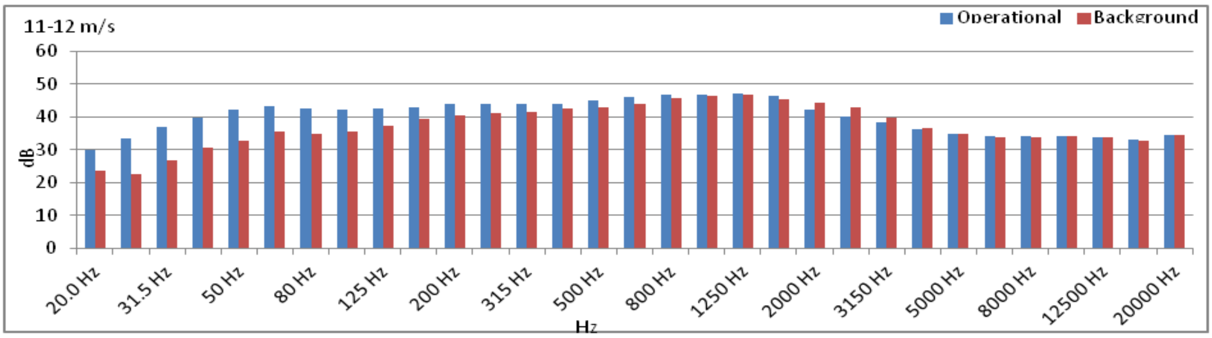
11-12 m/s
Operational
Background
60
50
40
30
20
10
0
dB
20.0 Hz
31.5 Hz
50 Hz
80 Hz
125 Hz
200 Hz
315 Hz
500 Hz
800 Hz
1250 Hz
2000 Hz
3150 Hz
5000 Hz
8000 Hz
12500 Hz
20000 Hz
Hz

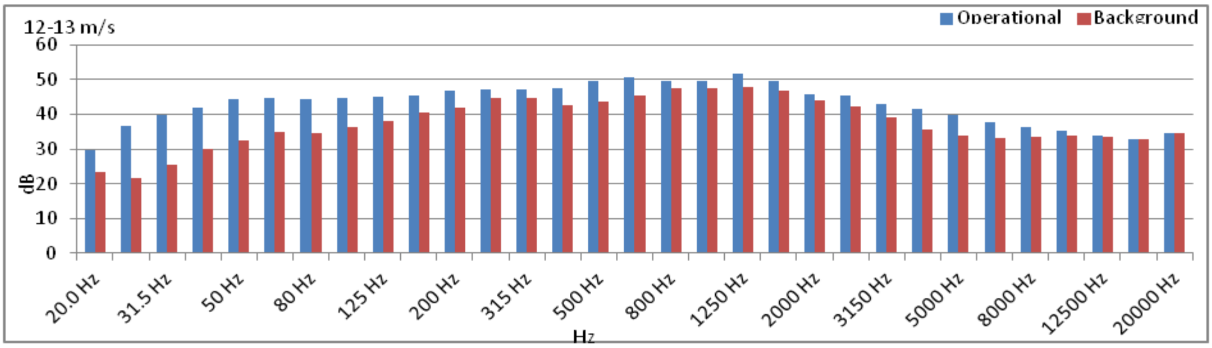
12-13 m/s
Operational
Background
60
50
40
30
20
10
0
dB
20.0 Hz
31.5 Hz
50 Hz
80 Hz
125 Hz
200 Hz
315 Hz
500 Hz
800 Hz
1250 Hz
2000 Hz
3150 Hz
5000 Hz
8000 Hz
12500 Hz
20000 Hz
Hz

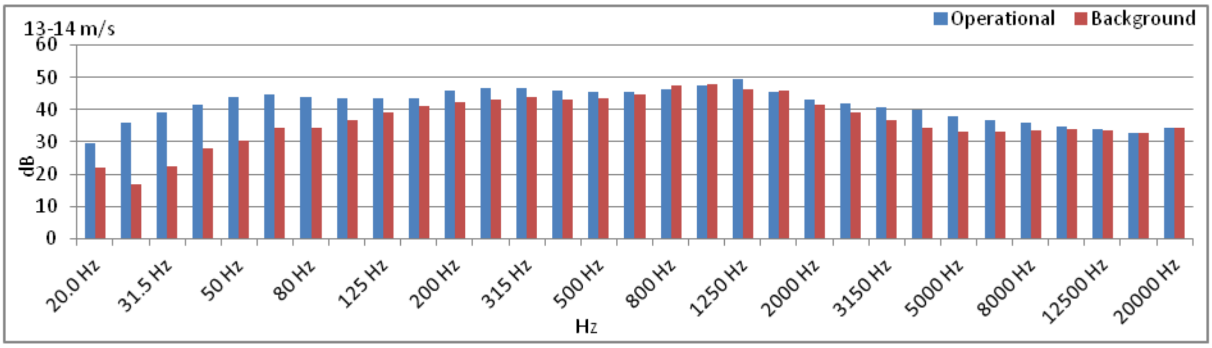
13-14 m/s
Operational
Background
60
50
40
30
20
10
0
dB
20.0 Hz
31.5 Hz
50 Hz
80 Hz
125 Hz
200 Hz
315 Hz
500 Hz
800 Hz
1250 Hz
2000 Hz
3150 Hz
5000 Hz
8000 Hz
12500 Hz
20000 Hz
Hz

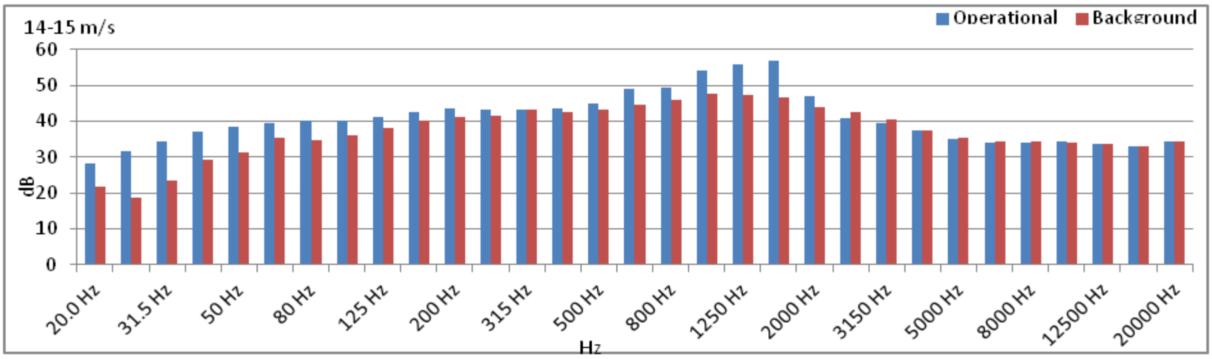
14-15 m/s
Operational
Background
dB
0
10
20
30
40
50
60
20.0 Hz
31.5 Hz
50 Hz
80 Hz
125 Hz
200 Hz
315 Hz
500 Hz
800 Hz
1250 Hz
2000 Hz
3150 Hz
5000 Hz
8000 Hz
12500 Hz
20000 Hz
Hz

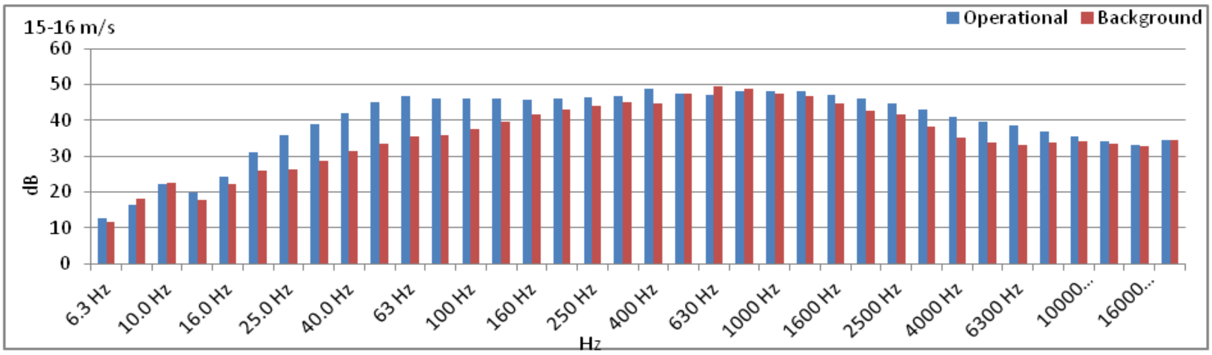
15-16 m/s
Operational
Background
dB
0
10
20
30
40
50
60
6.3 Hz
10.0 Hz
16.0 Hz
25.0 Hz
40.0 Hz
63 Hz
100 Hz
160 Hz
250 Hz
400 Hz
630 Hz
1000 Hz
1600 Hz
2500 Hz
4000 Hz
6300 Hz
10000...
16000...
Hz

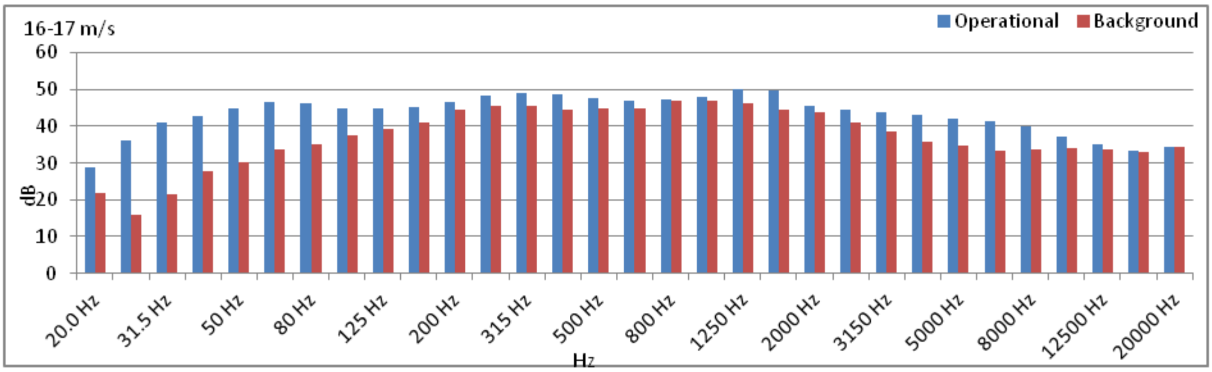
16-17 m/s
Operational
Background
dB
0
10
20
30
40
50
60
20.0 Hz
31.5 Hz
50 Hz
80 Hz
125 Hz
200 Hz
315 Hz
500 Hz
800 Hz
1250 Hz
2000 Hz
3150 Hz
5000 Hz
8000 Hz
12500 Hz
20000 Hz
Hz

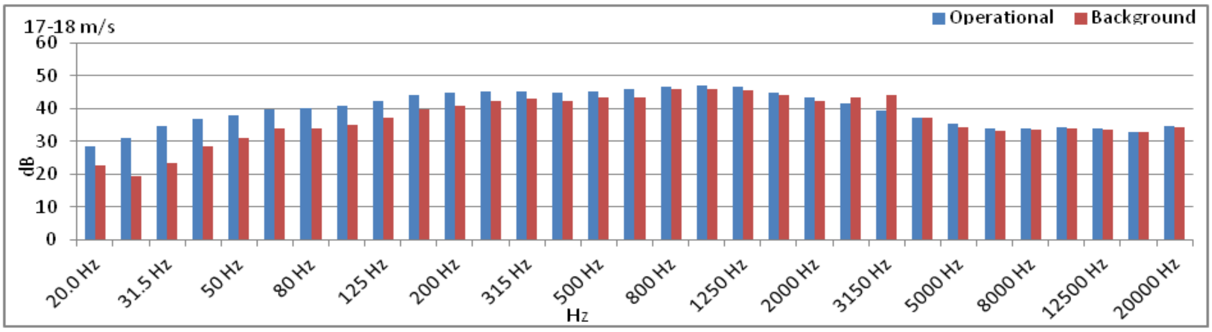
17-18 m/s
Operational
Background
dB
0
10
20
30
40
50
60
20.0 Hz
31.5 Hz
50 Hz
80 Hz
125 Hz
200 Hz
315 Hz
500 Hz
800 Hz
1250 Hz
2000 Hz
3150 Hz
5000 Hz
8000 Hz
12500 Hz
20000 Hz
Hz

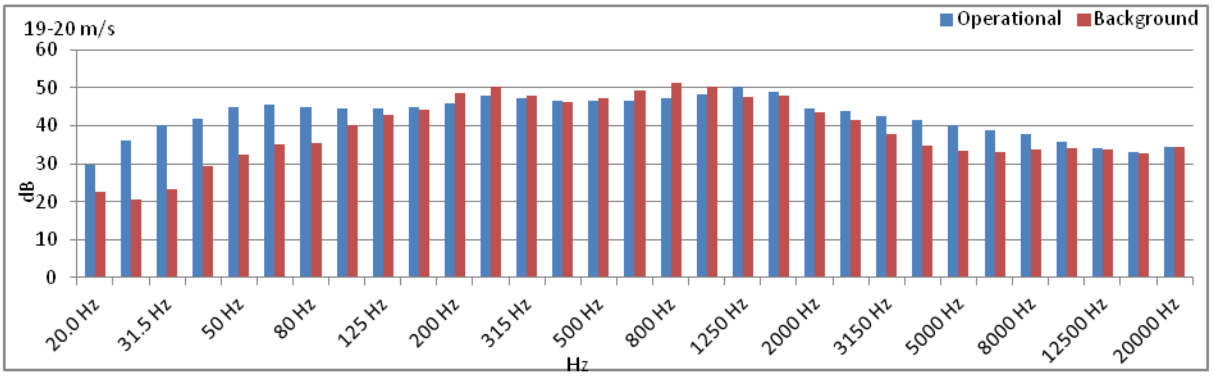
19-20 m/s
Operational
Background
dB
0
10
20
30
40
50
60
20.0 Hz
31.5 Hz
50 Hz
80 Hz
125 Hz
200 Hz
315 Hz
500 Hz
800 Hz
1250 Hz
2000 Hz
3150 Hz
5000 Hz
8000 Hz
12500 Hz
20000 Hz
Hz

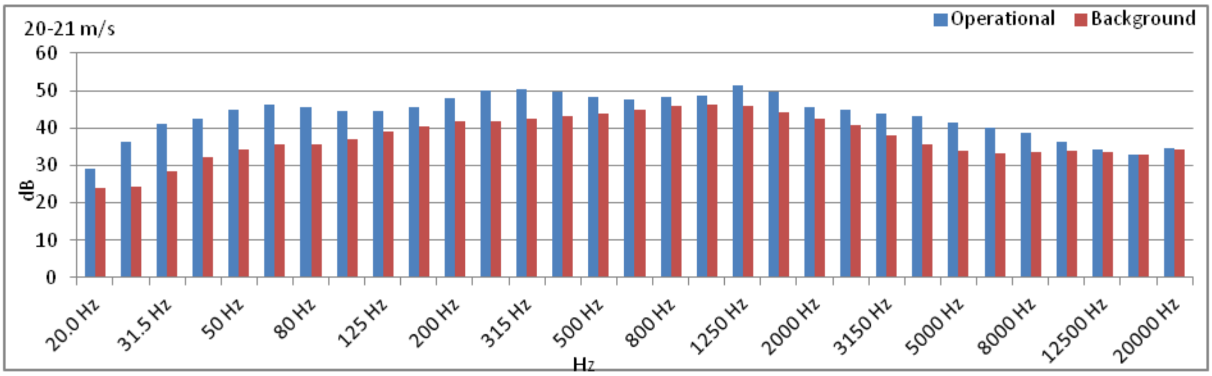
20-21 m/s
Operational
Background
dB
Hz
20.0 Hz
31.5 Hz
50 Hz
80 Hz
125 Hz
200 Hz
315 Hz
500 Hz
800 Hz
1250 Hz
2000 Hz
3150 Hz
5000 Hz
8000 Hz
12500 Hz
20000 Hz

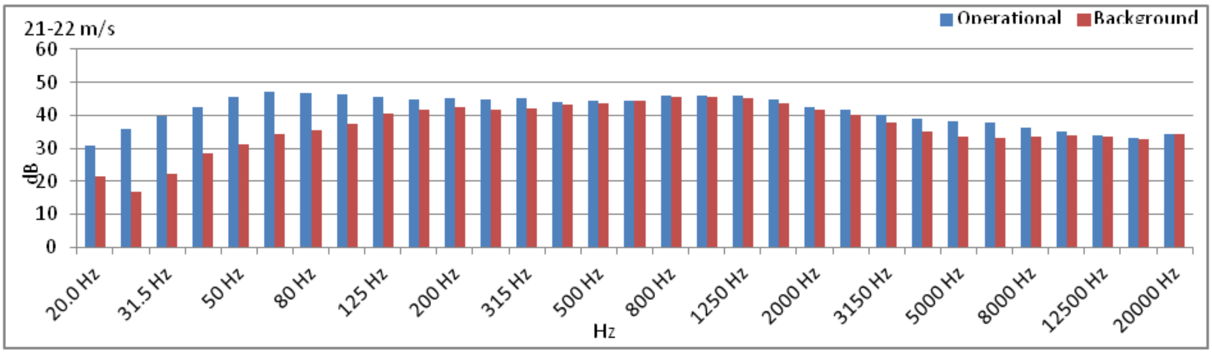
21-22 m/s
Operational
Background
dB
Hz
20.0 Hz
31.5 Hz
50 Hz
80 Hz
125 Hz
200 Hz
315 Hz
500 Hz
800 Hz
1250 Hz
2000 Hz
3150 Hz
5000 Hz
8000 Hz
12500 Hz
20000 Hz

APPENDIX R Wind Speed Frequency distributions Strata 2013

Year:	2013	MMLM - 10 MINUTE AV. DATA ANALYSIS				
INTERVAL	WIND SPEED BINS (m/s)	FREQUENCY	MEDIAN WIND SPEED (m/s)	INTERVAL TOTAL, vi (m/s)	AV WIND SPEED, vi (m/s)	ln(vi)
0	0 < v ≤ 0.5	4893	0.5	363.87	0.07	-2.599
1	0.5 < v ≤ 1.5	7585	1	6917.05	0.91	-0.092
2	1.5 < v ≤ 2.5	7235	2	14666.20	2.03	0.707
3	2.5 < v ≤ 3.5	5978	3	20441.08	3.42	1.229
4	3.5 < v ≤ 4.5	5004	4	21257.99	4.25	1.446
5	4.5 < v ≤ 5.5	3831	5	25051.09	6.54	1.878
6	5.5 < v ≤ 6.5	3128	6	19698.15	6.30	1.840
7	6.5 < v ≤ 7.5	2555	7	19278.80	7.55	2.021
8	7.5 < v ≤ 8.5	2099	8	18937.56	9.02	2.200
9	8.5 < v ≤ 9.5	1772	9	16257.80	9.17	2.216
10	9.5 < v ≤ 10.5	1623	10	17294.11	10.66	2.366
11	10.5 < v ≤ 11.5	1135	11	13862.81	12.21	2.503
12	11.5 < v ≤ 12.5	920	12	12297.86	13.37	2.593
13	12.5 < v ≤ 13.5	708	13	10500.25	14.83	2.697
14	13.5 < v ≤ 14.5	609	14	9532.86	15.65	2.751
15	14.5 < v ≤ 15.5	484	15	7704.54	15.92	2.767
16	15.5 < v ≤ 16.5	390	16	7842.85	20.11	3.001
17	16.5 < v < 17.5	313	17	6283.21	20.07	2.999
18	17.5 < v < 18.5	250	18	5130.82	20.52	3.022
19	18.5 < v < 19.5	225	19	4090.36	18.18	2.900
20	19.5 < v < 20.5	180	20	4083.38	22.69	3.122
21	20.5 < v < 21.5	126	21	2912.82	23.12	3.141
22	21.5 < v < 22.5	77	22	1997.94	25.95	3.256
23	22.5 < v < 23.5	82	23	2003.51	24.43	3.196
24	23.5 < v < 24.5	55	24	1554.34	28.26	3.341
25	24.5 < v < 25.5	36	25	1144.24	31.78	3.459
26	25.5 < v < 26.5	27	26	958.52	35.50	3.570
27	26.5 < v < 27.5	20	27	675.16	33.76	3.519
28	27.5 < v < 28.5	20	28	505.29	25.26	3.229
29	28.5 < v < 29.5	17	29	492.62	28.98	3.367
30	29.5 < v < 30.5	8	30	299.01	37.38	3.621
31	30.5 < v < 31.5	2	31	184.81	92.41	4.526
32	31.5 < v < 32.5	9	32	160.69	17.85	2.882
33	32.5 < v < 33.5	2	33	196.06	98.03	4.585
34	33.5 < v < 34.5	1	34	101.52	101.52	4.620
35	34.5 < v < 35.5	2	35	0.00	35.00	3.555
36	35.5 < v < 36.5	2	36	143.17	71.58	4.271

37	36.5 < v < 37.5	0	37	0.00	37.00	3.611
38	37.5 < v < 38.5	0	38	0.00	38.00	3.638
39	38.5 < v < 39.5	0	39	0.00	39.00	3.664
40	39.5 < v < 40.5	0	40	0.00	40.00	3.689
41	40.5 < v < 41.5	0	41	0.00	41.00	3.714
42	41.5 < v < 42.5	0	42	0.00	42.00	3.738
		51202		**268406.9**		

Mean wind speed:	5.24	m/s

Total number of missing wind data:	1358	2.6 %

p(vi) ACTUAL	**vi^k1**	**FUNCTION A: vi^k . ln(vi) . P(vi)**	**FUNCTION B: vi^k . P(vi)**	**FUNCTION C: ln(vi) . P(vi)**	**WEIBULL**	**RAYLEIGH**
0.096	0.0800166113165	-0.020	0.008	-0.248	0.208	0.028
0.148	0.9143105435484	-0.012	0.135	-0.014	0.164	0.056
0.141	1.9871449590430	0.198	0.281	0.100	0.129	0.102
0.117	3.3029210986566	0.474	0.386	0.144	0.097	0.133
0.098	4.0784808656078	0.577	0.399	0.141	0.083	0.145
0.075	6.2019537374055	0.871	0.464	0.140	0.053	0.140
0.061	5.9790712577644	0.672	0.365	0.112	0.056	0.123
0.050	7.1277206989079	0.719	0.356	0.101	0.044	0.099
0.041	8.4797960909056	0.765	0.348	0.090	0.033	0.073
0.035	8.6191871013280	0.661	0.298	0.077	0.032	0.051
0.032	9.9681952109775	0.748	0.316	0.075	0.025	0.033
0.022	11.3820761901072	0.631	0.252	0.055	0.018	0.020
0.018	12.4251979277592	0.579	0.223	0.047	0.015	0.011
0.014	13.7453558983528	0.513	0.190	0.037	0.011	0.006
0.012	14.4855554329428	0.474	0.172	0.033	0.010	0.003
0.009	14.7239565678715	0.385	0.139	0.026	0.009	0.001
0.008	18.4787167460645	0.422	0.141	0.023	0.004	0.001
0.006	18.4468018815183	0.338	0.113	0.018	0.004	0.000
0.005	18.8477624010509	0.278	0.092	0.015	0.004	0.000
0.004	16.7524007871966	0.214	0.074	0.013	0.006	0.000
0.004	20.7746806833125	0.228	0.073	0.011	0.003	0.000
0.002	21.1591968634847	0.164	0.052	0.008	0.002	0.000
0.002	23.6720142399720	0.116	0.036	0.005	0.004	0.000
0.002	22.3282836796166	0.114	0.036	0.005	0.002	0.000
0.001	25.7206376166617	0.092	0.028	0.004	0.001	0.000
0.001	28.8319412995198	0.070	0.020	0.002	0.001	0.000
0.001	32.1029216107377	0.060	0.017	0.002	0.000	0.000

0.000	30.5703536957169	0.042	0.012	0.001	0.000	0.000
0.000	23.0663825496021	0.029	0.009	0.001	0.002	0.000
0.000	26.3541914963681	0.029	0.009	0.001	0.001	0.000
0.000	33.7497020955534	0.019	0.005	0.001	0.000	0.000
0.000	81.3381617970085	0.014	0.003	0.000	0.000	0.000
0.000	16.4614939985823	0.008	0.003	0.001	0.007	0.000
0.000	86.1465482052165	0.015	0.003	0.000	0.000	0.000
0.000	89.1271242534667	0.008	0.002	0.000	0.000	0.000
0.000	31.6626438956217	0.004	0.001	0.000	0.000	0.000
0.000	63.4651224286488	0.011	0.002	0.000	0.000	0.000
0.000	33.4195523278791	0.000	0.000	0.000	0.000	0.000
0.000	34.2969938561891	0.000	0.000	0.000	0.000	0.000
0.000	35.1737847224595	0.000	0.000	0.000	0.000	0.000
0.000	36.0499420781851	0.000	0.000	0.000	0.000	0.000
0.000	36.9254822052296	0.000	0.000	0.000	0.000	0.000
0.000	37.8004205800584	0.000	0.000	0.000	0.000	0.000
1.000	**283.96**	**10.108**	**4.948**	**1.014**	**1.0168**	**1.024**

Weibull factors:	(Iterative) k =	0.9718
	k =	2.0000
	c =	5.1825

Proven Power Curve (W)	Measured		Weibull PDF		Rayleigh PDF			Guestimate Cp = 0.20		
	p(vi) ACTUAL	Energy Yield (kWh)	Weibull	Energy Yield (kWh)	Rayleigh	Energy Yield (kWh)	Power in the wind (kW)	Coefficient of Power	Power in Wind with Cp Applied (kW)	Power x Frequency (kW)
	0		0		0					
0	0.096	0.00	0.115	0.00	0.028	0.00	0.00	0.20	0.000	0.000
0	0.148	0.00	0.164	0.00	0.056	0.00	0.00	0.20	0.000	0.000
0	0.141	0.00	0.129	0.00	0.102	0.00	0.00	0.20	0.000	0.000
0	0.117	0.00	0.097	0.00	0.133	0.00	0.00	0.20	0.000	0.000
200	0.098	100.08	0.083	84.68	0.145	148.21	0.20	0.20	0.040	200.160
400	0.075	153.24	0.053	108.93	0.140	286.49	0.40	0.20	0.080	306.480
2000	0.061	625.60	0.056	570.36	0.123	1255.23	2.00	0.20	0.400	1251.200
4000	0.050	1022.00	0.044	899.78	0.099	2019.93	4.00	0.20	0.800	2044.000
6700	0.041	1406.33	0.033	1140.99	0.073	2518.58	6.70	0.20	1.340	2812.660
9000	0.035	1594.80	0.032	1489.40	0.051	2341.33	9.00	0.20	1.800	3189.600
11700	0.032	1898.91	0.025	1467.95	0.033	1964.83	11.70	0.20	2.340	3797.820
13900	0.022	1577.65	0.018	1305.46	0.020	1408.91	13.90	0.20	2.780	3155.300

15900	0.018	1462.80	0.015	1206.36	0.011	911.10		15.90	0.20	3.180	2925.600
17100	0.014	1210.68	0.011	990.66	0.006	519.53		17.10	0.20	3.420	2421.360
18000	0.012	1096.20	0.010	896.54	0.003	272.23		18.00	0.20	3.600	2192.400
18200	0.009	880.88	0.009	863.45	0.001	128.75		18.20	0.20	3.640	1761.760
18300	0.008	713.70	0.004	403.81	0.001	56.93		18.30	0.20	3.660	1427.400
18200	0.006	569.66	0.004	404.22	0.000	23.43		18.30	0.20	3.660	1145.580
18000	0.005	450.00	0.004	368.43	0.000	9.02		18.20	0.20	3.640	910.000
17000	0.004	382.50	0.006	533.26	0.000	3.12		18.00	0.20	3.600	810.000
0	0.004	0.00	0.003	0.00	0.000	0.00		17.00	0.20	3.400	612.000
0	0.002	0.00	0.002	0.00	0.000	0.00		0.00	0.20	0.000	0.000
0	0.002	0.00	0.004	0.00	0.000	0.00		0.00	0.20	0.000	0.000
0	0.002	0.00	0.002	0.00	0.000	0.00		0.00	0.20	0.000	0.000
0	0.001	0.00	0.001	0.00	0.000	0.00		0.00	1.20	0.000	0.000
0	0.001	0.00	0.001	0.00	0.000	0.00		0.00	2.20	0.000	0.000
0	0.001	0.00	0.000	0.00	0.000	0.00		0.00	3.20	0.000	0.000
0	0.000	0.00	0.000	0.00	0.000	0.00		0.00	4.20	0.000	0.000
0	0.000	0.00	0.002	0.00	0.000	0.00		0.00	5.20	0.000	0.000
0	0.000	0.00	0.001	0.00	0.000	0.00		0.00	6.20	0.000	0.000
0	0.000	0.00	0.000	0.00	0.000	0.00		0.00	7.20	0.000	0.000
0	0.000	0.00	0.000	0.00	0.000	0.00		0.00	8.20	0.000	0.000
0	0.000	0.00	0.007	0.00	0.000	0.00		0.00	9.20	0.000	0.000
0	0.000	0.00	0.000	0.00	0.000	0.00		0.00	10.20	0.000	0.000
0	0.000	0.00	0.000	0.00	0.000	0.00		0.00	11.20	0.000	0.000
0	0.000	0.00	0.000	0.00	0.000	0.00		0.00	12.20	0.000	0.000
0	0.000	0.00	0.000	0.00	0.000	0.00		0.00	13.20	0.000	0.000
0	0.000	0.00	0.000	0.00	0.000	0.00		0.00	14.20	0.000	0.000
0	0.000	0.00	0.000	0.00	0.000	0.00		0.00	15.20	0.000	0.000
0	0.000	0.00	0.000	0.00	0.000	0.00		0.00	16.20	0.000	0.000
0	0.000	0.00	0.000	0.00	0.000	0.00		0.00	17.20	0.000	0.000
0	0.000	0.00	0.000	0.00	0.000	0.00		0.00	18.20	0.000	0.000
0	0.000	0.00	0.000	0.00	0.000	0.00		0.00	19.20	0.000	0.000
	0.982	**14312.53**	**0.903**	**12734.26**	**1.023**	**13867.63**					30963

APPENDIX S Wind Speed Frequency distributions Strata 2014

Year: 2014	**MMLM - 10 MINUTE AV. DATA ANALYSIS**	**Year:** 2014

INTERVAL	**WIND SPEED BINS (m/s)**	**FREQUENCY**	**MEDIAN WIND SPEED (m/s)**	**INTERVAL TOTAL, vi (m/s)**	**Av WIND SPEED, vi (m/s)**	**ln(vi)**
0	0 < v ≤ 0.5	5280	0.5	513.79	0.10	-2.330
1	0.5 < v ≤ 1.5	7822	1	6974.10	0.89	-0.115
2	1.5 < v ≤ 2.5	7660	2	15911.25	2.08	0.731
3	2.5 < v ≤ 3.5	6249	3	20954.02	3.35	1.210
4	3.5 < v ≤ 4.5	5063	4	22153.45	4.38	1.476
5	4.5 < v ≤ 5.5	3996	5	23939.07	5.99	1.790
6	5.5 < v ≤ 6.5	3367	6	21633.03	6.43	1.860
7	6.5 < v ≤ 7.5	2517	7	20036.09	7.96	2.074
8	7.5 < v ≤ 8.5	2018	8	18312.21	9.07	2.205
9	8.5 < v ≤ 9.5	1517	9	15545.40	10.25	2.327
10	9.5 < v ≤ 10.5	1337	10	14404.81	10.77	2.377
11	10.5 < v ≤ 11.5	920	11	11223.50	12.20	2.501
12	11.5 < v ≤ 12.5	753	12	10285.10	13.66	2.614
13	12.5 < v ≤ 13.5	611	13	8639.42	14.14	2.649
14	13.5 < v ≤ 14.5	449	14	7726.34	17.21	2.845
15	14.5 < v ≤ 15.5	421	15	6169.88	14.66	2.685
16	15.5 < v ≤ 16.5	337	16	6580.65	19.53	2.972
17	16.5 < v < 17.5	290	17	5099.31	17.58	2.867
18	17.5 < v < 18.5	239	18	4913.58	20.56	3.023
19	18.5 < v < 19.5	176	19	3894.39	22.13	3.097
20	19.5 < v < 20.5	132	20	2916.86	22.10	3.095
21	20.5 < v < 21.5	147	21	2749.03	18.70	2.929
22	21.5 < v < 22.5	74	22	2299.14	31.07	3.436
23	22.5 < v < 23.5	76	23	1698.39	22.35	3.107
24	23.5 < v < 24.5	49	24	1747.57	35.66	3.574
25	24.5 < v < 25.5	48	25	1202.59	25.05	3.221
26	25.5 < v < 26.5	39	26	1040.23	26.67	3.284
27	26.5 < v < 27.5	43	27	1242.96	28.91	3.364
28	27.5 < v < 28.5	17	28	782.73	46.04	3.830
29	28.5 < v < 29.5	20	29	581.08	29.05	3.369
30	29.5 < v < 30.5	10	30	419.30	41.93	3.736
31	30.5 < v < 31.5	11	31	342.51	31.14	3.438
32	31.5 < v < 32.5	10	32	353.68	35.37	3.566
33	32.5 < v < 33.5	10	33	298.69	29.87	3.397

34	33.5 < v < 34.5	8	34	375.71	46.96	3.849
35	34.5 < v < 35.5	1	35	0.00	35.00	3.555
36	35.5 < v < 36.5	7	36	144.85	20.69	3.030
37	36.5 < v < 37.5	3	37	258.47	86.16	4.456
38	37.5 < v < 38.5	4	38	76.34	19.08	2.949
39	38.5 < v < 39.5	3	39	155.61	51.87	3.949
40	39.5 < v < 40.5	1	40	80.12	80.12	4.384
41	40.5 < v < 41.5	3	41	82.77	27.59	3.318
42	41.5 < v < 42.5	1	42	84.05	84.05	4.431
43						
		51451		**254572.8**		

	Mean wind speed:	4.95	m/s

Total number of missing wind data:					1109	2.1
p(vi) ACTUAL	**vi^k1**	**FUNCTION A: vi^k . ln(vi) . P(vi)**	**FUNCTION B: vi^k . P(vi)**	**FUNCTION C: ln(vi) . P(vi)**	**WEIBULL**	**RAYLEIGH**
0.103	0.1025655943755	-0.025	0.011	-0.239	0.213	0.032
0.152	0.8939143803763	-0.016	0.136	-0.017	0.172	0.062
0.149	2.0431743998541	0.222	0.304	0.109	0.132	0.113
0.121	3.2627934046525	0.479	0.396	0.147	0.101	0.144
0.098	4.2321001176533	0.615	0.416	0.145	0.082	0.154
0.078	5.7533725191851	0.800	0.447	0.139	0.059	0.144
0.065	6.1606788606510	0.750	0.403	0.122	0.054	0.121
0.049	7.5959569553156	0.771	0.372	0.101	0.040	0.093
0.039	8.6335111503586	0.747	0.339	0.087	0.032	0.066
0.029	9.7228077942855	0.667	0.287	0.069	0.025	0.043
0.026	10.2108089513268	0.631	0.265	0.062	0.023	0.026
0.018	11.5293715325768	0.516	0.206	0.045	0.017	0.015
0.015	12.8756866488266	0.493	0.188	0.038	0.013	0.008
0.012	13.3186735779522	0.419	0.158	0.031	0.012	0.004
0.009	16.1368482592184	0.401	0.141	0.025	0.006	0.002
0.008	13.7930805962549	0.303	0.113	0.022	0.011	0.001
0.007	18.2595543838891	0.355	0.120	0.019	0.004	0.000
0.006	16.4813387446686	0.266	0.093	0.016	0.006	0.000
0.005	19.2020080953296	0.270	0.089	0.014	0.003	0.000
0.003	20.6324806242180	0.219	0.071	0.011	0.002	0.000
0.003	20.6053456007374	0.164	0.053	0.008	0.002	0.000
0.003	17.5040241682767	0.146	0.050	0.008	0.005	0.000
0.001	28.7494638798826	0.142	0.041	0.005	0.004	0.000
0.001	20.8330015573068	0.096	0.031	0.005	0.002	0.000
0.001	32.8988770316866	0.112	0.031	0.003	0.000	0.000

0.001	23.2961092310829	0.070	0.022	0.003	0.001	0.000
0.001	24.7659914875954	0.062	0.019	0.002	0.001	0.000
0.001	26.7911738409516	0.075	0.022	0.003	0.001	0.000
0.000	42.2281953372825	0.053	0.014	0.001	0.000	0.000
0.000	26.9253492705238	0.035	0.010	0.001	0.001	0.000
0.000	38.5373623595958	0.028	0.007	0.001	0.000	0.000
0.000	28.8109803366645	0.021	0.006	0.001	0.000	0.000
0.000	32.6313859568922	0.023	0.006	0.001	0.000	0.000
0.000	27.6634645070067	0.018	0.005	0.001	0.001	0.000
0.000	43.0532312497917	0.026	0.007	0.001	0.000	0.000
0.000	32.2994903987566	0.002	0.001	0.000	0.000	0.000
0.000	19.3239873454388	0.008	0.003	0.000	0.003	0.000
0.000	77.9082572636459	0.020	0.005	0.000	0.000	0.000
0.000	17.8553076119683	0.004	0.001	0.000	0.004	0.000
0.000	47.4438552625952	0.011	0.003	0.000	0.000	0.000
0.000	72.5676235624838	0.006	0.001	0.000	0.000	0.000
0.000	25.5998156672464	0.005	0.001	0.000	0.001	0.000
0.000	76.0463272679996	0.007	0.001	0.000	0.000	0.000
1.000	288.53	9.431	4.729	0.971	1.0187	1.026

Weibull factors:	(Iterative) k =	0.9774
	k =	2.0000
	c =	4.9022

Proven Power Curve (W)	**Measured**		**Weibull PDF**		**Rayleigh PDF**			**Guestimate Cp = 0.20**		
	p(vi) ACTUAL	**Energy Yield (kWh)**	**Weibull**	**Energy Yield (kWh)**	**Rayleigh**	**Energy Yield (kWh)**	**Power in the wind (kW)**	**Coefficient of Power**	**Power in Wind with Cp Applied (kW)**	**Power x Frequency (kW)**
	0		0		0					
0	0.103	0.00	0.115	0.00	0.032	0.00	0.00	0.20	0.000	0.000
0	0.152	0.00	0.172	0.00	0.062	0.00	0.00	0.20	0.000	0.000
0	0.149	0.00	0.132	0.00	0.113	0.00	0.00	0.20	0.000	0.000
0	0.121	0.00	0.101	0.00	0.144	0.00	0.00	0.20	0.000	0.000
200	0.098	101.26	0.082	84.06	0.154	158.07	0.20	0.20	0.040	202.520
400	0.078	159.84	0.059	121.02	0.144	296.07	0.40	0.20	0.080	319.680
2000	0.065	673.40	0.054	554.27	0.121	1248.18	2.00	0.20	0.400	1346.800
4000	0.049	1006.80	0.040	814.42	0.093	1919.24	4.00	0.20	0.800	2013.600
6700	0.039	1352.06	0.032	1092.19	0.066	2270.62	6.70	0.20	1.340	2704.120
9000	0.029	1365.30	0.025	1162.10	0.043	1988.87	9.00	0.20	1.800	2730.600
11700	0.026	1564.29	0.023	1361.07	0.026	1561.65	11.70	0.20	2.340	3128.580

13900	0.018	1278.80	0.017	1220.13	0.015	1040.44		13.90	0.20	2.780	2557.600
15900	0.015	1197.27	0.013	1047.24	0.008	620.78		15.90	0.20	3.180	2394.540
17100	0.012	1044.81	0.012	1024.77	0.004	324.32		17.10	0.20	3.420	2089.620
18000	0.009	808.20	0.006	591.81	0.002	154.62		18.00	0.20	3.600	1616.400
18200	0.008	766.22	0.011	985.79	0.001	66.06		18.20	0.20	3.640	1532.440
18300	0.007	616.71	0.004	382.99	0.000	26.21		18.30	0.20	3.660	1233.420
18200	0.006	527.80	0.006	556.08	0.000	9.61		18.30	0.20	3.660	1061.400
18000	0.005	430.20	0.003	308.29	0.000	3.27		18.20	0.20	3.640	869.960
17000	0.003	299.20	0.002	214.81	0.000	1.00		18.00	0.20	3.600	633.600
0	0.003	0.00	0.002	0.00	0.000	0.00		17.00	0.20	3.400	448.800
0	0.003	0.00	0.005	0.00	0.000	0.00		0.00	0.20	0.000	0.000
0	0.001	0.00	0.004	0.00	0.000	0.00		0.00	0.20	0.000	0.000
0	0.001	0.00	0.002	0.00	0.000	0.00		0.00	0.20	0.000	0.000
0	0.001	0.00	0.000	0.00	0.000	0.00		0.00	1.20	0.000	0.000
0	0.001	0.00	0.001	0.00	0.000	0.00		0.00	2.20	0.000	0.000
0	0.001	0.00	0.001	0.00	0.000	0.00		0.00	3.20	0.000	0.000
0	0.001	0.00	0.001	0.00	0.000	0.00		0.00	4.20	0.000	0.000
0	0.000	0.00	0.000	0.00	0.000	0.00		0.00	5.20	0.000	0.000
0	0.000	0.00	0.001	0.00	0.000	0.00		0.00	6.20	0.000	0.000
0	0.000	0.00	0.000	0.00	0.000	0.00		0.00	7.20	0.000	0.000
0	0.000	0.00	0.000	0.00	0.000	0.00		0.00	8.20	0.000	0.000
0	0.000	0.00	0.000	0.00	0.000	0.00		0.00	9.20	0.000	0.000
0	0.000	0.00	0.001	0.00	0.000	0.00		0.00	10.20	0.000	0.000
0	0.000	0.00	0.000	0.00	0.000	0.00		0.00	11.20	0.000	0.000
0	0.000	0.00	0.000	0.00	0.000	0.00		0.00	12.20	0.000	0.000
0	0.000	0.00	0.003	0.00	0.000	0.00		0.00	13.20	0.000	0.000
0	0.000	0.00	0.000	0.00	0.000	0.00		0.00	14.20	0.000	0.000
0	0.000	0.00	0.004	0.00	0.000	0.00		0.00	15.20	0.000	0.000
0	0.000	0.00	0.000	0.00	0.000	0.00		0.00	16.20	0.000	0.000
0	0.000	0.00	0.000	0.00	0.000	0.00		0.00	17.20	0.000	0.000
0	0.000	0.00	0.001	0.00	0.000	0.00		0.00	18.20	0.000	0.000
0	0.000	0.00	0.000	0.00	0.000	0.00		0.00	19.20	0.000	0.000
	0.984	**12462.76**	**0.901**	**11521.04**	**1.026**	**11689.01**					**26884**

APPENDIX T Strata Sound Transmission Loss Calculations

Living Room		**Area**	**Hz**							
			63	**125**	**250**	**500**	**1000**	**2000**	**4000**	**8000**
Floor	Wood	61.5	0.15	0.15	0.11	0.1	0.07	0.06	0.07	0.07
Ceiling	Plaster board	35.34	0.15	0.15	0.11	0.04	0.04	0.07	0.08	0.08
Wall	Glass	23.6	0.18	0.18	0.06	0.04	0.03	0.02	0.02	0.02
Wall	Plaster board	72.3	0.29	0.29	0.1	0.06	0.05	0.04	0.04	0.04
	R Façade		49.4	55.3	61.3	67.3	73.4	79.4	85.4	91.4
	S Façade	**357**								
	A =	**Sα**	**39.7**	**39.7**	**19.3**	**12.8**	**10.0**	**9.5**	**10.5**	**10.5**
		$L_{Turbine}$	75.4	73.6	66.2	62.1	65.3	60.5	64.7	61.8
		L_{in}	35.5	27.9	17.6	9.2	7.5	-3.1	-5.4	-14.3
Bed Room		**Area**	**Hz**							
			63	**125**	**250**	**500**	**1000**	**2000**	**4000**	**8000**
Floor	Carpet	13.4	0.01	0.01	0.02	0.06	0.15	0.25	0.45	0.45
Ceiling	Plaster board	13.4	0.15	0.15	0.11	0.04	0.04	0.07	0.08	0.08
Wall	Glass	15	0.18	0.18	0.06	0.04	0.03	0.02	0.02	0.02
Wall	Drapes	15	0.07	0.07	0.31	0.49	0.75	0.7	0.6	0.6
Wall	Plaster board	40.2	0.29	0.29	0.1	0.06	0.05	0.04	0.04	0.04
	R Façade		49.4	55.3	61.3	67.3	73.4	79.4	85.4	91.4
	S Façade	**357**								
	A =	**Sα**	**16.5**	**16.5**	**6.7**	**4.4**	**5.0**	**6.2**	**9.0**	**9.0**
	A =	**Sα**	**14.9**	**14.9**	**10.4**	**11.1**	**15.8**	**16.4**	**17.7**	**17.7**
		$L_{Turbine}$	75.4	73.6	66.2	62.1	65.3	60.5	64.7	61.8
		L_{in}	39.4	31.7	22.2	13.9	10.5	-1.2	-4.7	-13.7
		L_{in}	39.8	32.2	20.3	9.8	5.5	-5.5	-7.6	-16.6
ρ concrete	2600	**kg/m³**								
t	0.45	**m**								
m	1170	**kg/m²**								

Table 91: Displays calculated expected internal noise levels (L_{in}) due to direct transmission through the concrete partition. Levels are calculated with and without drawing the bedroom drapes. Drawn levels are highlighted in blue.

Living Room		Area	Hz							
			63	125	250	500	1000	2000	4000	8000
Floor	Wood	61.5	0.15	0.15	0.11	0.1	0.07	0.06	0.07	0.07
Ceiling	Plaster board	35.34	0.15	0.15	0.11	0.04	0.04	0.07	0.08	0.08
Wall	Glass	23.6	0.18	0.18	0.06	0.04	0.03	0.02	0.02	0.02
Wall	Plaster board	72.3	0.29	0.29	0.1	0.06	0.05	0.04	0.04	0.04
	R Façade		12.5	18.4	24.5	30.5	36.5	42.5	48.5	54.6
	S Façade	23.6								
	A =	Sα	39.7	39.7	19.3	12.8	10.0	9.5	10.5	10.5
		Lturbine	75.4	73.6	66.2	62.1	65.3	60.5	64.7	61.8
		Lout	40.9	39.2	31.8	27.7	30.9	26.1	30.3	27.4
		Lin	32.2	24.5	14.2	5.8	4.1	-6.5	-8.7	-17.7
Bed Room		Area	Hz							
			63	125	250	500	1000	2000	4000	8000
Floor	Carpet	13.4	0.01	0.01	0.02	0.06	0.15	0.25	0.45	0.45
Ceiling	Plaster board	13.4	0.15	0.15	0.11	0.04	0.04	0.07	0.08	0.08
Wall	Glass	15	0.18	0.18	0.06	0.04	0.03	0.02	0.02	0.02
Wall	Drapes	15	0.07	0.07	0.31	0.49	0.75	0.7	0.6	0.6
Wall	Plaster board	40.2	0.29	0.29	0.1	0.06	0.05	0.04	0.04	0.04
	R Façade		12.5	18.4	24.5	30.5	36.5	42.5	48.5	54.6
	S Façade	15								
	A =	Sα	16.5	16.5	6.7	4.4	5.0	6.2	9.0	9.0
	A =	Sα	14.9	14.9	10.4	11.1	15.8	16.4	17.7	17.7
		Lturbine	75.4	73.6	66.2	62.1	65.3	60.5	64.7	61.8
		Lout	40.9	39.2	31.8	27.7	30.9	26.1	30.3	27.4
		Lin	34.0	26.4	16.9	8.6	5.2	-6.6	-10.0	-19.0
		Lin	34.5	26.8	14.9	4.5	0.2	-10.8	-13.0	-21.9
ρ glass	2800	kg/m^3								
t	0.006	m								
m	16.8	kg/m^2								

Table 92: Displays predicted external (Lout) and internal (Lin) sound levels (dB) at the Strata apartments in closest proximity to the operational turbines. Levels are calculated with and without drawing the bedroom drapes. Drawn levels are highlighted in blue.

APPENDIX U Strata averaged RMS Acceleration per wind speed bin

Bin	Range	Freq	Ave RMS A m/s^2 X	Std Dev	Ave RMS A m/s^2 Y	Std Dev	Ave RMS A m/s^2 Z	Std Dev
1	0 < V < 1	121	0.01	0.002	0.01	0.002	0.02	0.005
2	1 < V < 2	332	0.01	0.002	0.01	0.003	0.02	0.007
3	2 < V < 3	357	0.01	0.002	0.01	0.003	0.02	0.008
4	3 < V < 4	262	0.01	0.003	0.01	0.003	0.02	0.006
5	4 < V < 5	193	0.01	0.008	0.01	0.008	0.02	0.006
6	5 < V < 6	147	0.01	0.002	0.01	0.003	0.02	0.008
7	6 < V < 7	127	0.01	0.003	0.01	0.003	0.02	0.009
8	7 < V < 8	62	0.01	0.003	0.01	0.004	0.02	0.010
9	8 < V < 9	85	0.01	0.003	0.01	0.003	0.02	0.010
10	9 < V < 10	87	0.01	0.002	0.01	0.002	0.02	0.007
11	10 < V < 11	50	0.01	0.002	0.01	0.003	0.02	0.007
12	11 < V < 12	34	0.01	0.002	0.01	0.002	0.02	0.007
13	12 < V < 13	32	0.01	0.002	0.01	0.003	0.02	0.007
14	13 < V < 14	28	0.01	0.002	0.01	0.002	0.02	0.007
15	14 < V < 15	11	0.01	0.002	0.01	0.003	0.02	0.007
16	15 < V < 16	13	0.01	0.001	0.01	0.002	0.02	0.008
17	16 < V < 17	15	0.01	0.002	0.01	0.003	0.02	0.007
18	17 < V < 18	8	0.01	0.001	0.01	0.002	0.01	0.003
19	18 < V < 19	4	0.01	0.003	0.01	0.004	0.03	0.012
20	19 < V < 20	3	0.01	0.001	0.01	0.004	0.02	0.013
21	20 < V < 21	6	0.01	0.001	0.01	0.002	0.02	0.009
22	21 < V < 22	4	0.01	0.002	0.01	0.003	0.02	0.004
23	22 < V < 23	8	0.01	0.002	0.01	0.002	0.02	0.008

Table 93: Displays background average RMS A [m/s^2] recorded per wind speed bin at the Strata turbine base.

Bin	Range	Freq	Ave RMS A m/s^2 X	Std Dev	Ave RMS A m/s^2 Y	Std Dev	Ave RMS A m/s^2 Z	Std Dev
1	0 < V < 1	167	0.01	0.002	0.01	0.002	0.01	0.003
2	1 < V < 2	250	0.01	0.004	0.01	0.006	0.02	0.039
3	2 < V < 3	277	0.01	0.004	0.01	0.006	0.02	0.040
4	3 < V < 4	256	0.01	0.004	0.01	0.005	0.02	0.037
5	4 < V < 5	267	0.01	0.003	0.01	0.005	0.03	0.028
6	5 < V < 6	190	0.01	0.006	0.01	0.009	0.02	0.063
7	6 < V < 7	189	0.01	0.004	0.01	0.005	0.03	0.032
8	7 < V < 8	114	0.01	0.005	0.01	0.007	0.04	0.047
9	8 < V < 9	138	0.01	0.007	0.01	0.010	0.03	0.074
10	9 < V < 10	114	0.01	0.007	0.01	0.010	0.03	0.071
11	10 < V < 11	84	0.01	0.006	0.01	0.009	0.03	0.059
12	11 < V < 12	45	0.01	0.006	0.01	0.010	0.03	0.058
13	12 < V < 13	40	0.01	0.004	0.01	0.005	0.02	0.038
14	13 < V < 14	36	0.01	0.008	0.01	0.011	0.05	0.082
15	14 < V < 15	28	0.01	0.006	0.01	0.008	0.03	0.052
16	15 < V < 16	19	0.01	0.008	0.02	0.012	0.05	0.084
17	16 < V < 17	11	0.02	0.011	0.02	0.014	0.06	0.088
18	17 < V < 18	13	0.01	0.006	0.01	0.009	0.04	0.065
19	18 < V < 19	10	0.01	0.004	0.01	0.004	0.02	0.010
20	19 < V < 20	12	0.01	0.008	0.01	0.011	0.04	0.078
21	20 < V < 21	9	0.01	0.004	0.01	0.004	0.02	0.011
22	21 < V < 22	9	0.01	0.004	0.01	0.004	0.02	0.012

Table 94: Displays operational average RMS A[m/s^2] levels recorded per wind speed bin at the Strata turbine base.

APPENDIX V Weibull & Rayleigh distribution curves for an elevated LSBU site

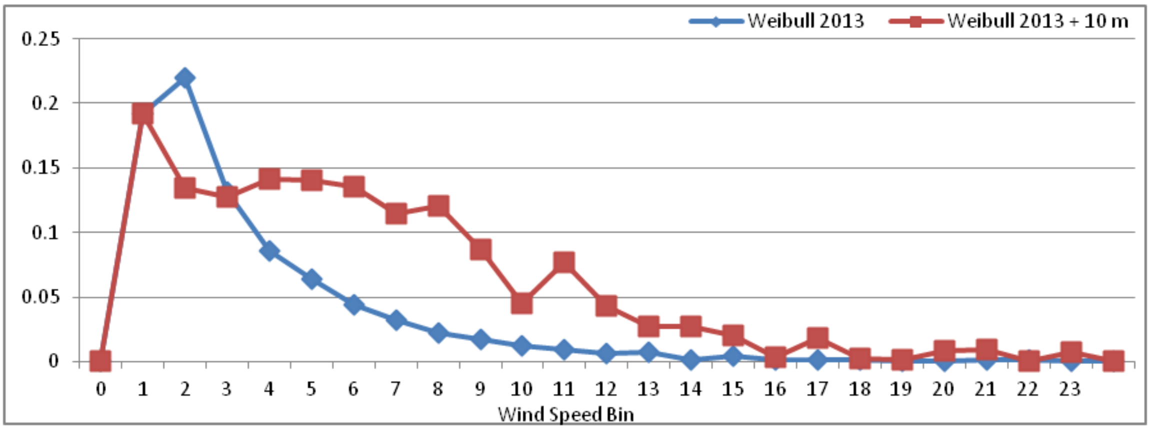

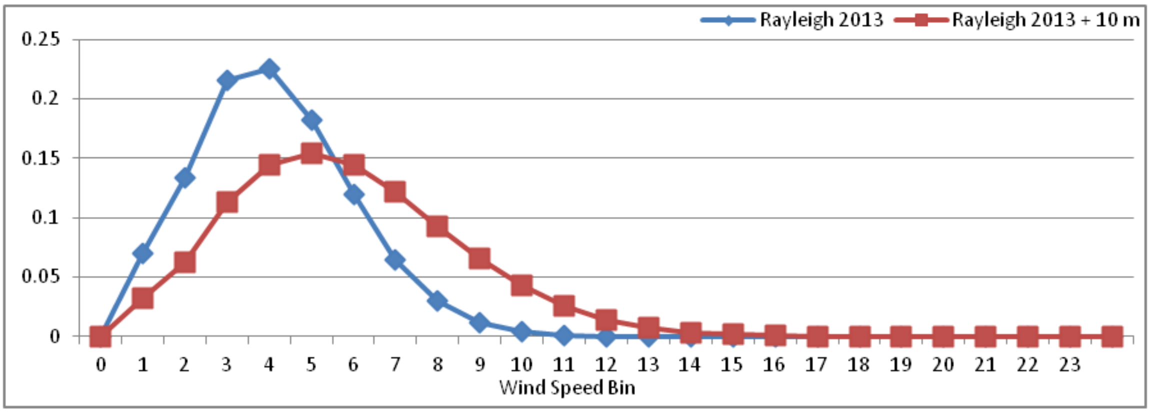

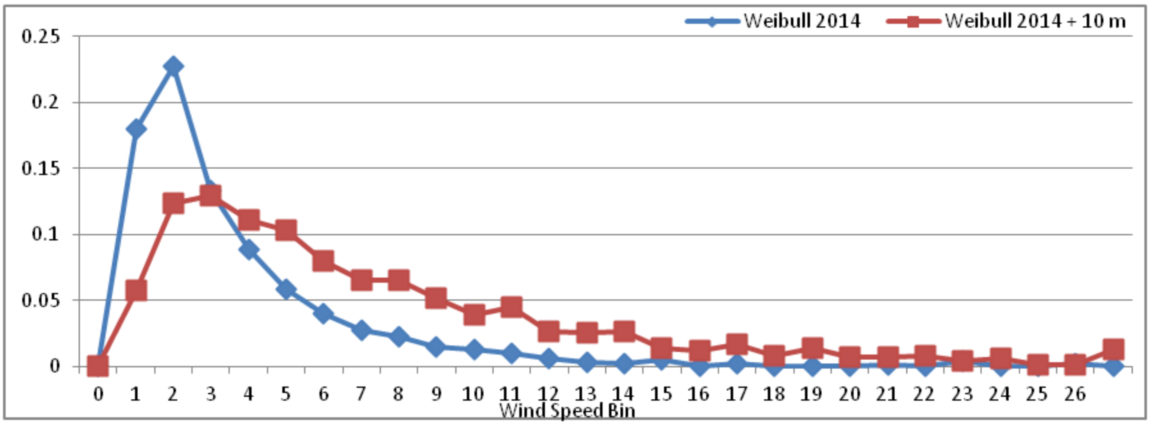

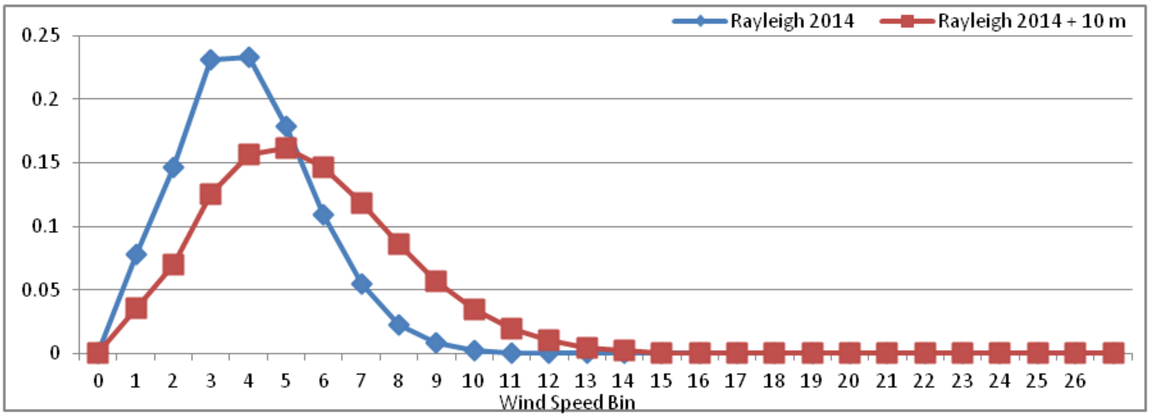

APPENDIX W Strata Weibull & Rayleigh curve comparison post optimisation